Dissertation

submitted to the
Combined Faculties for the Natural Sciences and for Mathematics
of the Ruperto-Carola University of Heidelberg, Germany
for the degree of
Doctor of Natural Sciences

presented by
Dipl.-Biol. Lisa von Paleske, geb. Dohrn
born in: Lübeck
Oral-examination: 02.12.2014

Identification of a novel enhancer region 1.7 Mb downstream of the *c-myc* gene controlling its expression in hematopoietic stem and progenitor cells

Referees:

Prof. Dr. Andreas Trumpp

Prof. Dr. Hanno Glimm

To my wonderful husband Stefan

The most exciting phrase to hear in science, the one that heralds new discoveries, is not 'Eureka!' (I found it!) but 'That's funny....'

Isaac Asimov

ABSTRACT

Identification of a novel enhancer region 1.7 Mb downstream of the *c-myc* gene controlling its expression in hematopoietic stem and progenitor cells

The transcription factor and proto-oncogene c-Myc is a central regulator of cellular proliferation, growth, metabolism and differentiation in many cell types including stem cells. Although it is known that c-Myc expression is tightly controlled and can drive tumorigenesis if de-regulated, the mechanisms of its transcriptional regulation remain largely elusive. Besides its promoter, which is not sufficient to account for endogenous *c-myc* expression, only a few *cis*-regulatory elements have been defined. The *c-myc* gene is located on mouse chromosome 15 within a 4 Mb-long gene-poor region, which coincides with a large topologically associating domain (TAD). At the distal end of this TAD, 1.7 Mb downstream of the mouse *c-myc* gene, we identified a cluster of enhancer-associated chromatin marks which were present only in hematopoietic tissues. A *LacZ* reporter gene inserted next to this cluster showed specific expression in hematopoietic stem cells (HSCs) and progenitor cells. Mice homozygous for a deletion of this enhancer region showed decreased myeloid and B cells, while HSCs, multipotent progenitors and megakaryocytes accumulated in the bone marrow. Mutant HSCs were non-functional, as they lost multipotency and showed differentiation defects at the progenitor level, which resulted in their accumulation *in vivo*. This phenotype closely mimicked the phenotype of mice in which the *c-myc* gene was conditionally deleted by the Cre/loxP technique in the adult hematopoietic system using MxCre (MxCre; c-myc$^{flox/flox}$). Importantly, gene expression analysis showed that the deletion of this enhancer region led to a dramatic reduction of *c-myc* expression in HSCs, multipotent progenitors and most mature cell types. Furthermore, compound heterozygous mice with one allele carrying the enhancer deletion and a *c-myc* null allele on the other chromosome displayed hematopoietic defects highly similar to MxCre; c-myc$^{flox/flox}$ animals, demonstrating genetic allelism between the *c-myc* coding region and the newly identified enhancer region. Altogether, these data provide genetic evidence that this enhancer region directly controls, *in cis*, *c-myc* expression in HSC/progenitor cells. Within the 126 kb enhancer region 8 modules of sizes between 0.4 kb and 1.9 kb were

identified and analyzed for relative enrichment of the enhancer-associated H3K27ac histone mark by ChIP/qRT-PCR. This was performed in different hematopoietic lineages and revealed that distinct enhancer modules differentially control *c-myc* expression in granulocytes or HSC/progenitors. Interestingly, this evolutionary highly conserved enhancer region was shown to be focally amplified in a number of tumor samples from patients with acute myeloid leukemia (AML), suggesting that this enhancer may be a critical component driving increased c-MYC expression found in certain leukemias. In summary, we identified a very distant hematopoietic and stem/progenitor specific enhancer region for *c-myc* and provide genetic data supporting its critical function as a key regulatory region in normal hematopoiesis and a putative role in human AML.

ZUSAMMENFASSUNG

Identifizierung einer neuen Enhancerregion 1.7 Mb strangabwärts des *c-myc* Gens, die dessen Transkription in hämatopoietischen Stamm- und Vorläuferzellen steuert

Der Transkriptionsfaktor c-Myc ist ein Proto-Onkogen und ein zentraler Regulator von zellulärer Proliferation, Wachstum, Metabolismus und Differenzierung in vielen Zelltypen einschließlich Stammzellen. Obwohl bekannt ist, dass die Expression von c-Myc streng kontrolliert erfolgt und bei Fehlregulation zu Tumorgenese führen kann, bleiben die Mechanismen seiner transkriptionellen Regulation weitestgehend unklar. Neben seinem Promoter, der alleine nicht ausreicht, um die endogene Expression von *c-myc* zu ermöglichen, wurden bisher nur wenige *cis*-regulierende Elemente bestimmt. Das *c-myc* Gen befindet sich auf dem Maus-Chromosom 15 in einer 4 Mb-langen, genarmen Region, die sich mit einer topologisch assoziierenden Domäne (TAD) überschneidet. Am distalen Ende dieser TAD, 1.7 Mb strangabwärts des murinen *c-myc* Genes, haben wir eine Gruppe von Enhancer-assoziierten Chromatinmodifikationen identifiziert, die ausschließlich in blutbildenden Geweben vorhanden waren. Ein *LacZ* Reportergen, das neben dieser Gruppe ins Genom eingefügt wurde, zeigte spezifische Expression in hämatopoetischen Stamm- (HSZ) und Vorläuferzellen. Mäuse, in denen diese Region homozygot deletiert wurde, zeigten eine verringerte Anzahl an myeloischen und B Zellen, während sich HSZ, multipotente Vorläuferzellen und Megakaryozyten im Knochenmark anreicherten. Die HSZ waren nicht funktionell, denn sie zeigten den Verlust ihrer Multipotenz und Differenzierungsdefekte beginnend auf der Vorläuferstufe, die zur Akkumulierung dieser Vorläuferzellen *in vivo* führte. Dieser Phänotyp glich in großem Maße dem Phänotyp von Mäusen, in denen das *c-myc* Gen mittels des Cre/loxP-Verfahrens durch MxCre im adulten hämatopoetischen System konditionell deletiert wurde (MxCre; c-myc$^{flox/flox}$). Genexpressionsanalysen zeigten, dass die Deletion der Enhancerregion zu einer dramatischen Verminderung der *c-myc* Expression in HSZ, multipotenten Vorläuferzellen und den meisten reifen Zelltypen führte. Doppelt heterozygote Mäuse,

die ein Allel mit deletiertem Enhancerbereich sowie ein deletiertes *c-myc* Allel auf dem anderen Chromosom besaßen, zeigten äußerst ähnliche hämatopoetische Defekte wie MxCre; c-myc$^{flox/flox}$ Tiere. Dies belegte den genetischen Allelismus zwischen der *c-myc* kodierenden Region und der neu identifizierten Enhancerregion. Insgesamt erbringen unsere Daten den genetischen Beweis, dass diese Enhancerregion die Expression von *c-myc* direkt und *in cis* in HSZ und Vorläuferzellen reguliert. Innerhalb der 126 kb umfassenden Enhancerregion identifizierten wir 8 Module mit Größen zwischen 0.4 kb und 1.9 kb und untersuchten die relative Anreicherung der Enhancer-assoziierten Histonmodifikation H3K27ac durch ChIP/qRT-PCR. Dies wurde in verschiedenen hämatopoietischen Zelltypen durchgeführt und zeigte, dass ausgewählte Enhancermodule die Expression von *c-myc* in Granulozyten oder HSZ/Vorläuferzellen differenziell steuert. Interessanterweise wurde eine fokale Amplifizierung dieser evolutionär hochkonservierten Enhancerregion in einer Reihe von Tumorproben von Patienten mit akuter myeloischer Leukämie (AML) nachgewiesen, was darauf hindeutet, dass dieser Enhancer entscheidend an der erhöhten Expression von c-MYC beteiligt ist, die in einigen Leukämien beobachtet wurde. Zusammenfassend lässt sich sagen, dass wir eine sehr weit entfernt gelegene Enhancerregion für *c-myc* identifiziert haben, die spezifisch für das hämatopoetische System, insbesondere für Stamm- und Vorläuferzellen ist. Unsere Daten belegen die entscheidende Funktion dieses Enhancerbereichs als regulatorische Schlüsselregion in der normalen Blutbildung und zeigen eine mögliche Rolle bei der humanen AML auf.

CONTENTS

1 INTRODUCTION

1.1 Regulation of gene expression

The complete hereditary information of an eukaryotic organism is comprised in the series of deoxyribonucleic acid (DNA) base pairs which are packed and organized in chromosomes. This information provides the blueprint for each cell to fulfill all biological reactions that constitute the living organism. The most well characterized class of elements within this information are the protein coding genes, hence it was termed the "genome". However, analysis of the human sequence limited their number to roughly 20,500 protein coding genes, which comprise only 1.5% of all base pairs of the human genome. Thus the largest part of the genome consists of non-coding sequences (CLAMP *et al.* 2007; LANDER *et al.* 2001; VENTER *et al.* 2001).

Almost every cell within an individual contains the same genomic set of instructions since they originate from a single zygote. However, cell types differ greatly in their appearance and function. This diversity originates from different gene expression patterns in each cell type, thus regulating their differentiation or their response to internal or external stimuli. Since the process of gene expression requires a tight and highly specific adjustment, various regulatory mechanisms exist at different levels. The two main steps for the transmission of the genetic information from DNA into protein are transcription and translation. In the process of transcription the gene serves as a template for the generation of a messenger RNA (mRNA) molecule. This molecule is subsequently exported from the nucleus into the cytoplasm where the encoded genetic information is translated into a sequence of amino acids of a polypeptide. Both steps are tightly regulated and followed by further regulatory mechanisms like splicing, 5'-capping, 3'-polyadenylation, export regulation and mRNA decay of the transcript or folding, cutting, chemical modification and degradation of the

polypeptide (LACKNER and BAHLER 2008; WALSH *et al.* 2005). The following chapters focus on regulatory mechanisms of the transcription.

1.1.1 Transcriptional machinery

The transcription of genes is performed by RNA polymerases. Eukaryotes possess three types of this enzyme, each of them specialized in the production of certain types of RNA species. RNA-Polymerase I is responsible for the synthesis of most rRNAs that are part of the ribosomes. RNA Polymerase II (RNAPII) is responsible for the synthesis of messenger RNAs (mRNAs) and most small nuclear RNA (snRNAs) and microRNAs (miRNAs). RNA Polymerase III synthesizes transfer RNAs (tRNAs), the 5S subunit of ribosomar RNAs (rRNAs) and furthermore some small RNAs (WHITE 2011). Most attention was drawn to the function of RNAPII as it mediates transcription of the protein coding genes. The RNAPII cannot bind to the DNA and start transcription on its own but requires certain factors, the general transcription factors (GTFs). Together these proteins form the pre-initiation complex (PIC) at the promoter (chapter 1.1.2.1.1), which is sufficient to account for a basal transcription level. Besides the GTFs a large, multisubunit complex termed Mediator assists in transcriptional stimulation. Altogether theses factors form the RNAPII transcriptional machinery (WOYCHIK and HAMPSEY 2002).

The assembly of the transcriptional machinery happens stepwise starting with the binding of the TATA-binding protein (TBP) as part of GTF TFIID near the site of transcription initiation on the template DNA. This complex serves as a platform for the assembly of the other GTFs TFIIA, TFIIB, TFIIE, TFIIF and TFIIH, which allow in concert the positioning of the RNAPII to the DNA strand. Local melting of the DNA at the transcription start site supports the open complex formation. Phosphorylation on serine 5 (Ser5P) of the RNAPII of the carboxy-terminal domain (CTD) domain of its largest subunit allows clearance and escape of the complex from the promoter region. The RNAPII is subsequently released from the promoter region, leaves the scaffold complex behind and forms a fully functional elongation complex, which goes along with another phosphorylation step (Ser2P). This complex moves down the DNA strand in the 3’ to 5’ direction inserting the ribonucleotides adenine, cytosine, guanine and uracil into a growing strand of RNA. At the termination site transcription stops, the RNAPII complex is disassembled and recycled to its unphosphorylated form by a phosphatase (HAHN 2004; MASTON *et al.* 2006; REINBERG *et al.* 1998).

1.1.2 Transcriptional regulation

Transcriptional regulation occurs primarily at the level of transcription initiation, but also the release from promoter-proximal pausing emerges as another level of regulation (ADELMAN and LIS 2012). The assembly of the RNAPII complex is regulated through the integrated activity of different regulatory elements and their cognate transcription factors. *Cis*-regulatory elements can be divided into two categories, proximal regulatory elements, like promoters, and distal regulatory elements, like enhancers, silencers, insulators and locus control regions that are reported to be located up to 1 Mb pairs away from the promoter (MASTON *et al.* 2006; RIETHOVEN 2010).

1.1.2.1 *Cis*-regulatory elements

1.1.2.1.1 Promoters

The promoter is a stretch of DNA located close to the transcription start site (TSS) of a gene and mediates the initiation of transcription. It is composed of a core promoter, which directs the transcriptional machinery to the TSS, and proximal promoter elements, which contain multiple binding sites for activator proteins (MASTON *et al.* 2006). The core promoter typically spans up to 1000 base pairs and can have a complex structure. Sequence elements found common to many core promoters include the TATA element (TBP-binding site), Inr (initiator element), BRE (TFIIB-recognition site), DPE (downstream promoter element), DCE (downstream core element) and MTE (motif ten element). These elements possess characteristic consensus sequences and are located at specific distances relative to the TSS. They mediate the binding of several GTFs and cofactors, thus enabling the assembly of the pre-initiation complex (SMALE and KADONAGA 2003).

The TATA box was first believed to be highly conserved and an essential part of every promoter, however sequencing and gene analysis efforts in recent years diminished the prevalence of the TATA element. Similarly it was found that all human core promoters are very diversely organized. Less than half of ~10,000 analyzed predicted promoters contain the most abundant Inr element, while other elements are represented at even lower frequencies (GERSHENZON and IOSHIKHES 2005). Also the combination of different elements within a single promoter varies and it was shown that initiation of the transcription at promoters is driven by synergy of its core elements. However, identification of promoter sequences cannot solely rely on the known core

elements. More motifs remain to be determined, which is in the focus of bioinformatics analyses.

One feature observed in 72% of human promoters is the abundance of CpG islands (SAXONOV *et al.* 2006). In regulatory sequences CpGs remain unmethylated whereas in most other regions the cytosine within CpGs is methylated thus increasing the probability of the cytosine becoming mutated to adenosine. Therefore the enrichment of CpGs can be used as a tool for mapping promoter sequences (IOSHIKHES and ZHANG 2000).

Another part of the promoter structure consists of proximal promoter elements. They were identified in 1982 by linker-scanning mutagenesis (MCKNIGHT and KINGSBURY 1982). This study localized transcriptional regulatory elements towards the region approximately 100 bp upstream of the TSS. Motifs present within this region are binding sites for transcriptional activators. The relative locations of these activator binding sites and the core promoter elements determine the directionality of transcription (MASTON *et al.* 2006; SMALE and KADONAGA 2003).

Transcription initiation at promoter usually occurs according to two patterns, termed focused and dispersed transcription initiation (JUVEN-GERSHON and KADONAGA 2010). The former is associated with a transcription start from a single TSS or a localized cluster of TSSs in less than 10 bp and is used predominantly in simple organisms. The latter displays multiple but weak start sites over a broad region of 50 to 100 nucleotides. In vertebrates, focused transcription is observed with the minority of promoters that typically belong to regulated promoters whereas dispersed transcription is typically associated with constitutive promoters in CpG islands. Differences in the presence of core promoter elements have been observed for these two types of transcription initiation. Notably, also intermediate promoters exist that share characteristics of both modes, multiple weak start sites with one dominant peak (JUVEN-GERSHON and KADONAGA 2010; SANDELIN *et al.* 2007).

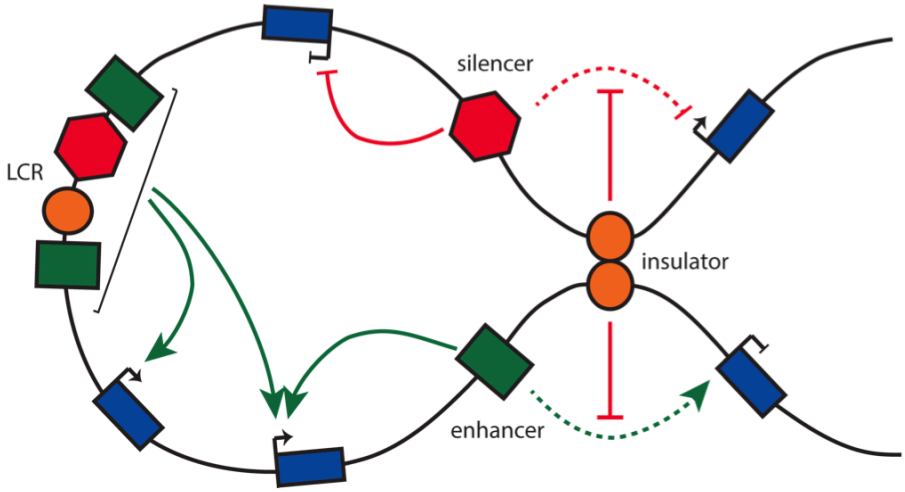

Figure 1.1: Distal regulatory elements
Transcription can be induced by enhancers and reduced by silencers. Insulators block enhancer or silencer activity when they are located in between the regulatory element and the target gene promoter by DNA loop formation. Locus control region (LCR) is composed of several elements that act in concert on multiple genes in a locus. Black arrows indicate the transcriptional activity of the promoters of target genes (blue).

1.1.2.1.2 Enhancers

Enhancers are distal elements that activate transcription of their respective target gene (Figure 1.1). They act on genes of the same DNA molecule, however most enhancers in the vertebrate genome are located more than 1000 bp away from their target gene (VISEL *et al.* 2009). The first enhancer was described in 1981 in SV40 DNA sequences, showing that transcription is activated independent of the enhancers location, distance or orientiation relative to its target gene (BANERJI *et al.* 1981). The so far greatest distance of an enhancer was observed for the limb enhancer of *Shh*, which is located 1 Mb upstream of its target gene (LETTICE *et al.* 2003). However, although enhancer and target gene might be far away from each other on the DNA strand, they are thought to come into close proximity by 3-dimensional folding of the chromatin (SCHOENFELDER *et al.* 2010) (discussion of interaction models in chapter 1.1.3.3).

Enhancers contain multiple binding sites for several different transcription factors. The motif composition but also the way these sequence motifs are arranged within the enhancer are essential for the transcriptional regulation (SPITZ and FURLONG 2012). In enhancer structures called enhanceosomes binding of the transcription factors in a characterized interferon-β enhancer. Expression is only driven when eight transcription factors are binding cooperatively to the enhancer (PANNE 2008). Therefore expression of the target gene interferon-β can be switched on rapidly, which might be critical in the response to a viral infection. However, many enhancers are organized in a less ordered manner, where binding of a subset of transcription factors is sufficient to activate

transcription and the positioning is less strict. The binding dynamics of additional transcription factors can modulate the target gene expression, thus having an additive effect (ARNOSTI and KULKARNI 2005; KULKARNI and ARNOSTI 2003). In contrast to the enhanceosome regulation this more flexible enhancer structure rather allows a fine-tuning of the target gene expression.

Due to the differential expression and activity of transcription factors in different cell types the regulation of transcriptional activity by enhancers is tissue- and/or developmental stage-specific (ONG and CORCES 2011).

The ways how enhancers activate transcription can occur at multiple levels. On the one hand recruited transcription factors regulate the transcriptional machinery, either by increasing its recuitment and therefore the initiation of transcription, but also the elongation and termination of transcription can be regulated. On the other hand enhancers function by mediating local remodelling of the chromatin, thus leading to an open formation with increased accessibility (ONG and CORCES 2011).

Recently a more direct interaction between enhancers and the transcriptional machinery was discovered. A genome-wide study in mouse cortical neurons revealed binding of the RNAPII to a subset of enhancers and moreover the bidirectional expression of short, non-coding RNAs, termed enhancer RNAs (eRNAs). eRNA expression was correlated to mRNA synthesis from nearby genes and at least for the example given in the study seemed to require interaction with the relevant promoter. It is proposed that they might be necessary for the maintenance of an open chromatin state, however function and mechanism of eRNAs remain to be elucidated (KIM *et al.* 2010).

1.1.2.1.3 Silencers

Silencers have a negative effect on the transcription of their target gene (Figure 1.1). Like enhancers they can be located at distant sites of the promoter, but they can also be located close by as well as in exons and introns of genes. Silencers contain binding sites for transcription factors that exhibit a repressive function, therefore these are called repressors. In some cases these factors recruit other corepressors to exert their repressive influence (OGBOURNE and ANTALIS 1998).

One example for silencer sequences is the polycomb response element (PRE). The first PRE was discovered in 1991 in *Drosophila* using a reporter construct with the mini-*white* gene that leads to a dark eye color (KASSIS *et al.* 1991). An insertion of a 2.4-kb fragment into the mini-*white* vector led to a white eye color of the flies,

suggesting that the reporter gene was completely silenced. The DNA fragment was then shown to contain two PREs, binding sites for polycomb repressive complexes (PRC) (AMERICO *et al.* 2002; DEVIDO *et al.* 2008; KASSIS 1994). Several motifs have been identified to account for PRC binding in *Drosophila*, however for a long time mammalian sequences were not identified until the recent discovery of two murine PREs (SING *et al.* 2009; WOO *et al.* 2010). Apart from that PRCs are recruited indirectly by several DNA-binding targeting factors (BEISEL and PARO 2011).

Polycomb repressive complexes are large complexes build of polycomb group (PcG) and other proteins. Originally PcG proteins were discovered as regulators of the homeotic (Hox) genes controlling the body segmentation in *Drosophila* (LEWIS 1978). Several genome-wide studies in flies, mice and humans revealed that PRCs have beside the Hox genes a multitude of predominantly development related targets (BOYER *et al.* 2006; LEE *et al.* 2006; NEGRE *et al.* 2006; SCHWARTZ *et al.* 2006; TOLHUIS *et al.* 2006). Depending on the composition of the subunits two major PRCs have been identified: PRC1 and PRC2. PRC2 contains a methyltransferase as catalytical subunit that mediates di- and trimethylation of lysine 27 of histone H3 (H3K27me2/H3K27me3) (CAO *et al.* 2002; CZERMIN *et al.* 2002; KUZMICHEV *et al.* 2002; MÜLLER *et al.* 2002), which act as repressive epigenetic marks (PENGELLY *et al.* 2013). In turn, H3K27me3 is recognized by a subunit of PRC1 complexes (FISCHLE *et al.* 2003; MIN *et al.* 2003). PRC1 contains two ubiquitin E3 ligases that monoubiquitinates histone H2A at lysine residue 119 (WANG *et al.* 2004). This histone mark is associated with transcriptional silencing mediated by chromatin compaction and RNAPII pausing (STOCK *et al.* 2007). In addition a direct interaction between the PcG protein EZH2 and DNA methyl transferases (DNMTs) has been shown, thus linking histone and DNA methylation at repressed promoters (VIRE *et al.* 2006).

In summary PcG proteins are important epigenetic regulators for the transcription of many developmental genes. PREs have been predominantly identified in flies but also mouse and are examplary for silencers.

1.1.2.1.4 Insulators

Insulators are also known as boundary elements and they restrict the activity of enhancers or silencer by blocking their interaction with the promoter. Two distinct (but not exclusive) functions can be attributed to an insulator. Either the insulator marks the border between regions of heterochromatin and euchromatin (barrier insulator), thus

preventing the spread of repressive chromatin or it prevents enhancer-promoter or silencer-promoter communication (known as blocking activity) (MASTON *et al.* 2006).

The barrier activity is thought to be mediated by recruitment of gene-activating factors or histone-modifying enzymes that render the chromatin permissive thus blocking the spread of heterochromatin (BUSHEY *et al.* 2008; MASTON *et al.* 2006).

For the enhancer blocking activity three potential mechanisms were postulated (BUSHEY *et al.* 2008). One model proposes that the insulator mimics the promoter structure, thus recruiting the transcriptional machinery. In this case the insulator would compete with the real promoter for interaction with the enhancer (GEYER 1997). In support with this model enhancer DNA and insulator DNA were shown to colocalize (YOON *et al.* 2007; ZHU *et al.* 2007). However, experiments where the position of the insulator was changed relative to the promoter-enhancer structure revealed that insulator function was dependent on the position in between enhancer and promoter, but not outside this structure (GOHL *et al.* 2011). This challenged the first model as one could have expected activity also when the insulator is positioned on the opposite site of the enhancer.

The second model suggests that the insulator directly acts as a physical barrier that stops the RNAPII from proceeding along the strand towards the promoter (ZHAO and DEAN 2004). However, some insulators were shown to be located in introns, still they were functional without truncating the gene product (GEYER and CORCES 1992). Furthermore, loss of insulator activity was shown for an insulator being inserted with two copies as opposed to a single copy in between an enhancer and promoter (CAI and SHEN 2001; MURAVYOVA *et al.* 2001). These two examples argue against a universal application of this mechanism for insulator function.

The third model proposes the formation of distinct compartments in the genome. It is assumed that elements can only interact when they are part of the same compartment (Figure 1.1). Such a partitioning is thought to occur by formation of DNA loops, that are formed by interaction between two insulators. One molecule involved in this loop formation is the CCCTC-binding factor (CTCF). Genome-wide studies revealed that a lot of CTCF-binding sites are located in between genes that display reduced correlation in gene expression compared to adjacent genes that are not separated by CTCF-binding sites (HUANG *et al.* 2007). Indeed CTCF-focused chromatin interaction analyses revealed that CTCF interactions lead to higher order chromatin organization. However, the results not only supported a role for CTCF in enhancer blocking function but also provided evidence that CTCF binding is necessary for a

number of enhancers to activate their target genes (HANDOKO *et al.* 2011). These results are in agreement with a more global chromatin organization that will be discussed in chapter 1.1.3.3.

In summary insulators are genetic boundary elements that block the interaction between enhancers and promoters. This is achieved by two main functions, however the detailed mechanisms still remain to be elucidated.

1.1.2.1.5 Locus Control Region (LCR)

A locus control region is defined as a *cis*-acting sequence element consisting of multiple regulatory elements that confer tissue-specific, copy-number dependent but position independent expression of a gene cluster (GROSVELD *et al.* 1987). Several LCRs have been identified in vertebrates, the most well studied is the LCR regulating the mouse *β-globin* locus (LI *et al.* 2002).

Transgenic mice carrying a 5 kb fragment of the *β-globin* locus still express the *β-globin* gene, however only at a very small fraction of the normal rate. Thus the more distant genomic region surrounding the *β-globin* gene was investigated for regulatory activity. 5 Sites showing hypersensitivity for DNase I treatment (5'HS1-5; chapter 1.1.3) are located 6 - 22 kb 5' to the first *globin* gene in the locus. Only if these sites were included, the LCR was fully functional and transgenic mice expressed the *β-globin* gene at normal levels (GROSVELD *et al.* 1987).

Experiments where the *β-globin* LCR was coupled to a *LacZ* gene driven by a Hsp68 promoter revealed LacZ expression not only in erythrocytes but also in the yolk sac, the tissue in which the Hsp68 promoter is normally active (TEWARI *et al.* 1996). This result suggests that the promoter structure contributes to the tissue-specificity and is not solely defined by the LCR.

Molecular dissection of the single HSs revealed enhancer (5'HS2-4) and insulator (5'HS5) functions within the distal part of the LCR. Enhancer activity was detectable in transient transfection assays for 5'HS2, whereas 5'HS3 and 5'HS4 only exhibited enhancer activity when they were integrated into chromatin (HARDISON *et al.* 1997). Thus regulation by these two enhancers seems to be dependent on chromatin alterations. Further hints come from the observation that β-thalassemia patients with a deletion upstream of 5'HS1 but intact globin locus show no expression of the globin genes due to alterations in the chromatin conformation (FORRESTER *et al.* 1990). Indeed interaction studies reveal that active transcription coincides with loop formation that brings the LCR in close proximity to the globin genes (TOLHUIS *et al.* 2002).

In summary a LCR is a multi-component regulatory element where the single elements within the LCR act cooperatively and synergistically.

1.1.2.2 Epigenetic regulation of the chromatin structure

As it has become apparent already in the description of the regulatory elements the chromatin structure plays an essential role in the regulation of gene expression. In eukaryotic cells the DNA is tightly packed into chromatin within the nucleus. The basic unit of the chromatin is the nucleosome, which consists of ~146 bp of DNA that is wrapped around a histone octamer (LUGER *et al.* 1997). The complete folding of the DNA leads to an organized structure with specific regions that are relatively uncondensed (euchromatin) and other regions that are densely packed (heterochromatin) (CAMPOS and REINBERG 2009). Transcriptional activity of genes is dependent on their chromatin structure as only euchromatin allows accessibility for most DNA-binding factors. The assembly and compaction of the chromatin is regulated by several epigenetic mechanisms, including posttranslational modifications of histone proteins, DNA methylation and ATP-dependent remodeling (KOUZARIDES 2007).

1.1.2.2.1 Histone modifications

Typically the histone octamer consists of two copies of each of the core histone proteins: H2A, H2B, H3 and H4. Histones are highly basic proteins, thus they are able to efficiently bind the negatively charged DNA. The N-terminal tails of the histones are protruding outward from the nucleosome and are therefore accessible for histone modifying enzymes as well as for proteins that recognize these modifications. For this reason most modifications occur at this tail, however also the short but accessible C-terminus can be modified. Histone modifications exert their function in two ways, either directly by changing the overall structure of the chromatin or by regulating the binding of effector molecules. Posttranslational modifications include acetylation, methylation, phosphorylation, ubiquitylation, and ADP-ribosylation of the histone proteins (BANNISTER and KOUZARIDES 2011).

1.1.2.2.1.1 Histone acetylation

All four core histones can be acetylated at several specific lysine residues (K), which is catalyzed by histone acetyltransferases (HATs). This modification is reversible as acetyl residues can be removed by histone deacetylases (HDACs). Histone acetylation is generally associated with transcriptionally active chromatin. The acetylation causes a decrease in the net positive charge of the N-terminal tail resulting

in a lower affinity for the negatively charged DNA. Therefore the chromatin has a more open structure and provides increased accessibility of regulatory factors to the DNA (GRUNSTEIN 1997). Additionally to the effect on histone charge histone acetylation can serve as a binding motif for regulators. Some transcription coactivators and chromatin remodeling complexes contain a domain termed bromodomain that is specific to the recognition of histone acetylation (WINSTON and ALLIS 1999).

1.1.2.2.1.2 Histone methylation

The two core histones H3 and H4 can be methylated at several lysine (K) and arginine (R) residues by methyltransferases. Compared to histone acetylation the functions of histone methylation are more diverse. In part this can be attributed to the more complex modification pattern as lysine residues can be mono-, di- or trimethylated, arginine residues can be mono- or dimethylated. In general methylation is associated with both transcriptional activation as well as repression. This is mostly regulated by promoting binding of activators and blocking of repressors (examples shown in (FLANAGAN *et al.* 2005; LI *et al.* 2006; NISHIOKA *et al.* 2002; SCHNEIDER *et al.* 2004)). In higher eukaryotes methylation of the fourth lysine residue at histone H3 (H3K4me) is generally associated with active promoter structures, whereas trimethylation of the 9^{th} and 27^{th} lysine residue of the same histone (H3K9me3 and H3K27me3) has been reported to mediate repressive function (compare polycomb repressive complexes, chapter 1.1.2.1.3) (KOUZARIDES 2007). However, in embryonic stem cells the existence of so-called bivalent domains has been reported. These cells exhibit both active H3K4me and repressive H3K27me marks at promoters of genes encoding developmentally important transcription factors (BERNSTEIN *et al.* 2006). It is assumed that this feature keeps the genes in a repressed but primed state to allow activation when the right signals are received. Another example for histone methylation is the methylation of the ninth lysine residue of histone 3 (H3K9), which marks transcriptionally silent heterochromatin (BARSKI *et al.* 2007; LEHNERTZ *et al.* 2003).

1.1.2.2.2 Chromatin remodeling

Chromatin remodeling is an important process of gene regulation as it enables access of transcription factors to specific genes and facilitates transcription elongation. Also other processes are dependent on chromatin remodeling, such as DNA repair, replication or chromatin assembly. It is catalyzed by chromatin remodeling complexes (CRCs) that use the energy from ATP hydrolysis to exchange or eject histones and to reorganize nucleosomes. They lack intrinsic DNA sequences that trigger them to their

target sites, hence they are typically recruited by sequence-specific transcription factors (NEELY *et al.* 1999; YUDKOVSKY *et al.* 1999). In eukaryotes five main families of CRCs are known: SWI/SNF, ISWI, CHD and INO80 and SWR1 (SAHA *et al.* 2006). Dependent on protein domains and subunits within the complex the functions of the different family members are different. The well characterized SWI/SNF complex for example contains a bromodomain in the ATPase subunit thus it recognizes acetylated histones (HASSAN *et al.* 2002) (see also chapter 1.1.2.2.1.1). The organization of multiple bromodomains within a complex can specify the selectivity of the complex towards particular nucleosomes (KASTEN *et al.* 2004).

1.1.2.2.3 DNA methylation

Gene expression can be also controlled by another epigenetic mechanism, the methylation of DNA. DNA methyltransferases (DNMTs) are responsible for the addition of methyl residues to the cytosine nucleotides, converting them to 5-methylcytosine (GOLL and BESTOR 2005). Usually only cytosine residues located next to guanine nucleotides can be methylated (CpG). Across the human genome 60-80% of all CpGs are methylated. Methylated cytosine residues within CpGs spontaneously deaminate without being repaired, therefore due to the evolutionary mutagenesis CpGs are underrepresented in the human genome (JABBARI and BERNARDI 2004). However, the human genome possesses several areas with high C+G content that show low DNA methylation. These areas are termed CpG islands and are often associated with promoters (DEATON and BIRD 2011) (see chapter 1.1.2.1.1).

Methylation of CpG islands located at TSSs is associated with long-term gene silencing and occurs e.g. in X-chromosome inactivation, genomic imprinting or for genes expressed predominantly in germ cells. In general CpG island methylation blocks the start of transcription (JONES 2012). The mechanism of silencing is not clear yet, it is thought to occur either by direct inhibition of transcription factor binding or by indirect recruitment of chromatin-modifying enzymes mediated by methyl-binding domain (MBD) proteins (DEATON and BIRD 2011). Also, there is a strong correlation between CpG islands and PRC2 binding, however sequence-specific DNA binding proteins that guide the PRC2 complex to CpG islands have not yet been identified in mammals (ZHOU *et al.* 2011).

A study in plants connects chromatin remodeling with DNA methylation by showing that incorporation of the histone variant H2A.Z by a SWR1 complex protects

gene promoters from DNA methylation. Deficiency of H2A.Z leads to general hypermethylation and therefore to gene silencing (ZILBERMAN *et al.* 2008).

1.1.3 Identification of enhancers

Many protein-coding genes have been identified due to an apparent phenotype as e.g. a disease that becomes evident upon mutation. Similarly some enhancers have been found as their mutation lead to diseases like thalassaemias (*HBB* enhancer), preaxial polydactyly (*SHH* enhancer) or Hirschsprung's disease (*RET* enhancer) (VISEL *et al.* 2009). Apart from such apparent phenotypes the identification of enhancers is a major challenge. However, they display certain features that can be used for their prediction and identification.

1.1.3.1 Evolutionary conservation

As mentioned in the beginning only 1.5% of the base pairs in the human genome encode for protein coding genes (CLAMP *et al.* 2007; LANDER *et al.* 2001; VENTER *et al.* 2001). The availability of further genome sequences from other organisms revealed a high conservation rate for these genes. However, comparison of the whole sequence of mouse and human demonstrated that ~5% of the human genome is under evolutionary constraint (WATERSTON *et al.* 2002) thus implying that these regions serves a sequence dependent function. Hence, 3.5% of the genome seems to contain functional elements without encoding a protein. A large cohort of putative enhancer elements defined by comparative analysis from human to fish and human to rodents have been tested for enhancer activity *in vivo* using a LacZ reporter assay in transgenic mouse embryos. 45% of the tested elements displayed tissue-specific enhancer activity at embryonic day (E) 11.5. This read-out most probably even underestimates the actual proportion of enhancers by restricting the analysis to a single time point (PENNACCHIO *et al.* 2006). Therefore comparative genomics can provide a potent approach for the prediction of regulatory elements. However, some functional enhancers have been identified that lack sequence conservation thus this feature is not always a property of enhancers (FISHER *et al.* 2006; HARE *et al.* 2008; MCGAUGHEY *et al.* 2008).

1.1.3.2 Transcription factor binding and chromatin state

Enhancers act as binding sites for several transcription factors which often exert chromatin-modifying activity thereby changing the local chromatin state. The development of techniques like ChIP-chip and ChIP-seq offers a genome-wide view on

transcription factor binding sites and the chromatin state and assists in functional annotation of the genome. Different combinations of histone variants, histone modifications, DNase I hypersensitivity and binding of cofactors mark e.g. gene bodies, promoters or regulatory elements (ZHOU *et al.* 2011) (Figure 1.2). Approaches to confine enhancer related features will be discussed in the following paragraph.

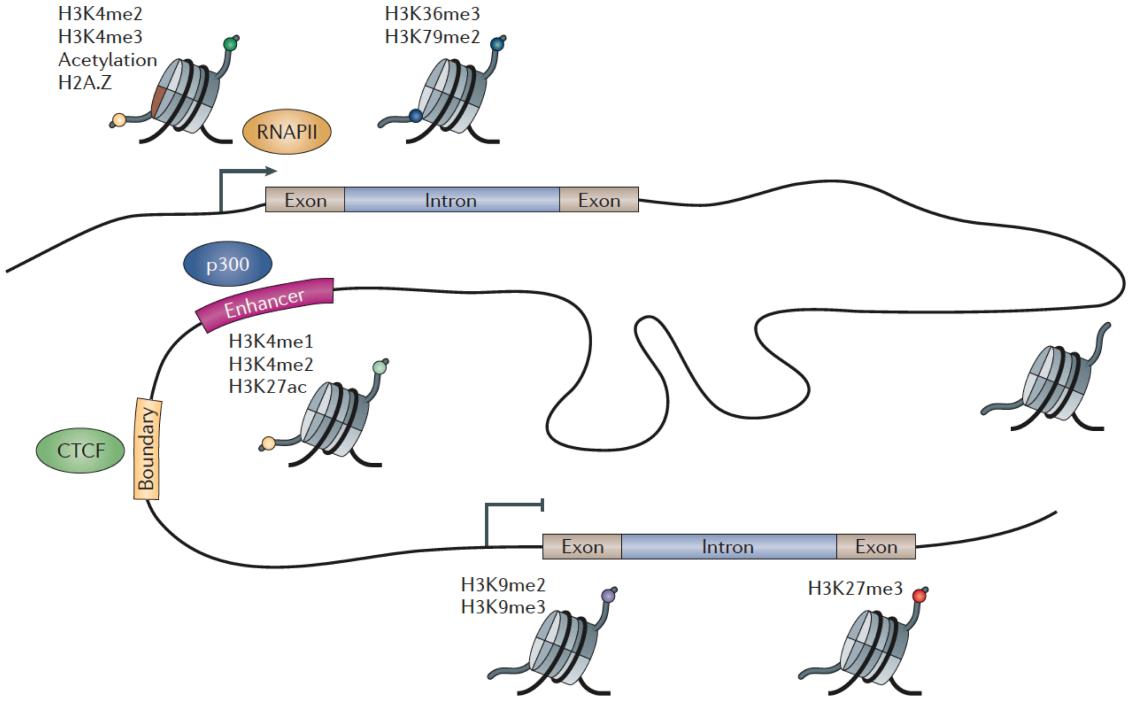

Figure 1.2: Histone modifications used for functional annotation of the mammalian genome
Reported histone modifications particularly enriched in each functional element are indicated adjacent to the respective structure (ZHOU *et al.* 2011).

The accessibility of the chromatin can be identified by assessment of the sensitivity for DNase I treatment (BIRNEY *et al.* 2007; BOYLE *et al.* 2008; CRAWFORD *et al.* 2006a; CRAWFORD *et al.* 2006b; SABO *et al.* 2004a; SABO *et al.* 2004b; THURMAN *et al.* 2012; XI *et al.* 2007). However, DNase I hypersensitivity sites (DHS) mark not only enhancers but also other regulatory regions such as promoters, silencers, insulators and locus control regions.

In another approach the acetyltransferase and transcriptional coactivator p300 was used. Studies fo the IFNβ enhanceosome showed that p300 is associated with active transcription (MERIKA *et al.* 1998). Genome-wide ChIP-seq for p300 in different embryonic mouse tissues revealed between 500 to 2500 potential enhancer regions. Functional validation of 86 predicted elements using the same approach as mentioned above augmented the prediction rate from 45% by comparative genomics to 87% (VISEL *et al.* 2009). The strength of this method over comparative genomics was further

shown by identification and validation of weakly conserved enhancers from developmental heart tissue (BLOW *et al.* 2010).

Analysis of distal p300-binding sites for certain histone methylations revealed an enrichment for H3K4 monomethylation (H3K4me1) with a concurrent absence of H3K4 trimethylation (H3K4me3). This distinguishes enhancers from active promoters marked by H3K4me3 (HEINTZMAN *et al.* 2007). Furthermore, the acetylation of the 27th lysine residue at histone H3 (H3K27ac) could also be linked to enhancers (HEINTZMAN *et al.* 2009) which was validated by two other studies. Moreover, these studies indicate that enrichment for H3K27ac distinguishes active from poised enhancers compared to H3K4me1 alone (CREYGHTON *et al.* 2010; RADA-IGLESIAS *et al.* 2011).

In summary an integrative analysis based on data about sequence conservation, transcription factor and cofactor binding sites, nucleosome positioning and histone modifications provides a powerful tool for the prediction of enhancers. However, enhancer prediction does not provide information about the spatiotemporal activity of the enhancer and which genes are targeted. Thus enhancer activity needs to be validated in functional assays (VISEL *et al.* 2009).

1.1.3.3 Long-range interaction between enhancer and promoter

The sonic hedgehog (*Shh*) enhancer displays with 1 Mb the so far greatest distance between an enhancer and its target promoter (LETTICE *et al.* 2003). It serves also as an example for an enhancer that is separated by another gene (*Rnf32*) from its target gene and that is located in an intron of another gene. Hence, enhancers are often located at a distant site and thus need to apply certain mechanism(s) to communicate specifically with their target promoter.

Several models have been proposed for enhancer function. One is called the "tracking" model where an enhancer-bound complex scans along the DNA sequence until it reaches the promoter and then would activate transcription. Another more indirect model based on nuclear positioning proposes that an active enhancer brings the promoter into regions of the nucleus that are transcriptionally active (PTASHNE 1986). However, the most widely favored model is based on the interaction between the enhancer and the promoter that is achieved by looping out of the intervening DNA. Advances over the last years in elucidating the interaction between promoters and enhancers have been summarized in recent reviews (BULGER and GROUDINE 2011; PLANK and DEAN 2014).

The global structure of the genome has been assessed by chromosome conformation capture assays (3C) and its derivative technologies (4C, 5C, Hi-C). These methods are based on crosslinked cells or nuclei that are subjected to digestion with restriction enzymes. Subsequently religation is promoted, however under dilute conditions so that religations only occur among crosslinked fragments. The religation frequency is then quantified and provides a linear mapping of DNA interactions, either locally of globally (DE WIT and DE LAAT 2012).

The first global study on the human genome using Hi-C showed the clustering of active regions as well as of inactive regions, respectively (LIEBERMAN-AIDEN *et al.* 2009). However, this study had only a limited sequency depth of 1 Mb which was outreached by the study performed in Bing Ren's lab (DIXON *et al.* 2012). With a resolution of 40-60 kb they discovered that the mammalian genome is organized in so called topologically associating domains (TADs) that are 500 kb to 3 Mb in size. The TAD structure is highly conserved in different cell types as well as from human to mouse. The borders of the domains are called boundaries and have been shown to be enriched for CTCF sites. TADs encompass genomic regions that display a high frequency of interactions within the TAD but much less frequently to sequences of another TAD. Functional relevance for the TAD structure was given by a study that showed that disruption of a TAD boundary in the X chromosome resulted in new chromosomal contacts and long-range transcriptional misregulation (NORA *et al.* 2012). Furthermore, analysis of regulatory landscapes defined large regulatory domains that strongly correlate with the TAD domains (SYMMONS and SPITZ 2013). However, interactions within a TAD have been reported to vary in a tissue-specific manner (PHILLIPS-CREMINS *et al.* 2013).

Insights into more specific interactions between enhancer and promoter structures come from ChIA-PET (chromatin interaction analysis by paired-end tag sequencing) experiments that combine the technology of ChIP with 3C-type analysis. RNAPII centered analysis of human and murine cell lines of progressive lineage commitment revealed extensive colocalization among promoters and distal-acting enhancers (LI *et al.* 2012; ZHANG *et al.* 2013).

In summary theses interaction studies support a model of DNA looping to get enhancers and promoters in close proximity. However, the molecular mechanisms driving these interactions are yet unknown.

1.2 The hematopoietic system

1.2.1 Hematopoietic stem cells

The blood system is one of the most highly regenerative adult tissues with billions of cells being produced every day that perform different specialized tasks. Red blood cells (erythrocytes) are the most abundant cells and transport oxygene to the peripheral tissues. White blood cells (leukocytes) are cells of the immune system that battle against infections and phagocyte foreign invaders. Furthermore, the blood contains a large number of platelets (thrombocytes) that prevent bleeding by forming blood clots (ALBERTS *et al.* 2008). Due to the high turn-over of these blood cells they have to be replaced efficiently by precursor cells. The question of the existence of a common precursor cell for the various cell types in the blood system emerged already end of the 19th century. However, due to the lack of experimental methods it took several decades until definitive evidence of hematopoietic stem cells (HSCs) was proved (RAMALHO-SANTOS and WILLENBRING 2007). In 1956 two groups showed that the blood system of irradiated recipient mice was repopulated by donor cells after transplantation of spleen or bone marrow cells from mice or rats (FORD *et al.* 1956; NOWELL *et al.* 1956). Work of James Till, Ernest McCulloch and co-workers in the 1960s proved that a subset of bone marrow cells was able to form colonies of myeloid and erythroid cells in the spleens of irradiated mice (BECKER *et al.* 1963; TILL and MCCULLOCH 1961). By demonstrating that spleen colonies were formed even after secondary transplantation the defining properties of HSCs were established – multipotency and self-renewal (SIMINOVITCH *et al.* 1963). Tracking of single cells by inducing chromosomal aberrations revealed that these splenic colonies developed from a single precursor cell, thus proving differentiation of a single precursor cell into different lineages (WU *et al.* 1967). These findings were until then however limited to the myeloid/erythroid lineage. Although it was later shown that these spleen colonies preferentially reflect progenitor potential the initial definition of HSCs remained valid. The definitive proof that single bone marrow cells were able to generate cells of the myeloid and the lymphoid lineage came another decade later in long-term transplantation experiments (ABRAMSON *et al.* 1977). Since then major effort was put on prospective isolation and detailed characterization of this rare population, however transplantation assays still serve as gold standard in functional evaluation of HSCs.

1.2.1.1 Functional assays for hematopoietic stem cells

Several *in vitro* and *in vivo* methods have been developed to adress the functional evaluation of HSCs and to distinguish them from other hematopoietic cell types such as progenitors or terminally differentiated cells. *In vitro* assays such as colony-forming unit (CFU) assays provide information about the function of progenitors rather than HSCs, but have the advantage of giving a read-out within a short time. To assess self-renewal potential, quantity and quality of HSCs time-consuming long-term assays have to be performed.

Among the *in vitro* assays the CFU assay is the most commonly used (CASHMAN *et al.* 1983). A given population is cultured for 7 to 14 days in a semi-solid methyl-cellulose cultur medium supplemented with defined growth factors. The progeny of single progenitors forms distinct colonies that remain well separated, thus their number can be quantified microscopically. In addition this assay gives information about the differentiation potential towards certain lineages. More immature progenitors form mixed colonies containing different cell types whereas colonies of a single cell type derive from more restricted progenitors. This CFU assay allows a read-out mostly for myeloid restricted progenitors. The *in vitro* assessment of lymphocyte lineages in CFU assays requires more specialized culture conditions (PURTON and SCADDEN 2007; SCHMITT and ZUNIGA-PFLUCKER 2002; WHITLOCK and WITTE 1982).

The cobblestone area-forming cell (CAFC) assay is used to estimate the frequency of HSCs or progenitors in a given cell population. It is based on long-term culture together with a stromal cell layer, assuming that only HSCs can retain their clonogenic potential for a prolonged time. A CAFC integrates into the layer and forms a cobblestone area that can be quantified (PLOEMACHER *et al.* 1989). Although this assay most probably does not quantify solely HSCs it reflects at least a more immature population as compared to the CFU assay (VAN OS *et al.* 2004). A similar approach is taken by the long-term culture-initiating cell (LTC-IC) assay where cells are also grown on stromal layers for more than 4 weeks and subsequently analyzed for their colony-forming ability (SUTHERLAND *et al.* 1989). It remains controversial if these assays truly pinpoint HSC frequencies, however results obtained from assays with refined conditions were reported to give a good correlation compared to *in vivo* transplantation assays (WOEHRER *et al.* 2013).

The earliest *in vivo* stem cell assay was the spleen colony forming unit (CFU-S) assay as described above for the experiments of TILL and MCCULLOCH (1961). For this

assay cells are injected intravenously into irradiated recipient mice and form macroscopic colonies in the spleen within 10 to 14 days. Although splenic progenitors are able to repopulate the recipient mice for the first 2 to 3 weeks, they lack long-term reconstitution ability (PURTON and SCADDEN 2007). Therefore this assay, similar to the *in vitro* assays described above, gives conclusions about progenitor potential rather than stem cell potential of the tested cells.

The only experimental approach to evaluate frequency and potential of bona fide HSCs is given by long-term repopulating assays since only HSCs are able to serially reconstitute the entire blood system over the life-time of an organism. In these *in vivo* assays, bone marrow cells are transplanted into recipient mice. Donor and recipient cells can be distinguished using either cytogenetic, immunological or biochemical markers. A widespread method is the use of congenic mice that differ in the Ly-5 antigen (CD45), which is expressed on all bone marrow derived cells except erythrocytes and platelets (KOMURO *et al.* 1975; MILLER *et al.* 1985; RALPH and BERRIDGE 1984; SCHEID and TRIGLIA 1979; SPANGRUDE *et al.* 1988; SYKES *et al.* 1989). Donor cell engraftment can thus be followed by peripheral blood analysis over time as well as bone marrow analysis after several months. Multipotent progenitors can reconstitute the blood system of lethally irradiated recipients up to several months, however they are not able to do so in a secondary or tertiary transplant. Thus serial rounds of transplantation allow the discrimination between multipotent progenitor cells and HSCs by defining their long-term repopulation capacity (LEMISCHKA *et al.* 1986).

In competitive transplantation assays cells of interest are transplanted together with a competitor cell population containing a known number of HSCs in a defined ratio into recipients. This assay allows determining the frequency of repopulating units (RU), being a measure for the functional potential of HSCs within the tested cell population compared to a control population (HARRISON *et al.* 1993; YUAN *et al.* 2005). Although this assay allows evaluation about the reconstitution potential of the different lineages, it does not provide information on the HSC frequency in the tested population. The most common assay to determine HSC frequencies is the limiting dilution assay. Decreasing cell numbers of donor populations are transplanted together with a standard dose of competitor bone marrow (SZILVASSY *et al.* 1990; TASWELL 1981). Determining the number of non-engrafted mice in each dilution allows calculation of the competitive repopulating units (CRUs) and therefore the frequency of HSCs based on Poisson statistics. So far HSCs cannot be isolated to 100% purity (chapter 1.2.1.2), thus enriched populations are still heterogeneous and have different potentials to contribute to blood

lineages. Single cell transplantation assays allow functional and quantitative read-out of single cells instead of cell populations, however such experiments are technically challenging, time-consuming and expensive (DYKSTRA *et al.* 2007; EMA *et al.* 2006; YAMAMOTO *et al.* 2013).

In research transplantation assays are usually performed with recipient mice that are preconditioned for example by lethal irradiation in order to empty the HSC niche and thus allow for donor cell engraftment. However, it has to be kept in mind that irradiation significantly damages cells and tissues within the bone marrow and induces a state of severe inflammation, which both may influence HSC homing, engraftment and function. To avoid this effect mutant mouse models can be used, which allow long-term engraftment without conditioning of the recipient mice, as for example mice with mutations of the receptor tyrosine kinase c-Kit, such as c-kit$^{W/Wv}$ mice (MILLER and EAVES 1997; NOCKA *et al.* 1990; WASKOW *et al.* 2009). Using such mouse strains in transplantation assays allows the analysis of HSCs under more physiological conditions.

1.2.1.2 Identification of hematopoietic stem cells by cell surface markers

Since HSCs were discovered scientists continously worked on defining markers that help to recognize and isolate HSCs prospectively. Initially HSCs were reported to be enriched in cells that are negative for lineage markers such as the B cell marker B220, the granulocyte markers CD11b and Gr-1 as well as the T cell markers CD4 and CD8 (MÜLLER-SIEBURG *et al.* 1988; MÜLLER-SIEBURG *et al.* 1986). Additionally these studies showed that HSCs express the cell surface protein Thy-1 at low levels, a marker that was also included when Sca-1 was identified to positively mark HSCs (SPANGRUDE *et al.* 1988). This combined marker set enriched the stem cell purity from 1 HSC in 10^5 in total bone marrow cells to 1 HSC in 30 Lin$^-$Thy1^{low}Sca-1$^+$ cells. The immuno-phenotype of HSCs was further refined by adding the stem cell factor receptor c-Kit (IKUTA and WEISSMAN 1992; OGAWA *et al.* 1991). Since then, the marker combination Lin$^-$Sca-1$^+$c-kit$^+$ (LSK) has been generally used for HSC enrichment. Although all HSC activity resides in this population, it is still a heterogeneous mixture of HSCs and other non-self-renewing progenitor cells. Thus in the following years other markers were identified to further enrich for HSCs within the LSK population. LSK cells negative for CD34 or Flk2/Flt3 (CD135) purify HSCs up to 1 in 5 cells (ADOLFSSON *et al.* 2001; CHRISTENSEN and WEISSMAN 2001; OSAWA *et al.* 1996). Moreover the CD34 marker distinguishes between long-term (CD34$^-$) and short-term (CD34$^+$) reconstituting

capacity. An alternative gating strategy was proposed by the Morrison group, which investigated the expression of members of the signaling lymphocytic activation molecule (SLAM) protein family on HSCs (KIEL *et al.* 2005). Based on this study HSCs are positive for CD150 and negative for CD48. Combined with the LSK marker set the SLAM markers identify HSCs to almost 50% purity. Other positive markers for HSCs are endoglin, EPCR and ESAM, but these seem not to add further enrichment (BALAZS *et al.* 2006; CHEN *et al.* 2002; OOI *et al.* 2009; YOKOTA *et al.* 2009).

Another method to isolate HSCs is based on their high efflux activity (BAINES and VISSER 1983; BERTONCELLO *et al.* 1985; GOODELL *et al.* 1996; WOLF *et al.* 1993). Staining with intravital dyes such as the mitochondrial-binding dye Rhodamine 123 or the DNA-binding dye Hoechst 33342 allows identification of HSCs as low retaining cells. Visualization of Hoechst 33342 efflux by emitting at two wavelengths serves to identify the so called side population enriched for HSCs. Stringent gating for Hoechst staining in combination with LSK and CD34 marker was shown to enrich for HSCs to 96% purity (MATSUZAKI *et al.* 2004). However, this technique is prone to technical variability and has to be performed conscientiously (PURTON and SCADDEN 2007).

The study of WILSON *et al.* was the first to combine LSK with the Slam markers, CD34 and CD135 in a single assay providing a close enrichment for HSCs as opposed to multipotent progenitor populations present within the LSK population (WILSON *et al.* 2008).

1.2.1.3 Development of hematopoietic stem cells

Hematopoiesis during mammalian development occurs in multiple waves. The first murine hematopoietic progenitors emerge in the yolk sac at E7.5. In order to meet the immediate demand of oxygene supply in the developing embryo, they produce mainly primitive erythroid cells, which appear only transiently between 7 and 12 days postcoitus (dpc). The observation that blood cells and blood vessels are in close proximity led to the hypothesis of a common ancestor, the hemangioblast (MURRAY 1932; SABIN 1920). Studies using an embryonic stem (ES) cell differentiation assay identified the blast colony-forming cell (BL-CFC) *in vitro* (CHOI *et al.* 1998). Cells with highly similar characteristics of these BL-CFCs were found in the gastrulating mouse embryo further supporting the existence of the hemangioblast (HUBER *et al.* 2004). Despite this early occurrence of hematopoietic progenitors, explanted cells from early yolk sac are neither able to generate lymphoid progeny nor reconstitute adult mice

hematopoiesis, suggesting that this site is not the source of definitive HSCs (CUMANO *et al.* 1996; CUMANO *et al.* 2001).

The second wave of hematopoiesis is initiated at E8.25 in the yolk sac, allantois and paraaortic splanchnopleura, where hematopoietic progenitors display multipotent capacity but still lack self-renewal capacity. Transient erythromyeloid progenitors colonize the liver by E9.5 to E10.5, where they further mature to release definitive erythrocytes to the circulation at E11.5 (MCGRATH *et al.* 2011). These definitive erythroid cells differ from primitive erythroid cells e.g. by their size, the time point of enucleation, the tissues they are found in and the form of *globin* genes being expressed (BARON 2013). The first definitive HSCs occur from E10.5 to E11.5 in an intraembryonic region surrounding the dorsal aorta called the aorta-gonad-mesonephros (AGM) region and in the vitelline and umbilical arteries (DE BRUIJN *et al.* 2000; MEDVINSKY and DZIERZAK 1996; MÜLLER *et al.* 1994). These possess fully functional, long-term multilineage engraftment and repopulation capacity. Also the placenta appears to contain HSCs and some studies suggest that it is a true site of HSC generation (GEKAS *et al.* 2005; LEE *et al.* 2010; RHODES *et al.* 2008). From E11.5 onwards HSCs are spread through circulation into the fetal liver, thymus and spleen (JOHNSON and MOORE 1975) (Figure 1.3). The fetal liver serves as a site for massive HSC expansion and differentiation (EMA and NAKAUCHI 2000; MORRISON *et al.* 1995). The skeletal system starts to develop from E12.5, creating a niche for adult HSCs. Vascularization of the bones allows the migration of hematopoietic cells towards the bone marrow from E15.5 onwards. However, despite the presence of circulating functional HSCs already at that time these cells only start populating the bone marrow from E17.5 onwards (CHRISTENSEN *et al.* 2004). This delay implies that up to this time point the fetal bone marrow lacks attraction signals such as the cytokine SDF1 and other factors supporting HSC engraftment (ARA *et al.* 2003; MIKKOLA and ORKIN 2006). Perinatal HSCs are still highly proliferative and expand in the bone marrow. By 3 to 4 weeks after birth they switch to a more quiescent phenotype characteristic of adult bone marrow HSCs (BOWIE *et al.* 2007; BOWIE *et al.* 2006).

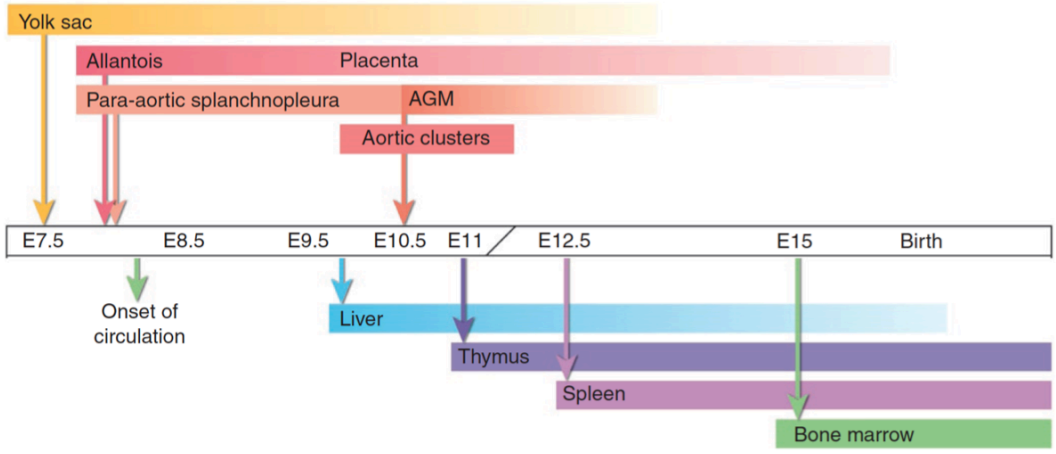

Figure 1.3: Timeline of hematopoietic events in the developing mouse
Arrows above the timeline indicate the onset of specific hematopoietic cell generation. Arrows below indicate the earliest time of colonization of the secondary hematopoietic territories (DZIERZAK and SPECK 2008).

1.2.2 The hematopoietic hierarchy

HSCs are characterized by their multipotency, self-renewal capability as well as proliferative potential. These characteristics are experimentally proven by transplantation experiments in which a single HSC serially reconstitutes all myeloid and lymphoid lineages over a prolonged time (chapter 1.2.1.1). Since HSCs represent only a small fraction of all bone marrow cells, mature effector cells however have to be replenished to billions of cells every day, lineage commitment occurs through extensive amplification steps on several progenitor levels. This hematopoietic hierarchy is classically viewed as a linear branching model with the HSC (LSK $CD150^{+}CD48^{-}$ $CD135^{-}CD34^{-}$) residing at its top (Figure 1.4) (BRYDER *et al.* 2006). HSCs are largely quiescent with about 80-90% of the cells in the G0 phase of the cell cycle. Label-retaining assays have revealed that the HSC population consists of two distinct populations: highly dormant HSCs that divide only about 5 times per lifetime of the animal, and activated HSCs that divide approximately once per month. The population of dormant HSCs harbors the vast majority of long-term self-renewal activity (WILSON *et al.* 2008).

In the classical bifurcation model (Figure 1.4), HSCs give rise to the multipotent progenitor population 1 (MPP1) by gain of CD34 expression. These cells are also often referred to as ST-HSCs because they have lost self-renewal capacity, but have not yet undergone any fate decision (CABEZAS-WALLSCHEID AND TRUMPP, unpublished data). Subsequent multipotent progenitor populations 2 to 4 (MPP2, 3 and 4) have been described based on expression of cell surface markers and their cycling behavior.

These have just recently been defined more closely in a global transcriptomics, proteomics and epigenomics study performed by our group (CABEZAS-WALLSCHEID *et al.* 2014). This study revealed by reconsitution assays that MPP2 cells are multipotent whereas MPP3 and MPP4 populations show a differentiation bias towards myeloid or lymphoid cell types, respectively. In the next step of lineage commitment multipotent progenitors give rise to two oligopotent progenitors, the common myeloid and common lymphoid progenitors (CMP and CLP) (AKASHI *et al.* 2000; KONDO *et al.* 1997). CMPs then give rise to granulocyte-macrophage progenitors (GMPs) and megakaryocyte-erythrocyte progenitors (MEPs). These in turn are restricted to generating granulocytes and macrophages or erythrocytes and platelets, respectively. CLPs exclusively give rise to B cells, T cells and natural killer (NK) cells. Both CMPs and CLPs are proposed to give rise to dendritic cells (MANZ *et al.* 2001).

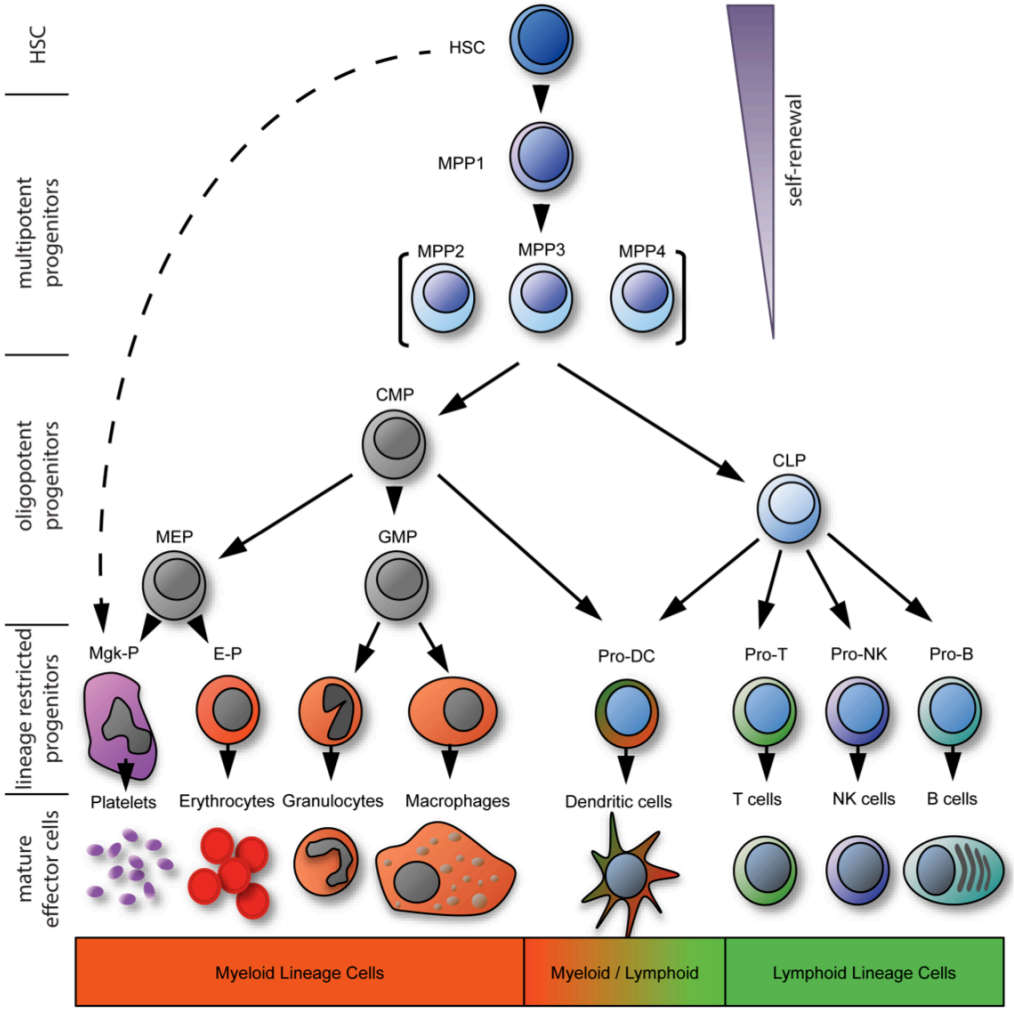

Figure 1.4: Hierarchical organization of the hematopoietic system
Classical view of the hematopoietic hierarchy with the HSC at the top of the hierarchy, containing the highest self-renewal capacitiy and long-term multilineage reconstitution capacity (BRYDER *et al.* 2006). Self-renewal capacity is gradually lost until the multipotent progenitors branch off into myeloid or lymphoid restricted oligopotent progenitors which further differentiate towards lineage restricted progenitors that finally give rise to mature effector cells. Recent studies suggest the presence of a direct link between HSCs and the megakaryocytic lineage.

Recent studies have challenged this classical view of the hematopoietic hierarchy by demonstrating a strong heterogeneity within the HSC pool. MÜLLER-SIEBURG *et al.* identified lineage biased HSCs by using limiting dilution assays dividing the HSC pool into myeloid-biased, lymphoid-biased and balanced HSCs based on the ratio of lymphoid to myeloid cell output (MÜLLER-SIEBURG *et al.* 2004; MÜLLER-SIEBURG *et al.* 2002). Another classification was based on myeloid to lymphoid chimerism levels taking the competitor level into account, hence leading to the definition of 4 different classes of HSCs (α, β, γ and δ) (BENZ *et al.* 2012; DYKSTRA *et al.* 2007). α and β HSCs were both able to reconstitute myeloid and lymphoid cells in secondary transplantations. However, α HSCs showed a higher myeloid cell output, while β HSCs were biased towards lymphoid cells. γ HSCs are not serially transplantable despite robust engraftment for 6-7 months and δ HSCs show only limited self-renewal capacity therefore closely resembling the MPP1 population. A third challenging study was performed by ADOLFSSON *et al.* which proposed the presence of lymphoid-primed multipotent progenitor cells (LMPPs) that give rise to B and T cells as well as granulocytes and macrophages, but lack erythro-megakaryocytic potential (ADOLFSSON *et al.* 2005). This study suggested an earlier branching point of a megakaryocyte/ erythrocyte progenitor population (MkEPs) that occurs before separation of the lymphoid and myeloid lineage. These MkEPs reside within the $CD135^-$ fraction of LSK cells whereas LMPPs are $CD135^+$. In contrast a subsequent study suggested that at least a minor fraction of the $CD135^+$ LMPP population still retains megakaryocyte-erythroid potential (FORSBERG *et al.* 2006). Furthermore, a recent study combined a paired daugther cell analysis with single cell transplantations (YAMAMOTO *et al.* 2013). This analysis suggested first that a single division of LSK $CD34^-$ HSCs can result in several types of committed progenitors and second that the HSC compartment contains a myeloid restricted progenitor population which retains long-term self-renewal capability. These myeloid restricted progenitors comprise progenitors with differentiation potential equivalent to CMPs and MEPs as well as sole megakaryocyte potential. Therefore this study proposes a myeloid-biased branch in the hematopoietic hierarchy and additionally challenges the hypothesis that long-term self-renewal is a unique property of multipotent stem cells. Further proof of a close hierarchical relation between HSCs and megakaryocytes emerged from a study, which identified von Willebrand factor (vWF) positive cells as platelet-primed HSCs at the apex of the HSC hierarchy (SANJUAN-PLA *et al.* 2013). These cells showed enhanced short- and long-

term platelet reconstitution and also had the ability to generate vWF$^-$ lymphoid-biased HSCs.

In summary the classical hierarchical model of hematopoiesis is subject to changes due to the appearance of increasing numbers of HSC and progenitor subtypes. Single cell assays revealed great heterogeneity of several immunophenotypically defined stem and progenitor populations and call for further refinement. Future studies will add more information to these differentiation processes and also to their regulation.

1.3 The oncogenic transcription factor Myc

c-Myc was initially identifed as the cellular homologue of the *v-myc* oncogene in the avian myelocytoma virus MC29, which causes leukemia and sarcoma in chicken (SHEINESS *et al.* 1978; VENNSTROM *et al.* 1982). Its oncogenic potential in humans became apparent by its altered expression in Burkitt lymphoma patients. In these patients the c-Myc coding region is translocated, so that it is under the control of immunoglobulin gene enhancer elements (DALLA-FAVERA *et al.* 1982; TAUB *et al.* 1982). Soon after c-Myc's discovery two more family members, N-Myc and L-Myc, were identified in neuroblastoma cell lines/tumors and small lung cell carcinomas, respectively (KOHL *et al.* 1983; NAU *et al.* 1985; SCHWAB *et al.* 1983).

Approximately 70% of human cancers are associated with overexpression or deregulation of c-Myc. However, this is not driven by activating mutations within the coding sequence, instead chromosomal translocation and gene amplification cause oncogenic activation (MEYER and PENN 2008). In leukemias and lymphomas c-Myc overexpression is often caused by translocations whereas in solid tumors it is commonly driven by amplification of the *c-Myc* gene (DANG 2012).

1.3.1 Myc on the molecular level

1.3.1.1 Molecular function of Myc

The *myc* gene encodes for a basic-helix-loop-helix leucine zipper (bHLH-Zip) transcription factor that can act as an activator and repressor. The mechanisms how it regulates its multiple targets have been nicely summarized in two review articles (ADHIKARY and EILERS 2005; VAN RIGGELEN *et al.* 2010) (Figure 1.5).

Myc binds to E-box sequences (CACGTG), thereby regulating the respective target genes (BLACKWELL *et al.* 1993; BLACKWELL *et al.* 1990). However, Myc can only bind these sequences when it is bound to its partner protein Max (Myc-associated

factor X) (AMATI *et al.* 1993; BLACKWOOD and EISENMAN 1991; BLACKWOOD *et al.* 1992). This heterodimer recruits a co-activator complex (TRRAP) and histone acetylases (HATs) such as GCN5 and TIP60, which leads to the activation of target genes (BOUCHARD *et al.* 2001; FRANK *et al.* 2003; FRANK *et al.* 2001; MCMAHON *et al.* 2000). Max itself however can also form homodimers or heterodimers. As a homodimer Max neither activates nor represses transcription at E-box containing promoters. In contrast upon dimerization with Mad family proteins like Mad1-4 and Mnt (AYER *et al.* 1993; HURLIN *et al.* 1997; HURLIN *et al.* 1996; ZERVOS *et al.* 1993) it performs repressive functions by recruitment of histone deacetylases (HDACs) via Sin3 (AYER *et al.* 1995; HASSIG *et al.* 1997; LAHERTY *et al.* 1997; SCHREIBER-AGUS *et al.* 1995). Mad proteins are often accumulated in differentiating cells, thus leading to repression of Myc-induced proliferative genes (ADHIKARY and EILERS 2005).

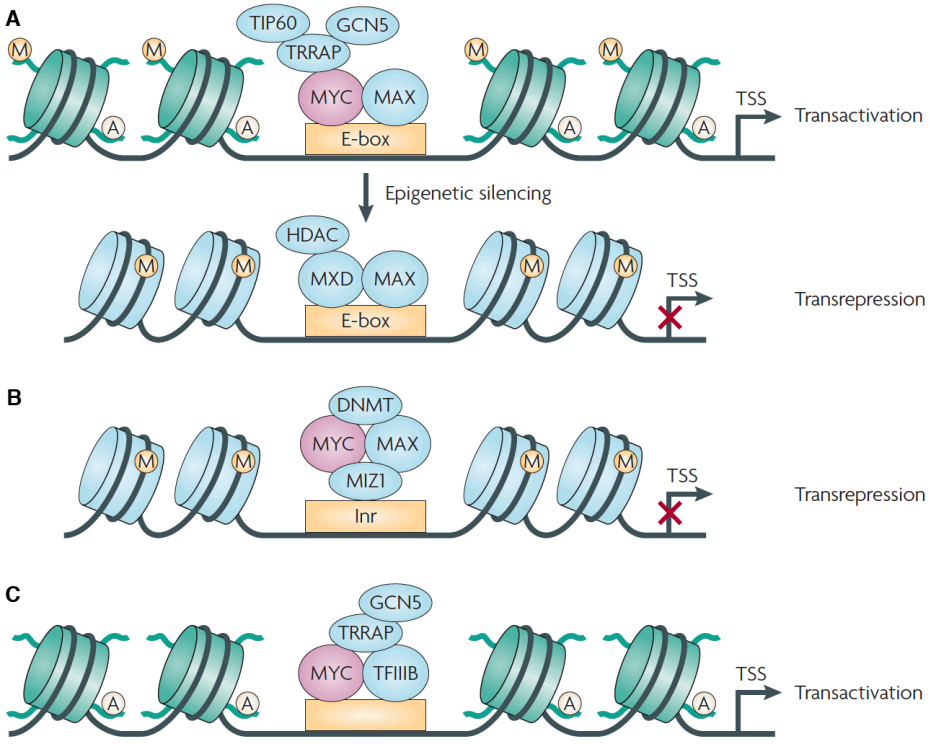

Figure 1.5: Gene regulation by Myc
A Myc forms heterodimers with Myc-associated factor X (Max) that bind to the E-Box sequence motif. This leads to recruitment of cofactors, including histone acetylases (HATs) like GCN5, TIP60 and TRRAP (part of a large HAT complex) and therefore by opening the chromatin to an activation of transcription. However, Max can also dimerize with Mad family proteins (MXD), which antagonizes Myc-Max binding to E-boxes. MXD-Max dimers recruit histone deacetylases (HDACs), resulting in transcriptional repression. **B** Myc-Max dimers can be recruited by the transcription factor Miz1 to core promoter elements of several promoters (initiator element - Inr), leading to transcriptional repression via recruitment of DNA-methyltransferase 3a (DNMT). **C** Myc also forms Max-independent complexes with transcription factor IIIB (TFIIIB) to promote the transcription of RNA polymerase III targets. This involves recruitment of TRRAP and GCN5. A, acetylation; M, methylation; TSS, transcription start site (VAN RIGGELEN *et al.* 2010).

Two other important interaction partners of Myc are the zinc finger proteins Miz1 and Sp1, which can recruit Myc-Max also to promoters lacking the E-box sequence CACGTG. Miz1 itself is a transcriptional activator when bound to the promoter in the absence of Myc (GARTEL *et al.* 2001; PEUKERT *et al.* 1997). By binding to Miz1, Myc-Max causes transrepression of specific Miz1 target genes, which is in part mediated by DNA methylation (BRENNER *et al.* 2005).

A third way of Myc regulation emerged from Max-independent complex formation with TFIIB, thereby promoting transcription catalzyed by RNA polymerase III (GOMEZ-ROMAN *et al.* 2003; STEIGER *et al.* 2008).

1.3.1.2 Target genes and regulation mechanisms of Myc

The global search for Myc target genes revealed that Myc binds very ubiquitously throughout the genome to a myriad of genomic sites encompassing up to 15% of all genes but also including some intergenic sites (BIEDA *et al.* 2006; CAWLEY *et al.* 2004; FERNANDEZ *et al.* 2003; LI *et al.* 2003; ORIAN *et al.* 2003; PATEL *et al.* 2004; ZELLER *et al.* 2006). However, not all genes bound by Myc are associated with increased expression, which could be explained by either lack of necessary coactivators or by its repressive function (e.g. via Miz1). Within the list of target genes several functional groups have been identified by gene ontology analysis (Figure 1.6).

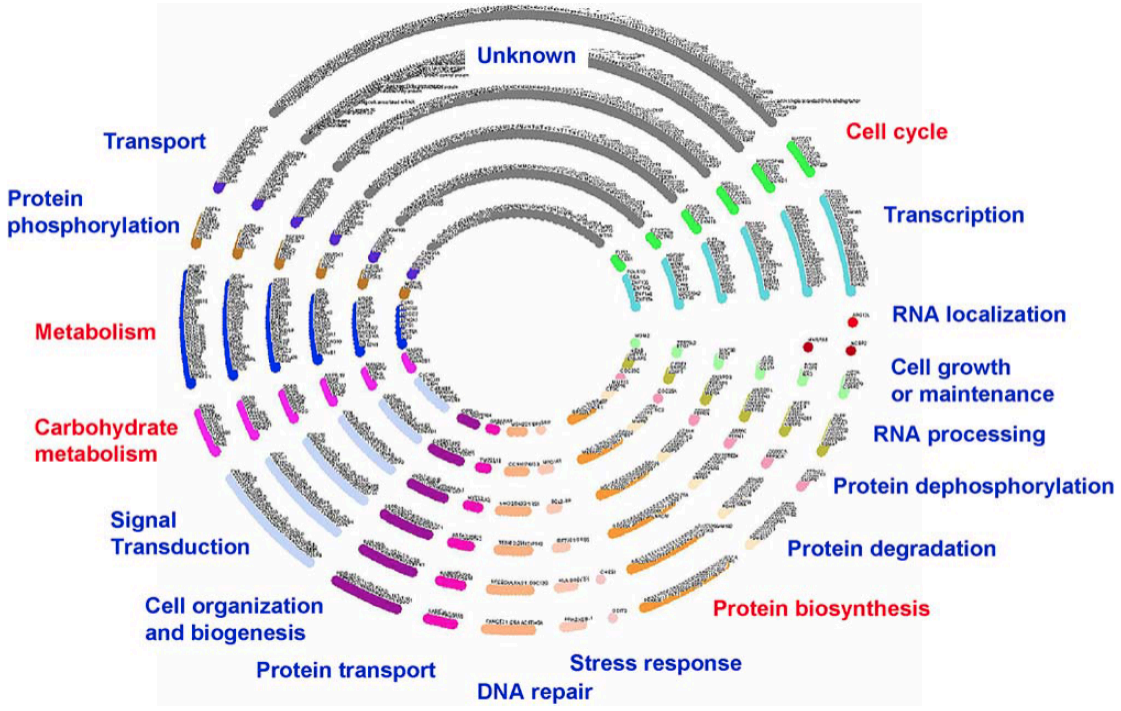

Figure 1.6: Gene ontology analysis of Myc target genes
Distribution of Myc target genes by gene ontology (GO) analysis as determined in (DANG *et al.* 2006). Statistically overrepresented GOs are highlighted in red.

c-Myc potently stimulates proliferation and inhibits differentiation. Exemplary for the regulation of the cell cycle, c-Myc represses expression of the cell cycle inhibitor p21 and regulates expression of several cyclins and cyclin-dependent kinases (CDKs), thus mediating its cell cycle promoting function (BOUCHARD *et al.* 2001; CLAASSEN and HANN 2000; HERMEKING *et al.* 2000; SEOANE *et al.* 2002; SEOANE *et al.* 2001; WU *et al.* 2003). Another prominent function that is regulated by c-Myc is the protein synthesis, which occurs through multiple mechanisms (VAN RIGGELEN *et al.* 2010). On the one hand c-Myc regulates the RNAPII-mediated transcription of ribosomal proteins and auxiliary cofactors but also translation initiation factors and other translation modifiers. On the other hand transcription of rRNAs and tRNAs via RNA polymerase I and III is regulated by c-Myc. Moreover c-Myc has been reported to have a non-transcriptional role in modulating translation. This includes first, the phosphorylation of RNAPII at its CTD, driving it into the elongation phase. Second c-Myc augments cap-dependent translation (COLE and COWLING 2008; COWLING and COLE 2007). Regulation of microRNAs (miRNAs) opens another field of c-Myc activity. For instance oncogenic miRNAs such as miR-17-92 cluster, are activated, tumor suppressor miRNAs, such as let-7 are repressed by c-Myc (CHANG *et al.* 2008; CHANG *et al.* 2009; O'DONNELL *et al.* 2005). Finally, another non-transcriptional regulation has been observed for DNA replication as c-Myc binds to the pre-replicative complex and increases activity at DNA replication origins (DOMINGUEZ-SOLA *et al.* 2007). In summary, many genes regulated by c-Myc are directed towards cell cycling and cell growth, the latter regulated by changes in ribosome biogenesis, protein synthesis, and metabolism.

Transcription was long thought to be regulated mainly at the level of recruitment of the transcriptional machinery (see chapter 1.1.2). However, recent data suggest that promoter-proximal pausing is a general feature of RNAPII transcription in mammals and that c-Myc plays a major role in the release auf RNAPII from this state (RAHL *et al.* 2010). Two studies on activated lymphocytes, ES cells and tumor cells attribute a general function to c-Myc as an universal amplifier of transcription (LIN *et al.* 2012; NIE *et al.* 2012). It is shown that elevated levels of c-Myc do not lead to binding and activation of new target genes with e.g. lower affinity non-canonical E-box sequences but to increased expression of already previously bound c-Myc targets. However, this general amplification model has been partly challenged by two recent publications, showing that c-Myc indeed selectively regulates gene expression (SABÒ *et al.* 2014; WALZ *et al.* 2014). Although SABÒ *et al.* also observed the general increase in mRNA

production this seemed to be rather an indirect effect mediated by c-Myc target genes. In contrast to the amplifier model studies, which question a direct suppressive function of c-Myc, they identified genes with differential expression, including genes that are repressed by c-Myc, which is mediated by Miz1 interaction (WALZ *et al.* 2014). Therefore besides transcription regulation by increased c-Myc promoter binding other factors direct the specific induction of target gene, making c-Myc regulation an interplay between chromosome structure, c-Myc-DNA binding affinity and other transcription factors.

1.3.1.3 Transcriptional regulation of Myc levels

c-Myc plays a critical role in many different pathways and is essential for normal cell function. However, it exerts oncogenic function if deregulated, therefore its expression needs to be tightly regulated. This occurs by many signals on multiple levels. Under normal physiological conditions c-Myc levels are relatively low and additionally c-Myc has a short half-life both on mRNA and protein level (LIU and LEVENS 2006). Thus small changes can yield large consequences and therefore regulation mechamisms exist at transcriptional, translational and posttranslational levels (KING *et al.* 2013; LEVENS 2010; PENN *et al.* 1990a; PENN *et al.* 1990b; REAVIE *et al.* 2013). Focus in this chapter will be set on the transcriptional regulation.

The *c-Myc* gene consists of three exons, however the prevalent c-Myc protein variant is encoded by exons 2 and 3 only. Transcription initiation starts from the two major TATA-containing promoters P1 and P2 at the 5' end of exon I, while other minor promoters are used to a lesser extent. Upon translocation in some Burkitt lymphoma patients P1 and P2 are displaced and c-Myc is driven from promoter P3. Extensive research has been done on the transcriptional control of c-Myc promoters. This very complex regulation has been summarized by Wierstra and Alves (WIERSTRA and ALVES 2008). In general the c-Myc promoter integrates transcription factor input and a multitude of signaling pathways as e.g. from mitogens, growth factors and cytokines. Of note, this regulation has been shown to be highly dependent on the cellular context. Furthermore, chromatin remodeling and the methylation state of the DNA influences promoter regulation as does the DNA conformation and topology (LIU and LEVENS 2006).

Expression of a reporter gene driven by the c-Myc promoter failed to recapitulate normal c-Myc expression, even if 50 kb of the flanking regions were included (LAVENU *et al.* 1994; MAUTNER *et al.* 1996). Thus, although c-Myc promoter regulation is already

very complex, further control elements have to be located outside this 50 kb fragment that are necessary for normal c-Myc expression.

1.3.2 Physiological functions of Myc

1.3.2.1 Function of Myc in development and stem cells

The first attempt to assess c-Myc function in cellular proliferation, differentiation and embryogenesis by generating homozygous *c-myc* knockout (KO) mice revealed that the null mutation is embryonic lethal between 9.5 and 10.5 days of gestation. Homozygous embryos displayed a reduced body size and a strong delay in development with some pathologic abnormalities. Heterozygous deletion of *c-myc* did not display any morphological changes in embryos, however adult females were less fertile (DAVIS *et al.* 1993). Next, the generation of several mouse lines with stepwise decreasing c-Myc levels allowed a closer look at its physiological consequences not only in embryos but also in adult mice. Reduction of c-Myc expression went along with progressive growth and body size reduction. In contrast to Drosophila dMyc mutants that show reduced cell size but unchanged cell numbers, murine c-Myc mutants have reduced cell numbers without a change in cell size (JOHNSTON *et al.* 1999; TRUMPP *et al.* 2001). First observations pointed to an involvement of the hematopoietic system in the *c-myc* KO phenotype, which is subject of the following chapter.

Conditional deletion of *c-myc* using several tissue-specific Cre recombinases was investigated for a number of tissues and revealed a role for c-Myc in intestinal crypt formation, cell size and ploidy of liver cells, the number of neuronal stem cells, proliferation of renal stem and progenitor cells, differentiation in pancreatic cells, the mammary gland and melanocyte development (BAENA *et al.* 2005; BETTESS *et al.* 2005; BLANCO-BOSE *et al.* 2008; BONAL *et al.* 2009; COUILLARD and TRUDEL 2009; MUNCAN *et al.* 2006; NAGAO *et al.* 2008; PSHENICHNAYA *et al.* 2012; STOELZLE *et al.* 2009; ZANET *et al.* 2005).

Deletion of *N-myc* led to embryonic lethality at E10.5 to E12.5 and embryos displayed neuroectodermal and heart abnormalities (CHARRON *et al.* 1992; SAWAI *et al.* 1993; STANTON *et al.* 1992). Conditional deletions revealed involvement of N-Myc in proliferation and survival of neural and retinal progenitors, lung epithelial cells, limb bud mesenchyme, ear development and hair cell formation (HATTON *et al.* 2006; KNOEPFLER *et al.* 2002; KOPECKY *et al.* 2011; KOPECKY *et al.* 2012; MARTINS *et al.* 2008; OKUBO *et al.* 2005; OTA *et al.* 2007).

Expression of L-Myc is normally detected in cerebellar cortex, cerebellum, lung, kidney, and intestine tissues. However, in contrast to the other two family members *L-myc* KO mice are viable without an apparent phenotype (HATTON *et al.* 1996).

In summary straight and conditional deletions demonstrated a critical role for Myc in embryonic development and especially in stem and progenitor cells (LAURENTI *et al.* 2009). In addition gain of function studies underline its role in proliferation and differentiation, as e.g. shown for skin stem cells (BERTA *et al.* 2010; OSKARSSON *et al.* 2006; WATT *et al.* 2008).

Not surprisingly, also a role for c-Myc in embryonic stem (ES) cells has been identified. Murine ES cells express elevated levels of Myc and their growth usually depend on the growth factor LIF (leukemia inhibitory factor). However, a mutant Myc version capable to escape GSK3β dependent degradation kept the self-renewal and pluripotency state of ES cells independent of leukemia inhibitory factor (LIF). In contrast expression of a dominant negative form of Myc antagonized self-renewal and promoted differentiation (CARTWRIGHT *et al.* 2005). Although no gros effect on ES cells has been reported for the single deletion of *c-myc* or *N-myc*, conditional knockout of both *myc* genes in murine ES cells exhibited severely disrupted self-renewal, pluripotency and survival along with enhanced differentiation (SMITH *et al.* 2010; VARLAKHANOVA *et al.* 2010).

1.3.2.2 Function of Myc in hematopoietic cells

The studies summarized so far in chapter 1.3.2.1 do not explain in detail the primary reason for the embryonic lethality of *c-myc* KO mice. Besides some non-hematopoietic defects these embryos had severe defects in establishing the primitive yolk sac hematopoiesis. Those few cells formed failed on colony formation assays (TRUMPP *et al.* 2001). More light was shed on the involvement of the hematopoietic system by using a Sox2Cre recombinase, which deleted *c-myc* specifically in the epiblast while trophoectoderm and primitive endoderm structures retained wild type *c-myc*. Embryos with this tissue-restricted deletion appeared morphologically normal, not exhibiting any obvious proliferation defect. Thus most of the developmental defects observed in *c-myc* KO embryos were attributed to placental insufficiency. However, embryos with epiblast-specific *c-myc* deletion did only survive until E12 and were completely pale as they lacked red blood cells both in the liver and dorsal aorta. Thus the hematopoietic system is particularly dependent on c-Myc function (DUBOIS *et al.* 2008).

1.3.2.2.1 Deletion of *c-myc* in hematopoietic stem cells

The role of Myc in adult HSCs has been addressed by our and other laboratories using conditional deletion by the MxCre recombinase (BAENA *et al.* 2007; GUO *et al.* 2009; WILSON *et al.* 2004). Following induction by polyinosinic-polycytidylic acid (polyI:C) *Mx1*-promoter driven Cre led to an efficient deletion of *c-myc* in hematopoietic cells already at the stem cell level (KÜHN *et al.* 1995). Mice suffered from severe anemia and a loss of most committed hematopoietic lineages, while HSCs accumulated in the bone marrow (WILSON *et al.* 2004). In contrast overexpression of c-Myc led to a loss of HSCs. HSC accumulation upon *c-myc* deletion was accompanied by upregulation of several adhesion molecules such as N-cadherin and integrins. Based on these results a model was proposed where c-Myc does not impair self-renewal and proliferative capacity of HSCs but that they are retained in the niche by high expression of adhesion molecules and fail to differentiate (Figure 1.7). In conclusion, c-Myc controls the balance between HSC self-renewal and differentiation.

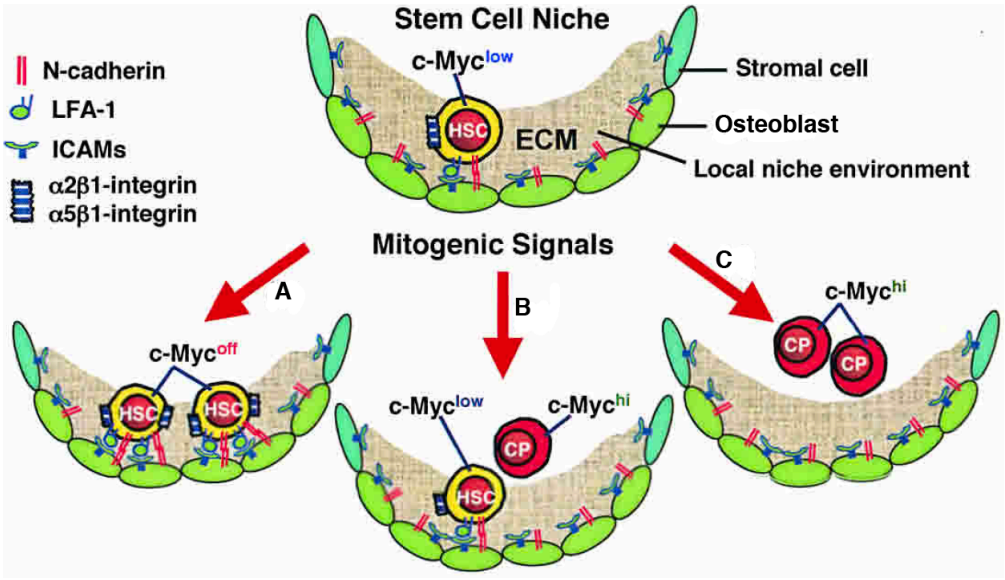

Figure 1.7: c-Myc controls the balance between HSC self-renewal and differentiation
Quiescent hematopoietic stem cells (HSCs) expressing low levels of c-Myc are retained in the stem cell niche by modest expression of the indicated cell surface receptors. The response of HSCs to mitogenic signals is dependent on c-Myc levels. **A** c-Myc deletion leads to upregulation of adhesion molecules that retain both daughter cells in the niche, thereby promoting expansion of HSCs at the expense of differentiation. **B** Induced c-Myc expression leads to downregulation of adhesion molecules, thereby attachment to the niche is untightened. This daughter cell differentiates towards a committed progenitor (CP) while the daughter cell with low c-Myc expression remains as HSC in the niche. **C** High expression of Myc switches the balance towards differentiation leading to exhaustion of the stem cell pool (adapted from (WILSON *et al.* 2004)).

Another study using the same mouse model focused on the lineage commitment of c-Myc deficient HSCs (GUO *et al.* 2009). Consistent with the previously published data by WILSON *et al.* they observed anemia and leukopenia as well as an increase in LSK cells in mice conditionally deleted for *c-myc*. However, they also observed a 3- to 5-fold increase in platelet numbers, which was the result of enhanced megakaryopoiesis. c-Myc deficiency led to a smaller size of megakaryocytes with lower polyploidy, however maturation and platelet formation was not impaired. Finally they showed that the thrombocytosis phenotype was the result of HSC cell intrinsic defects.

1.3.2.2.2 Deletion of *c-myc* and *N-myc* in hematopoietic stem cells

The fact that c-Myc deficient HSCs were not impaired in their proliferative potential was thought to be due to compensation by other Myc family members. Therefore LAURENTI *et al.* investigated the effect of *N-myc* as well as combined *c-* and *N-myc* deletion in HSCs (LAURENTI *et al.* 2008). Whereas N-Myc deficiency alone did not impact on HSC numbers or function, simultaneous deletion of *c-* and *N-myc* resulted in severe pancytopenia and rapid lethality of the mice. The HSC pool as well as most progenitors and differentiated cell types were depleted due to impaired proliferation, differentiation and increased apoptosis. Strikingly, the most primitive dormant HSCs, which give rise to highly proliferative progenitor, survived without expression of c-Myc and N-Myc under homeostatic conditions.

In conclusion of the described functions of Myc in different stem cell types, requirement for Myc activity seems to correlate with the proliferative status of the stem cell. While Myc ensures proliferation and self-renewal in actively dividing stem cells, dormant non-dividing stem cells are independent of Myc activity. For these cells overexpression of Myc rather induces their exit form the normal stem cell compartment (LAURENTI *et al.* 2009; WATT *et al.* 2008; WILSON *et al.* 2004).

1.3.3 The *c-myc*/*Pvt1* gene locus

The *c-myc* gene is located in the 8q24 region in the human genome and at 61.8 Mb region on chromosome 15 in the mouse genome. The murine *c-myc* gene is located in the middle of a 4 Mb-long, gene-poor region (Figure 1.8). Right next to *c-myc* is the *Pvt1* gene located. In humans expression of this long non-coding RNA (lncRNA) has been reported to be low in normal tissue, but highly expressed in many transformed cell lines (CARRAMUSA *et al.* 2007). Moreover, copy number of PVT1 was

co-increased in more than 98% of cancers with increased copy numbers of MYC (TSENG *et al.* 2014).

1.3.3.1 Conservation of the *c-myc*/*Pvt1* flanking locus

By comparison of genomic sequences from different species conserved areas within the genomes can be identified. Despite being gene poor the flanking regions of the *c-myc*/*Pvt1* locus are highly conserved both on the synteny as well as the sequence level between mouse and human (Figure 1.8). Pairwise alignment of both sequences revealed 48% conservation of the sequence between *A1bg* and *c-myc* and between *Pvt1* and *Gsdmc*. In contrast the gene poor regions centromeric to *A1bg* and telomeric to *Acdy8* show lower conservation (38% and 31%, respectively). As high conservation in non-coding areas of the genome points towards a functional role of these sequences such as in transcriptional regulation (see chapter 1.1.3.1) the *c-myc*/*Pvt1* flanking region is likely to contain regulatory elements.

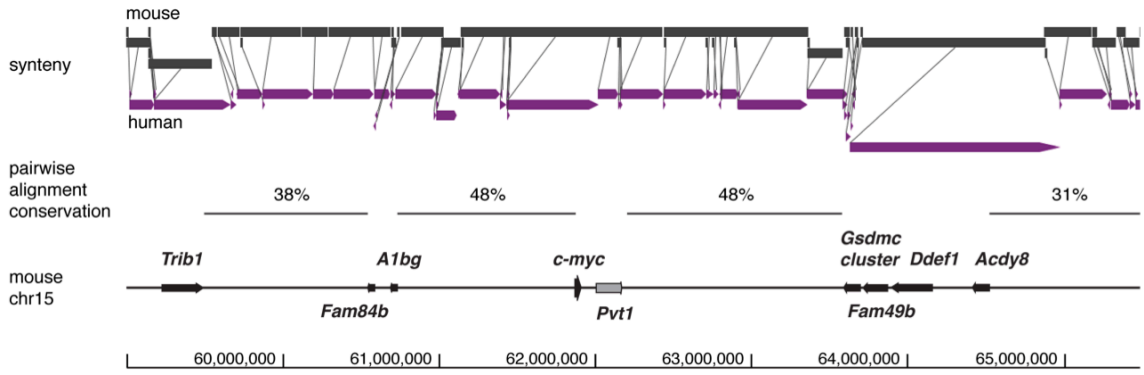

Figure 1.8: Conservation of the *c-myc*/*Pvt1*-flanking locus in humans
The mouse (grey) and human (purple) *c-myc*/*Pvt1* flanking locus displays a high synteny (visualized using the VISTA Browser (MAYOR *et al.* 2000)). Pairwise alignment of the mouse and human sequence reveals a higher conservation of the *c-myc*/*Pvt1* flanking locus sequence (spanning the sequence between *A1bg* and *Gsdmc*) as compared to the gene poor regions on the centromeric side of *A1bg* and the telomeric side of *Acdy8* (alignment of mm9 and hg19 genomes using UCSC genome browser). Overall nucleotide alignment indicates that 40% of the human genome can be aligned to the mouse genome.

Gene duplication events early during evolution resulted in the formation of the different Myc family members (ATCHLEY and FITCH 1995). Also the synteny of the *N-myc* locus is highly preserved as the locus possesses the paralogous genes *Trib2, Fam84a* and *Fam49a*. A knock-in study, in which the *c-myc* coding region was replaced by that of *N-myc*, showed that N-Myc can replace c-Myc without any survival or reproductive consequences and only mild effects on skeletal muscle, body weight, and cell growth response (MALYNN *et al.* 2000). These results suggested that Myc

expression and function is not only determined by the coding sequences but also by distinct *cis*-regulatory elements in the genomic context.

1.3.3.2 Long-range regulatory elements in the *c-myc*/*Pvt1* flanking locus

Global analysis of a diverse set of tissues and cell types in the mouse provided a map of *cis*-regulatory sequences, pointing towards a multitude of potential enhancers in the entire *c-myc*/*Pvt1* flanking locus (SHEN *et al.* 2012). Indeed, recent studies have identified in this region distant enhancer modules that physically contact the *c-myc* promoter (AHMADIYEH *et al.* 2010; HALLIKAS *et al.* 2006; POMERANTZ *et al.* 2009; SOTELO *et al.* 2010). These regions contain disease related single nucleotide polymorphisms (SNPs) linked to prostate, breast and colon cancer. Deletion of such a potential enhancer region important for colorectal cancer susceptibility located 335 kb upstream of *c-myc* did not change *c-myc* expression in vivo but conferred resistance to intestinal tumors (SUR *et al.* 2012).

Work by our collaborators recently proved the existence of very remote *cis*-acting enhancers that control *c-myc* expression in the developing face (USLU *et al.* 2014). These enhancer elements are spread across a large area of the non-coding region located telomeric to the *c-myc*/*Pvt1* flanking locus. Deletion of this region alters the facial morphology in mouse embryos mildly and leads sporadically to a cleft lip/cleft palate phenotype.

2 AIM OF THE THESIS

c-Myc is an essential transcription factor regulating a myriad of genes in human and mouse. Therefore it controls critical pathways that act in concert for proper functioning of the cell. Deregulation of c-Myc can have serious consequences as evidenced by its involvement in many types of cancer. Since Myc as discovered many studies aimed to illuminate the regulatory mechanisms of c-Myc expression. Despite these efforts, not all regulatory elements that account for proper c-Myc expression were identified. Since most of these studies were focused on the vicinity of the *c-myc* gene, we hypothesized that there are enhancer elements that are located more distantly. In line with this hypothesis, the *c-myc* gene is flanked by a large non-coding region that is highly conserved, suggesting the presence of regulatory elements within this locus. Indeed, our collaborators identified enhancer activity in the developing face within a large part of this non-coding region located telomerically of *c-myc* (USLU *et al.* 2014). Deletion of this broad region abolishes c-Myc expression in this tissue. Since many regulatory enhancers are acting in a tissue-dependent manner and due to Myc's important function in HSCs, we focused our study on the hematopoietic system. First, we aimed to characterize the broad deletion of the region covered by the embryonic face enhancer. Then, by using a set of transgenic mouse lines carrying a regulatory sensor integrated into the genome, we aimed to screen the *c-myc*/*Pvt1* flanking locus for regulatory input. Following this screen the specificity of these elements needed to be determined. The consequences of this deletion would then be further indicative for the functional role of the enhancer element in the hematopoietic system. In summary, our study aimed at defining distal regulatory elements of the murine *c-myc* gene in hemaopoietic stem cells. Finally, we wanted to extend this regulatory input to the human *c-MYC* gene and investigate its implication in leukemia.

3 RESULTS

3.1 Strategy for the transposon-mediated generation of transgenic mice

The group of François Spitz at the European Molecular Biology Laboratory (EMBL) in Heidelberg is interested in the identification of regulatory sequences and understanding how their arrangement controls gene expression. For this purpose they developed an *in vivo* system based on the transposition of *Sleeping Beauty* transposons called GROMIT (Genome Regulatory Organization Mapping with Integrated Transposons) (RUF *et al.* 2011). These transposons contain a regulatory sensor composed of a *LacZ* gene driven by a minimal promoter. The promoter region corresponds to a 50 bp long fragment adjacent to the start site of the human *β-globin* gene (YEE and RIGBY 1993) and does not show specific activity when inserted into the mouse genome. However, it is very sensitive to endogenous regulatory input, therefore *LacZ* reporter expression reflects the presence of *cis*-regulatory elements. These elements are either in close proximity to the genomic site of the insertion or distant but acting in a long-range manner.

The incorporation of this regulatory sensor within the *Sleeping Beauty* transposon allows a fast and simple way to remobilize the sensor *in vivo*. Transposition is induced by a hyperactive form of the Sleeping Beauty transposase (HSB16) (BAUS *et al.* 2005) under the control of a mouse *Prm1* promoter fragment. Transposase expression is therefore restricted to spermatogenesis (PESCHON *et al.* 1989). Male mice carrying the transposon and the transposase transgene are bred to wild type females and the progeny is screened for new insertions. In contrast to other transposons the *Sleeping Beauty*

transposon does not show an integration bias towards particular regions like transcription start sites, gene bodies or intergenic sequences (HORIE *et al.* 2003; RUF *et al.* 2011; YANT and KAY 2003). However, it preferentially integrates close to its starting site (KENG *et al.* 2005; LUO *et al.* 1998), therefore new insertions are frequently observed within 1 to 2 Mb distance to the initital insertion. This feature allows the fast generation of mice with different insertions within a particular region of interest.

The transposon contains in addition to the regulatory sensor a *loxP* site (SAUER and HENDERSON 1988; STERNBERG and HAMILTON 1981), which can be used for Cre-mediated chromosomal rearrangements (HERAULT *et al.* 1998; RUF *et al.* 2011; WU *et al.* 2007). The recombination can lead to either deletion, duplication or inversion of the sequence between two insertion loci. After recombination the reporter remains present at the locus, thus allowing the comparison of reporter expression at the breakpoints with reporter expression after the recombination event.

Dr. Veli V. Uslu, postdoctoral fellow in François Spitz' laboratory, generated multiple mouse lines carrying the transposon on chromosome 15 at different positions in the flanking region of the *c-myc* gene (USLU *et al.* 2014). Furthermore, he generated several mouse lines carrying deletions or duplications in that region. Using these mice he analyzed the *c-myc*/*Pvt1* flanking region for regulatory elements in E11.5 embryos and identified distant *cis*-acting enhancers that control *c-myc* expression in the developing face (USLU *et al.* 2014).

3.2 Deletion of a 882 kb long region downstream of *c-myc* impacts on the hematopoietic system

Since *c-myc* plays an important role in the hematopoietic system (chapter 1.3.2.2) we first aimed to analyze the influence of a large deletion in the *c-myc/Pvt1* flanking locus on hematopoietic cells, knowing that this region contains enhancer elements acting on *c-myc* in the embryonic face. Cre-mediated recombination between transposon insertion 8a (located 800 kb telomeric to *c-myc*) and 17a (located 1.7 Mb telomeric to *c-myc*) led to the generation of del(8-17) mice carrying a 882 kb deletion between both insertions (Figure 3.1) (RUF *et al.* 2011; USLU *et al.* 2014).

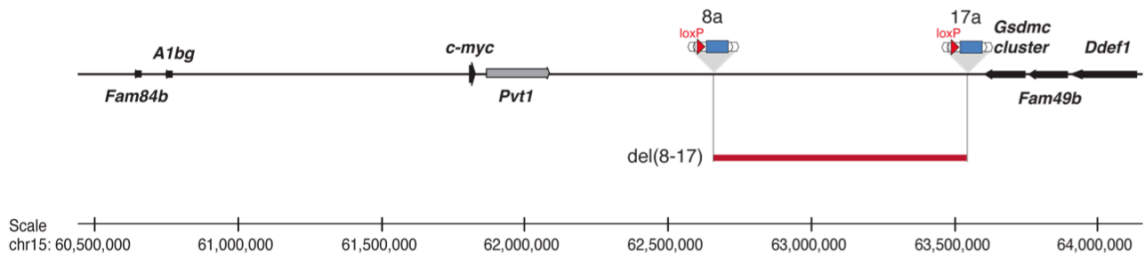

Figure 3.1: The *c-myc*/*Pvt1* gene locus is flanked by a large non-coding region
Organization of the mouse locus on chromosome 15. Protein coding genes are indicated by black arrows, non-coding genes by grey arrows. The two transposon insertions 8a and 17a are depicted that were used to generate the del(8-17) deletion (red bar).

Homozygous del(8-17) mice were born in normal mendelian ratios and did not show gross abnormalities at the day of birth. However, further monitoring revealed that these mice have a postnatal growth defect and showed some postnatal mortality until weaning age (USLU *et al.* 2014). Similarly, mice with a heterozygous *c-myc* deletion and accordingly diminished *c-myc* expression levels also displayed a reduction in body size (TRUMPP *et al.* 2001), however this did not result in postnatal mortality. Assuming that the enhancer is only active in specific tissues but leads to a greater reduction of *c-myc* expression levels in these tissues as compared to overall heterozygous deletion of *c-myc*, one or more of these affected tissues can account for the postnatal mortality.

3.2.1 Effect of del(8-17) on the distribution of hematopoietic cells in the bone marrow

Due to postnatal mortality we sacrificed mice at day 10 after birth for the analysis of the hematopoietic system. At this age, homozygous del(8-17) mice were 30.4%±5.3 smaller than wild type mice (Figure 3.2 A). The number of bone marrow (BM) cells was reduced almost to a similar extent as it is indicated by the BM cellularity (Figure 3.2 B,C). However, analysis of the BM by flow cytometry revealed a strongly disturbed appearance of mature hematopoietic effector cells (Figure 3.2 D,E). While numbers of red blood cells (Ter119$^+$) and T cells (CD4$^+$, CD8$^+$) remained unchanged, numbers of B cells (B220$^+$) and granulocytes (CD11b$^+$ Gr-1$^+$) were dramatically reduced. In contrast, del(8-17) mice did have increased numbers of megakaryocytes (Mgk; CD41$^+$). These changes in the distribution of differentiated cells closely resembled the phenotype of adult mice with conditional deletion of *c-myc* in the hematopoietic system induced by MxCre (GUO *et al.* 2009; WILSON *et al.* 2004).

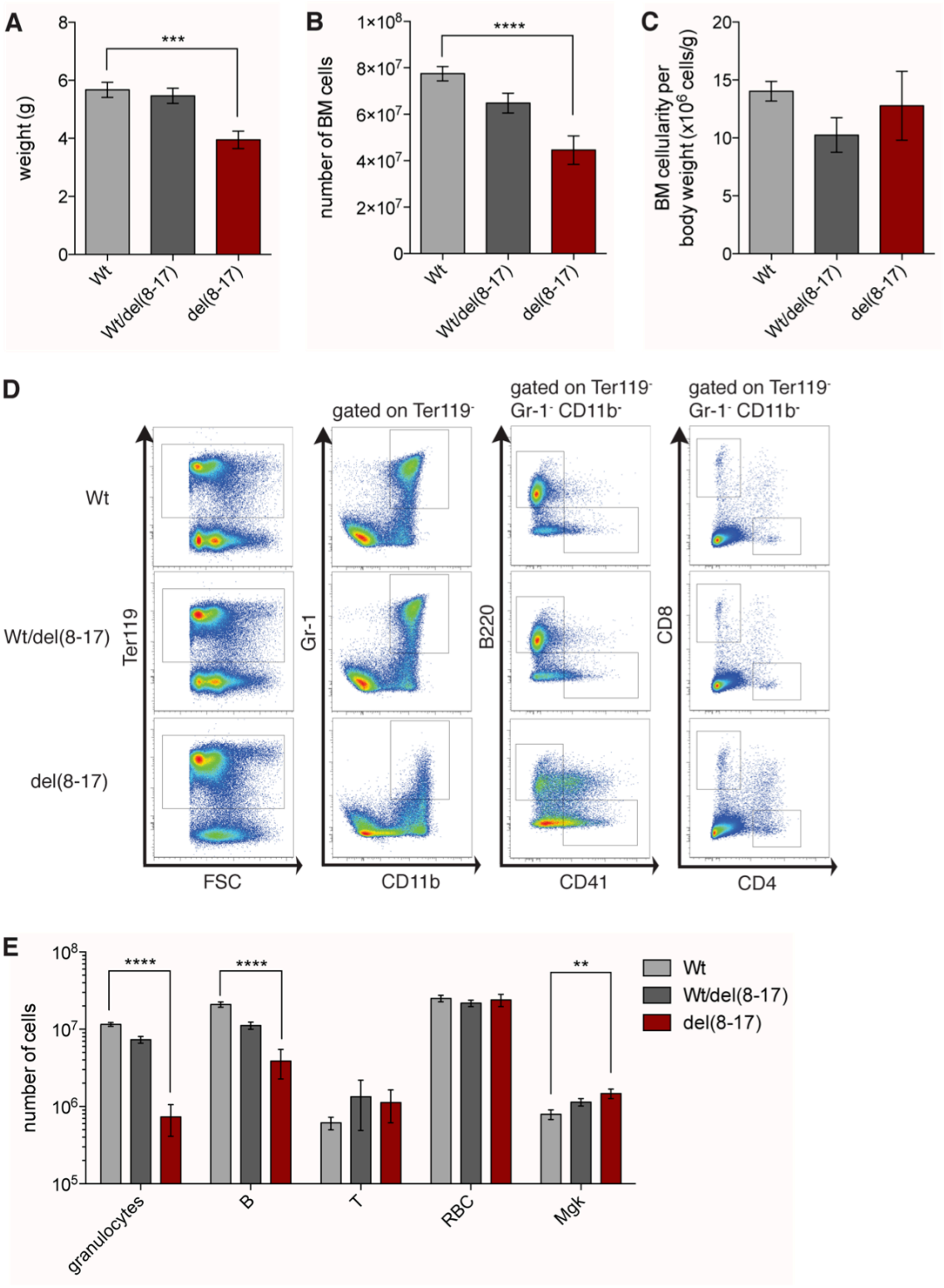

Figure 3.2: The deletion del(8-17) disturbs the differentiated cells
Comparison of 10 days old wild type (Wt) or heterozygous Wt/del(8-17) mice to homozygous del(8-17) mice. **A** Body weight. **B** Number of BM cells from two femurs, tibias, ilia, and the vertebrae. **C** BM cellularity. **D** Representative flow cytometry profiles of BM cells stained for differentiated cell types. **E** Quantitative and statistical analysis of numbers of differentiated cell types in the BM (B, B cells; T, T cells; RBC, red blood cells; Mgk, megakaryocytes).
Data shown are mean (±SEM) values (n = 5-16). Statistical significance is indicated for the comparison of del(8-17) to Wt mice; **p≤0.01; ***p≤0.005; ****p≤0.001.

The aforementioned conditional deletion of *c-myc* has been shown to result in an accumulation of hematopoietic stem and progenitor cells (HSPCs; Lineage$^-$ Sca-1$^+$ cKit$^+$ (LSK)) in the BM (GUO *et al.* 2009; WILSON *et al.* 2004), therefore we analyzed the BM cells of del(8-17) mice for this HSPC population. The frequency of LSK cells was about 10-fold higher in homozygous del(8-17) mice than in wild type mice. Due to the decrease in total BM cells (Figure 3.2 B) the net increase of LSK cells was 7.6-fold (Figure 3.3 A, B).

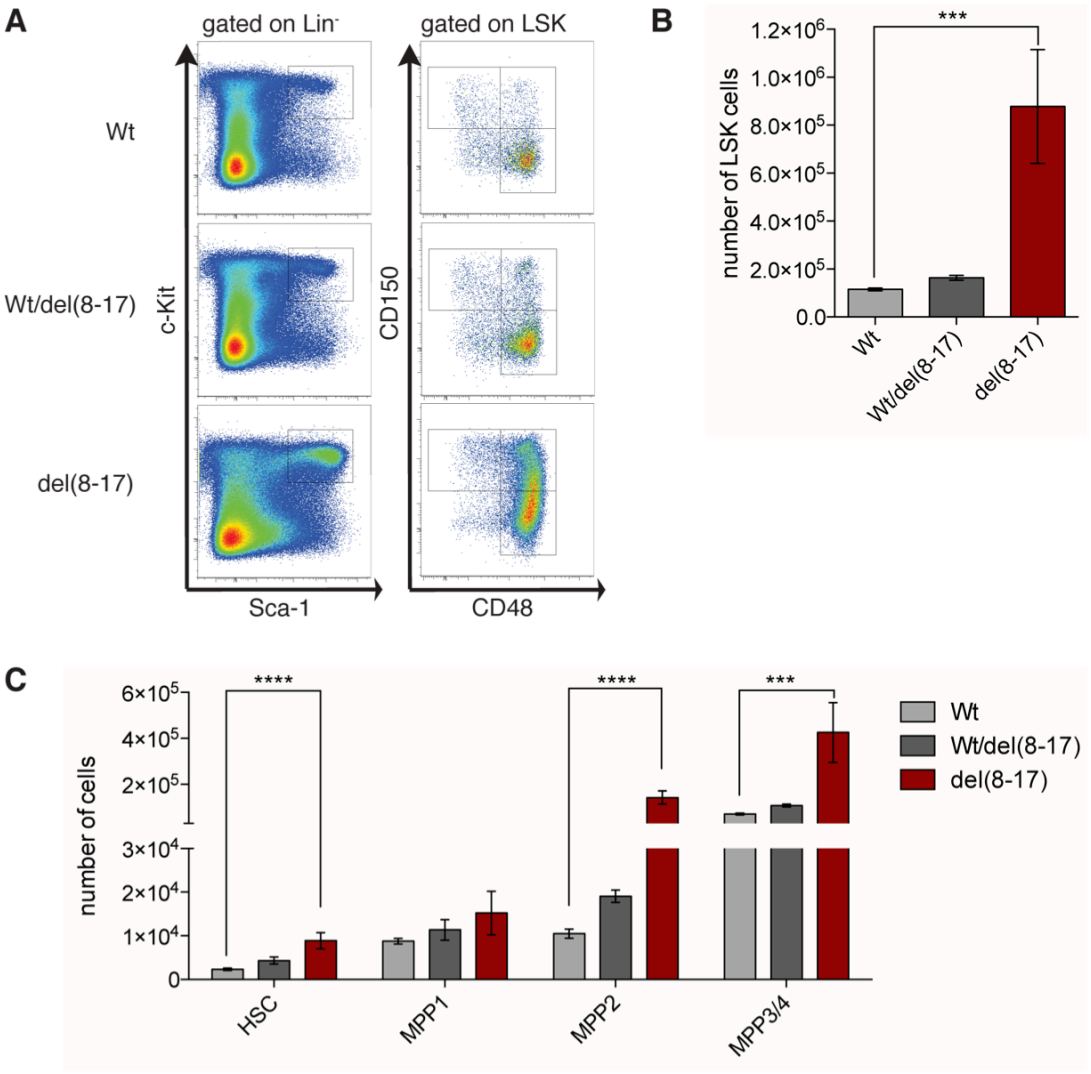

Figure 3.3: The deletion del(8-17) leads to an increase of the hematopoietic stem and progenitor cell population
Comparison of the hematopoietic stem and progenitor compartment in the BM of 10 days old wildtype (Wt), heterozygous Wt/del(8-17) mice and homozygous del(8-17) mice. **A** Representative flow cytometry plot of Lin$^-$ gated and LSK gated BM cells. **B** Quantitative and statistical analysis of stem and progenitor cell numbers in the BM.
Data shown are mean (±SEM) values (n = 5-16). Statistical significance is indicated for the comparison of del(8-17) to Wt mice; ***p≤0.005; ****p≤0.001.

WILSON *et al.* and GUO *et al.* used the cell surface marker CD135 (Flk2/Flt3R) to further define the HSCs within the LSK cell population. Conditional deletion of *c-myc* led to an enrichment specifically in LSK CD135$^-$ cells, thus the authors concluded that HSCs accumulated in the BM of *c-myc* deficient mice. To investigate the HSC population in del(8-17) mice we used CD34 (OSAWA *et al.* 1996) and the Slam markers CD150 and CD48 (KIEL *et al.* 2005) in addition to the LSK marker set. This analysis revealed that the number of HSCs defined by LSK CD150$^+$ CD48$^-$ CD34$^-$ was almost 4-fold increased (Figure 3.3 D). Even more prominent was the increase of the CD48$^+$ population within the LSK population (Figure 3.3 A). These cells correspond to the multipotent progenitor populations MPP2 (LSK CD150$^+$ CD48$^+$ CD34$^+$), MPP3 and 4 (LSK CD150$^-$ CD48$^+$ CD34$^+$). Quantification of these populations revealed a 14-fold and 6-fold increase of MPP2 and MPP3/4 respectively (Figure 3.3 D). In summary, dramatic accumulation of late multipotent progenitor cells but not HSCs or MPP1 cells account for the increase of LSK cells.

3.2.1.1 Deletion of del(8-17) keeps stem and progenitor cells in a more active state

Since c-Myc is known to play an important role in the control of proliferation we assessed the cycling behavior of stem and progenitor cells in the BM of del(8-17) mice. We stained BM cells of del(8-17) mice for intracellular Ki67, only expressed by cycling cells, combined with Hoechst33342, which stains DNA stochiometrically. This staining allows the identification of cells in the G0 (Ki67^{neg}Hoechst^{low}), the G1 (Ki67^{pos}Hoechst^{low}) and the S, G2 and M (Ki67^{pos}Hoechst^{high}) phases of the cell cycle. Wild type HSCs displayed only very low cycling activity and 90% of the cells were in G0 (Figure 3.4 A,C). Upon differentiation along the multipotent progenitor populations the cell cycle stage moved progressively from G0 to G1 (Figure 3.4 A,D,E,F). Strikingly only 35% of del(8-17) HSCs were in G0. Also the other progenitor populations displayed a significantly reduced number of cells in G0 compared to wild type cells except for the MPP3/4 population where the level of cells in G0 is already very low. Only the HSC population exhibited a slight increase in cells that are actively cycling, which might account for the accumulation of HSPCs in the BM of del(8-17) mice. Overall deletion of del(8-17) kept stem and progenitor cells in a more active state.

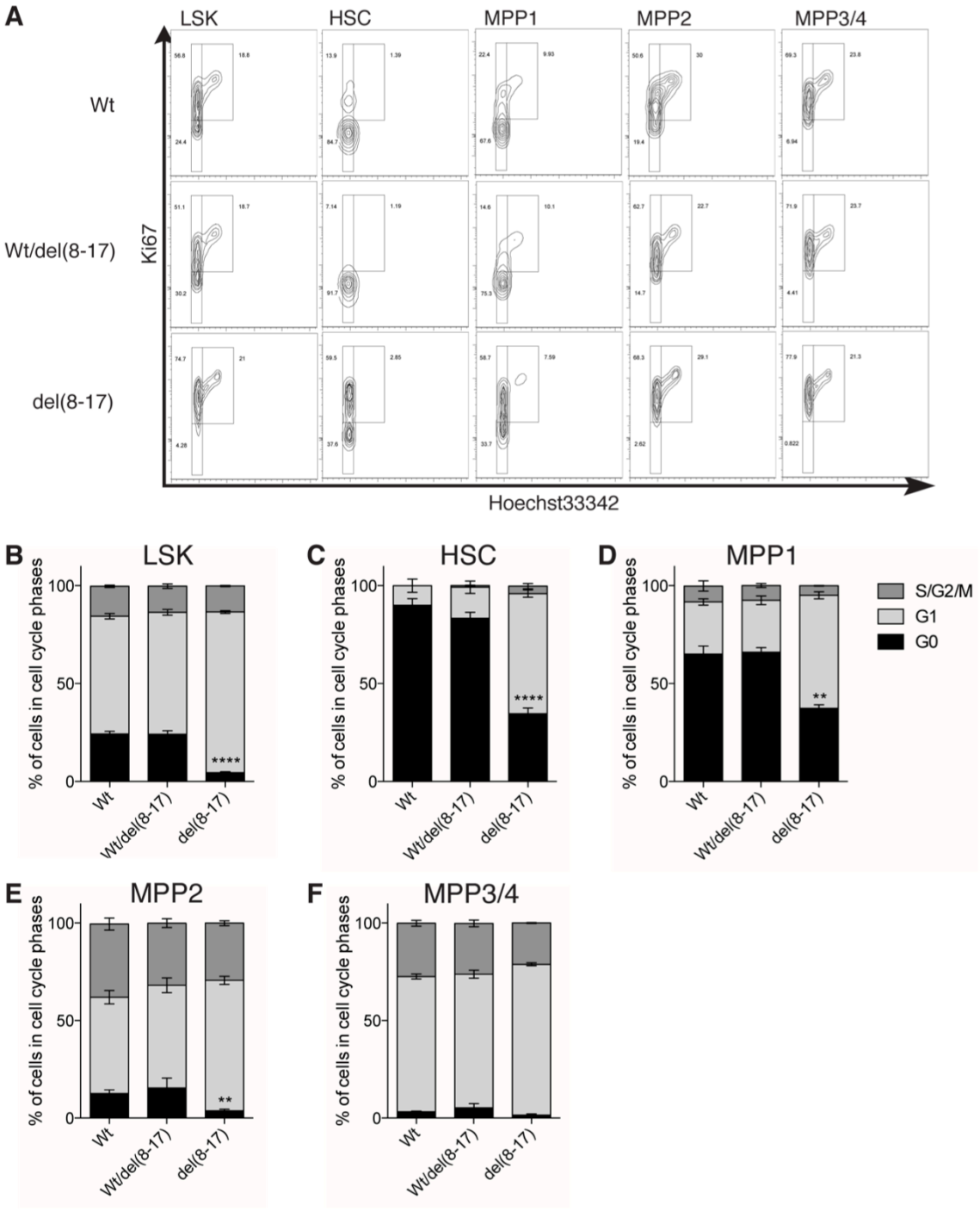

Figure 3.4: The deletion del(8-17) leads to a more active cell cycle state of hematopoietic stem and progenitor cells

Cell cycle analysis by Ki67/Hoechst33342 staining of hematopoietic stem and progenitor cells of 10 days old wild type (Wt), heterozygous Wt/del(8-17) or homozygous del(8-17) mice. **A** Representative flow cytometry profiles of cells gated for the indicated populations. **B-F** Quantitative and statistical analysis of the cell cycle in the indicated populations.

Data shown are mean (±SEM) values (n = 3-5). Statistical significance is indicated for the comparison of the G0 cell cycle phase between del(8-17) and Wt mice; **p≤0.01; ****p≤0.001.

3.2.2 The accumulation of del(8-17) stem and progenitor cells already manifests in the fetal liver

During embryonic development HSCs are not located initially in the BM but migrate through different embryonic tissues. As described in chapter 1.2.1.3 the first functional HSCs could be isolated from the AGM region of mouse embryos starting from E10.5 (DE BRUIJN *et al.* 2000; DZIERZAK and SPECK 2008; KUMARAVELU *et al.* 2002; MEDVINSKY and DZIERZAK 1996; MÜLLER *et al.* 1994). From E11.5 they start to colonize the fetal liver where they undergo expansion and maturation, followed by migration to the BM from E17.5 onwards (MIKKOLA and ORKIN 2006). Fetal HSCs in the liver are markedly different to adult HSCs especially regarding their cell cycle status and proliferative capacity (BOWIE *et al.* 2007; BOWIE *et al.* 2006).

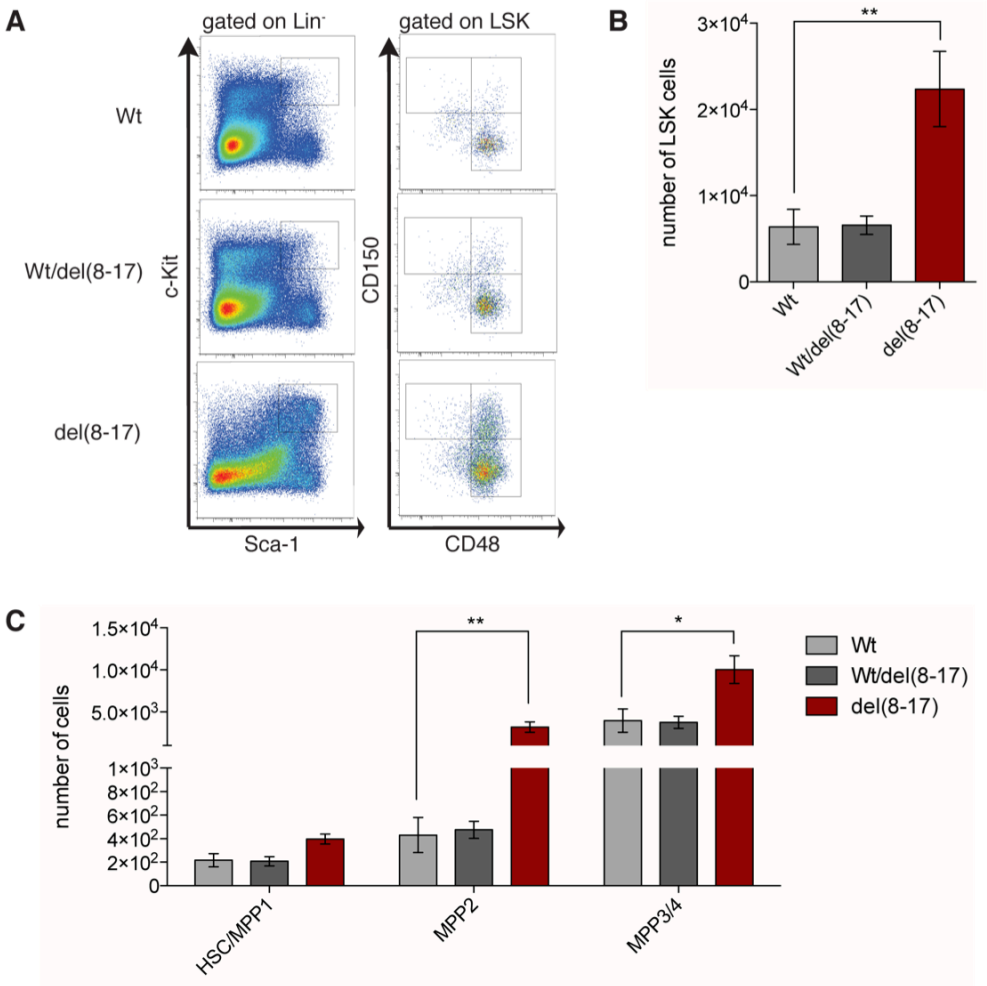

Figure 3.5: Accumulation of hematopoietic stem and progenitor cells in the liver of newborn del(8-17) mice
Comparison of the hematopoietic stem and progenitor compartment in the liver of 10 days old wild type (Wt), heterozygous Wt/del(8-17) or homozygous del(8-17) mice. **A** Representative flow cytometry profiles of Lin$^-$ gated and LSK gated liver cells. **B** Quantitative and statistical analysis of stem and progenitor cell numbers in the liver.
Data shown are mean (±SEM) values (n = 3-6). Statistical significance is indicated for the comparison of del(8-17) to Wt mice; *p≤0.05; **p≤0.01.

Since we analyzed the del(8-17) mice at the age of 10 days and observed an accumulation of stem and progenitor cells in the BM with a more active cell cycle profile we wanted to assess the number of HSCs in the liver of these animals. In this quantification HSCs and MPPs were characterized without gating for CD34 as expression of this marker on HSCs changes during developmental stages (MATSUOKA *et al.* 2001). Similar to the accumulation in the BM the number of LSK cells in the liver was increased by more than 3-fold (Figure 3.5 A,B). Again correlating to the BM this accumulation was mainly due to the increase of MPP2 (7.5-fold) and MPP3/4 (2.5-fold) whereas the HSC/MPP1 population displayed only a non-significant 1.8-fold increase (Figure 3.5 A,C).

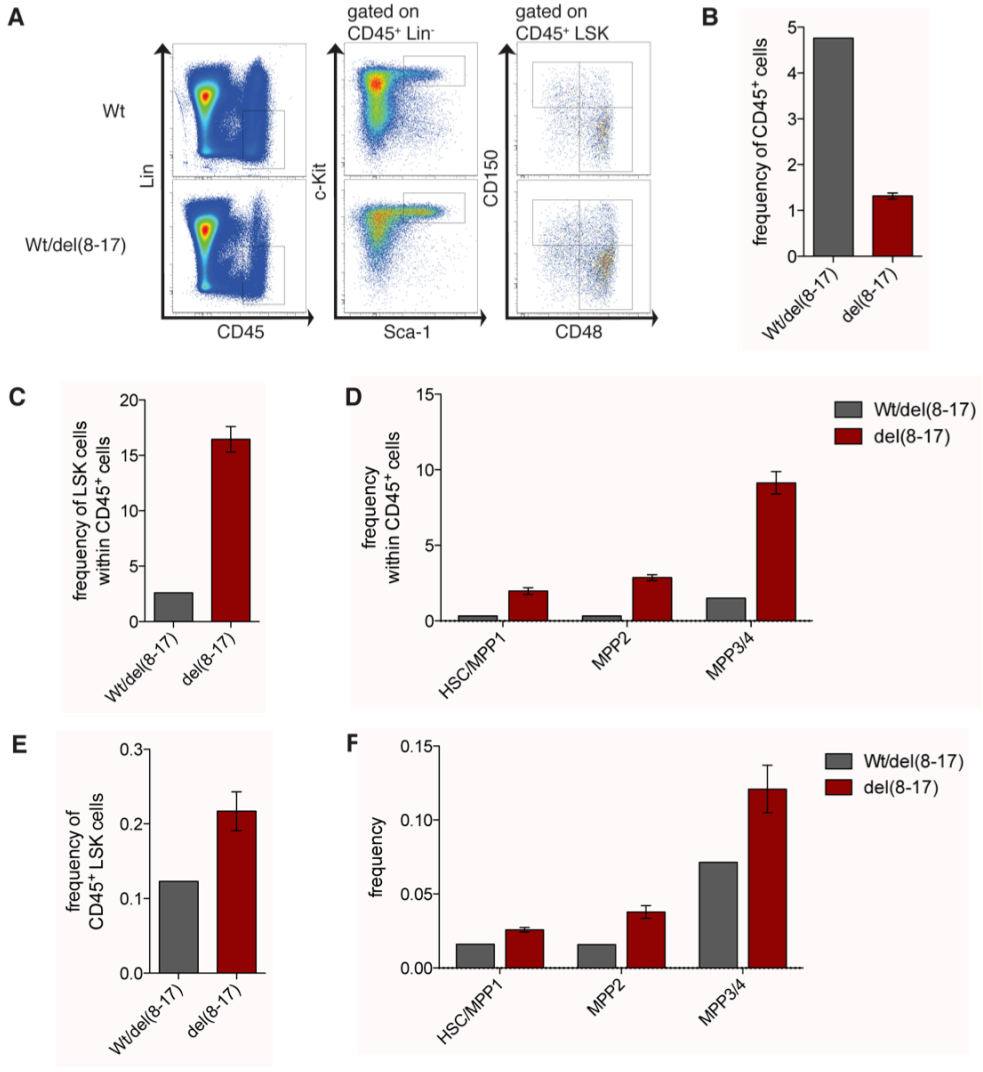

Figure 3.6: Accumulation of hematopoietic stem and progenitor cells in the fetal liver of del(8-17) mice
Comparison of the hematopoietic stem and progenitor compartment in the liver of heterozygous Wt/del(8-17) and del(8-17) embryos at E15.5. **A** Representative flow cytometry profiles of Lin^- gated and LSK gated liver cells. **B** Frequency of hematopoietic cells ($CD45^+$) in the fetal liver. **C** Frequency of LSK cells within the blood cell population in the fetal liver. **C** Frequency of HSC/MPP1, MPP2 and MPP3/4 cells within the blood cell population in the fetal liver. **E,F** Absolute frequencies of the populations shown in C and D. Data shown are mean (±SEM) values (n = 1-2).

In a pilot experiment with 1 and 2 mice per genotype we stained fetal liver cells from E15.5 embryos for hematopoietic stem and progenitor populations. In addition the CD45 marker was used to identify hematopoietic cells among the hepatocytes. The fetal livers of embryos carrying the del(8-17) deletion contained 4-fold less $CD45^+$ blood cells compared to the control liver (Figure 3.6 A,B), however among these blood cells the frequency of HSC and MPP populations was strongly increased (Figure 3.6 C,D). With regard to the reduced amount of $CD45^+$ blood cells the absolute amount of HSC and MPP cells in the liver might have been unchanged. However, absolute frequencies still showed an increase for each population (Figure 3.6 E,F). In summary the phenotype we observed in the BM of newborn mice already manifests in the fetal liver where a number of HSCs is retained at least till day 10 after birth.

3.2.3 The del(8-17) deletion leads to reduced *c-myc* expression in stem and progenitor cells

Since these mice displayed a very similar phenotype compared to the conditional *c-myc* deletion and we knew about potential regulatory input of the deleted region on *c-myc* we next assessed the expression of *c-myc* and other nearby genes in the *c-myc*/*Pvt1* flanking region. For this purpose we sorted LSK cells as well as myeloid committed progenitor cells (LS^-K) and analyzed the mRNA levels by qRT-PCR. *c-myc* levels dropped dramatically upon del(8-17) deletion in LSK cells to 3% of wildtype levels. However, LS^-K cells showed only a minor reduction to 65% of wildtype levels. In contrast *Fam49b*, a gene located 210 kb telomeric from the deletion breakpoint did not show a significant change in expression. Furthermore, *Gsdmc* expression levels were very low (data not shown) and we could not detect *Pvt1*.

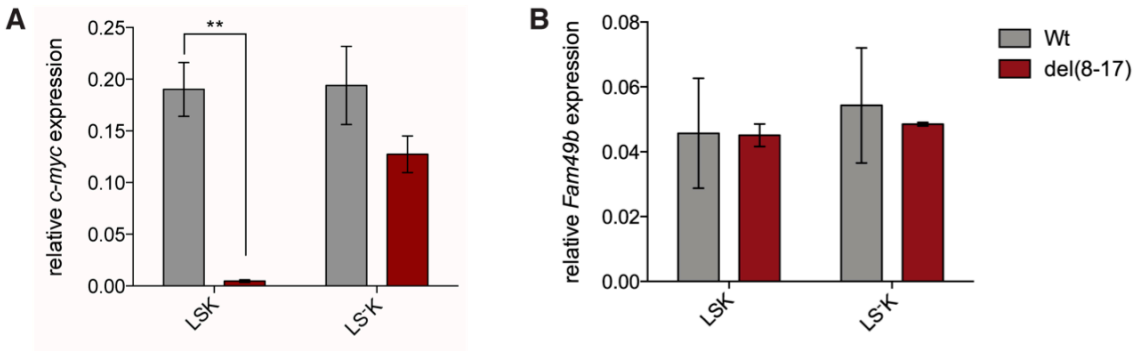

Figure 3.7: Analysis of gene expression in the *c-myc*/*Pvt1* flanking locus upon del(8-17)
Relative mRNA expression levels of *c-myc* (**A**) and *Fam49b* (**B**) measured by qRT-PCR in LSK and LS^-K BM cells from 10 days old wildtype and del(8-17) mice. Data shown are mean (±SEM) values (n = 4-8).

3.2.4 Competitive transplantation reveals a critical role for the del(8-17) region for HSC self renewal and differentiation

The lack of many mature effector cells, the accumulation of stem and progenitor cells in the BM of del(8-17) mice and the fact that *c-myc* levels were significantly reduced in LSK cells led us to test the self renewal and differentiation potential of del(8-17) HSCs by a reconstitution experiment. Lethally irradiated mice transplanted solely with conditionally *c-myc* deleted BM cells did not survive (WILSON *et al.* 2004). As a similar phenotype for the transplantation of del(8-17) BM cells could be expected we decided to co-transplant competing wild type BM cells that generate a functional hematopoietic system and thus ensure the survival of the recipient mice. We isolated BM cells of 10 days old del(8-17) and control mice and transplanted them together with CD45.1/2 BM cells from an adult mouse in an overall 80:20 ratio intravenously into lethally irradiated $CD45.1^+$ mice. Due to the higher frequency of stem cells in the BM, 4 times more HSCs from del(8-17) mice as from wild type mice were transplanted. The engraftment was monitored over time by bleeding the mice every 4 weeks and determining the percentage of $CD45.2^+$ in the blood. As shown in Figure 3.8 B del(8-17) derived cells did not contribute to the peripheral blood already 4 weeks after transplant while control cells efficiently reconstituted the periphery. After 16 weeks mice were sacrificed and the engraftment was analyzed in the BM. Similar to the peripheral blood differentiated cell types were hardly reconstituted by del(8-17) HSCs, however the stem cell compartment was reconstituted to 63% (Figure 3.8 C,D). Multipotent progenitor populations MPP1, MPP2, MPP3/4 and myeloid committed progenitors LS^-K of del(8-17) transplanted mice showed a gradually declining contribution to the BM from 62% to 24% (Figure 3.8 D).

In summary these results show that del(8-17) HSCs were functionally defective as they were unable to reconstitute mature hematopoietic lineages upon transplantation in a competitive setting. At the same time del(8-17) HSCs retained their self-renewal capacity as they remained present and accumulated in the BM to an amount of 68% of wild type levels.

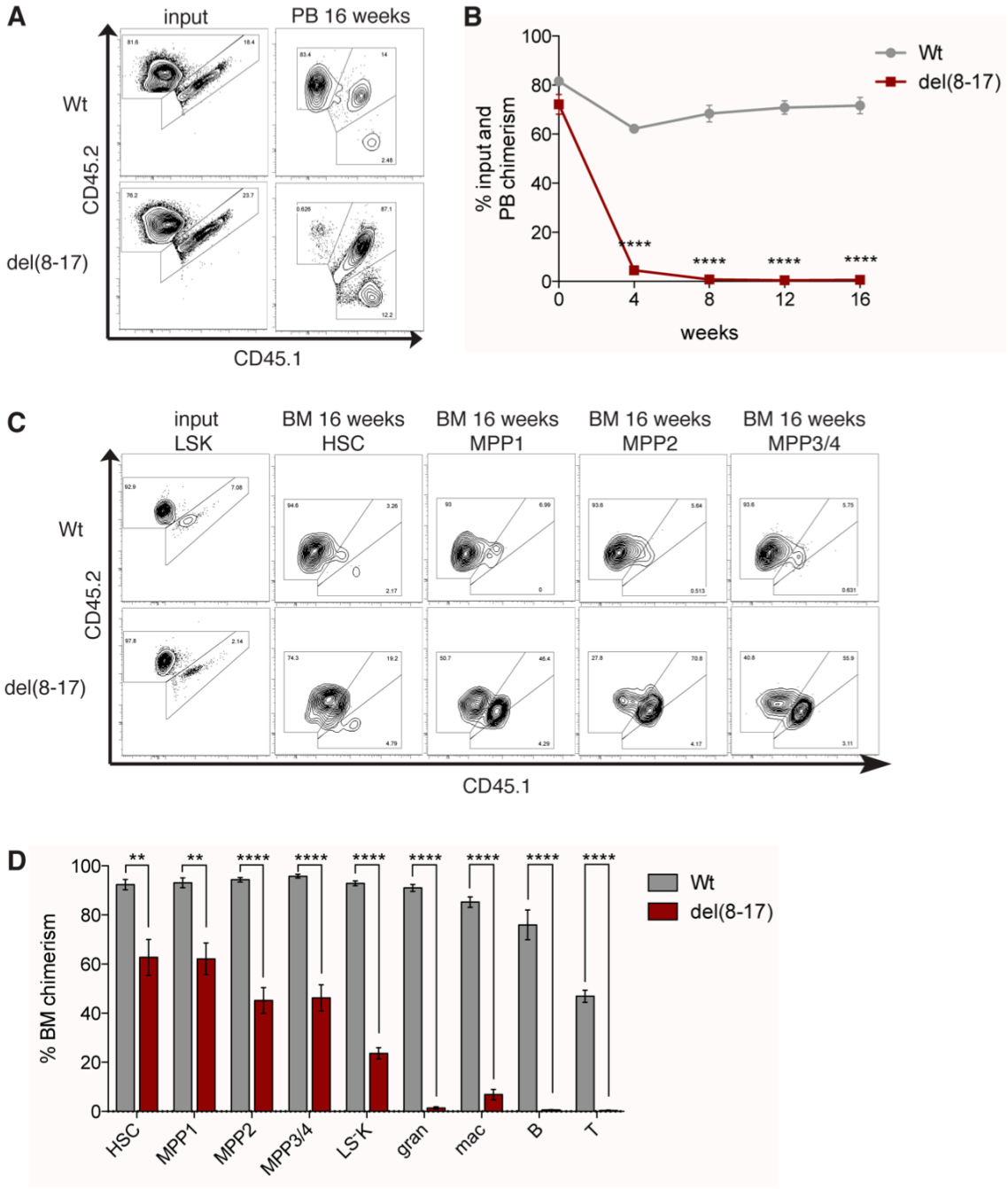

Figure 3.8: Competitive transplantation shows an impaired differentiation potential but retained self-renewal of del(8-17) HSCs

BM cells of 10 days old CD45.2$^+$ del(8-17) or wild type mice were transplanted together with competing CD45.1/2 BM cells in an overall 80:20 ratio intravenously into lethally irradiated CD45.1$^+$ recipient mice. The engraftment of the CD45.2$^+$ was monitored by bleeding the mice every 4 weeks, after 16 weeks the blood and the BM was analyzed for engraftment of different cell populations. **A** Representative flow cytometry profiles of the input ratio as well as engraftment of peripheral blood cells in recipient mice 16 weeks after transplant. **B** Percentage of CD45.2$^+$ cells in the peripheral blood of recipient mice over time. **C** Representative flow cytometry profiles of the LSK input ratio as well as engraftment of different stem and progenitor cells in the BM of recipient mice 16 weeks after transplant. **D** Percentage of CD45.2$^+$ cells from different populations in the BM of recipient mice.

Data shown are mean (±SEM) values (n = 6-8). Statistical significance is indicated for the comparison of del(8-17) to Wt mice; **p≤0.01; ****p≤0.001.

3.3 Enhancer activity in the *c-myc* gene desert

The del(8-17) region does not contain any protein coding gene (chapter 1.3.3, Figure 3.1), nevertheless its deletion causes a dramatic downregulation of *c-myc* in HSPCs and a similar phenotype as mice with a conditional deletion of *c-myc* in hematopoietic cells. As described in chapter 3.1 Dr. Veli V. Uslu generated several mouse lines carrying insertions of the *LacZ* reporter gene at different positions in the *c-myc*/*Pvt1* flanking locus. The positions of selected insertions are indicated in Figure 3.9 A. To screen for possible regulatory input we assessed the expression of these enhancer sensors in several hematopoietic cell types.

We used fluorescein di-(β-D-galactopyranoside) (FDG), a fluorogenic substrate of galactosidase, to measure LacZ expression in BM cells (GUO and WU 2008). After hypotonic loading of the substrate into the cells galactosidase cleaves FDG and releases the fluorescent product FITC, which can then be detected by flow cytometry. We found that when the transposon is inserted at position 17a, the sensor showed strong LacZ expression in HSPCs (LSK) as well as myeloid committed progenitors (LS^-K). LacZ expression from 17a was however very weak in cells positive for the lineage markers (Figure 3.9 B,C). We then assessed LacZ expression in separate stainings for more defined stem and progenitor (Figure 3.9 D), committed progenitor (Figure 3.9 E) and differentiated cell populations (Figure 3.9 F) to see if different cell types show distinct enhancer activity. Within the LSK population LacZ expression declined slightly from HSC to MPP3, while MPP4 showed similar levels as HSCs. Among the committed progenitor populations GMPs had the highest enhancer activity in a similar range as HSCs and MPP4 cells, while LacZ expression in CMPs, MEPs and CLPs was slightly reduced. Among the differentiated cell types only very subtle LacZ expression could be observed, which was highest in erythroblasts and megakaryocytes (Figure 3.10 C). Interestingly, other insertions showed hardly any expression, only a weak, but significant LacZ signal, was detected for 14c and 16a in hematopoietic stem and precursor cells (Figure 3.10 A,D). Thus, this hematopoietic specific expression of the enhancer sensor seemed to be limited to the distal part of the *c-myc*/*Pvt1* flanking locus and it did not extent as a large regulatory domain (SYMMONS *et al.* 2014) contrarily to other enhancers identified in the region (USLU *et al.* 2014).

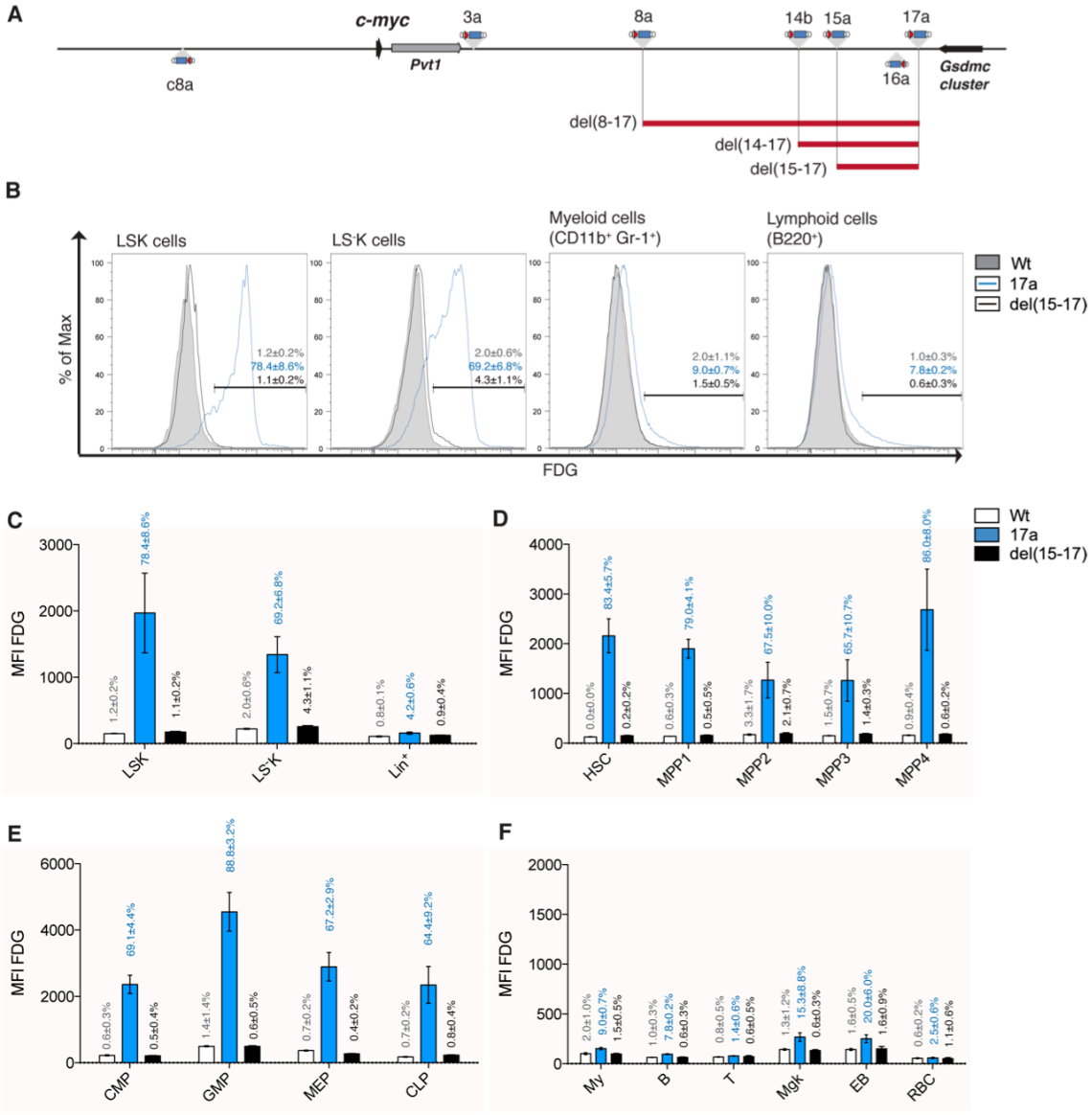

Figure 3.9: Enhancer activity at the distal end of the *c-myc*/*Pvt1* flanking locus
A Murine *c-myc* gene locus on chromosome 15 with flanking regions. Protein coding genes are indicated by black arrows, non-coding genes by grey arrows. Location of insertion sites of transposons are indicated, deletions are depicted as red bars. **B** Representative flow cytometry histograms of FDG stained hematopoietic cells. **C** Quantification of LacZ expression in BM stem and progenitor cells (LSK), myeloid committed progenitors (LS^-K) and differentiated (Lin^+) cells of wild type (Wt), heterozygous 17a and heterozygous del(15-17) mice measured by FDG staining. Bars represent the mean fluorescent intensity (geometric mean) ±SEM and vertically plotted values represent the percentage of positively stained cells ±SD. **D-F** LacZ expression as in **C** in immunophenotypically more defined (**D**) hematopoietic stem and multipotent progenitor populations, (**E**) committed progenitor populations and (**F**) mature effector cells. Data shown are mean values from two independent experiments (n = 3).

To further characterize the function of this enhancer region, we assessed LacZ expression in hematopoietic cells from mice carrying deletions within this region as they retained the *LacZ* reporter gene at the breakpoint (Figure 3.9 A). Besides del(8-17) two more deletions were tested that encompass the sequence in between transposons 14b and 17a (del(14-17)) or 15a and 17a (del(15-17)) (Figure 3.9 A). All three deletions

have the insertion 17a as the telomeric breakpoint, however they differ in size, i.e. 882 kb for del(8-17), 367 kb for del(14-17) and 259 kb for del(15-17). We found that all deletions showed a concomitant loss of LacZ expression in the different hematopoietic cell types, indicating that only the very telomeric part of the *c-myc*/*Pvt1* flanking locus is required for this activity (Figure 3.9 and Figure 3.10). This regulatory region is more than 1.4 Mb away from the *c-myc* gene.

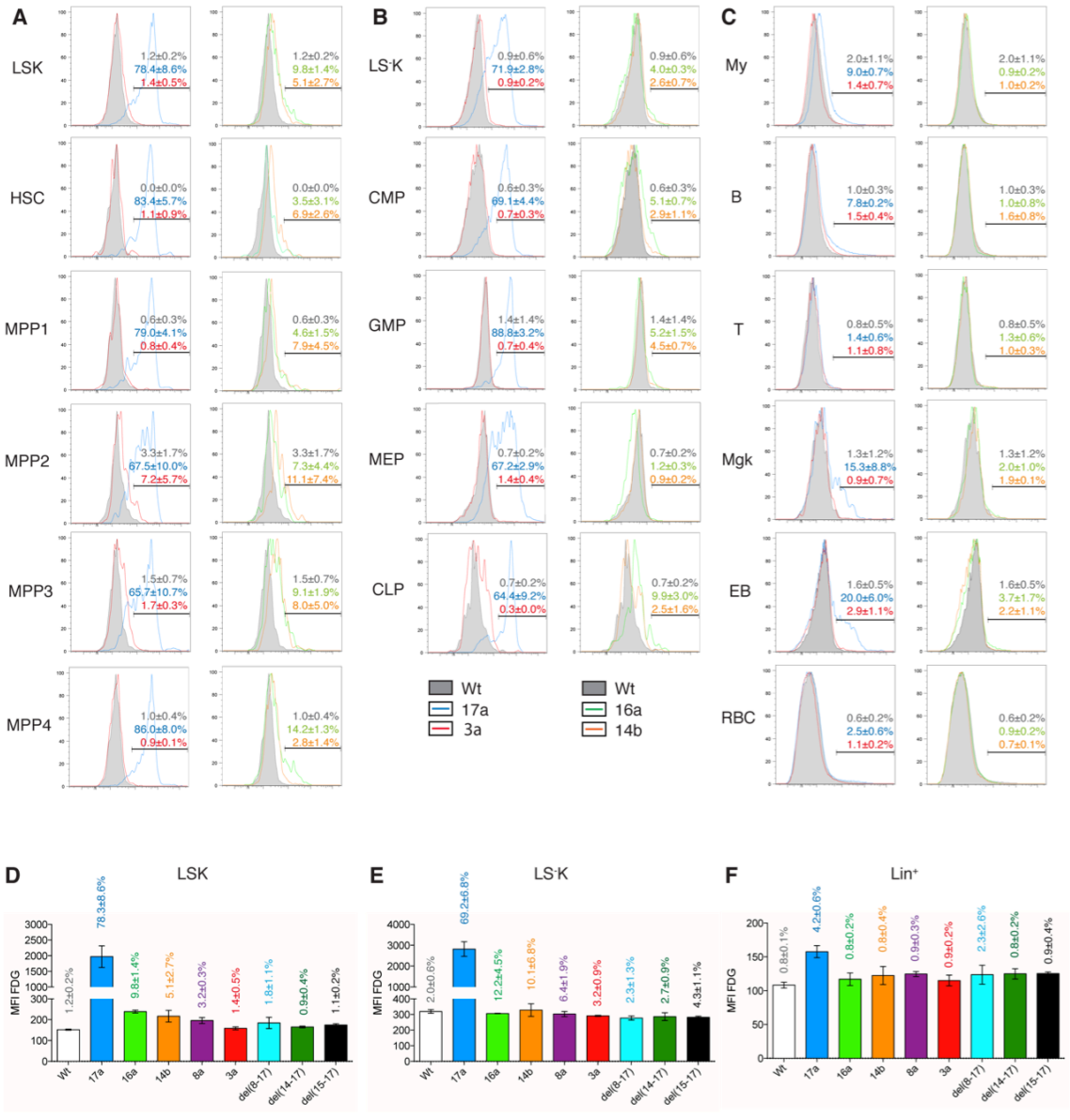

Figure 3.10: Enhancer activity across the *c-myc* gene desert
A-C Representative flow cytometry histograms of FDG stained hematopoietic cells from wild type and heterozygous mice with insertions at 17a, 3a, 14b or 16a. **D-F** Quantification of LacZ expression in BM stem and progenitor cells (LSK), myeloid committed progenitors (LS^-K) and differentiated (Lin^+) cells of wild type (Wt) and heterozygous mice with the indicated insertions measured by FDG staining. Bars represent the mean fluorescent intensity (geometric mean) ±SEM and vertically plotted values represent the percentage of positively stained cells ±SD. Data shown are mean values (n = 2) representative from two independent experiments (n = 3).

3.4 Identification of regulatory elements in the *c-myc*/*Pvt1* flanking locus

3.4.1 The *c-myc* gene is located in a TAD domain

The spatial organization of the genome is intrinsically tied to its biological function, therefore several key aspects can be learned about the relationship between higher order chromatin structure and genome function from global studies of 3D genome organization. Hi-C is a method based on Chromosome Conformation Capture (3C), in which chromatin is crosslinked with formaldehyde, resulting in covalent links between spatially adjacent chromatin segments. Next, the chromatin is digested with a restriction enzyme and the resulting sticky ends are filled with biotinylated nucleotides. Re-ligation is performed under conditions that lead to the creation of chimeric molecules consisting only of fragments that are covalently linked, i.e. they were originally in close spatial proximity. After shearing of the DNA these molecules are isolated by streptavidin beads. DNA sequencing reveals a genome-wide interaction map that can be visualized as two-dimensional contact matrices for each chromosome or specific regions (LIEBERMAN-AIDEN *et al.* 2009).

The REN lab performed as part of the MOUSE ENCODE PROJECT Hi-C analyses of embryonic stem cells and terminally differentiated cell types of human and mouse (DIXON *et al.* 2012). Due to their high sequencing depth they could observe highly self-interacting regions that appear as triangles in the two-dimensional heat map. These large, megabase-sized local chromatin interaction domains were termed topological associating domains (TAD) and were bounded by narrow segments where the chromatin interactions appeared to end abruptly, the TAD boundaries. Of note it was observed that TADs are stable across different cell types and also throughout both organisms tested, suggesting that they reflect an inherent property of mammalian genomes.

Hi-C data can be accessed at http://yuelab.org/hi-c/database.php where genomic interactions are graphically illustrated as a heat-map for a selected region in a chosen cell type. Analysis of the *c-myc*/*Pvt1* flanking locus in murine embryonic stem cells revealed that the *c-myc* gene is located in the middle of a large TAD domain that spans over 3 Mb and ends telomerically close to the *Gsdmc* cluster (Figure 3.11). We located the enhancer activity to the del(15-17) region, which is more than 1.4 Mb away from the *c-myc* gene. Still it belongs to the same TAD domain as can be seen in Figure 3.11,

making the interaction between the enhancer within the del(15-17) region and the *c-myc* promoter region a likely event. The genes located at the telomeric site of the del(15-17) region belong to the neighboring TAD, therefore a *cis*-regulation of these genes by an enhancer element within the del(15-17) region is unlikely as the probability of physical interaction is very low. Accordingly we did not observe changes in *Fam49b* expression in del(8-17) LSK cells (Figure 3.7) although this gene is located closer to the enhancer containing del(15-17) region than *c-myc*.

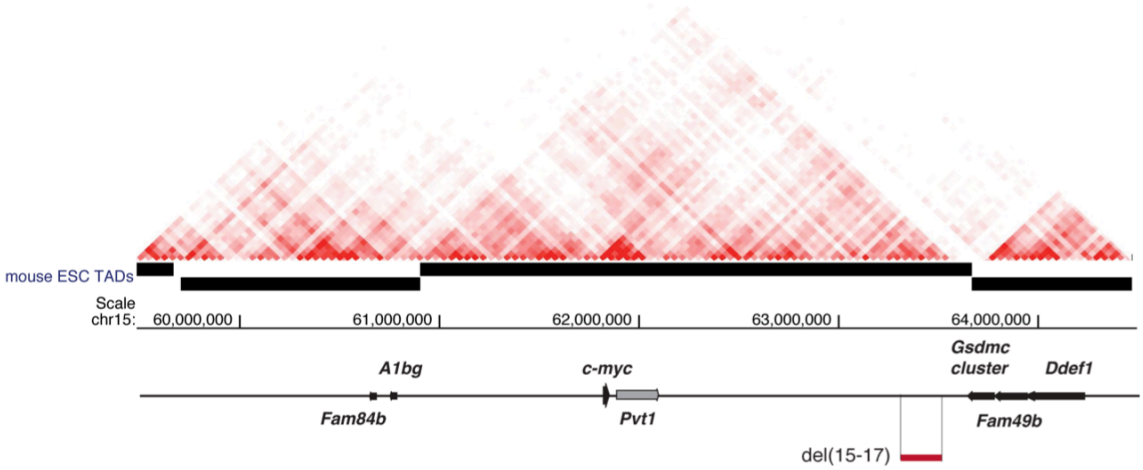

Figure 3.11: The *c-myc*/*Pvt1* flanking locus is located in a large TAD domain
Heat map of Hi-C data of mouse embryonic stem cells (ESC) for the *c-myc*/*Pvt1* flanking locus accessed at http://yuelab.org/hi-c/database.php. Interaction between two loci is viewed as the point where the diagonals originating from each locus intersect. Black bars represent separate mouse ESC TAD domains. Genes and deletion are depicted as in Figure 3.9 A.

3.4.2 Enhancer associated chromatin marks define a distal hematopoietic enhancer cluster (DHEC)

To identify regions that regulate *c-myc* expression during hematopoiesis, we examined publicly available chromatin profiles from hematopoiesis-related tissues (Figure 3.12) (SHEN *et al.* 2012). RNA-seq and promoter-associated marks (H3K4me3, H3K36me3, Pol2) confirmed that the *c-myc*-TAD is located in a large gene desert, comprising only c-*myc* and the non-coding *Pvt1* gene, flanked centromerically by *A1bg* and *Fam84b* and telomerically by the *Gsdmc* gene cluster. Enhancer-associated marks (H3K27ac, H3K4me1) highlighted a number of peaks across this interval in hematopoietic tissues: two isolated peaks are located centromerically (450-550 kb from *c-myc*), a proximal cluster of multiple peaks overlapping with *Pvt1* (from 50 kb to 450 kb away from *c-myc*), and another very remote cluster of peaks located at the distal end of the TAD, 1.7 Mb away from *c-myc*. This distal hematopoietic enhancer cluster (DHEC) was observed in BM, bone marrow derived macrophages (BMDM) and fetal

liver, but not in other non-hematopoietic tissues, suggesting that this region may act as a tissue-specific enhancer.

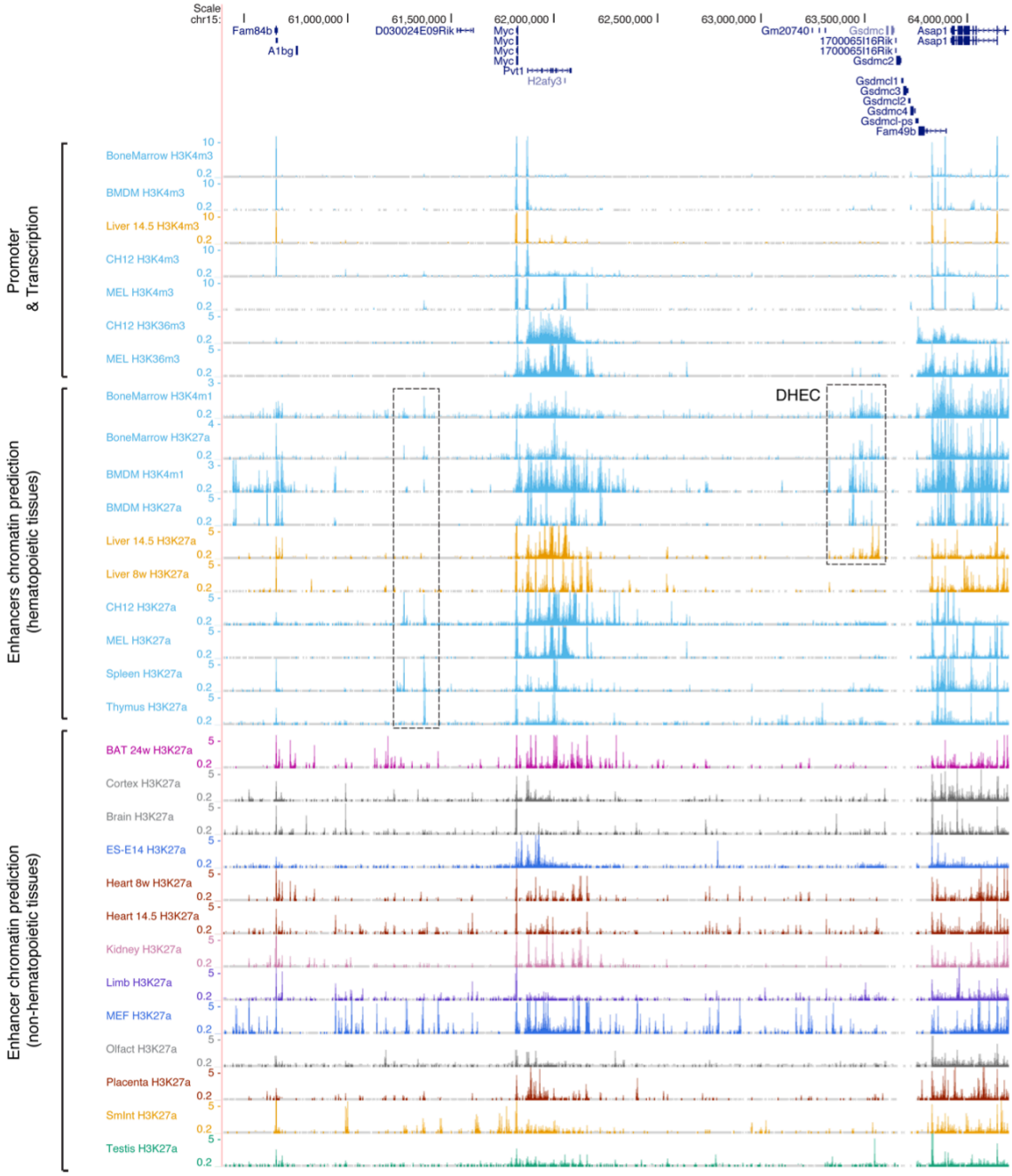

Figure 3.12: Regulatory elements in the *c-myc* gene desert
Murine *c-myc* gene locus on chromosome 15 with flanking regions. Annotated genes are indicated. Top lines show chromatin modifications in different hematopoietic tissues associated with promoter and active transcription (H3K4me3 and H3K36me3). Middle lines show chromatin modifications in different hematopoietic tissues associated with enhancers (H3K4me1 and H3K27ac). Bottom lines show chromatin modifications in different non-hematopoietic tissues associated with enhancers (H3K4me1 and H3K27ac). Only hematopoietic tissues show enhancer marks at the distal end of the *c-myc*/*Pvt1* flanking locus, entitled DHEC.
Abbreviations: DHEC: distant hematopoietic enhancer cluster; H3K4m3: trimethylation of 4th lysine residue of histone 3; H3K4m3: monomethylation of 4th lysine residue of histone 3; H3K27a: acetylation of 27th lysine residue of histone 3; BMDM: BM derived macrophages; CH12: B-cell lymphoma cell line (GM12878 analog); MEL: leukemia cell line (K562 analog); BAT: Brown adipocytes tissue; ES-E14: mouse embryonic stem cell line E14; MEF: mouse embryonic fibroblast; Olfact: Olfactory bulb; Smint: Small intestine.

3.5 Characterization of the DHEC by del(15-17) deletion

3.5.1 Effect of del(15-17) deletion on the distribution of hematopoietic cells in the bone marrow

The greatest part of the DHEC is located within the del(15-17) region therefore we had the possibility to address the phenotypical consequences upon its deletion in homozygous del(15-17) mice. In contrast to del(8-17) mice (chapter 3.2), where the deletion encompassed the DHEC and additional 774 kb of its centromerically located sequence, this smaller deletion did not lead to postnatal lethality. Instead, del(15-17) mice were viable, fertile and did not show any overt phenotype.

Although the body weight of adult del(15-17) mice was within the normal range we observed a significant reduction in BM cellularity (Figure 3.13 A,B) as compared to control mice having one *c-myc* allele flanked by *loxP* sites. This genomic modification did not alter *c-myc* expression levels as shown by TRUMPP *et al.* (2001), neither in a heterozygous nor homozygous setting.

Similar to what we found in mice carrying the 882 kb deletion, we found a more than 3-fold accumulation of LSK cells (Figure 3.13 C). Further refinement of this population using the Slam markers CD150 and CD48 as well as CD135 and CD34 (CABEZAS-WALLSCHEID *et al.* 2014; WILSON *et al.* 2008) revealed an accumulation of the multipotent progenitor populations MPP2, 3 and 4, whereas the number of HSCs and MPP1 remained unchanged (Figure 3.13 D,E). Flow cytometric analysis of the mature lineages in the BM revealed a strong decrease in granulocytes and B cells while the number of T cells, macrophages ($CD11b^+$ $Gr\text{-}1^-$) and erythrocytes remained unchanged. In contrast the number of megakaryocytes defined by expression of CD41 increased significantly (Figure 3.13 F,G). Thus the hematopoietic phenotype closely resembled the one found in 10 days old del(8-17) mice, suggesting that the overall changes in the hematopoietic system regarding stem, progenitor and differentiated cell populations did not account for the postnatal lethality and reduced body size of del(8-17) pups.

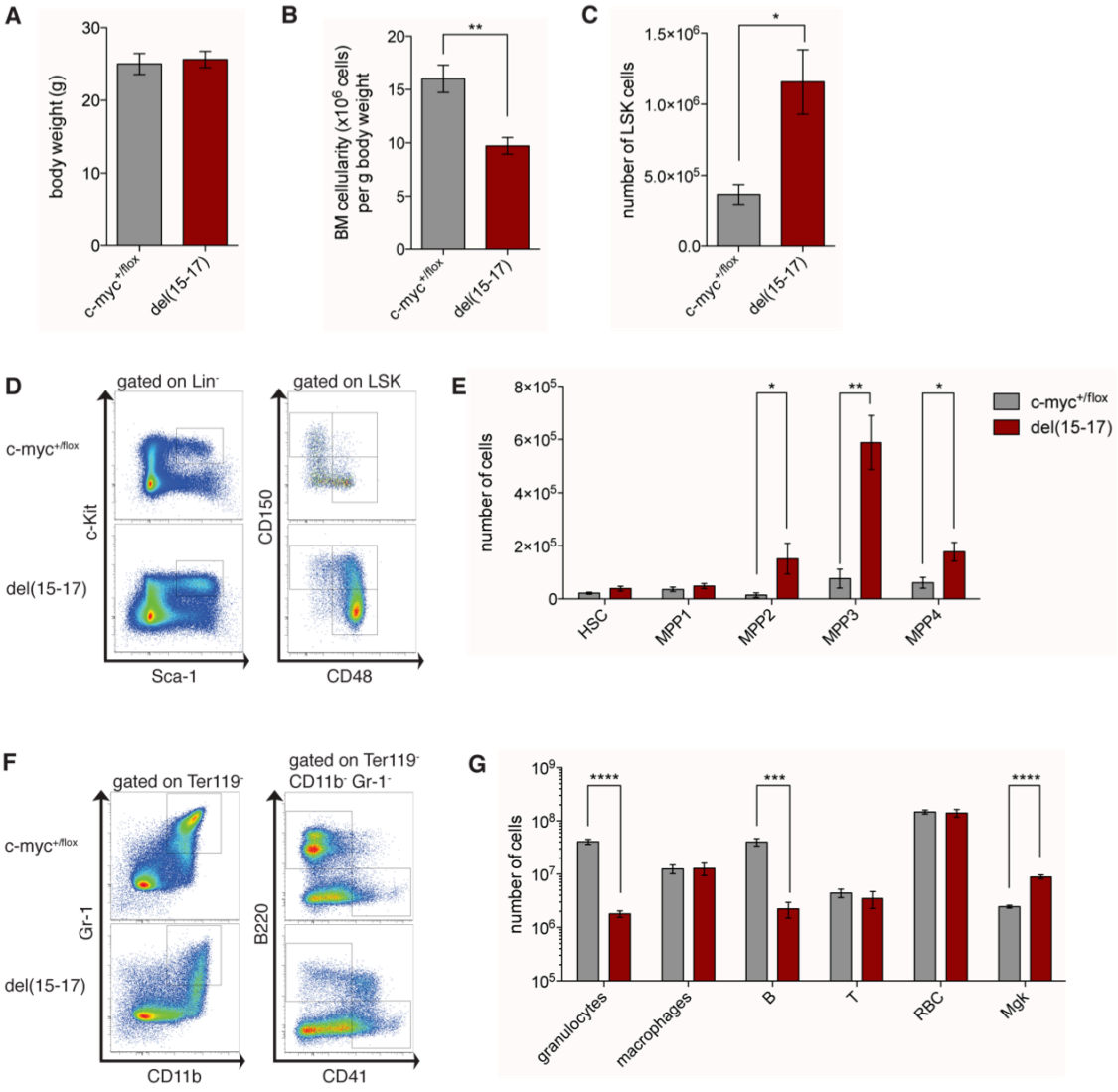

Figure 3.13: Deletion of the del(15-17) region leads to an accumulation of multipotent progenitor cells and a disturbed appearance of mature effector cells
Comparison of adult homozygous del(15-17) mice to control c-myc$^{+/flox}$ mice. **A** Body weight. **B** BM cellularity per g body weight. **D** Representative flow cytometry profiles of Lin$^-$ gated and LSK gated BM cells. **E** Quantitative and statistical analysis of stem and progenitor cell numbers in the BM (n = 4-5). **F** Representative flow cytometry profiles of BM cells stained for differentiated cell types. **E** Quantitative and statistical analysis of numbers of differentiated cell types in the BM (B, B cells; T, T cells; RBC, red blood cells; Mgk, megakaryocytes) (n = 5).
Data shown are mean (±SEM) values. Statistical significance is indicated; *p≤0.05; **p≤0.01; ***p≤0.005; ****p≤0.001.

3.5.2 Del(15-17) HSCs reconstitute stem and progenitor cells but lack differentiation potential after competitive transplantation

To investigate the repopulation potential of del(15-17) HSCs we performed a competitive transplantation assay in a similar setting as for the del(8-17) mice (chapter 3.2.4). Since del(15-17) mice did not show any postnatal lethality as opposed to del(8-17) mice (chapter 3.2), we could transplant adult BM cells to assess HSCs function. In contrast the previous transplantation had to be performed with BM cells from 10 days old mice due to their postnatal lethality. Since HSCs pass through some essential changes during development, they might exhibit different characteristics in transplantation experiments compared to adult HSCs (MIKKOLA and ORKIN 2006).

BM cells were harvested from homozygous del(15-17) as well as wild type mice (CD45.2) and were intravenously transplanted into lethally irradiated congenic recipients (CD45.1) together with BM competitor cells (CD45.1/2) in a 80:20 ratio. Since the absolute frequency of HSCs in the BM of the donor del(15-17) mice was higher than in the control donor mouse the amount of transplanted HSCs was 4-fold higher.

Already 4 weeks post transplant, del(15-17) HSCs failed to reconstitute the peripheral blood compartments of recipient mice (Figure 3.14 B). Strikingly, analysis of BM chimerism 16 weeks after transplantation revealed an accumulation of del(15-17) HSCs (Figure 3.14 C,D). The accumulation of immunophenotypically defined multipotent progenitor cells observed in del(15-17) mice did not become evident in competitively transplantated mice. Although under homeostatic conditions del(15-17) HSCs are capable to generate macrophages, T cells, red blood cells and megakaryocytes at normal or even increased numbers, almost no mature effector cell type was derived from del(15-17) HSCs in the transplantation situation. Red blood cells and platelets do not express the hematopoietic cell marker CD45, therefore they are usually not evaluated in transplantation assays. However, very early erythrocyte progenitors and megakaryocytes still express intermediate levels of CD45 (DARZYNKIEWICZ *et al.* 2009), therefore we also assessed the BM chimerism of recipient mice for $CD71^+$ erythrocyte progenitors (EP) and $CD41^+$ megakaryocytes (Mgk). Donor derived cells were detectable from both populations in mice transplanted with wild type BM cells, however del(15-17) HSCs did hardly give rise to these cell types.

In summary, del(15-17) HSCs accumulated almost to wild type levels in the BM of transplanted mice. While control donor HSCs generated normal proportions of stem

and progenitor cell types as well as of mature lineages, del(15-17) chimerism levels decreased continuously along the hematopoietic hierarchy.

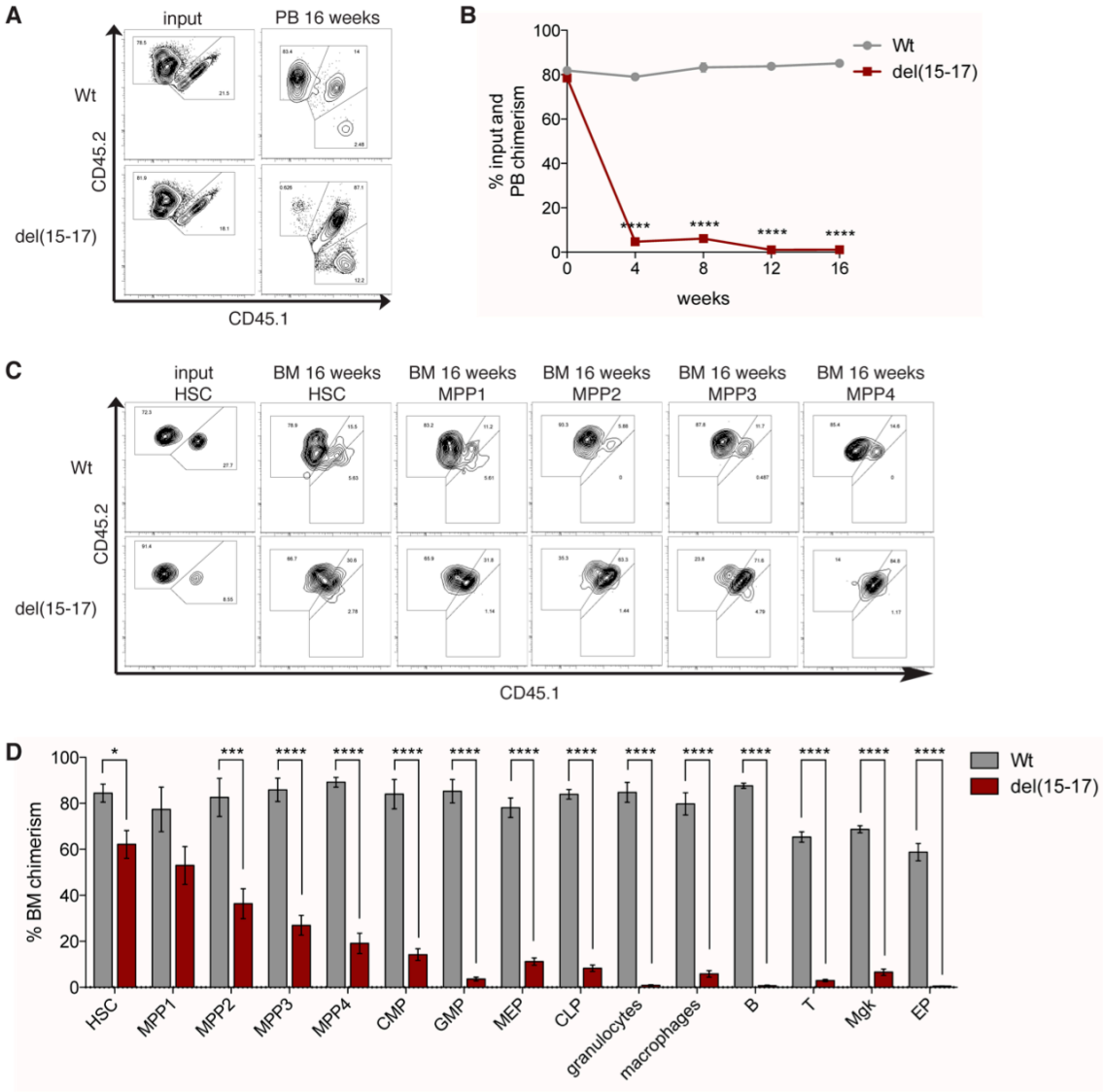

Figure 3.14: Competitive transplantation shows an impaired differentiation potential but retained self-renewal of del(15-17) HSCs

BM cells of adult CD45.2$^+$ del(8-17) or wild type mice were transplanted together with competing CD45.1/2 BM cells in an overall 80:20 ratio intravenously into lethally irradiated CD45.1$^+$ recipient mice. The engraftment of the CD45.2$^+$ was monitored by bleeding the mice every 4 weeks, after 16 weeks the blood and the BM was analyzed for engraftment of different cell populations. **A** Representative flow cytometry profiles of the input ratio as well as engraftment of peripheral blood cells in recipient mice 16 weeks after transplant. **B** Percentage of CD45.2$^+$ cells in the peripheral blood (PB) of recipient mice over time. **C** Representative flow cytometry profiles of the HSC input ratio as well as engraftment of different stem and progenitor cells in the BM of recipient mice 16 weeks after transplant. **D** Percentage of CD45.2$^+$ cells from different populations in the BM of recipient mice.

Data shown are mean (±SEM) values (n = 6-8). Statistical significance is indicated for the comparison of del(8-17) to Wt mice; *p≤0.05; ***p≤0.005; ****p≤0.001.

3.6 The DHEC is acting *in cis* on *c-myc*

3.6.1 Compound heterozygous mice prove allelism between DHEC and *c-myc*

Deletion of the del(15-17) region and therefore of the DHEC led to a phenotype closely related to the phenotype observed by deleting *c-myc* in hematopoietic cells (GUO *et al.* 2009; WILSON *et al.* 2004). In addition deletion of the del(8-17) region that also encompasses the DHEC led to a dramatic *c-myc* downregulation in a population containing stem and progenitor cells, suggesting that the DHEC acts upstream of *c-myc* in these cells. To prove if this regulation is direct we crossed a heterozygous del(15-17) mouse with heterozygous *c-myc*^{KO} mice (c-myc$^{flox/KO}$) to generate compound heterozygous mice carrying one enhancer deletion allele and one *c-myc* null allele (del(15-17)/c-myc^{KO}). Similar results described in this chapter were obtained by using del(14-17)/c-myc^{KO} mice (data not shown).

Heterozygosity for either *c-myc* deletion (c-myc$^{KO/Wt}$) or the enhancer deletion (del(15-17)/c-myc^{flox}) did not lead to any overt changes compared to c-myc$^{flox/Wt}$ mice (hereafter also termed wild type mice). Compound heterozygous mice however demonstrated very similar hematopoietic defects to that shown by homozygous del(15-17) mice, thereby proving allelism between *c-myc* and the enhancer region (Figure 3.15). The BM cellularity was significantly decreased whereas the LSK population increased about 4-fold (Figure 3.15 A,B). HSC and MPP1 populations did not differ in absolute cell numbers, but the multipotent progenitor populations MPP2, 3 and 4 expanded (12.8-fold; 8.9-fold; 3.5-fold respectively; Figure 3.15 C,D).

Among the differentiated cell types granulocyte and B cell numbers dropped dramatically, while macrophage and T cell numbers remained stable and the number of megakaryocytes increased. In contrast to the previously described phenotype of homozygous del(15-17) mice compound heterozygotes displayed a reduced number of erythrocytes (62.3% of wild type levels). Thus, *c-myc* expression of the two alleles in homozygous del(15-17) seemed to be sufficient to allow for normal erythrocyte cell numbers (Figure 3.13 F), whereas compound heterozygous mice displayed a mild haploinsuffiency (Figure 3.15 C,D). In support of this conclusion the erythrocyte population of heterozygous c-myc$^{KO/Wt}$ mice decreased to 87.3% of wild type levels, however not significantly.

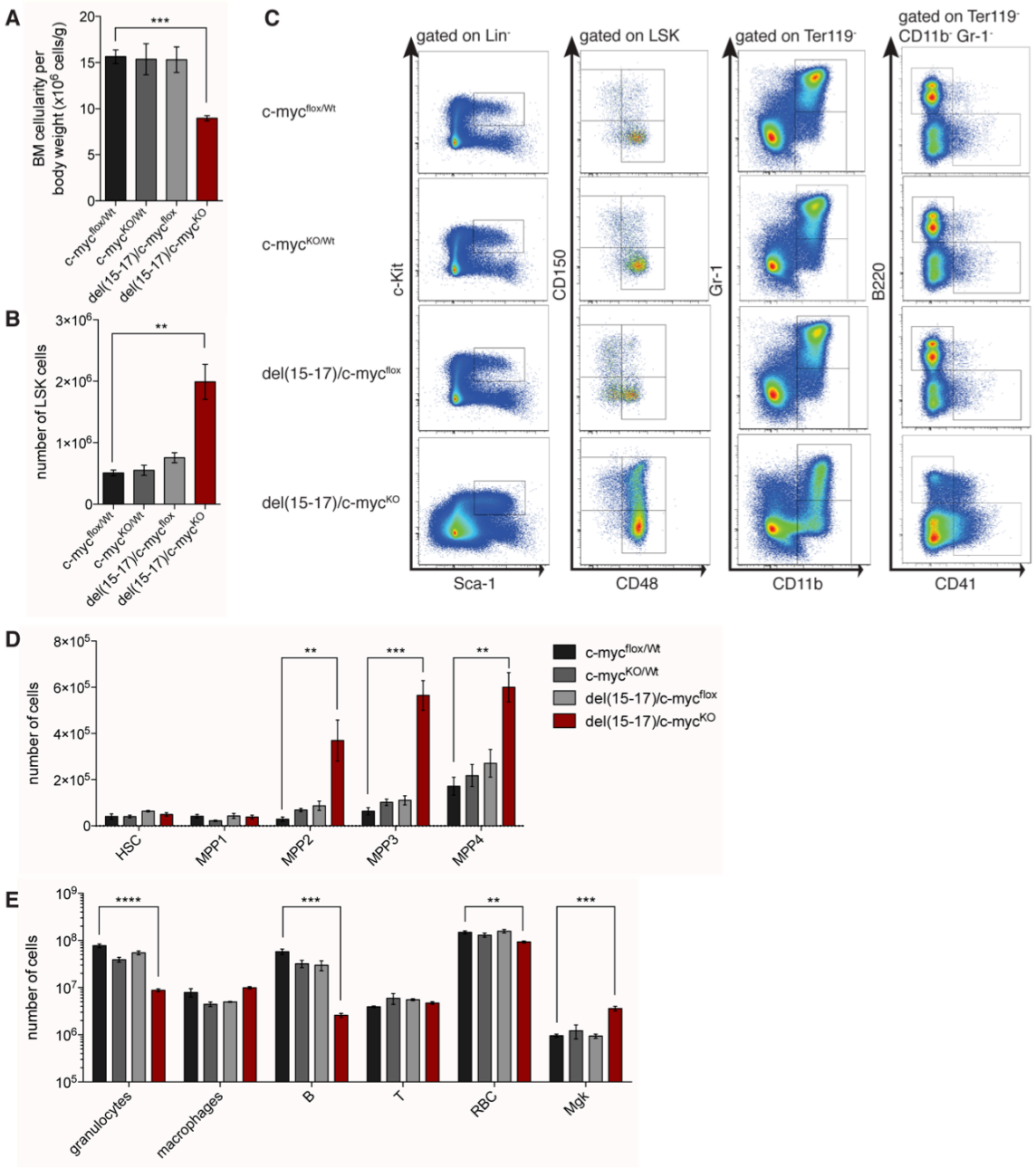

Figure 3.15: Compound heterozygous mice display a similar phenotype as homozygous del(15-17) mice

Comparison of adult c-myc$^{flox/Wt}$, c-myc$^{flox/KO}$, del(15-17)/c-myc^{flox} and del(15-17)/c-myc^{KO} mice. **A** BM cellularity per g body weight. **B** Quantitative and statistical analysis of LSK cell numbers in the BM. **C** Representative flow cytometry profiles of BM cells stained for hematopoietic stem and progenitor cells as well as for differentiated cell types. **D** Quantitative and statistical analysis of stem and progenitor cell numbers in the BM. **E** Quantitative and statistical analysis of numbers of differentiated cell types in the BM (B, B cells; T, T cells; RBC, red blood cells; Mgk, megakaryocytes).

Data shown are mean (±SEM) values (n = 4). Statistical significance is indicated; **p≤0.01; ***p≤0.005; ****p≤0.001.

To also address the functional ability we performed a colony-forming unit assay. Using this system it is possible to quantify differentiation potential of multipotent and lineage-restricted progenitors *in vitro* (chapter 1.2.1.1). Isolated BM cells from control (del(15-17)/c-myc^{flox}) and compound heterozygous (del(15-17)/c-myc^{KO}) mice were cultured in M3434 medium, a semi-solid methylcellulose medium supplemented with nutrients and cytokines. Within ten days the progenitors from control BM cells did proliferate, resulting in the formation of discrete colonies. In contrast del(15-17)/myc^{KO} progenitors showed a greatly reduced colony formation (Figure 3.16 A,C). In addition colonies were much smaller in size and cell number (Figure 3.16 B), thus proving that del(15-17)/myc^{KO} progenitor cells have a defect in differentiation towards mature cells.

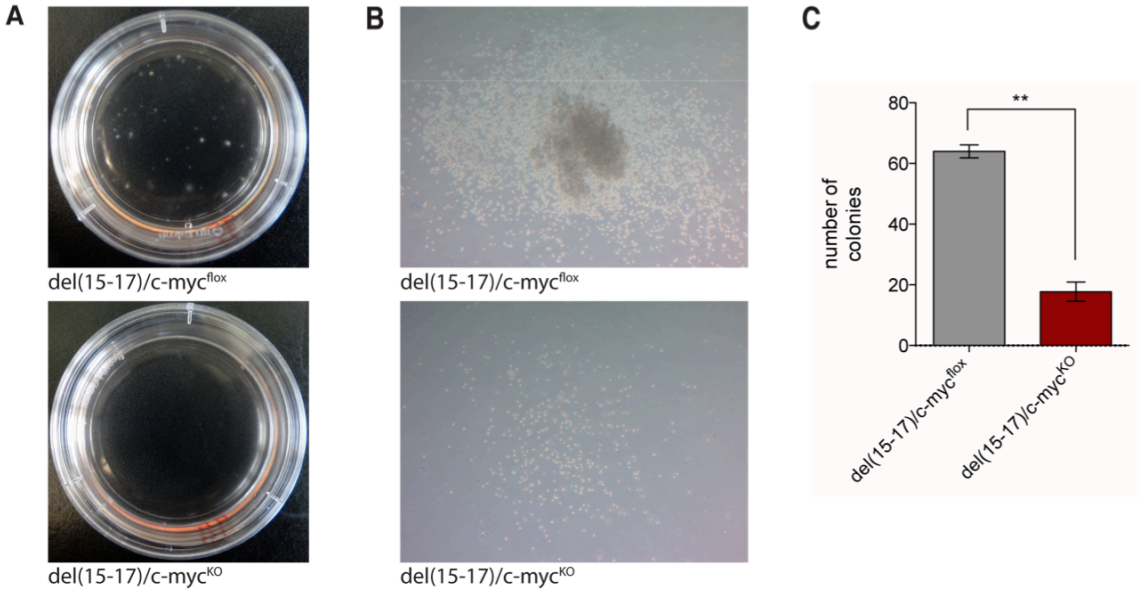

Figure 3.16: Compound heterozygous mice display reduced colony formation ability
20.000 BM cells of del(15-17)/c-myc^{flox} and del(15-17)/c-myc^{KO} mice were seeded into supplemented methylcellulose medium and evaluated after 10 days. **A** Pictures of representative dishes. **B** Microscope images of representative colonies. **C** Quantitative and statistical analysis of counted colony numbers.
Data shown are mean (±SEM) values (n = 4). Statistical significance is indicated; **p≤0.01.

3.6.2 Gene expression upon deletion of the DHEC

We sought to determine the relevance of the DHEC for endogenous gene expression in hematopoietic cells in detail. This issue was already addressed using the del(8-17) mice which showed a reduction of *c-myc* expression to barely detectable levels in LSK cells (Figure 3.7). Next we wanted to examine expression levels in better defined stem and progenitor populations and also committed progenitor and differentiated cell types. For this reason we sorted the different cell types from compound heterozygous mice as well as c-myc$^{flox/Wt}$ (wild type) and heterozygous c-myc$^{KO/Wt}$ mice and performed qRT-PCR analyses. Wild type expression of *c-myc* was

highest in stem and progenitor populations as opposed to the differentiated cell types (Figure 3.17 A). In detail, HSCs, MPPs, GMPs and MEPs showed equal *c-myc* expression levels, whereas CMP levels were almost 2-fold higher and CLP levels 2-fold decreased as compared to the HSC level. Differentiated cell types reached only between 0.5% (granulocytes) to 26.7% (megakaryocytes) of HSC level as illustrated in Figure 3.17 A. Upon deletion of the DHEC *c-myc* expression was lost in HSCs, all MPPs, CMP, GMP and CLP cells. It was also strongly reduced in most mature cell types, except T-cells. Expression of *c-myc* in megakaryocyte-erythrocyte progenitor cells (MEP) was less affected as it was only reduced to 48.3% of c-myc$^{KO/Wt}$ and 30.6% of c-myc$^{flox/Wt}$ levels. In contrast to these effects on hematopoietic cell types, deletion of del(15-17) had no effect on *c-myc* expression in other tissues, such as the embryonic face, limbs, heart and liver (USLU *et al.* 2014).

Moreover we determined expression levels of genes flanking the DHEC. *Gsdmc* expression is very low in HSPCs as we have seen before in del(8-17) LSK cells (chapter 3.2.3), therefore we determined the expression of another telomerically located gene. As expected *Ddef1* expression was not significantly changed by the DHEC deletion (Figure 3.17 C). On the centromeric side *Pvt1* expression was hardly detectable. *Fam84b* expression was not significantly diminished upon deletion of the DHEC, instead we observed significantly upregulation for some progenitor cell types and granulocytes (Figure 3.17 D).

To check for compensatory mechanisms we also determined *N-myc* expression in all samples. In contrast to *c-myc*, *N-myc* was highly expressed only in HSCs and decreased steadily in subsequent populations. These results overall confirmed the published gene expression levels of the Myc family members and proved the predominant role of *c-myc* in the hematopoietic system while only the most primitive cells at the top of the hierarchy concomitantly expressed *c-myc* and *N-myc* (LAURENTI *et al.* 2008). Interestingly, we found that deletion of the DHEC led to a compensatory upregulation of *N-myc* in most populations (Figure 3.17 B). Of note, *N-myc* levels were not changed in HSCs suggesting that in these cells no transcriptional feedback loop is active.

Together, these data showed that the del(15-17) region is allelic to *c-myc*, proving that the DHEC acts as a very distant, yet critical *cis*-acting enhancer for *c-myc* in almost all hematopoietic cell types except T cells and MEPs.

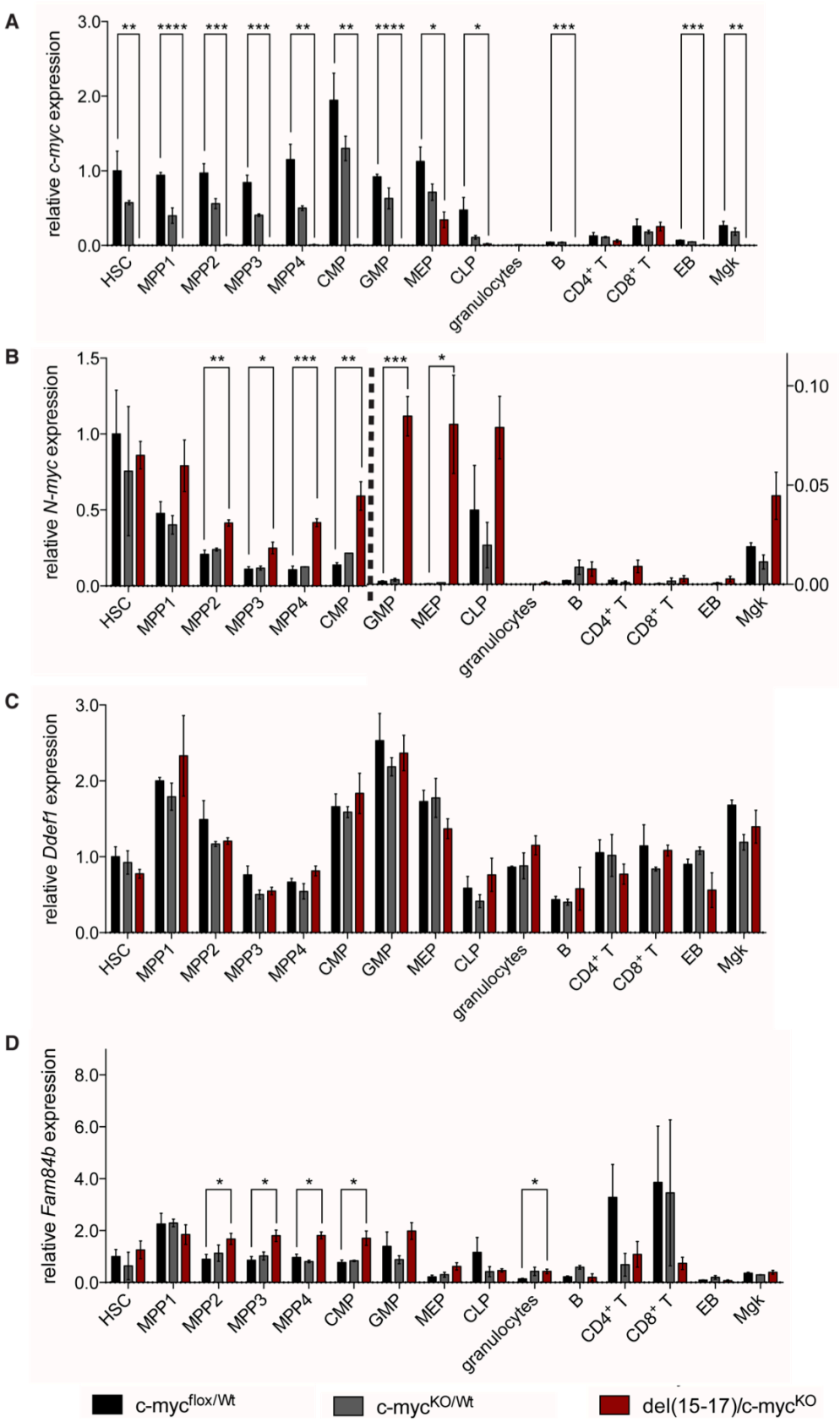

Figure 3.17: Relative gene expression in compound heterozygous mice
mRNA expression of *c-myc* (**A**), *N-myc* (**B**), *Ddef1* (**C**) and *Fam84b* (**D**) by hematopoietic cells of the BM was measured by qRT-PCR in c-myc$^{flox/Wt}$, c-myc$^{KO/Wt}$ and del(15-17)/c-myc^{KO} mice. The scale for *N-myc* expression levels (**B**) is separated; values to the left of the dashed line refer to the left scale, values to the right of the dashed line to the right scale.
Data shown are mean (±SEM) values (n = 3-4); Statistical significance is indicated; *p≤0.05; **p≤0.01; ***p≤0.005; ****p≤0.001.

3.7 Reduction of the distance between *c-myc* and DHEC does not impact on cell frequencies within the hematopoietic system

Next, we were wondering if a reduction of the distance between the DHEC and *c-myc* would impact on its regulation. In a pilot experiment we analysed a del(8-14) mouse compared to a wild type mouse and took the frequencies of hematopoietic cell types as an immediate readout for a potential change in regulation. This deletion excised a 516 kb region between the insertions 8a and 14b (Figure 3.9), thus reducing the distance from 1.7 Mb to 1.2 Mb.

BM cell numbers were in the normal range upon deletion of the del(8-14) region (Figure 3.18 A). Flow cytometric analysis did not reveal strong differences in most quantified hematopoietic populations (Figure 3.18 B-D). Only the number of LSK cells was decreased to 78% of wild type level, which was mostly due to a reduction in numbers of MPP4 cells. However, this tendency is rather contrary to the phenotype upon deletion of the DHEC. Although a larger cohort of mice have to be analyzed to validate this initial experiment and gene expression levels have to be determined, these data suggested that a reduction of the distance between the DHEC and the *c-myc* gene by deletion of the 516 kb spanning del(8-14) region did not impact on *c-myc* expression in hematopoietic cells. Furthermore, this experiment proved that the centromeric part indeed did not account for the hematopoietic phenotype observed in del(8-17) mice. Thus, although the del(8-14) region exhibited enhancer activity regulating *c-myc* in the developing face (USLU *et al.* 2014), these regulatory elements seem not be active in hematopoietic cells. This is in accordance with the locally restricted sensor expression in hematopoietic cells (chapter 3.3) and the broader sensor expression in the embryonic face (USLU *et al.* 2014).

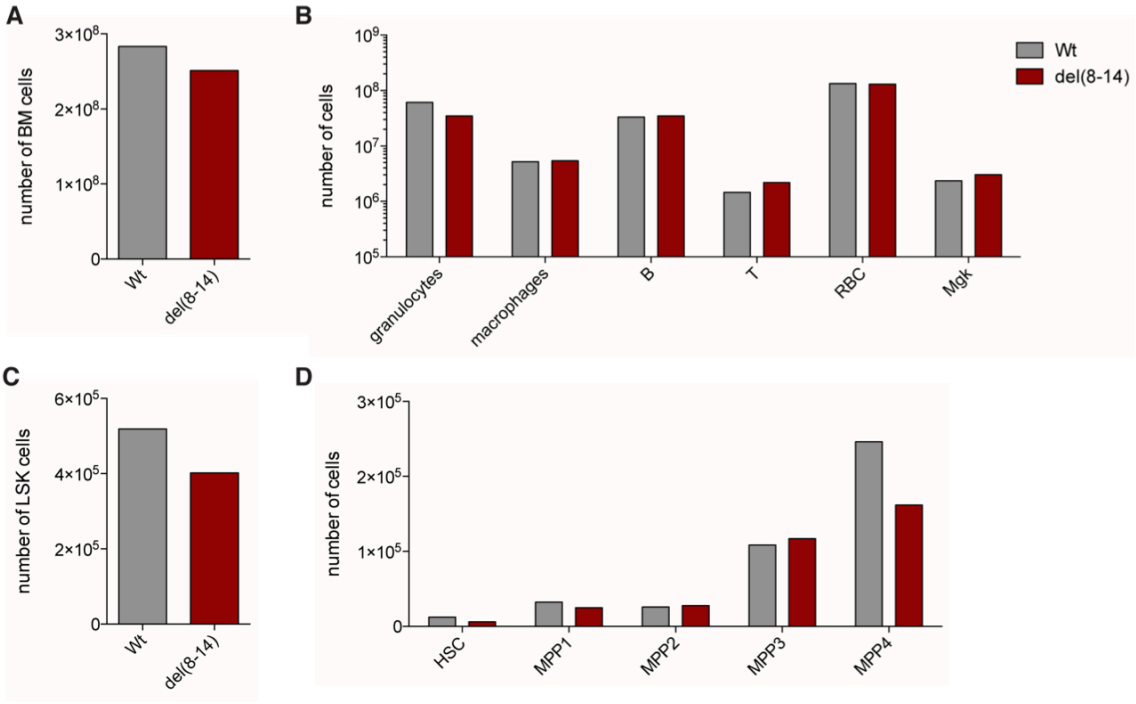

Figure 3.18: A reduced distance between the DHEC and *c-myc* does not change hematopoietic cell frequencies
Comparison of adult wild type and del(8-14) mice. **A** Number of BM cells. **B-D** Quantitative analysis of cell numbers of (**B**) differentiated cell types, (**C**) LSK cells and (**D**) stem and multipotent progenitor cell types in the BM.
Data shown are values from an experiment with 1 mouse per genotype (n = 1).

3.8 Deletion of the DHEC closely but not completely mimicks conditional deletion of *c-myc*

So far the hematopoietic phenotype upon DHEC deletion has only been compared to data of *c-myc* deletion published a decade ago (WILSON *et al.* 2004). However, we were interested to directly compare both phenotypes and also to specify the *c-myc* deletion phenotype in greater detail using additional cell markers to define the hematopoietic stem and progenitor cell compartment. *c-myc* deletion in hematopoietic cells was achieved by treatment of MxCre c-myc$^{flox/flox}$ mice with polyinosinic-polycytidylic acid (poly(I:C)), hereafter termed c-myc$^{\Delta Mx}$. c-myc$^{flox/flox}$ mice that did not have the Cre transgene served as control mice. Since this mouse strain was on a C57Bl/6 background, but the del(15-17) mice that were used for this part of the experiments were on a mixed background we used separate control mice (c-myc$^{+/flox}$). All mice were treated identically with poly(I:C) in order to control for interferon-mediated effects. Interferons have been shown to directly induce proliferation of HSCs (BALDRIDGE *et al.* 2010; ESSERS *et al.* 2009; SATO *et al.* 2009), thus to circumvent this transient effect we analyzed the mice 4 weeks after the first poly(I:C) injection. At this

time point c-myc$^{\Delta Mx}$ mice were reported to display already a clear phenotype (WILSON *et al.* 2004). Del(15-17) mice treated with poly(I:C) did not show any differences to PBS treated animals (data not shown) and untreated del(15-17) animals (chapter 3.5). Hence, in the following part the differences of c-myc$^{\Delta Mx}$ mice to control mice and to del(15-17) deleted mice will be highlighted.

c-myc$^{\Delta Mx}$ mice displayed a reduced body size to 82% of that of control mice (Figure 3.19 A), which was already apparent before treatment of the mice (data not shown). As lowered *c-myc* levels result in reduced body size (TRUMPP *et al.* 2001), the observation of a lower body weight suggested either a leakiness of the transgene and/or interferon production in the mice that can be caused e.g. by stress. The former situation would cause an overall *c-myc* downregulation in all cells of the body, the latter only reduced *c-myc* levels in MxCre targeted cell types. Which of the two scenarios (or both) were valid could be easily addressed by determining gene expression by qRT-PCR and the status of genomic deletion by PCR, however we did not address this question so far as it was not in the scope of this experiment.

To account for the reduced body size the number of BM cells was corrected for the body weight. Both deletions, deletion of *c-myc* and deletion of the del(15-17) region, resulted in a similar reduction of the BM cellularity (Figure 3.19 B).

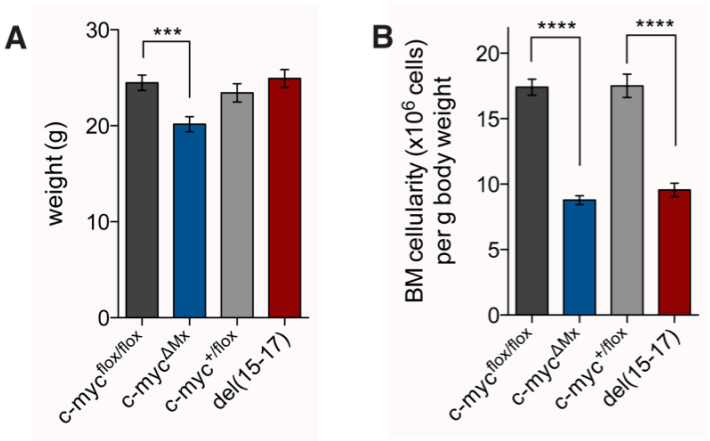

Figure 3.19: The BM cellularity is equally reduced upon *c-myc* and del(15-17) deletion
Comparison of mice with MxCre driven *c-myc* deletion and mice with del(15-17) deletion compared to the respective control mice. **A** Body weight before poly(I:C) injections. **B** BM cellularity 4 weeks after 1st poly(I:C) injection.
Data shown are mean (±SEM) values (n = 6-18). Statistical significance is indicated for the comparison between c-myc$^{flox/flox}$ and c-myc$^{\Delta Mx}$ and between c-myc$^{+/flox}$ and del(15-17); ***p≤0.005; ****p≤0.001.

3.8.1 HSC and progenitor populations upon *c-myc* deletion and DHEC deletion

Flow cytometric quantification of the stem and progenitor cell compartment revealed a similar increase in the number of LSK cells as a result of both deletions (Figure 3.20 A,B). Our analysis revealed that the HSC and MPP compartments in BM cells of c-myc$^{\Delta Mx}$ mice very closely resembled that of del(15-17) mice (Figure 3.13 and Figure 3.20). In both cases the number of the most primitive cells, the HSC and MPP1 cells, were unchanged compared to control populations (Figure 3.20 A,D). This is a striking new observation since so far it was reported that *c-myc* deletion would lead to an increase in HSCs (GUO *et al.* 2009; WILSON *et al.* 2004). However, at that time HSCs were only defined as LSK CD135^{-} cells, a population comprising HSCs, MPP1, MPP2 and MPP3 cells using a much better defining marker combination (CABEZAS-WALLSCHEID *et al.* 2014; WILSON *et al.* 2008). Instead of a change in HSC numbers both deletions led to an increase in the multipotent progenitor populations 2-4.

Analysis of the LS^{-}K population that contains myeloid committed progenitor cells revealed a strong decrease upon *c-myc* deletion to only 6.7% of control levels. The del(15-17) progenitors instead showed only a reduction to 48.6% of control LS^{-}K cells (Figure 3.20 A,C). Further refinement of this committed progenitor population demonstrated a general loss of CLPs, CMPs, GMPs, and in particular MEPs (Figure 3.20 A,E) upon *c-myc* deletion. These results stand in contrast to data from GUO *et al.* (2009), where *c-myc* deletion was associated with preservation of MEP cell numbers. The only difference that could explain this discrepancy lies in the design of the experiment. GUO *et al.* used mice that were 3 weeks old when they started the induction, while in our experiment we used adult mice. The dose of GUO *et al.* was 5 times as much as we used so one might consider a less effective deletion. However, efficiency of deletion was checked in Lin^{-} cells by PCR and showed a clear deletion (Figure 3.20 F).

Del(15-17) mice showed a similar decrease for CLP and GMP cell numbers whereas CMP cell numbers remained present to 59% of control levels and MEPs even to 79%. This represented a remarkable difference between mice deleted for *c-myc* and mice deleted for the DHEC. Most likely this difference is linked to the intermediate *c-myc* levels detected in MEPs upon DHEC deletion (Figure 3.17 A).

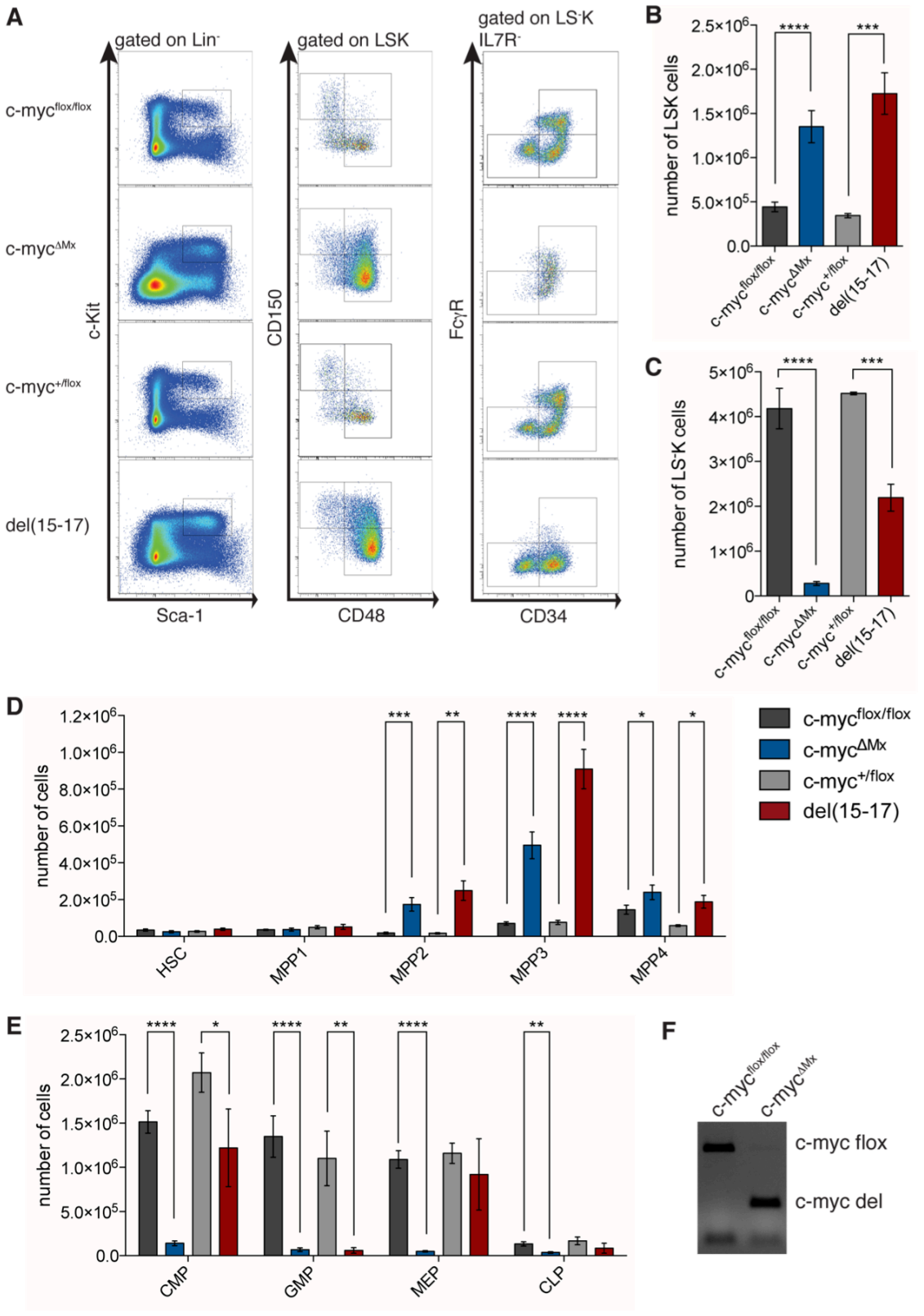

Figure 3.20: The distribution of stem, multipotent progenitor and committed progenitor cells is equally affected by *c-myc* and del(15-17) deletion except for CMPs and MEPs
A Representative flow cytometry profiles of BM cells stained for stem, multipotent progenitor and committed progenitor cells. **B-E** Quantitative and statistical analysis of numbers of (**B**) LSK cells, (**C**) LS$^-$K cells, (**D**) stem and multipotent progenitor cells and (**E**) committed progenitor cells in the BM. **F** Genotyping by PCR of c-myc$^{flox/flox}$ and c-myc$^{\Delta Mx}$ Lin$^-$ cells.
Data shown are mean (±SEM) values (n = 6-17; except for **C,E**: n = 4-8). Statistical significance is indicated for the comparison between c-myc$^{flox/flox}$ and c-myc$^{\Delta Mx}$ and between c-myc$^{+/flox}$ and del(15-17); *p≤0.05; **p≤0.01; ***p≤0.005; ****p≤0.001.

To elucidate the cycling behavior of the stem and progenitor cell compartment we performed a cell cycle analysis by Ki67/Hoechst33342 staining in these cells (Figure 3.21). Firstly, cell cycle analysis revealed a clear difference in the cycling behavior between the control mice of each mouse strain. Control mice of del(15-17) displayed a slightly higher proportion of cells in the G0 phase of the cell cycle for all multipotent progenitor populations which was most prominent in MPP2 cells. Since mice were age and sex matched and the *flox* allele should not have an influence on *c-myc* expression this difference had to originate from the different backgrounds of these mice (C57Bl/6 for *c-myc* deleted mice and mixed background for del(15-17) mice).

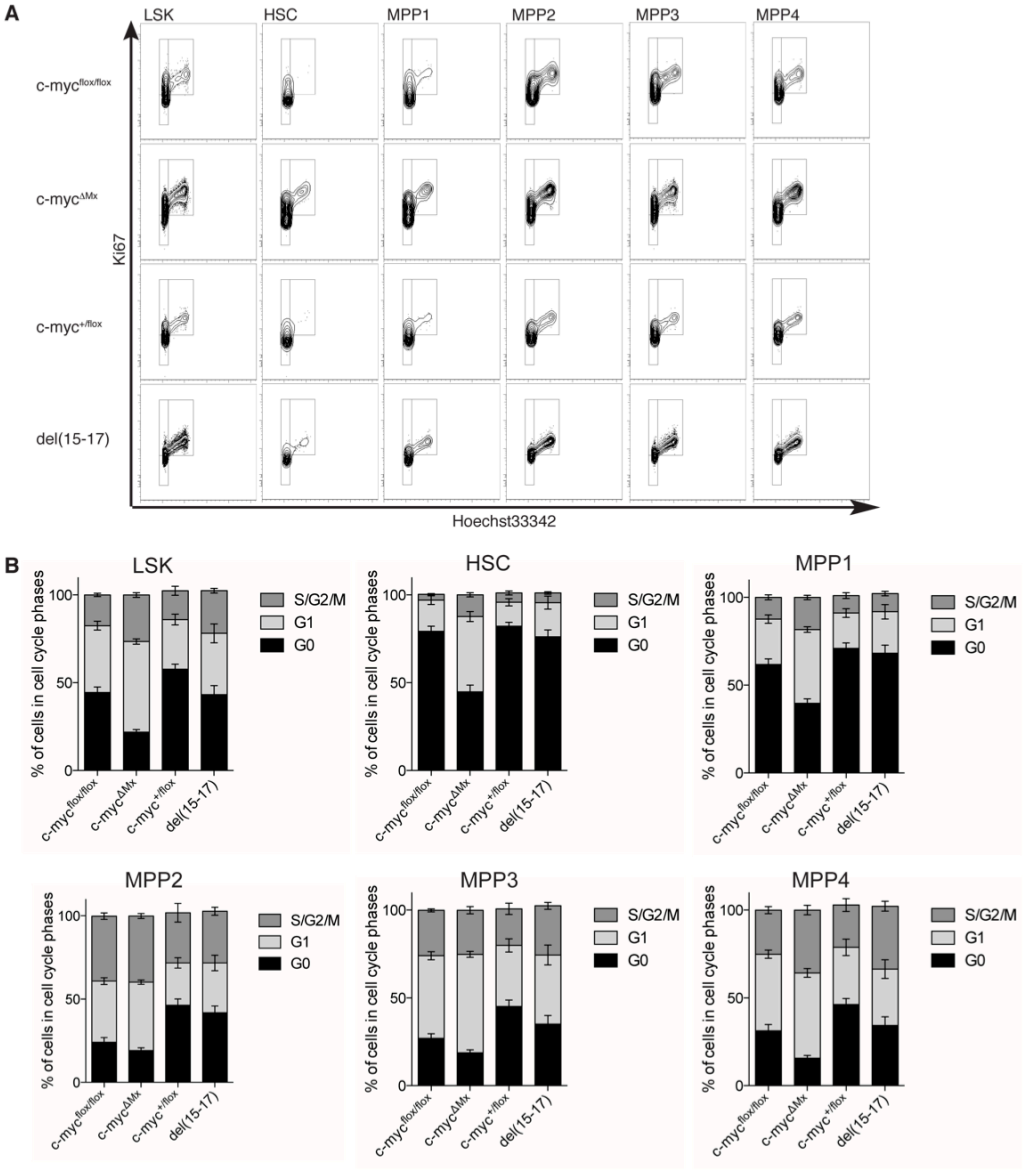

Figure 3.21: The effect of *c-myc* and del(15-17) deletion on the cell cycle profiles of hematopoietic stem and progenitor cell populations
Cell cycle analysis by Ki67/Hoechst33342 staining of stem and multipotent progenitor cell types of *c-myc* deleted and del(15-17) mice compared to the respective controls. **A** Representative flow cytometry profiles of cells gated for the indicated populations. **B-F** Quantitative analysis of the cell cycle in the indicated populations.
Data shown are mean (±SEM) values (n = 6-15).

Compared to their respective control mice, a reduction of cells in the G0 phase could be observed in LSK cells for both deletions. However, it was less extensive for the DHEC deletion and was mostly attributed to the reduction of quiescent cells in MPP3 and MPP4 cells. In contrast *c-myc* deletion showed a greater reduction, which was propagated not only by MPP3 and MPP4, although these cells amount for more than 3 quarter of the LSK cell compartment (WILSON *et al.* 2008) and thus cover most differences in smaller populations. Analysis of the most primitive HSC and MPP1 cells revealed a strong reduction in the proportion of cells being in the G0 phase and a higher proportion of cycling cells.

The previous observation of increased megakaryocyte numbers in del(8-17), del(15-17) and compound heterozygous mice and the hypothesis of a potential short cut between the HSC compartment towards the megakaryocytic lineage prompted us to investigate the levels of the megakaryocytic cell surface marker CD41 in stem and multipotent progenitor cells. Cell surface staining of control BM cells mice and subsequent analysis by flow cytometry revealed the presence of CD41 expressing cells only in cell populations also expressing CD150 (HSC, MPP1 and MPP2) whereas MPP3 and MPP4 showed only a very low mean fluorescence intensity (Figure 3.22). Upon deletion of either *c-myc* or del(15-17) CD41 expression dropped significantly in HSCs and MPP1 while it increases in MPP4. Thus, both deletions lead to a similar shift of the proportion of CD41 expressing cells along the hierarchy towards the late multipotent progenitor cell population.

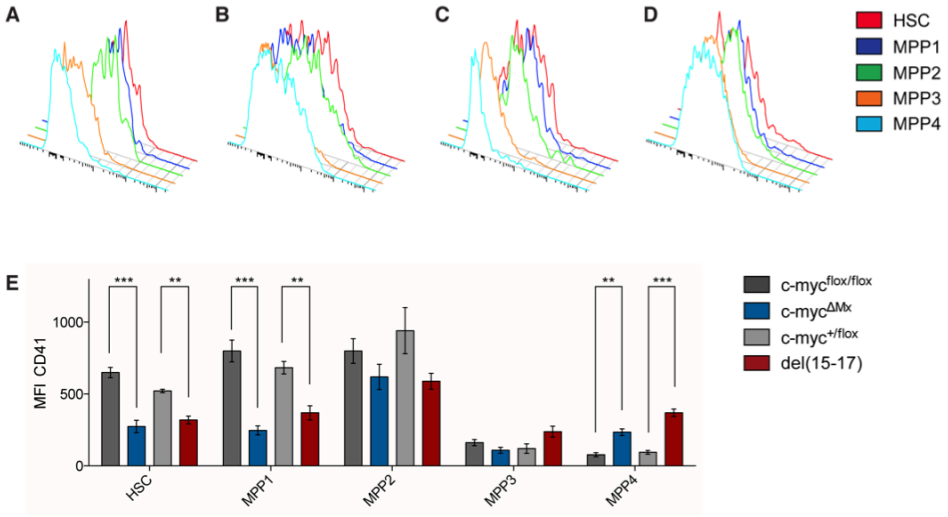

Figure 3.22: Expression of CD41 in HSCs and multipotent progenitor cells is changed upon deletion of *c-myc* and del(15-17)
A-D Representative flow cytometry histograms of CD41 expression in (**A**) c-myc$^{flox/flox}$ mice, (**B**) c-myc$^{\Delta Mx}$ mice, (**C**) c-myc$^{+/flox}$ mice and (**D**) del(15-17) mice. **E** Quantitative and statistical analysis of the mean fluorescence intensity (geometric mean) of CD41 expression in stem and progenitor cells. Data shown are mean (±SEM) values (n = 2-4). Statistical significance is indicated; *p≤0.05; **p≤0.01; ***p≤0.005.

3.8.2 Distribution of mature effector cells upon *c-myc* deletion and DHEC deletion

Flow cytometric analysis revealed similar tendencies between conditional *c-myc* deletion and del(15-17) deletion compared to the respective controls for most differentiated cell types (Figure 3.23). Both deletions led to a decrease in the number of granulocytes, while megakaryocyte numbers increased. Macrophages and T cell numbers remained unaltered when compared to the control mice.

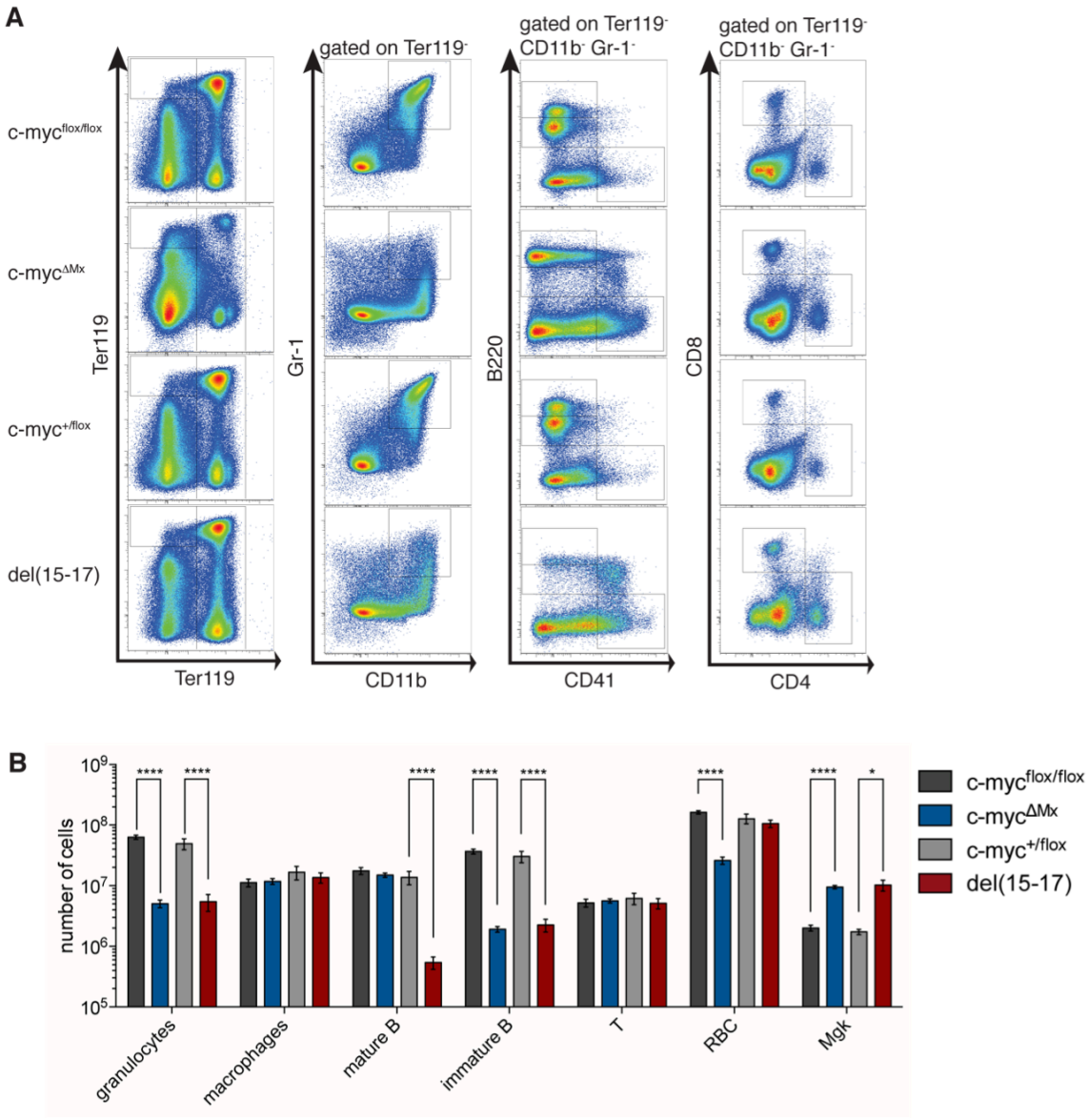

Figure 3.23: The distribution of differentiated cell types is equally affected by *c-myc* and del(15-17) deletion except for erythrocytes
A Representative flow cytometry profiles of BM cells stained for differentiated cell types. **B** Quantitative and statistical analysis of numbers of differentiated cell types in the BM (B, B cells; T, T cells; RBC, red blood cells; Mgk, megakaryocytes).
Data shown are mean (±SEM) values (n = 6-17). Statistical significance is indicated for the comparison between c-myc$^{flox/flox}$ and c-myc$^{\Delta Mx}$ and between c-myc$^{+/flox}$ and del(15-17); *p≤0.05; ****p≤0.001.

Total B cell numbers were less affected by conditional *c-myc* deletion than by del(15-17) deletion. However, the intensity of B220 fluorescence allowed distinguishing between mature ($B220^{high}$) and immature ($B220^{intermediate}$) B lymphocytes. Among these two populations, only the number of immature B cells was strongly reduced and this reduction had the same extend as for del(15-17) mice. The number of mature B cells was however unchanged in c-$myc^{\Delta Mx}$ mice. This could be explained by the longevity of the mature B cells as only 4 weeks had passed since the induction of the deletion (FULCHER and BASTEN 1997).

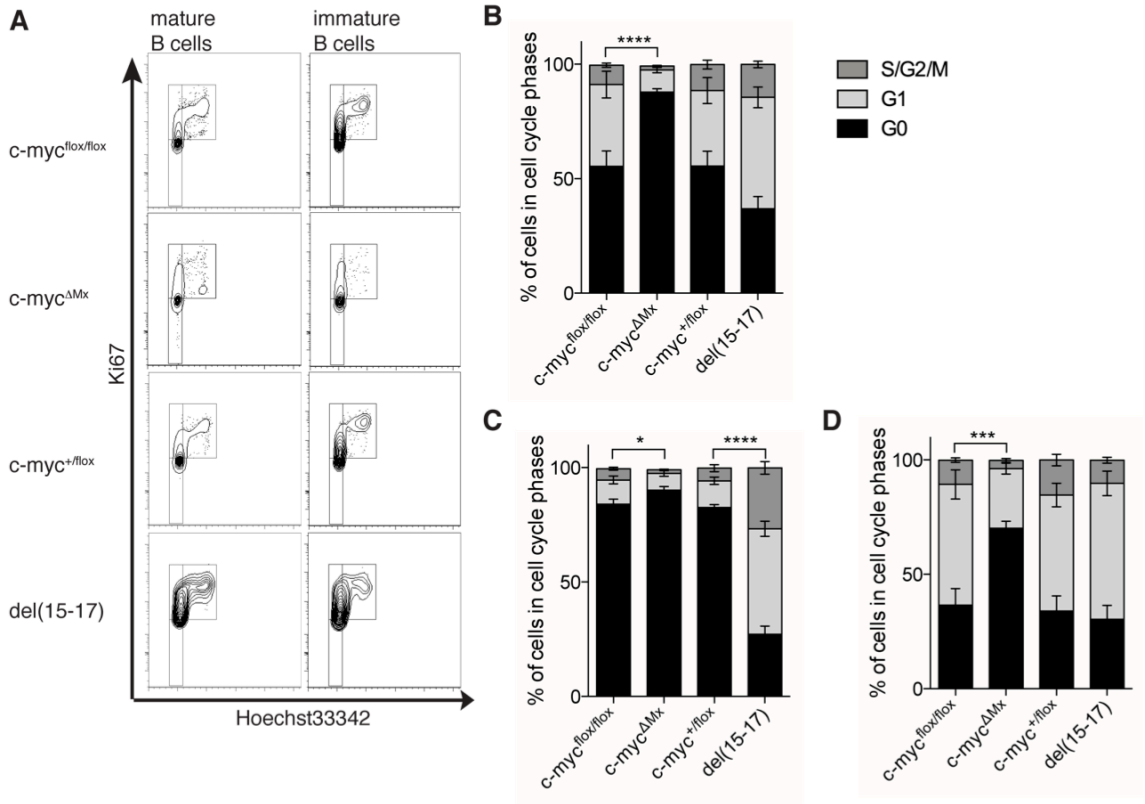

Figure 3.24: The effect of *c-myc* and del(15-17) deletion on the cell cycle profiles of B cells
Cell cycle analysis by Ki67/Hoechst33342 staining of B cells of *c-myc* deleted and del(15-17) mice compared to the respective controls. **A** Representative flow cytometry profiles of cells gated for the indicated populations. **B**-**D** Quantitative and statistical analysis of the cell cycle status in (**B**) overall B cells, (**C**) mature B cells and (**D**) immature B cells.
Data shown are mean (±SEM) values (n = 6-12). Statistical significance is indicated for the comparison in G0 between c-$myc^{flox/flox}$ and c-$myc^{\Delta Mx}$ and between c-$myc^{+/flox}$ and del(15-17); *p≤0.05; ***p≤0.005; ****p≤0.001.

90% of mature B cells of c-$myc^{\Delta Mx}$ mice were in the G0 phase of the cell cycle thus have reached their quiescent state (Figure 3.24 B). This resting population was virtually absent in the BM of del(15-17) mice (Figure 3.23). Among all present B cells in del(15-17) mice a proportion of 37% was in G0 phase of the cell cycle. Thus, these cells are in a more proliferative state similar to immature B cells of control mice (Figure 3.24 D). However, the percentage of cells in G0 was significantly increased for mature

B cells (and the almost depleted immature B cells) of c-myc$^{\Delta Mx}$ mice, reflecting the proliferative function of c-Myc. In summary, although *c-myc* deleted mice had a defect in generating new immature B cells, mature B cells were still present in the BM. Since the del(15-17) deletion was not conditional but straight, the failure in B cell generation was constantly present and thus more apparent in the overall cell number.

The analysis of the erythrocyte population in the BM of *c-myc* deleted mice revealed a decrease of the cell number to only 16% of the same population in control mice (Figure 3.23 B). As it can be seen from the representative flow cytometry profiles (Figure 3.23 A, second panel) all subpopulations within the Ter119^{+} population identified based on CD71 expression and cell size (FSC) were affected by this reduction in cell number, however the more immature cells (CD71^{+}) showed the greatest effect. In contrast del(15-17) erythrocyte numbers were barely changed. This lack in changes in erythrocyte numbers was already apparent as del(15-17) mice did not show signs of anemia like pale feet as reported in animals with a complete deletion of *c-myc* in hematopoietic cells (GUO *et al.* 2009; WILSON *et al.* 2004).

3.8.3 Erythrocytes are differentially affected in the peripheral blood upon *c-myc* or DHEC deletion

The BM is the primary site of hematopoiesis in adult mice, generating billions of cells that enter the blood stream for circulation. Analysis of the peripheral blood of mice with either *c-myc* deletion or del(15-17) deletion showed a similar decrease in the white blood cell count to about half of the cell numbers in blood from control animals (Figure 3.25 A). Both deletions led to increased platelet counts, which was more dramatic in c-myc$^{\Delta Mx}$ mice than in del(15-17) mice. This thrombocytosis was accompanied by a significantly enlarged platelet size as it has been reported by GUO *et al.* (2009) for *c-myc* deletion (Figure 3.25 B,C).

The red blood cell count confirmed the reported anemia in c-myc$^{\Delta Mx}$ mice as it was dramatically decreased, leading to a watery appearance of the blood. This went along with an equally reduced hematocrit (volume of red blood cells relative to blood volume) and hemoglobin concentration (Figure 3.25 D-E). In contrast the blood of del(15-17) had a normal red appearance, however red blood cell counts and the hemoglobin concentration in blood of del(15-17) mice were also reduced but to a lesser extent than for c-myc$^{\Delta Mx}$ mice. Notably, the hematocrit showed only a slight, non-significant reduction. In combination with the more reduced cell count this pointed

towards an increased volume of red blood cells (judged by the extent of fold changes in Figure 3.25 D,E).

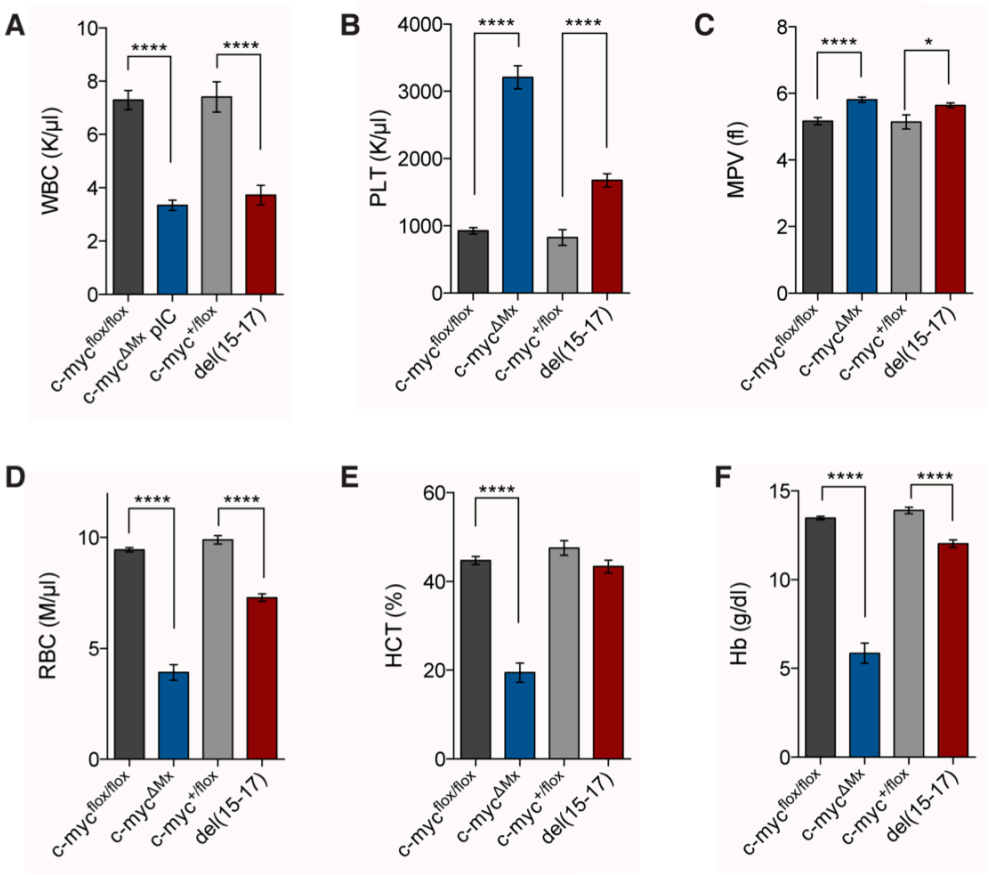

Figure 3.25: Peripheral blood analysis by an automated cell count reveals differences in the erythrocyte phenotype upon *c-myc* or del(15-17) deletion
Quantitative and statistical analysis of peripheral blood properties from c-myc$^{\Delta Mx}$ and del(15-17) mice compared to the respective control mice determined by the automated Hemavet counter. **A** White blood cell count. **B** Platelet count (3 out of 16 values were above the detection limit of 4000 and therefore counted as 4000). **C** Mean platelet volume. **D** Red blood cell count. **E** Hematocrit. **F** Hemoglobin concentration.
Data shown are mean (±SEM) values (n = 6-18). Statistical significance is indicated for the comparison between c-myc$^{flox/flox}$ and c-myc$^{\Delta Mx}$ and between c-myc$^{+/flox}$ and del(15-17); *p≤0.05; ****p≤0.001.

This observation led us to analyze the morphological appearance of erythrocytes and platelets in both mouse strains by peripheral blood smears stained with May-Grünwald/Giemsa. In this staining nuclei, granules of basophil granulocytes, granules of platelets and RNA molecules in the cytoplasm are stained by basic dyes, thus appearing purple, while red blood cells and granules of eosinophil granulocytes are stained by eosin and appear red. Besides of the apparent anemia deletion of *c-myc* promoted an aberrant red blood cell morphology. Erythrocytes were pale in color and contained a large, central pallor due to insufficient hemoglobin content. Additionally a higher number of large erythrocytes with a light blue staining appeared (Figure 3.26, green arrow heads) which are termed polychromatic erythrocytes.

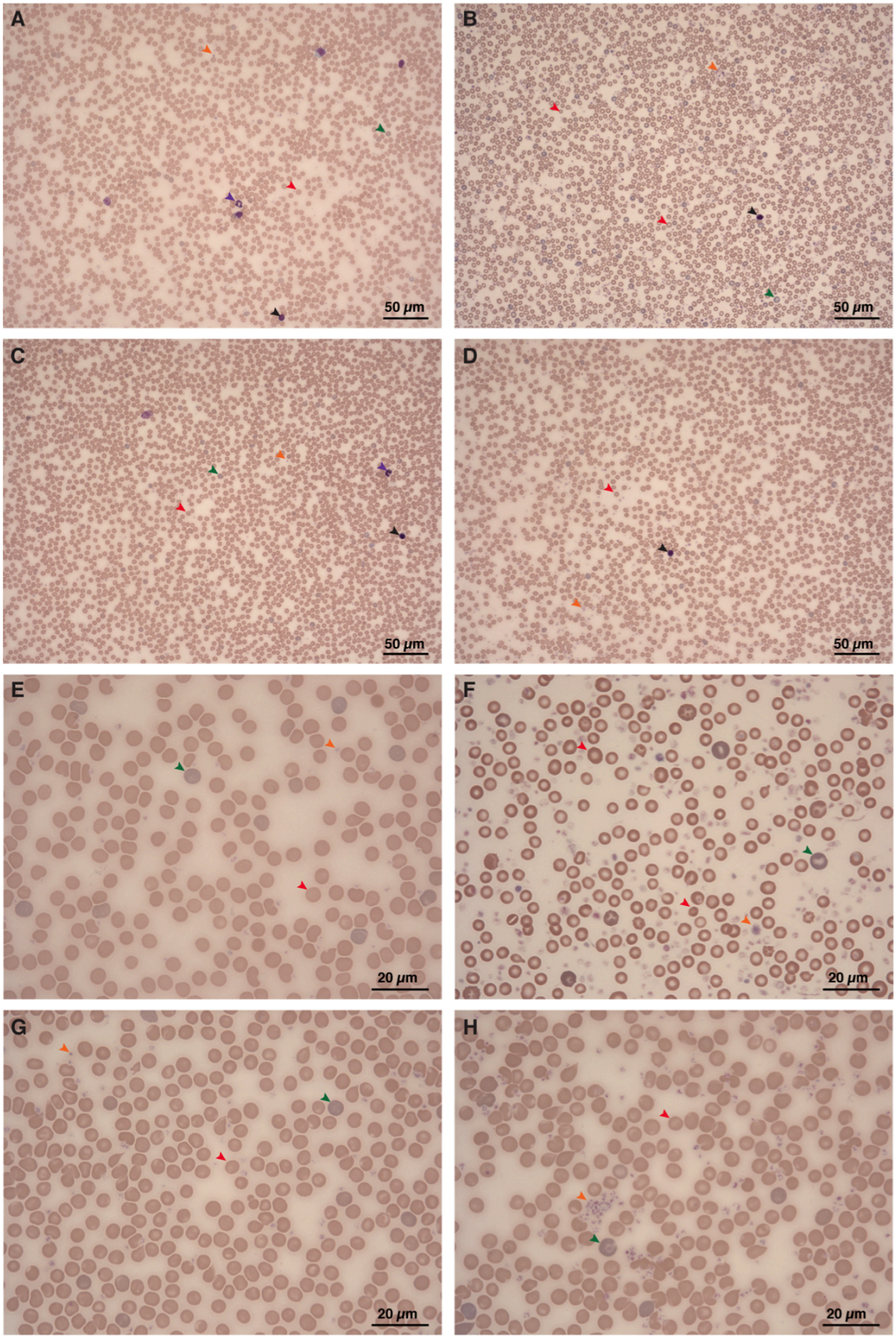

Figure 3.26: Peripheral blood smears show anemia in c-myc$^{\Delta Mx}$ mice which is not apparent in del(15-17) mice

A-D 20x and **E-H** 63x magnification of peripheral blood smears with May-Grünwald/Giemsa staining from (**A,D**) c-myc$^{flox/flox}$ mice, (**B,E**) c-myc$^{\Delta Mx}$ mice, (**C,F**) c-myc$^{+/flox}$ mice and (**D,G**) del(15-17) mice. Coloured arrow heads point at the following cell types: black=lymphocyte; purple=neutrophil; orange=platelet; red=erythrocyte; green=polychromatic erythrocyte.

Polychromatic cells are immature and recently released from the BM, which occurs e.g. in response to acute blood loss, hypoxia, or red blood cell destruction. Thus, their occurrence was in agreement with the strong anemia found in these mice. Furthermore, the erythrocytes showed a striking variation in cell size (Figure 3.26 B,F) which was quantified by measuring the cell perimeter (Figure 3.27 A). The median perimeter decreased significantly from 17.7 µm to 16.0 µm and the cell size showed a strong variability (quantified in (Figure 3.27 B).

In contrast to the erythrocytes of c-myc$^{\Delta Mx}$ mice the morphological appearance of erythrocytes of del(15-17) mice was not dramatically changed. The perimeter of del(15-17) erythrocytes showed a normal distribution width, however with an increased median perimeter (18.4 µm compared to 17.6 µm). At the same time these cells did not display hypochromasia. Instead, the hemoglobin content was in a normal range according to the increased cell size. Thus these observations confirmed the results of the automated cell counter (Figure 3.25). In addition no apparent increase in polychromatic cells was detectable.

The peripheral blood smears additionally confirmed the thrombocytopenia for both deletions (Figure 3.26 B,F,D,H). Increased numbers of platelets were detecable, which sometimes formed aggregates (exemplary in Figure 3.26 H, orange arrow head).

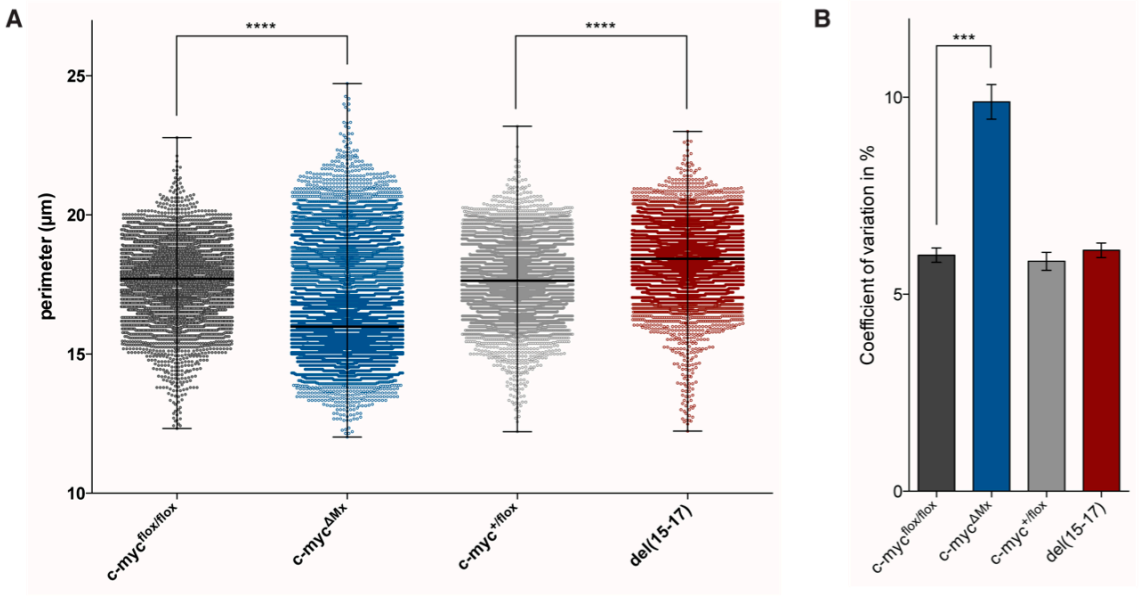

Figure 3.27: The size of erythrocytes in c-myc$^{\Delta Mx}$ mice is decreased and shows a higher variability

Quantitative and statistical analysis of erythrocytes in peripheral blood smears (20x magnification) from c-myc$^{\Delta Mx}$ and del(15-17) mice compared to the respective control mice. **A** Cell size quantified by the perimeter. Data are represented as scatter dot plot with the median values and range (n = 8165-10926 from 4-5 images analyzed). **B** Variability in cell size. Data shown are the mean (±SEM) values (n = 4-5 images).
Statistical significance is indicated for the comparison between c-myc$^{flox/flox}$ and c-myc$^{\Delta Mx}$ and between c-myc$^{+/flox}$ and del(15-17); ***p≤0.005; ****p≤0.001.

Analysis of erythroid progenitor populations in the BM revealed that the most immature proerythroblast population (EB) is slightly but significantly increased upon *c-myc* deletion (Figure 3.28). Similar results were shown by GUO *et al.* (2009). The successive populations EryA, B and C mark progressive steps of erythroblast maturation (KOULNIS *et al.* 2011). These populations were strongly affected by c-Myc deficiency, with most impact on the first two populations. Erythroblast cell numbers of DHEC deleted mice however were not significantly changed at all levels, showing only a slight decrease for EryA cells. Thus c-Myc deficiency led to loss of erythroblast populations in the BM which was not detectable for DHEC deletion.

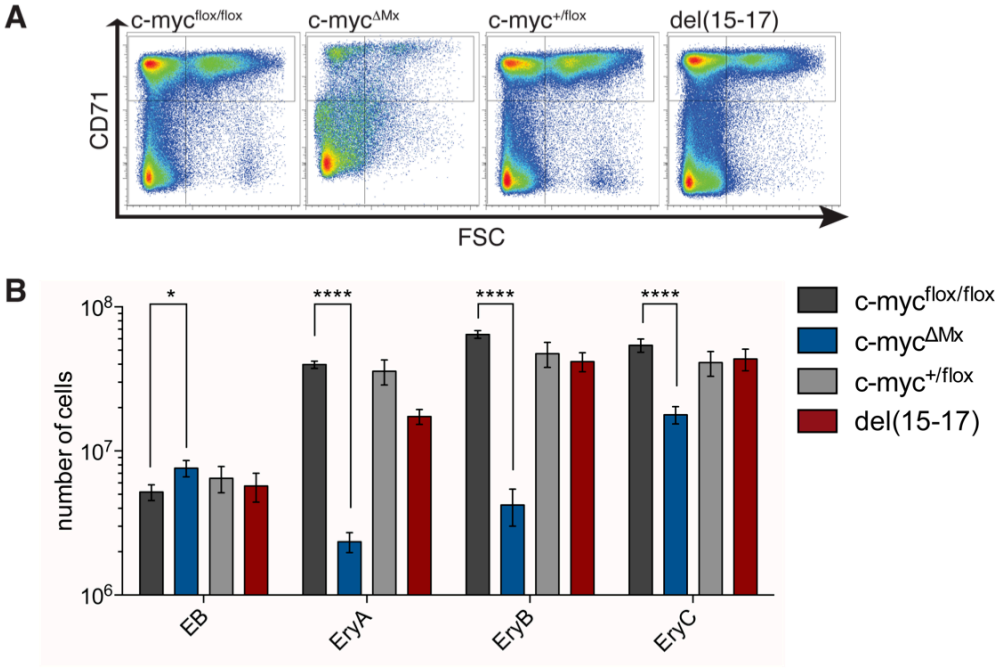

Figure 3.28: BM erythroid progenitor numbers are decreased upon *c-myc* deletion
A Representative flow cytometry profiles of BM cells stained for erythroblast populations, gated on Ter119$^+$ cells. EryA cells are gated for CD71$^+$ cells with high FSC, EryB cells are gated for CD71$^+$ cells with low FSC and EryC cells are gated for CD71$^-$ cells with low FSC. **B** Quantitative and statistical analysis of numbers of (pro-)erythroblasts in the BM (EB, proerythroblasts; EryA/B/C, erythroblast progenitors).
Data shown are mean (±SEM) values (n = 6-17). Statistical significance is indicated for the comparison between c-myc$^{flox/flox}$ and c-myc$^{\Delta Mx}$ and between c-myc$^{+/flox}$ and del(15-17); *p≤0.05; ****p≤0.001.

In summary deletion of *c-myc* promoted a strong anemia with anisocytosis, hypochromasia and polychromatosia of peripheral erythrocytes, whereas deletion of the DHEC caused mild anemia with a normochromatic macrocytosis. Both deletions however involved a strong thrombocytosis.

3.8.4 T cell development is impaired upon *c-myc* deletion but not upon DHEC deletion

In normal hematopoiesis lymphoid progenitors originating from the BM migrate to the thymus, the site of T cell development and maturation. At this site T cell progenitor cells lack CD4 and CD8 expression and are referred to as double negative (DN) cells. Among these cells four early differentiation stages (DN1-4) have been defined based on the expression of the cell surface molecules CD25 and CD44. DN4 cells differentiate further to the double positive stage (DP; $CD4^+CD8^+$), the last stage before final maturation to the $CD4^+$ or $CD8^+$ single positive (SP) cells. These cells leave the thymus and enter the peripheral circulation (PETRIE 2003).

The number of T cells were not changed neither in the BM of c-$myc^{\Delta Mx}$ nor of del(15-17) mice (Figure 3.23). However, a previous study reported a strong decrease in the cellularity of the thymus at 8 weeks after induction of *c-myc* deletion (WILSON *et al.* 2004). Thus, the normal T cell counts might be based on remaining long-lived T cells after induction of *c-myc* deletion (similar to the long-lived B cells, Figure 3.24). Therefore we analyzed the developmental stages of T cells in the thymuses of mice upon *c-myc* and upon del(15-17) deletion.

4 weeks after induction of *c-myc* deletion the cellularity of the thymus dropped dramatically (Figure 3.29 A). Furthermore, among the remaining thymic cells the $CD4^+/CD8^+$ DP population was virtually absent (Figure 3.29 B,C). Gating on the DN population revealed that basically only DN $CD44^-$ $CD25^-$ cells (DN4) remained (Figure 3.29 B,D). However, these could be also non-hematopoietic cells, e.g. epithelial cells, since these cells were only defined by negativity for the indicated cell surface molecules. Thus indeed the remaining mature T cells, that have been generated before the induction of *c-myc* deletion, accounted for the normal T cell counts in the BM as *c-myc* deletion impairs further T cell development.

In contrast del(15-17) mice displayed a normal thymus cellularity and normal T cell frequencies except for a slight, but significant increase in the overall DN population size that was due to an increase in DN3 cells. The change in numbers of this T cell progenitor cell type did not result in changes of mature T cells, neither in the thymus nor the BM.

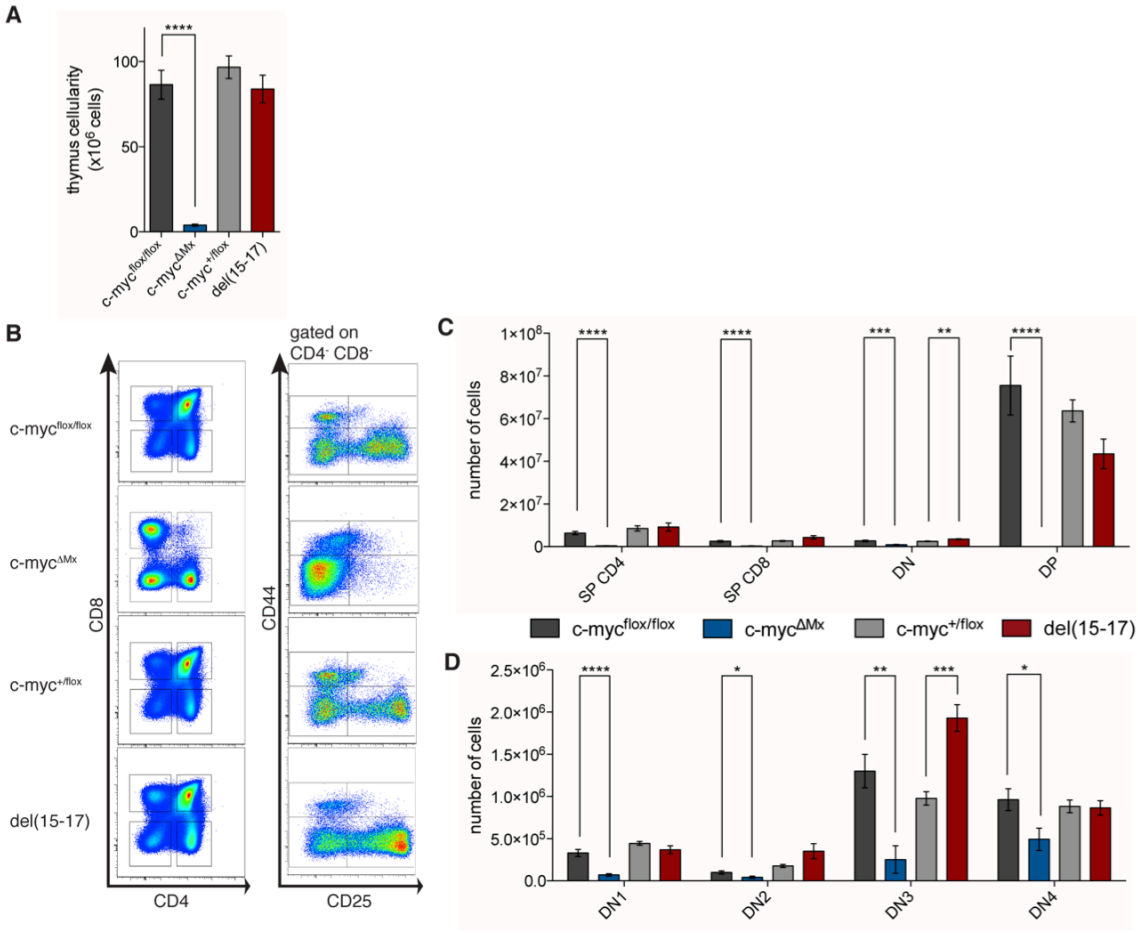

Figure 3.29: T cell development is impaired upon conditional *c-myc* deletion but not del(15-17) deletion
Comparison of mice with MxCre driven *c-myc* deletion and mice with del(15-17) deletion compared to the respective control mice. **A** Thymus cellularity 4 weeks after 1st poly(I:C) injection. **B** Representative flow cytometry profiles of thymic cells stained for thymocytes. **C** Quantitative and statistical analysis of numbers of developing and mature T cells in the thymus (SP CD4=single positive $CD4^+$ $CD8^-$ cells; SP CD8=single positive $CD8^+$ $CD4^-$ cells); DN=double negative ($CD4^-$ $CD8^-$) cells; DP=double positive ($CD4^+$ $CD8^+$) cells; **C** Quantitative and statistical analysis of numbers of developing T cells in the thymus gated on the $CD4^-$ $CD8^-$ double negative population (DN1= $CD44^+$ $CD25^-$; DN2= $CD44^+$ $CD25^+$; DN3= $CD44^-$ $CD25^+$; DN4= $CD44^-$ $CD25^-$).
Data shown are mean (±SEM) values (n = 5-8). Statistical significance is indicated for the comparison between c-myc$^{flox/flox}$ and c-myc$^{\Delta Mx}$ and between c-myc$^{+/flox}$ and del(15-17); *p≤0.05; **p≤0.01; ***p≤0.005; ****p≤0.001.

In summary deletion of *c-myc* has a strong effect on basically all mature effector cells, leading to life-threatening pancytopenia and thrombocytosis. Differentiated cell types in del(15-17) were similarly affected except for only a mild effect on erythrocytes and T cells. This was coherent with the rather mild decrease of *c-myc* expression upon deletion of the DHEC in MEPs (Figure 3.17). Altogether, these data indicate that the DHEC is active and contributes to *c-myc* expression in the erythrocyte-megakaryocyte lineage, but that one or several additional enhancers, located elsewhere in the locus, can maintain *c-myc* expression in these cells independently of the DHEC. T cell development is not impaired upon DHEC deletion and numbers of mature cells and *c-*

myc expression within these cells are similar to controls, thus suggesting that *c-myc* expression in T cells is completely driven by other enhancer(s) outside the DHEC.

3.9 The DHEC region consists of individual modules

The DHEC, identified by histone marks in hematopoietic tissues (Figure 3.12), spans across a 126 kb region and is almost entirely covered by the del(15-17) region, which covers a sequence of 259 kb. A closer look at the DHEC revealed the presence of multiple sites that are evolutionary conserved as it is visualized in Figure 3.30 (bottom panel: Genomic Evolutionary Rate Profiling (GERP), (COOPER *et al.* 2005)). This indicates an enrichment for functional elements at these conserved sites. Interestingly, some of these conserved regions correspond to clusters of hematopoietic transcription factor binding sites, defined by ChIP-seq in a hematopoietic progenitor cell line (HPC-7; Figure 3.30) (HANNAH *et al.* 2011; WILSON *et al.* 2010).

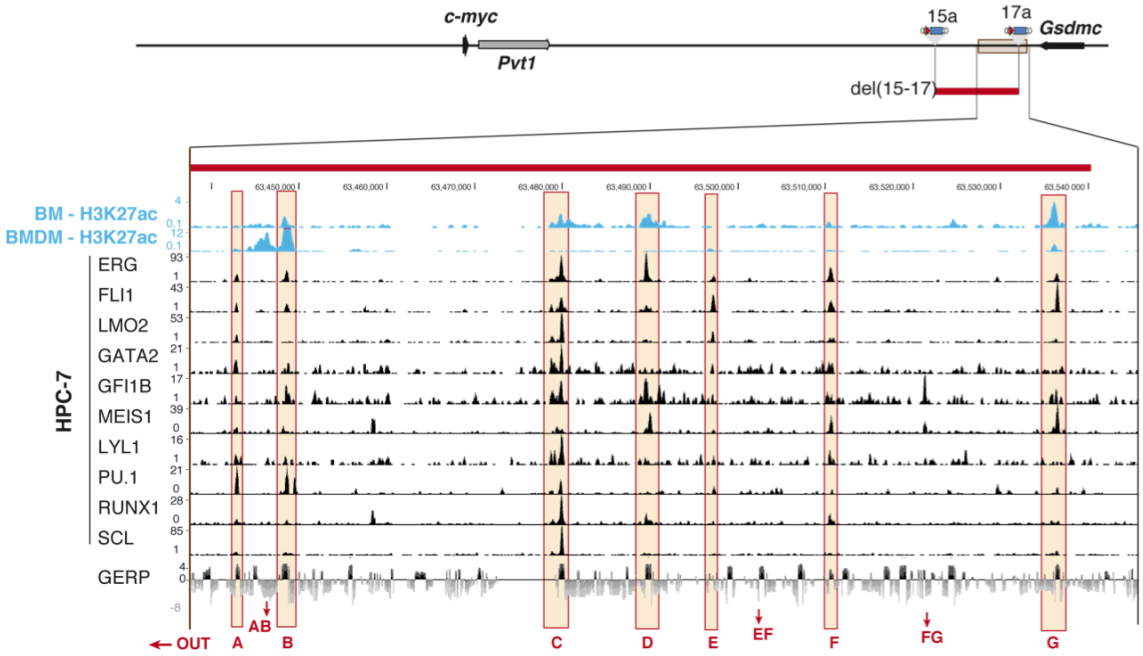

Figure 3.30: The enhancer region consists of individual modules
Enlarged view on the genomic region of the DHEC in the *c-myc*/*Pvt1* flanking locus. Top lines show H3K27 acetylation in BM and BM derived macrophages (BMDM), obtained from SHEN *et al.* (2012). Middle lines show ChIP-seq profiles of transcription factor occupancy performed in HPC-7 cells, obtained from Wilson *et al.* (2010). The bottom line shows the Genomic Evolutionary Rate Profiling (GERP) (COOPER *et al.* 2005). Location of individual modules within the DHEC are highlighted and termed with the indicated letters.

To get further insight into the involvement of the different modules that compose the DHEC, we sought to examine the enrichment of the H3K27ac enhancer mark over the different modules in different cell types (Figure 3.31). For this experiment we sorted

LSK cells, granulocytes, macrophages and B cells from wild type mice and subjected them to chromatin immunoprecipitation using an H3K27ac antibody and subsequent qRT-PCR. As controls served three independent loci of non enriched regions (according to several datasets from ENCODE) at other chromosomes and a locus located within the del(15-17) region but outside the DHEC (OUT). The locations of the different modules (A-G) as well as some interjacent locations (AB, EF, FG) are indicated in Figure 3.30.

We found that the extent of H3K27ac enrichment varied greatly depending of the cell type: in LSK cells modules D and G were particularly prominent whereas in granulocytes modules A, B, C and G showed high enrichment. Macrophages instead showed high enrichment for module G only, while B cells completely lacked any enrichment for the enhancer mark. Thus these data indicate that the activity of the DHEC is dependent on individual modules within the cluster and that the activity in individual cell types is driven by distinct modules.

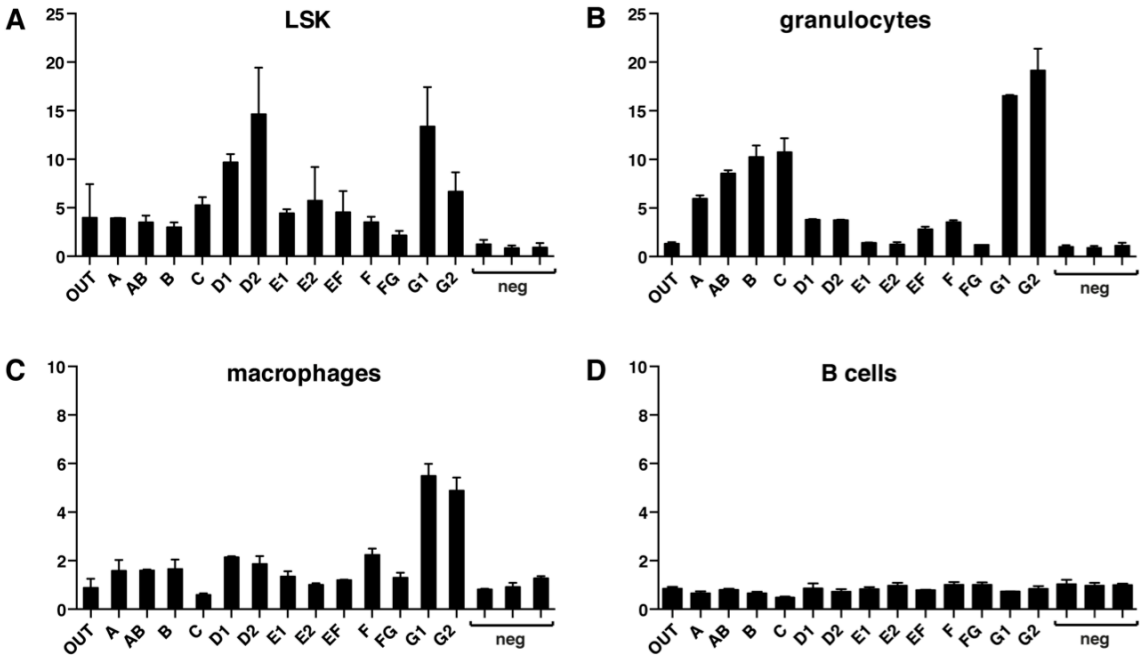

Figure 3.31: Relative enrichment for H3K27ac in the individual modules
Indicated cell types were sorted from wild type mice and subjected to ChIP using an H3K27ac antibody. Enrichment was measured by qRT-PCR for the in Figure 3.30 indicated positions compared to the input material and normalized to average negative control enrichment. **A** LSK cells, **B** granulocytes, **C** macrophages, **D** B cells.

3.10 The DHEC region is highly conserved in humans and implicated in leukemia

The human *c-MYC* locus is highly syntenic to the mouse orthologous region (Figure 1.8). The different modules composing the DHEC are also highly conserved in sequence, their locations on the human chromosome 8 are depicted in Figure 3.32. Most modules overlap with high enrichment for the enhancer-associated chromatin modifications H3K4 monomethylation and H3K27 acetylation in mobilized $CD34^+$ HSCs from healthy donors while H3K4 trimethylation is not enriched (BERNSTEIN *et al.* 2010). Furthermore, these modules display DNase hypersensitivity, a feature of active *cis*-regulatory sequences (BIRNEY *et al.* 2007; BOYLE *et al.* 2008; CRAWFORD *et al.* 2006a; CRAWFORD *et al.* 2006b; SABO *et al.* 2004a; SABO *et al.* 2004b; XI *et al.* 2007). Thus, the enhancer region is highly conserved in humans and exhibits enhancer features in human HSCs.

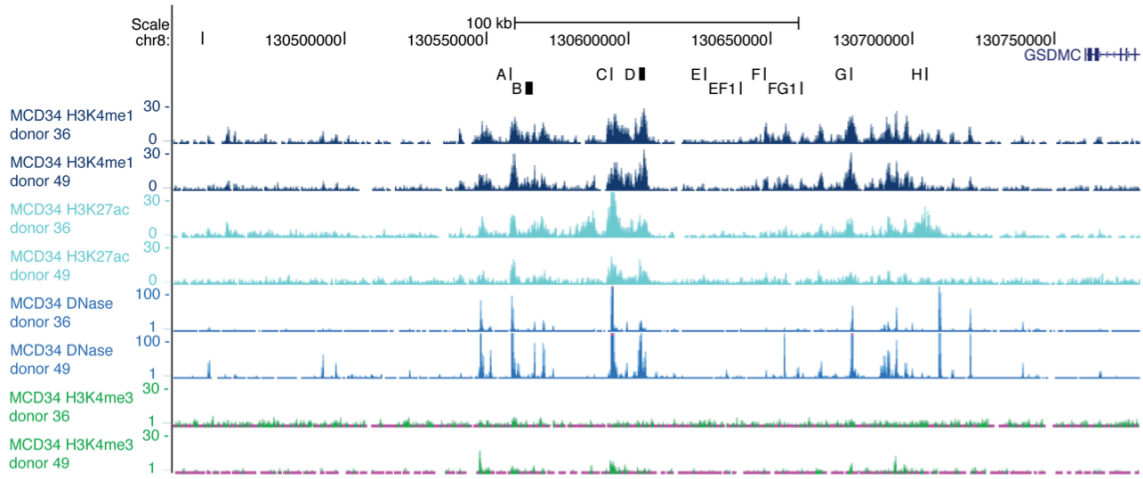

Figure 3.32: Evidence for the presence of a HSC specific enhancer cluster in the human *c-myc*/*Pvt1* flanking locus
The positions of the sequences equivalent to the DHEC modules are depicted for the human chromosome 8. Chromatin modifications (H3K4me1, H3K27ac, H3K4me3) and DNase hypersensitivity sites in mobilized $CD34^+$ hematopoietic stem cells (MCD34) from two healthy donors were obtained from the NIH Roadmap Epigenomics Mapping Consortium (BERNSTEIN *et al.* 2010).

Genome-wide association studies (GWAS) have identified thousands of single-nucleotide polymorphisms (SNPs) that are linked to human diseases. Many variations are located in non-coding regions, thus the evaluation of their direct function is complicated. 40% of GWAS SNPs are located in DNase hypersensitivity sites thus pointing towards a prevalent location of these disease- and trait associated variants in regulatory elements (MAURANO *et al.* 2012).

Five common SNPs are present within the human DHEC region that have been associated with human diseases (Figure 3.33). Two of them (rs10098310 and rs10956483) refer to hematopoiesis as they reflect changes in monocyte counts (NALLS *et al.* 2011; OKADA *et al.* 2011). These two GWAS SNPs do not directly overlap with any of the modules. However, visual examination of haplotype maps (HapMaps) for two populations (CEU=Utah residents of northern and western European ancestry; JPT+CHB=Japanese individuals from Tokyo, Japan and Han Chinese individuals from Beijing, China) revealed the presence of two blocks (highlighted in yellow and purple) spanning the DHEC, which are enriched for high linkage disequilibrium (LD) values (Figure 3.33, dark red marks high LD). Thus the two hematopoiesis related SNPs are very likely to be linked to their neighbouring areas containing the conserved DHEC modules.

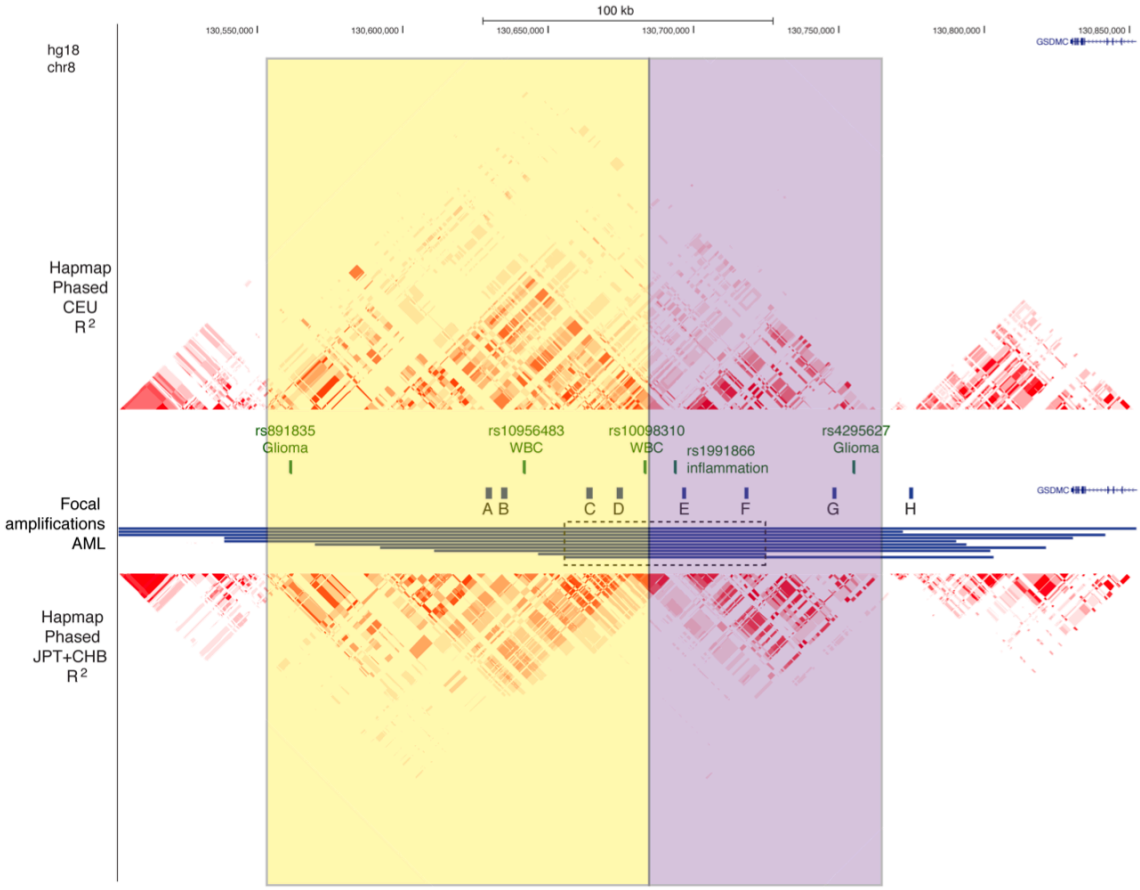

Figure 3.33: Implication of the DHEC in human diseases
The genomic coordinates on chromosome 8 (hg18) are shown at the top and the location of five GWAS SNPs with the affected traits is indicated in green. The pattern of linkage disequilibrium (LD) in the HapMap of CEU and JPT+CHB populations (HapMap release 22) reveals blocks (highlighted in yellow and purple) with high LD. Blue bars indicate the areas found to be focally amplified in AML patients (KUHN *et al.* 2012; RADTKE *et al.* 2009). The dashed box marks the common region.

Another more direct link to human disease appeared due to the recurrent observation of focal amplifications overlapping the DHEC region in acute myeloid leukemia (KUHN *et al.* 2012; RADTKE *et al.* 2009). As it is represented in Figure 3.33 the common region that is focally amplified in these patients encompasses the modules C to F, attributing the core function of the enhancer to this area.

c-MYC expression is found to be elevated in several cancers (DANG 2012; MEYER and PENN 2008). Its expression levels in AML however were contrarily reported. A first microarray based study on AML samples reported elevated levels (COURT *et al.* 2004), which was supported by further qRT-PCR experiments obtained in an independent study (SALVATORI *et al.* 2011). However, in other studies *c-MYC* was not detected as one of the highly overexpressed genes (ROSS *et al.* 2004; STIREWALT *et al.* 2008; VALK *et al.* 2004).

Since we had access to primary AML samples we sought to determine *c-MYC* expression by qRT-PCR (Figure 3.34). The levels are represented relative to *c-MYC* expression in cord blood (CB) samples. The analysis revealed a high diversity of *c-MYC* expression ranging from very low (light green) and normal (dark green) over modestly elevated levels (light red) to samples with more than 5-fold increased *c-MYC* levels (dark red). The underlying karyotype and mutational analysis for each patient sample did not reveal a general correlation between cytogenetic aberrations and the *c-MYC* expression pattern (Dr. Simon Raffel, personal communication).

The analysis of the DHEC region in high expressing compared to low expressing samples in respect to enhancer marks could provide a direct link between the enhancer region, *c-MYC* expression and leukemia. This will be addressed in future experiments.

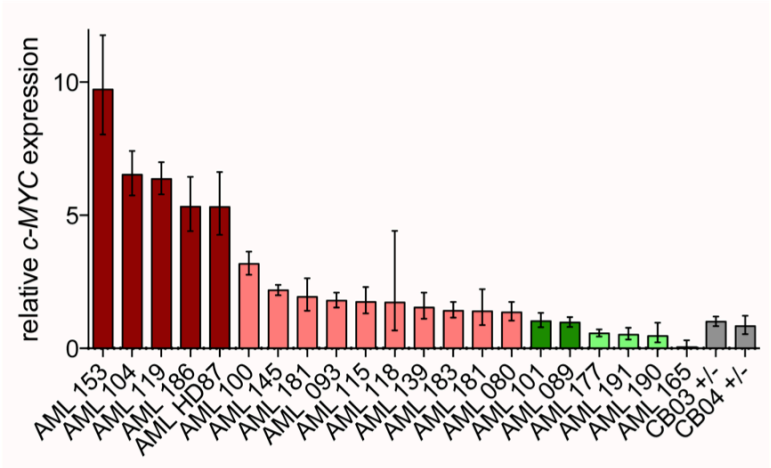

Figure 3.34: *c-MYC* expression levels in primary samples of AML
c-myc expression levels in primary samples of AML relative to levels in cord blood (CB, grey). Red bars highlight samples with 5 to 10-fold levels, light red bars samples with 1.3 to 5-fold levels, green bars samples with 0.7 to 1.3-fold levels and light green bars 0 to 0.7-fold levels. Data shown are mean values (with range).

For some enhancers it was shown that germline duplications can lead to malformations affecting the organ where they are active (DATHE *et al.* 2009; LOHAN *et al.* 2014). Similarly, it is possible that somatic duplications of the DHEC can constitute an alternative way to up- or misregulate *c-MYC* expression in a tissue-specific manner. A first attempt to test this hypothesis in the murine system was done by analyzing mice carrying a duplication of the enhancer region (Figure 3.35 A). However, neither mice carrying 3 nor 4 copies of the DHEC did display gross alterations in hematopoietic cell frequencies (Figure 3.35 B-D). Thus, a variation in the copy number of the DHEC did not manifest in a hematopoietic phenotype in these mice.

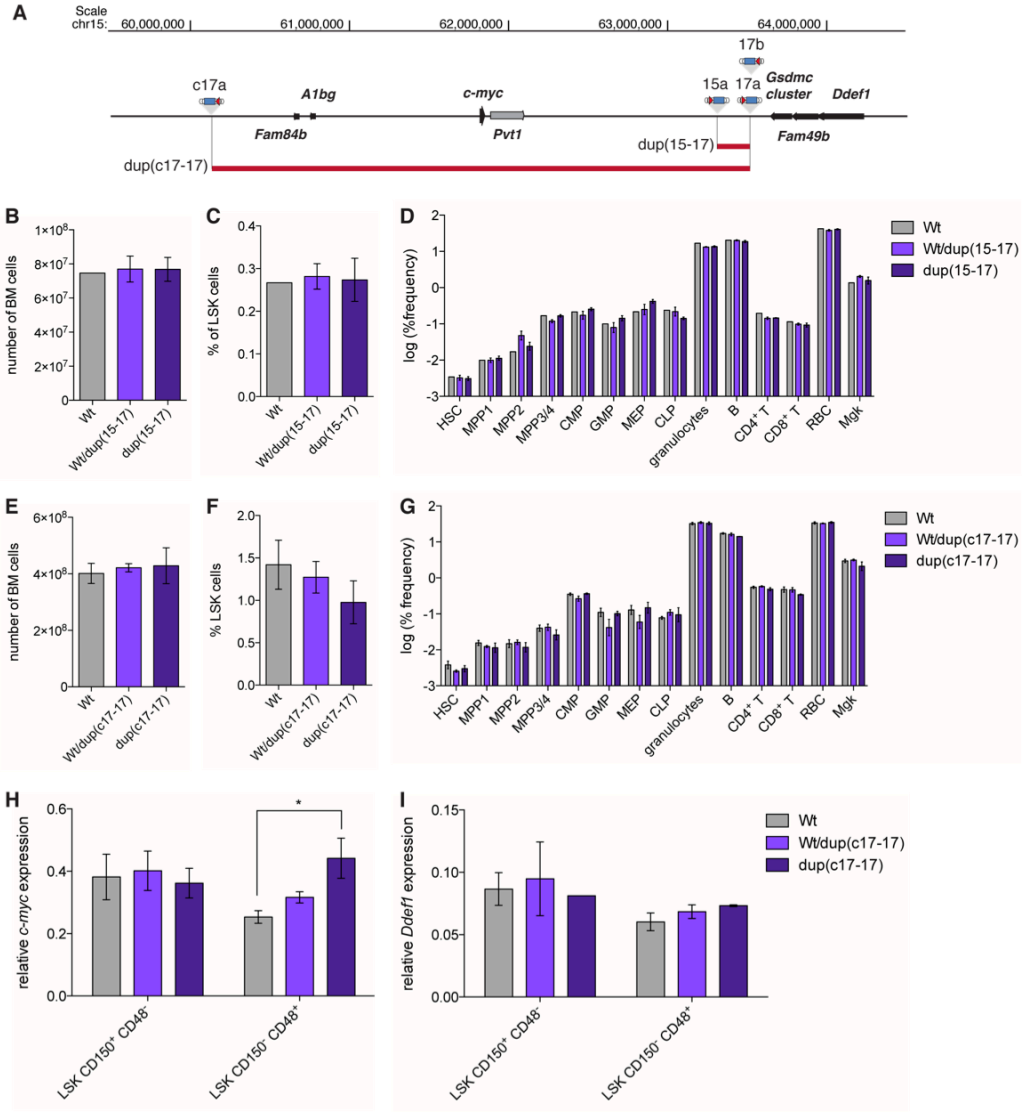

Figure 3.35: Murine duplication of the DHEC or a 3 Mb large region encompassing *c-myc* and the DHEC does not change cell frequencies

A Locations of the transposon insertions used to generate mice with duplications of the interjacent sequence. **B,E** Number of BM cells in (**B**) young dup15-17) mice (10 days old) and (**E**) adult dup(c17-17) mice. **B,C,F,G** Quantification of major hematopoietic cell types in (**C,D**) dup(15-17) mice and (**F,G**) dup(c17-17) mice. **H,I** mRNA expression of *c-myc* (**H**) and *Ddef1* (**I**) by hematopoietic stem and progenitor cells was measured by qRT-PCR in wild type, heterozygous and homozygous dup(c17-17) mice.
Data shown are mean (±SEM) values (n = 1-4 for dup(15-17) and n = 2-4 for dup(c17-17)).

Besides we also tested mice having the whole *c-myc* locus duplicated, spanning a 3.4 Mb region encompassing *Fam84b*, *A1bg*, *c-myc*, *Pvt1* and the DHEC. Also in these mice we did not detect significant differences in cell frequencies in the BM (Figure 3.35 E-F). However, analysis of gene expression levels revealed an increase in *c-myc* expression in multipotent progenitors (LSK $CD150^{-}CD48^{+}$) according to the copy number while the HSC and MPP1 population (LSK $CD150^{+}CD48^{-}$) showed no change in expression. As expected *Ddef1* expression was unaltered as this gene was located outside of the duplicated region. These results suggest another layer of transcriptional regulation of *c-myc* in hematopoietic stem and early progenitor cells.

In summary, the DHEC is highly conserved from mice to humans and mobilized human HSCs display similar enhancer-associated chromatin marks as murine hematopoietic cells. Furthermore, the human DHEC is linked to changes in white blood cell counts and AML, thus underscoring a function in human hematopoietic diseases. *c-MYC* is differentially expressed in primary AML samples, however a direct association between the DHEC and *c-MYC* in humans needs to be proven.

4 DISCUSSION

4.1 c-Myc expression in hematopoietic cells is regulated by a distal enhancer cluster

Hundreds of studies have been carried out to dissect the *c-myc* promoter region to identify the *trans*-acting factors and molecular mechanisms that may regulate its expression (reviewed in (WIERSTRA and ALVES 2008)). However, as the *c-myc* promoter proximal region does not recapitulate its expression and regulation *in vivo* (LAVENU *et al.* 1994; MAUTNER *et al.* 1996), regulatory elements have to be located outside the 50 kb region surrounding the *c-myc* gene. Our results demonstrate that *in vivo*, *c-myc* expression in HSPCs depends critically on the activity provided by a very remote enhancer region, located almost 1.7 Mb away from the promoter region. Importantly, our analysis of compound alleles showed that the regulatory interaction between *c-myc* and the DHEC are taking place *in cis*. Homozygous deletion of the DHEC critically affected almost all hematopoietic cell types in the BM. Specifically, it led to an increase in stem and progenitor cells and megakaryocytes accompanied by a decrease in myeloid and B cells.

This phenotype was already apparent in del(8-17) mice where the deletion encompassed in addition to the DHEC a large part located centromerically to this cluster. These mice showed a more dramatic phenotype as the homozygous deletion was perinatal lethal with only few surviving mice. For this reason we analyzed these mice 10 days after birth. The cell cycle status of HSCs in the BM of del(8-17) mice was dramatically changed, having less cells in G0 and more in G1. In accordance to the decreased body size this observation resembled a developmental retardation. In fact fetal HSCs in the mouse liver are actively cycling thereby satisfying the demand of expansion of the HSC pool during this developmental phase. Only after transition to the

BM HSCs enter a quiescent state (BOWIE *et al.* 2007; BOWIE *et al.* 2006). Analysis of the stem and progenitor compartment in the fetal liver at E15.5 showed that regulation by the enhancer is already occuring at a very early phase of hematopoiesis, thus it seems not to be temporarily restricted. It is possible that this kind of retardation is dependent on an increased retention of HSCs in the fetal liver as it was shown for c-Myc deficiency in adult HSCs and the BM niche. In this situation adhesion molecules were upregulated that are thought to attach the cells more tightly to cells of the surrounding niche (WILSON *et al.* 2004).

As shown by our collaborators the del(8-17) region possesses enhancer activity regulating *c-myc* in the developing face (USLU *et al.* 2014). Similarly *c-myc* expression was dramatically downregulated in stem and progenitor cells (LSK), however the myeloid committed cells (LS$^-$K) showed 85% *c-myc* expression on the mRNA level (Figure 3.7). *c-myc* expression in other tissues such as fetal heart and liver at E11.5 was not affected (USLU *et al.* 2014). At this stage, hematopoiesis is just starting to colonize the fetal liver, therefore a decrease in *c-myc* expression is not expected (KUMARAVELU *et al.* 2002; MEDVINSKY and DZIERZAK 1996; MÜLLER *et al.* 1994). Even at later stages, a decreased *c-myc* expression due to hematopoietic cells would not have become apparent in the whole organ as normal *c-myc* expression in the non-hematopoietic cells (e.g. at E15.5 > 95%; Figure 3.6) would have covered it. Overall these results showed that the enhancers in the del(8-17) region are acting only in specific tissues. Moreover, they suggest a cell-type specific regulation, showing specificity for the stem and progenitor cell compartment. Later, the extended analysis of *c-myc* expression in multiple hematopoietic cell types in compound heterozygous mice confirmed that all cells of the stem and progenitor compartment were affected by the DHEC deletion (Figure 3.17). However, most other cell types, including restricted progenitors as well as differentiated cell types were similarly affected. The only exceptions were MEPs with partial decrease in *c-myc* expression and T cells with normal *c-myc* expression levels (see also chapter 4.2), thus the observed partially retained *c-myc* expression in del(8-17) myeloid committed progenitor cell population was most probably due to *c-myc* expression in MEPs.

The genomic integration of the reporter gene enabled us to measure the activity of nearby enhancers. Several other methods are generally used to analyze the regulatory potential of a candidate sequence. These include classical reporter-gene assays carried out by cloning the respective sequence next to an easily accessible reporter gene such as green fluorescent protein (GFP), luciferase or β-galactosidase (LacZ). Activity is then

measured in transiently or stably transfected cultured cells. Most importantly the choice of a representative cell line is necessary to be able to draw conclusions about the tissue-specificity of the enhancer sequence. Still, cell lines are transcriptionally very different from their original tissues, thus this method has major limitations. Another possibility is to inject reporter constructs into embryos, which then allows following of the gene expression throughout development (PENNACCHIO *et al.* 2006). However, the *in vivo* activity might still not reflect the endogenous expression due to differences in the chromatin structure (MASTON *et al.* 2006). Furthermore, the cloned construct only allows the isolated view on the selected sequence but does not take into account cooperative activity with other regulatory sequences and not the respective distance between enhancer and target promoter. Usage of bacterial artifical chromosomes (BACs) to generate transgenic animals circumvented these latter limitations since this assay measures enhancer activity in its native position to the target promoter (VAN KEUREN *et al.* 2009). However, distance is limited to the maximum size (~500 kb) that can be cloned into the BAC, which is not sufficient for large, complex landscapes. Therefore the generation of transgenic mice with genomic integration of the reporter construct overcomes those limitations mentioned above and provides an integrated and non-gene-centric view of *cis*-regulatory activity (RUF *et al*. 2011).

LacZ activity of insertions tested across the *c-myc*/*Pvt1* flanking locus revealed that enhancer activity was present in hematopoietic stem, progenitor and committed progenitor cells, but almost absent in differentiated cells. Importantly, this assay restricted enhancer activity towards the telomeric end of the *c-myc*/*Pvt1* flanking locus. This is in contrast to the facial enhancer function which spreads much further to the telomeric side (USLU *et al*. 2014). The restriction towards the telomeric side became also apparent by RNA-seq results of cells from the medial faces of del(8–17) homozygous embryos (USLU *et al.* 2014). This analysis showed downregulation of several hematopoietic-related genes that arose from cells in small blood vessels in the dissected tissue. However, this observation was only made for the del(8-17) deletion but not the del(8-14) deletion, suggesting that the blood phenotype is mediated by an enhancer region in the latter region. Overall enhancer activity detected from the 17a insertion correlated well with *c-myc* expression detected by qRT-PCR. Although deletion of the several tested regions retained the reporter gene at the breakpoint, no lacZ expression could be detected in any tested cell type. This implicates that no regulatory input is acting on the reporter gene promoter, which means in turn that the regulatory input acting on 17a has been deleted by the minimum deletion of del(15-17).

Combined analysis of this enhancer activity assay and publicly available chromatin modifications as well as 3D organizational studies allowed the localization of a cluster of enhancer peaks in hematopoietic tissues that we termed DHEC (distal hematopoietic enhancer cluster).

We carried out a series of experiments with DHEC deleted mice to define the function of the DHEC. In contrast to the del(8-17) deletion del(15-17) deletion was not lethal. Instead, mice appeared with normal body size and no apparent defect. However, in the hematopoietic system these mice displayed with an accumulation of stem and progenitor cells (LSK) and a disturbed pattern within the differentiated lineages. Thus they closely resembled the phenotype of the MxCre mediated conditionally deleted *c-myc* mice which we proved by direct side-by-side comparison. Most important was the observation that compound heterozygous mice do exhibit the same phenotype as mice with DHEC deletion alone. This experiment nicely demonstrated genetic allelism between the c-myc knockout and the enhancer deletion alleles, thus providing genetic evidence for the hypothesis that the *c-myc* downregulation is a direct consequence of the DHEC deletion and not mediated by an indirect mechanism. Furthermore, this experiment proved the function of the enhancer *in cis* as expression could not be driven from the intact *c-myc* gene despite the presence of the intact enhancer region on the other chromosome.

An observation that was apparent throughout all experiments in DHEC and *c-myc* deleted mice was the accumulation of $CD48^+$ multipotent progenitor cells whereas HSC and MPP1 numbers remained unchanged. This is in contrast to the previous assumption that c-Myc deficiency leads to the accumulation of the most potent hematopoietic cells, the HSCs (GUO *et al.* 2009; WILSON *et al.* 2004). This former observation was based on a limited marker combination for the identification of HSCs. Reevaluation of the results confirmed that previous definition of HSCs as LSK $CD135^-$ ($Flk2^-/Flt3R^-$) cells comprises the populations HSC, MPP1, MPP2 and MPP3. Since MPP3 account for the largest amount of cells within the LSK $CD135^-$ population the drawn conclusion of an HSC accumulation was instead an increase in multipotent progenitor cells.

Previous analysis of the cell cycle, proliferation and apoptosis revealed that there was no difference in *c-myc* deleted LSK cells, thus the accumulation of these cells was thought not to occur due to increased proliferation or survival (WILSON *et al.* 2004). Our results comparing the cell cycle of *c-myc* deleted and del(15-17) deleted stem and progenitor cells to cells of the respective control mice at 4 weeks after poly(I:C) induction showed a different cell cycle profile (Figure 3.24). Although these data

showed a higher proliferation for *c-myc* deleted HSCs and MPP1 cells these cells did not accumulate in the BM. Moreover c-Myc deficient mice showed a similar distribution in the stem and multipotent progenitor compartment as del(15-17) mice, which did not show increased proliferation in the HSC and MPP1 population. This stronger cycling behavior might be a feedback mechanism to the more severe loss of committed progenitors (Figure 3.20 E) and mature effector cells (chapter 3.8.2). Further experiments such as BrdU incorporation assays and terminal deoxynucleotide transferase dUTP nick end labeling (TUNEL) assays will help to discriminate between apoptosis and self-renewal changes in these more defined cell populations.

Transplantation experiments of both del(8-17) and del(15-17) BM cells revealed reconstitution in the HSC compartment but hardly any contribution to differentiated cells in the periphery (Figure 3.8 and Figure 3.14). This phenotype closely resembled the published transplantation effect of *c-myc* deleted HSCs, however del(15-17) HSCs did not accumulate as dramatically as reported for c-Myc deficient HSCs (WILSON *et al.* 2004). Strikingly, donor derived cells showed a different distribution of hematopoietic cells in reconstituted mice compared to homeostatic del(15-17) mice, as the most primitive HSCs accumulated most with a concomitant decrease along the hierarchy. This in turn means that in the transplantation setting, deletion of the DHEC did not result in an increase in multipotent progenitor populations. Also, transplanted del(15-17) HSCs did not contribute to T cells or megakaryocytes although they were able to give rise to these cell types in del(15-17) mice. This difference may be due to the stress situation that occurs in the transplantation setting or may be caused by differences of Myc requirement for lineage differentiation in fetal and adult HSCs (mutant adult HSCs were transplanted but the enhancer deletion was present already during ontogeny in the mutant mice). Another possibility is that DHEC deletion leads in addition to hematopoietic changes also to changes in the BM niche that promotes the phenotype observed under homeostatic conditions. Upon transplantation this niche-dependent effect would be missing and could contribute to the described phenotype. We do not have any further evidence for a function of the DHEC in niche cells yet, but this will be investigated in future experiments for example by reverse chimera analysis. Notably, macrophages, T cells and megakaryocytes were at least reconstituted by del(15-17) HSCs in a range from 3 to 6.6% of total BM chimerism, while the other del(15-17) HSC derived mature effector cells were virtually absent (<1%). Since these transplantations were performed in a competitive setting, the differentiation potential towards these lineages might be covered by efficient hematopoiesis derived from competitor HSCs.

To investigate this further, three types of transplantations could be set up. Straight transplantation of del(15-17) BM into lethally irradiated recipient mice would circumvent the influence of competitor BM. This transplantation might lead to early lethality as observed in transplantation of *c-myc* deleted BM (WILSON *et al.* 2004). Furthermore, we would not be able to easily discriminate the origin of long-lived cells such as T cells, if they are either transplanted or newly derived from engrafted HSCs. Therefore as an alternative we would sort LSK cells and transplant them along with Sca-1 depleted competitor BM. The latter population ensures quick generation of effector cells for a limited in time. Meanwhile engrafted del(15-17) LSK cells have the possibility to re-establish the blood system and lack competition long-term. Third, we could generate del(15-17) compound heterozyogus mice carrying a floxed *c-myc* allele together with the MxCre transgene. After transplantation and establishment of a stable hematopoietic system by the donor HSCs, deletion of the floxed *c-myc* allele allows the evaluation of del(15-17) derived cells in blood and BM. In a similar experiment, GUO *et al.* (2009) showed that the thrombocytosis phenotype upon c-Myc deficiency is an HSC cell-intrinsic defect. It will be interesting to see if this holds true for deletion of the DHEC and especially the formation of other cells such as macrophages, T cells and red blood cells.

In summary, DHEC deletion generally resembled c-Myc deficiency, but in some instances it manifested to a slightly milder extend. This could likely be due to residual *c-myc* expression at a very low level.

4.2 Deletion of the enhancer affects some hematopoietic cell types differently than conditional *c-myc* deletion

Our experiments demonstrate that DHEC has a primordial role in controlling *c-myc* expression in most hematopoietic lineages, most prominently in HSCs and MPPs. Its regulatory input is particularly essential for the formation of granulocytes and B lymphocytes, which recalls the phenotype of MxCre driven *c-myc* deletion. However, not all hematopoietic cell types were similarly affected by deletion of the DHEC, which will be discussed in this chapter.

On the protein level immature thymocytes of the double negative compartment do express high levels of c-Myc, however only a very small subset of the maturing double positive thymocytes show c-Myc expression at a low level. Single positive thymocytes have an overall low but detectable expression of c-Myc whereas mature T cells in the

periphery do not express c-Myc anymore (HUANG *et al.* 2008; ZIMMERMAN and ALT 1990). Generation of chimeras using *c-myc* deficient ES cells and RAG-1$^{-/-}$ recipient blastocyts showed that c-Myc is necessary for populating the thymus in adult mice (DOUGLAS *et al.* 2001). Apparently N-Myc could not complement c-Myc deficiency to drive proper T cell development which is in accordance to its co-expression with c-Myc only in early stages of T cell development. Furthermore, deletion of *c-myc* induced by *Lck* promoter driven Cre recombinase, which ablates expression starting at the DN3 stage, suggests that c-Myc is required for the proliferation at that stage, however thymocytes are able to differentiate further to the DP stage. The adult thymus however contained a 10 times lower number of cells (DOSE *et al.* 2006).

A reduced thymic cellularity 8 weeks after induction of MxCre driven *c-myc* deletion has already been shown (WILSON *et al.* 2004) and is confirmed by our results 4 weeks after induction. The DP compartment was almost completely depleted, single positive thymocytes most probably were remaining long-lived thymocytes derived from c-Myc expressing cells prior to induction, which could easily be tested by PCR. However, the deletion of the DHEC resulted in almost normal T cell development with the only change of an increased DN3 population. Later stages were not affected as thymocytes further developed through the DP and SP stages to finally generate mature CD4^{+} and CD8^{+} lymphocytes in the periphery. Indeed *c-myc* expression in these mature T cells was not changed in compound heterozygous mice. Thus further enhancer elements located outside the del(15-17) region seem to be present that account for sufficient c-Myc expression during T cell development.

Recently, this T cell enhancer for *c-myc* expression has been identified and characterized (HERRANZ *et al.* 2014). The authors located the human T cell enhancer 1.4 Mb downstream of the *c-MYC* TSS and showed that it exhibits enhancer-associated chromatin marks in a human T-ALL cell line and physically interacts with the *c-MYC* promoter region. Furthermore, this enhancer contains a recognition site for NOTCH1, a ligand-activated transcription factor oncogene associated with T-ALL (TZONEVA and FERRANDO 2012; WENG *et al.* 2004). The equivalent region in mice is located 1.3 Mb downstream of the *c-myc* TSS thus 355 kb centromeric to the DHEC region. Homozygous deletion of the T cell enhancer showed that it is specifically required for thymocyte development beyond the DN3/DN4 stage, whereas many other hematopoietic cell types including the stem cell compartment were not affected. Moreover the enhancer was shown to be required for NOTCH1-induced T cell leukemogenesis.

Although our results support the presence of a T cell enhancer outside of the DHEC, part of our results are, on first sight, contradictory to the T cell enhancer described above. The del(8-17) region covers this enhancer thus one would expect similar defects in T cell development in mice with a homozygous deletion for this region. However, both control and homozygous mice, analyzed 10 days after birth, have comparable, albeit low numbers of mature $CD4^+$ and $CD8^+$ T lymphocytes in the BM. Although we did not look at T cell development in the thymus yet, an overall defect at this developmental stage would be expected to result in reduced numbers of mature cells in the periphery as it is the case for the study of the T cell enhancer by HERRANZ *et al.*. This issue requires further analyses for multiple reasons. First, with the available data we compare the lymphocyte populations at different developmental stages, and second, the comparison so far allows only an indirect observation since different tissues are evaluated (BM compared to thymus, spleen and lymph nodes). Del(8-17) mice were analyzed at 10 days age whereas T cell enhancer deleted mice were analyzed at 6 weeks age. T cell development at early stages is regulated differently compared to the adult situation (DOUAGI *et al.* 2002). In favor of a differential age-dependent requirement of c-Myc for T cell development are results from DOUGLAS *et al.*, which show that thymic colonization in the absence of c-Myc occurs more frequently at fetal stages than at postnatal stages. However, analysis of the fetal stage revealed a block at the late stage of DN cell maturation, thus c-Myc deficient thymocytes did not contribute to the periphery. Enhancers regulate target gene expression in a tissue- and stage specific manner (VISEL *et al.* 2009). Therefore it is possible that T cell development in the embryo and the newborn mouse gets different regulatory input than in the adult mouse. If another enhancer not deleted by del(8-17) exists that drives T cell development at least until 10 days after birth, T cell enhancer deleted mice present with mature T cells at wild type levels.

Notably, although null deletion of the T cell enhancer resulted in dramatically reduced thymic cellularity and reduced T cell numbers in the periphery as shown for spleen and lymph nodes this latter decrease was only modest to approximately 40% of wild type levels (HERRANZ *et al.* 2014). To test if this rather mild effect on mature T cells is equivalent to full c-Myc deficiency, mature T cells in c-$myc^{\Delta Mx}$ mice have to be analyzed for the presence of *c-myc* deleted cells. This can be done e.g. either by genotyping of sorted cells or by introducing a reporter construct such as the Rosa26EYFP$^{flox/flox}$ allele into the mouse that marks c-Myc deficient cells. Finally, although being performed with only a single mouse per group, the del(8-14) mouse

displayed normal T cell numbers. This deletion also encompasses the T cell enhancer but not the DHEC and since these mice were analyzed at an adult stage, the argument of regulation due to different requirement of c-Myc at the fetal stage is not valid for the observed phenotype. Therefore this issue needs to be addressed in more detail in future experiments.

Similar as for T lymphocytes c-Myc is also necessary for B lymphocyte development. Deletion of *c-myc* exclusively in B cells beginning at the very early pro-B cell stage via a Cre recombinase driven by the mb1 promoter led to a developmental defect at the pro- to pre-B cell transition in the BM (HOBEIKA *et al.* 2006; VALLESPINOS *et al.* 2011). Our experiments showed that deletion of the DHEC led to significantly downregulated *c-myc* expression in B cells and a similar effect on the immature B cell population as achieved directly by *c-myc* deletion via MxCre recombinase. Thus in contrast to T lymphocytes *c-myc* expression in early B cells is driven by the DHEC.

MEP progenitor cells are restricted to the megakaryocyte/erythrocyte lineage (AKASHI *et al.* 2000). In wild type mice mRNA expression levels of *c-myc* were similar to HSC, MPP and committed progenitor populations (Figure 3.17), however on the protein level this population showed highest expression among all hematopoietic cell types, which was a 7-fold increase compared to HSCs (EHNINGER *et al.* 2014). This discrepancy between the transcript and the protein level suggests posttranscriptional regulation mechanisms, as it was shown e.g. by the E3 ubiquitin ligase Fbw7 (REAVIE *et al.* 2010). Thus MEPs in particular seem to depend on high levels of c-Myc. Upon deletion of the DHEC *c-myc* expression was mildly reduced in these cells, suggesting that its expression depends only partially on this enhancer region (Figure 3.17). Moreover erythrocytes, progeny of the MEP population, barely showed a phenotype as opposed to c-Myc deficient erythrocytes.

Among the mature cell types, only red blood cells were shown to have detectable c-Myc at the protein level (EHNINGER *et al.* 2014), suggesting a functional role for c-Myc in this cell type. Indeed the deletion of *c-myc* led to a dramatic phenotype in the erythroid lineage as it was shown upon MxCre driven deletion in the BM (WILSON *et al.* 2004, GUO *et al.* 2009 and our results) and Sox2Cre driven deletion in the epiblast (DUBOIS *et al.* 2008). In the latter case apoptosis in the erythroblast population has been observed and was considered to contribute to or even cause the death of the embryos. Hemavet and peripheral blood smear analyses revealed a strong anemia with anisocytosis, hypochromasia and polychromatosia of the red blood cells upon c-Myc deficiency. Erythroblasts, the immediate progeny of erythrocytes in the BM, were

decreased. This could either cause the defect observed in the periphery and/or be the consequence of a feedback mechanism, that tries to replenish functional red blood cells in the periphery and leads to exhaustion of erythroid progenitors. The latter situation is supported by the finding of a high number of polychromatic cells, a sign of premature release. Conversely, the number of proerythroblasts was slightly increased, thus suggesting that c-Myc deficiency leads to a differentation block at that stage. Therefore both scenarios seem to cooperatively lead to the anemic phenotype. In sharp contrast deletion of the DHEC caused only a mild anemia with a normochromatic macrocytosis. It was not accompanied by a significant change in (pro-) erythroblast populations in the BM, thus the mild defect could be sufficiently compensated. Of note, LacZ profiles of the proerythroblast population revealed a small subpopulation that showed strong, DHEC-dependent, expression from insertion 17a (Figure 3.10). The activity of the enhancer in this subpopulation could account for the reduction of *c-myc* expression in erythroblasts in DHEC deleted mice (Figure 3.17). Most importantly DHEC deletion did not cause lethality. The only differences in the hematopoietic system between both mouse models manifested in T cell development and the erythroid phenotype. The former is dispensable for laboratory mice (e.g. in *Prkdc*^{scid} mice), therefore our results strengthen the hypothesis that lethality upon c-Myc deficiency is caused by the strong defect in erythroid development and function (DUBOIS *et al.* 2008; TRUMPP *et al.* 2001; WILSON *et al.* 2004). Altogether, these data indicated that the DHEC is active and contributes to *c-myc* expression in the erythrocyte-megakaryocyte lineage, but that one or several additional enhancers, located elsewhere in the locus, can maintain *c-myc* expression in these progenitors, independently of the DHEC.

A broad analysis of enhancer-associated marks across the respective cell types could assist in identification of such an enhancer. A global analysis of chromatin modifications across different stages of hematopoietic differentiation has recently been published (LARA-ASTIASO *et al.* 2014). A short description of these data as well as visualization of chromatin modifications in the DHEC and *c-myc* region can be found in the Appendix section 6.1.1 with Figure 6.1 and Figure 6.2. Overall these data are in accordance with our ChIP-PCR results, showing highest enrichment for the H3K27ac enhancer mark at the D and G module in stem and progenitor cells (compare Figure 3.31 to Figure 6.1), while granulocytes show higher enrichment at modules A, B and G. In our results B cells gave no specific enrichment for H3K27ac, which stands in contrast to the data shown in Figure 6.1. However, in these data combined analysis for H3K27ac and H3K4me1 also revealed an overall lower enhancer mark signal for all

lymphocytes compared to stem and progenitor cells. Most interestingly LARA-ASTIASO *et al.* provide data for enhancer-associated marks in MEPs and erythroblast cells. Strikingly, these profiles appear to be different to other progenitor or differentiated cell types. The modules A to G were less prominent, in contrast, a peak located next to module G and a peak at module H show highest signals. Thus this region might possess enhancer potential specific for regulation of *c-myc* expression in the erythroid lineage. Since the transposon 17a is located at position 63.550.550 on chromosome 15 and this insertion served as the breakpoint for del(15-17) deletion, module H was not deleted in all experiments performed throughout this thesis. This module could have caused the partially retained expression of *c-myc* in MEPs. However, if module H indeed would possess enhancer activity, one could have expected detection of LacZ expression in these cells upon deletion of del(15-17) as it keeps the reporter gene located close to module H. This was not the case (Figure 3.9), therefore other not yet defined regions are likely to be responsible for *c-myc* enhancer function in the erythroid lineage.

4.3 Thrombocytosis caused by *c-myc* downregulation

Platelets are critical elements in the blood system. They are not only important during homeostasis and thrombosis but also for tissue regeneration after injury and inflammation (GAWAZ *et al.* 2005; SEMPLE *et al.* 2011). Often patients suffering from critical thrombocytopenia, for example, as a result of a hematopoietic disease or chemotherapy, require platelet transfusions (LIEBERMAN *et al.* 2014). Platelets are derived from giant multinucleated cells in the BM, the megakaryocytes (PATEL *et al.* 2005; THON and ITALIANO 2010). Both, megakaryocyte and platelet numbers, were highly increased upon *c-myc* deficiency (GUO *et al.* 2009). Thus the megakaryocytic lineage is the only lineage in the hematopoietic system not being downregulated by the lack of *c-myc*. GUO *et al.* showed that c-Myc is required for polyploidy formation resulting in smaller megakaryocytes upon c-Myc deficiency. However, cytoplasmic maturation is not impaired, thus functional platelets are produced from these smaller megakaryocytes. Similar to c-Myc deficiency our results proved that deficiency of the DHEC also leads to an increase in the megakaryocytic lineage mediated by *c-myc* downregulation.

In situations of acute blood loss or other stress situations that lead to loss of cells of the megakaryocytic lineage these have to be rapidly and efficiently replenished to ensure survival of the organism. Although subsequently challenged by another study a

model has been suggested in 2005 favoring a direct shortcut within the hematopoietic hierarchy that connects the stem cell compartment with megakaryocytic progenitors (ADOLFSSON *et al.* 2005). Data from others but also our lab suggest the presence of megakaryocytic lineage primed HSCs or progenitors (HAAS *et al.* 2014; SANJUAN-PLA *et al.* 2013). More detailed, work from HAAS *et al.* allows a respective identification of megakaryocytic primed progenitors by analysing the primed transcriptome state on single cell level. Thus already at an very early stage of the hierarchy some cells carry determinants for their latter megakaryocytic identity. To gain a first insight into megakaryocytic differentiation potential at the stem and progenitor level upon c-Myc downregulation we determined the amount of CD41 expressing cells in these compartments. These results suggested that megakaryocytic progenitors are pushed from the HSC compartment further down the hierarchy, which is in accordance with the ultimately increased megakaryocyte numbers in the BM. It would be interesting to further track the megakaryocytic populations along the hierarchy using more defined markers (PRONK *et al.* 2007). Furthermore, transcriptome analysis on the single cell level could identify the proportion of megakaryocytic primed HSCs.

Concomitant deletion of *c-myc* and *N-myc* leads to the loss of all major BM cell types including megakaryocytes (LAURENTI *et al.* 2008). Furthermore, expression of *N-myc* is restricted to the very early HSC compartment. These observations argue for the requirement of functional Myc expression (either c-Myc or N-Myc) for the megakaryocytic differentiation potential, which could happen on the level of megakaryocytic priming on the HSC/progenitor level. To test this latter hypothesis, one could check for *N-myc* levels in the above mentioned single cell transcriptome analysis to see if megakaryocytic priming coincides with higher Myc levels. Also, N-Myc deficient mice should be analyzed for a potential defect in megakaryopoiesis, which was not addressed in the original paper (LAURENTI *et al.* 2008).

4.4 Mechanisms of DHEC function

The DHEC region has recently been described in murine leukemia cells to exert enhancer function (SHI *et al.* 2013). 3C and 4C experiments in this study showed long-range interaction between the enhancer region and *c-myc* in a murine and a human leukemia cell line but not in HEK293T cells. Due to the limitation in cell numbers we could not analyze the long-range interaction in mouse stem and progenitor cells by 3C techniques. Instead, we decided to show interaction indirectly by DNA-FISH

experiments. First analyses revealed that *c-myc* and enhancer probe signals nicely overlapped whereas combination with a probe located at the same distance telomeric to the enhancer showed distinct foci (data not shown). These results suggest that not only in leukemic cells but also under homeostatic conditions the DHEC physically contacts the *c-myc* gene locus and therefore enables transcriptional regulation (chapter 1.1.3.3).

As outlined in the introduction, the expression of enhancer RNAs (eRNAs) has been described only a few years ago (KIM *et al.* 2010; KOCH *et al.* 2011). Global analysis of transcription in human cells using cap analysis of gene expression (CAGE) showed that the majority of eRNAs are non-polyadenylated and only 10% to 20% of eRNAs exist in the polyadenylated state (ANDERSSON *et al.* 2014; DJEBALI *et al.* 2012). The polyadenylation status further correlates with the directionality of transcription and the size of the transcript. Non-polyadenylated eRNAs are transcribed bidirectional and are usually 500-2000 bp in size whereas polyadenylated eRNAs reach sizes greater than 3000 bp and are generated by unidirectional transcription (NATOLI and ANDRAU 2012). Since polyadenylation confers among other functions mRNA stability, non-polyadenylated eRNAs are thought to be quite unstable and sensitive to degradation.

Enhancer transcription correlates well with enhancer activity as shown by co-expression of nearby genes (HAH *et al.* 2011; HAH *et al.* 2013; KIM *et al.* 2010; WANG *et al.* 2011). Therefore enhancer transcription might be a useful indicator of enhancer activity (MELGAR *et al.* 2011). The concrete function and mechanism of eRNAs in enhancer activity is not yet clarified, however there is evidence for RNA-dependent (LAM *et al.* 2013; LI *et al.* 2013; MELO *et al.* 2013; MOUSAVI *et al.* 2013) and RNA-independent roles of eRNA transcription (KAIKKONEN *et al.* 2013).

The del(15-17) region so far contains no annotated gene except of a putative, unclassified sequence (AK040104), which gets disrupted by the deletion del(15-17) as the centromeric breakpoint lies within this sequence. Interestingly, analysis of recently published transcriptome data of murine HSCs (CHALLEN *et al.* 2014) revealed the presence of a transcript between module F and G (Figure 6.3). This transcript showed expression at a very low but significant level (signal range <35 units compared to >1000 units for *c-myc*; Figure 6.4) and displayed a size of ~5 kb without any intronic sequences. Therefore, since these RNA-seq data were derived after enrichment for polyadenylated transcripts, this transcript can be classified to the group of polyadenylated eRNAs. RNA-seq data for B cells and granulocytes from the same study revealed that this transcript is not expressed in these differentiated cell types and thus correlates with DHEC enhancer activity measured by LacZ expression. If this eRNA is

involved in mediating the phenotype observed upon DHEC deletion remains to be investigated. Similarly the presence of further eRNAs encoded within the DHEC could be examined by transcript analysis without polyA-enrichment.

The latter finding also prompted us to look further into the data of CHALLEN *et al.* (2012, 2014) who investigated the role of DNA methylation in HSCs. DNA methylation is an epigenetic mechanism involved in modulating many biological activities such as transcription (chapter 1.1.2.2.3), genomic imprinting and genome stability (CHEN and LI 2006). Among the different types of DNA methyltransferases Dnmt3a and Dnmt3b are responsible for modifying unmethylated DNA, thus they are called de novo methyltransferases (HATA *et al.* 2002; OKANO *et al.* 1999). Serial transplantation of Dnmt3a deleted HSCs led to an increased contribution of these donor cells to the peripheral blood while HSCs accumulated in the BM (CHALLEN *et al.* 2012). Combined deficiency of Dnmt3a and Dnmt3b (dKO) in HSCs led to further increase in HSC self-renewal while differentiation capacity declined after secondary transplantation (CHALLEN *et al.* 2014). Overall Dnmt3 deficiency resembled the *c-myc* KO phenotype on the long run. Therefore we asked for *c-myc* and *N-myc* expression levels after these serial transplantations. Indeed Dnmt3a KO and Dnmt3a/b dKO HSCs showed a strong downregulation of both genes compared to HSCs from age matched control mice (Figure 6.4). Thus Myc might be a key factor in mediating the phenotype upon Dnmt3 deficiency in HSCs.

Previous DNA methylation studies revealed an association of low methylated regions with cell-specific regulatory regions or transcription factor binding sites (HODGES *et al.* 2011; STADLER *et al.* 2011; ZILLER *et al.* 2013). In line with these studies analysis of DNA methylation in the DHEC region revealed some narrow valleys at the individual enhancer modules (Figure 6.3), while the surrounding sequences were highly methylated. Most interestingly, deletion of Dnmt3a and more prominently of Dnmt3a/b in HSCs from tertiary transplanted mice showed some differences in DNA methylation compared to the wild type control. Of note, a site of significant hypomethylation partially overlapped with the eRNA sequence mentioned above (Figure 6.3, dashed box). However, this hypomethylation was not accompanied by a decreased eRNA expression, instead it was slightly increased, which is contradictory to a direct connection between DNA methylation and *c-myc* regulation via enhancer function of this eRNA. A potential implication of regulation by the human homologues DNMT3A/c-MYC for leukemia development will be discussed at the end of the following chapter.

4.5 Function of the *MYC* enhancer region in leukemia

The identification of the murine *c-myc* enhancer region and the characterization of its physiological role for hematopoiesis have important implications for human health. Firstly, the human *MYC* locus is highly syntenic to the mouse orthologous region. The different blocks composing the DHEC are also highly conserved in sequence. Both myeloid/erythroid and lymphoblastoid cell lines show enhancer-associated chromatin modifications over some of the DHEC modules (ERNST *et al.* 2011) and more importantly most of the modules are covered by enhancer-associated chromatin marks in mobilized $CD34^+$ HSCs (Figure 3.32) (BERNSTEIN *et al.* 2010). Common SNPs present within the DHEC have been associated with different human traits linked to hematopoietic defects, including changes in monocyte counts (NALLS *et al.* 2011; OKADA *et al.* 2011). Also, focal amplifications overlapping the DHEC have been recurrently observed in acute myeloid leukemia (Kuhn et al. 2012; Radtke et al. 2009). Interestingly, also duplications of the T cell enhancer region are implicated specifically with T-cell acute lymphoblastic leukemia (HERRANZ *et al.* 2014). Both regions were not focally amplified, for example in chronic lymphocytic leukemia (EDELMANN *et al.* 2012), suggesting that duplications of specific enhancer modules may contribute to cancer in some but not all cell types. It is likely that these disease-associated patterns can be used to identify further enhancer modules active in hematopoiesis. For other enhancers it has been shown that their germline duplications can lead to malformations affecting the organ where they are active (DATHE *et al.* 2009; LOHAN *et al.* 2014). Our results showed that neither duplication of the DHEC nor of the whole *c-myc*/*Pvt1* flanking locus resulted in a misregulation of the hematopoietic system. It is likely that transcriptional and posttranscriptional regulatory mechanisms are involved in dosage compensation and keep Myc expression at physiological levels. Evidence for the former is e.g. shown in HSC/MPP1 cells that show no difference in *c-myc* expression upon duplication of the whole *c-myc*/*Pvt1* flanking locus. The importance for posttranscriptional regulation mechanisms have been discussed already in chapter 4.2. However, we looked at dup(15-17) mice at a very early time point soon after birth as this experiment was carried out along with a del(8-17) experiment. Detection of a potential contribution of the murine DHEC duplication to leukemia formation should be followed up in aged mice or can be addressed by breeding these mice to a mouse strain with a high susceptibility to leukemia formation. Similarly it was recently shown that duplication of the whole locus (*c-myc*/*Pvt1*/*Gsdmc*) promoted cancer development in

predisposed mice for mammary tumors (GUY *et al.* 1992; TSENG *et al.* 2014). In this context, cancer susceptibility by *c-myc* copy number increase was dependent on Pvt1 as duplication of *c-myc* alone or *Pvt1*/*Gsdmc* without *c-myc* did not show a reduced tumor-free survival rate.

Recent works have underlined that in cancerous cells *MYC* becomes regulated by so-called super-enhancers (LOVEN *et al.* 2013). This misregulation can occur due to translocations that juxtapose *MYC* to other enhancers (BERGSAGEL and KUEHL 2001; DALLA-FAVERA *et al.* 1982; TAUB *et al.* 1982). In the above mentioned study an altered *in cis* regulation due to juxtaposition of the *c-myc* gene close to a potential regulatory element could be ruled out since mice with a duplicated allele on one chromosome but a null allele on the other did not show pre-cancerous characteristics (TSENG *et al.* 2014).

In murine leukemia cells the DHEC region has recently been exposed as a super-enhancer, since it shows prominent and widespread deposition of H3K27ac, Mediator, and BET bromo-domain proteins (SHI *et al.* 2013). Our data suggest that in normal hematopoiesis, the DHEC is not acting as a super-enhancer, but instead coincides with a series of spatially close, but nonetheless separately acting modules that exert distinct activities. The conversion of enhancers into regions with higher enrichment of H3K27ac chromatin marks, a feature of super-enhancers, appeared common in cancers (HNISZ *et al.* 2013). This suggests that epigenetic alterations may contribute to this "super-enhancer transformation", either through chromatin changes or due to misregulated expression of transcription factors or epigenetic remodelers that may superimpose transcriptional programs normally separated in distinct cell types. The examination of enhancer-associated chromatin marks in the DHEC of primary AML samples and their association with *c-MYC* expression levels will help to shed more light on this process as data published so far rely mostly on cell lines.

As already mentioned above, MYC might not only be deregulated in established AML, but also be implicated together with DNMT3A in leukemia development. In 2010 DNMT3A has been first identified as a somatic mutation in AML patients (LEY *et al.* 2010). This study revealed a mutation frequency of 22% that frequently occured together with mutations in nucleophosmin (NPM1), FMS-related tyrosine kinase 3 (FLT3) and isocitrate dehydrogenase 1 (IDH1). Cancer is thought to be a clonal disease, meaning that all cancer cells descend from a single cell (GREAVES and MALEY 2012; YATES and CAMPBELL 2012). Somatic mutations accumulate in a stepwise manner until disease manifestation and upon diagnosis cancer cells consist of several clones bearing different mutations. Their dominance varies over time, also in response to cancer

treatment. A recent study tried to shed light on the clonal evolution of AML and found that HSCs acquire pre-leukemic mutations, which allow clonal expansion and subsequent acquisition of mutations leading to cancer (SHLUSH *et al.* 2014). Since these pre-leukemic cells can survive chemotherapy they then serve as a reservoir for new clones leading to relapse. DNMT3A mutations have been identified as such an early event in leukemogenesis. Transferring our observations from data of Dnmt3a KO mice to this model, DNMT3A mutations might lead to downregulation of MYC in HSCs. This in turn could account for the accumulation of these pre-leukemic HSCs, which upon acquisition of further mutations, lead to development of AML. Such further mutations might also account for deregulated c-MYC expression in the established leukemia, possibly by transforming the MYC enhancer.

4.6 Regulation of stem cells by Myc

In the hematopoietic system combined deficiency for c-Myc and N-Myc led to a rapid hematopoietic failure associated with impaired proliferation, differentiation and increased apoptosis (LAURENTI *et al.* 2008). Interestingly, under homeostatic conditions Myc deficiency in the dormant HSCs failed to proliferate but were maintained in the bone marrow and these Myc deficient dormant HSCs could even be transplanted. Since Myc function is closely associated with proliferative potential and we detected a dramatic downregulation of *c-myc* upon enhancer deletion, our observation of increased MPP cell numbers instead of HSCs was surprising at first sight. However, *c-myc* downregulation was accompanied by an upregulation of *N-myc* transcripts in all progenitor cells, which accounts for their proliferative potential up to the stage of MPPs. The wide loss of differentiation potential most likely is associated with retention of HSPCs in the niche as it was shown for the conditional *c-myc* deletion (WILSON *et al.* 2004). WILSON *et al.* observed an upregulation of N-cadherin and a number of adhesion receptors in *c-myc* deficient LSK cells, suggesting that c-Myc controls the balance between differentiation and HSPC accumulation by regulating HSPC interaction with the microenvironment. The fact that enhancer deleted mice were still able to generate T cells and red blood cells to an almost normal extent suggests that at least some cells can overcome this differentiation block, likely due to fluctuations in basal *c-myc* expression in HSCs/progenitors. Such escaping cells are either already committed to the distinct lineages or, in case they are still multi- or oligopotent, their expansion and differentiation within the respective lineage is driven by regulatory elements outside the

identified enhancer region (as it is the case for the T cell enhancer (HERRANZ *et al.* 2014)).

Interestingly, similar roles of Myc regulation as in hematopoietic cells have been observed in our laboratory in ES cells (SCOGNAMIGLIO AND TRUMPP, personal communication). ES cells grown under conventional culture conditions in medium containing serum have been shown to rapidly differentiate upon deletion of *c-myc* and *N-myc* (SMITH *et al.* 2010; VARLAKHANOVA *et al.* 2010). These culture conditions keep ES cells not in a stable pluripotent but a primed state that is sustained by Myc proteins. However, serum-free culture together with 2 inhibitors ("2i") targeting the mitogen-activated protein kinase kinase (Mek) and the glycogen synthase kinase-3 (Gsk3) can establish a naïve ground state of pluripotency (YING *et al.* 2008). Work by SCOGNAMIGLIO AND TRUMPP showed that under these culture conditions ES cells lacking c-Myc and N-Myc form only very small colonies that lack proliferation activity. They remain undifferentiated and retain their pluripotency network (unpublished). This observation highly resembles the situation in the most primitive HSC population lacking both c-Myc and N-Myc (LAURENTI *et al.* 2008).

In summary, Myc activity is dispensible for the most potent dormant stem cells at the top of their hierarchy which harbor the highest self-renewal capacitiy (naïve ESCs and HSCs). Myc is not only essential for proliferation of stem and progenitor cells but simultaneously also promotes stem cell differentiation. In contrast terminal differentiation is blocked by overexpression of Myc leading to an expansion of late progenitor cells.

4.7 Outlook

The characterization of the distal *c-myc* enhancer adds a valuable contribution to the understanding of *c-myc* transcription regulation in hematopoietic cells. However, thus far we only characterized the function regarding deletion of the whole cluster. By using the CRISPR/Cas-mediated genome engineering tool (YANG *et al.* 2014) mice have been generated by our collaborators that harbor deletion of single modules within the DHEC. Analysis of these mice will add further understanding in the differential usage of these single enhancer elements in hematopoiesis. Also, these experiments will elucidate the potential role of the eRNA, which can then be addressed further by overexpression or shRNA-mediated knockdown.

Furthermore, we want to extend our studies on the implication on leukemia initiation and maintenance. Forced c-Myc expression in transgenic mice results in a variety of malignancies (ADAMS *et al.* 1985; CHESI *et al.* 2008; LEDER *et al.* 1986). In most mouse models, however, secondary events are required for malignancy, as mice present with disease after a long latency (BEER *et al.* 2004; ELLWOOD-YEN *et al.* 2003; FELSHER and BISHOP 1999). Retrovirus-mediated expression of *c-myc* in BM cells leads to rapid development of acute myeloid leukemia (LUO *et al.* 2005). On one hand, we plan to use the mouse line with duplication of the DHEC (dup(15-17)) and see if the latency period of leukemia is shortened in theses mice. For this experiment a leukemia model with a long latency period is anticipated, as shown in leukemia induction by HoxA9 (KROON *et al.* 1998). On the other hand, we would like to assess whether this enhancer region is important for AML maintenance. Therefore we are currently breeding mice to gain compound heterozygous mice with a del(15-17) allele, a floxed *c-myc* allele and the inducible MxCre transgene. LSK cells will be transduced by retroviral overexpression of MLL-AF9 and transplanted into recipient mice. The impact of the enhancer region on leukemia maintenance will be determined by Cre-mediated *c-myc* deletion after first signs of leukemia onset.

5 MATERIAL & METHODS

5.1 Material

5.1.1 Reagents

Reagent	Company
Acetone	Sigma-Aldrich (St. Louis, USA)
ACK lysis buffer	Lonza (Walkersville, USA)
Agarose	Sigma-Aldrich (St. Louis, USA)
Ammonium sulfate ($(NH_4)_2SO_4$)	Roth (Karlsruhe, Germany)
BD Cytofix/Cytoperm™	Becton Dickinson (Franklin Lakes, USA)
BD Perm/Wash™ buffer	Becton Dickinson (Franklin Lakes, USA)
Boric acid	Sigma-Aldrich (St. Louis, USA)
Bromphenol blue	Sigma-Aldrich (St. Louis, USA)
bovine serum albumin (BSA)	PAA Laboratories, Pasching, Austria
Deoxyribonucleotide triphosphate (dNTP)	Thermo Fisher Scientific (Waltham, USA)
Dimethylsulfoxid (DMSO)	Sigma-Aldrich (St. Louis, USA)
Direct PCR Tail Lysis Reagent	Peqlab (Erlangen, Germany)
DNA Gene Ruler 100 bp	Thermo Fisher Scientific (Waltham, USA)
DNA oligonucleotides (primers)	Sigma-Aldrich (St. Louis, USA)
Entellan	Merck (Darmstadt, Germany)
Ethanol (EtOH)	Merck (Darmstadt, Germany)
Ethidium bromide	Roth (Karlsruhe, Germany)
Ethylenediamine tetra-acetic acid-disodium salt (EDTA)	Sigma-Aldrich (St. Louis, USA)
Fetal calf serum (FCS)	PAA Laboratories, Pasching, Austria
fluorescein di-(β-D-galactopyranoside) (FDG)	Sigma-Aldrich (St. Louis, USA)
Glacial acetic acid	Sigma-Aldrich (St. Louis, USA)
Giemsa	Sigma-Aldrich (St. Louis, USA)
Glycerol	Applichem (Darmstadt, Germany)

Hanks' Balanced Salt Solution (HBSS)	Thermo Fisher Scientific (Waltham, USA)
Hoechst33342	Thermo Fisher Scientific (Waltham, USA)
4-(2-hydroxyethyl)-1-piperazineethane-sulfonic acid (HEPES buffer)	Thermo Fisher Scientific (Waltham, USA)
Hydrochloric acid (HCl)	Roth (Karlsruhe, Germany)
Isopropanol	Sigma-Aldrich (St. Louis, USA)
May-Grünwald	Sigma-Aldrich (St. Louis, USA)
Methanol (MeOH)	Sigma-Aldrich (St. Louis, USA)
Magnesium chloride ($MgCl_2$)	VWR International (Radnor, USA)
MethoCult M3434 medium	StemCell Technology (Vancouver, Canada)
One Comp eBeads	eBioscience (San Diego, USA)
Paraformaldehyde (PFA)	Sigma-Aldrich (St. Louis, USA)
Penicillin-Streptomycin (10000 units/ml)	Thermo Fisher Scientific (Waltham, USA)
Phosphate buffered saline (PBS)	Sigma-Aldrich (St. Louis, USA)
Polyinosinic-polycytidylic acid (poly(I:C))	InvivoGen (Toulouse, France)
Potassium chloride (KCl)	Roth (Karlsruhe, Germany)
Potassium dihydrogen phosphate (KH_2PO_4)	Roth (Karlsruhe, Germany)
Power SYBR Green Master Mix	Thermo Fisher Scientific (Waltham, USA)
Rnase-free water	Thermo Fisher Scientific (Waltham, USA)
Rnase Zap	Thermo Fisher Scientific (Waltham, USA)
RPMI 1640	Sigma-Aldrich (St. Louis, USA)
Sodium chloride (NaCl)	Sigma-Aldrich (St. Louis, USA)
Sodium hydroxide (NaOH)	Sigma-Aldrich (St. Louis, USA)
Sodium dihydrogen phosphate (Na_2HPO_4)	Sigma-Aldrich (St. Louis, USA)
Trimethoprim/sulfamethoxazole	Ratiopharm (Ulm, Germany)
Sucrose	Sigma-Aldrich (St. Louis, USA)
Trisodium citrate	Sigma-Aldrich (St. Louis, USA)
tris(hydroxymethyl)aminomethane (Tris)	Sigma-Aldrich (St. Louis, USA)
Triton X-100	Applichem (Darmstadt, Germany)
Xylol	Sigma-Aldrich (St. Louis, USA)

Table 5.1: Reagents

5.1.2 Enzymes

Enzyme	Company
Dnase I	Qiagen (Hilden, Germany)
Proteinase K	Peqlab (Erlangen, Germany)
DreamTaq DNA polymerase	Thermo Fisher Scientific (Waltham, USA)
SuperScript Reverse Transcriptase	Thermo Fisher Scientific (Waltham, USA)

Table 5.2: Enzymes

5.1.3 Buffers

Buffers provided with the kits were used in the case of RNA isolation and reverse transcription. All other buffers used are listed in Table 5.3.

Buffer	Composition
10x TBE	890 mM Tris 890 mM boric acid 20 mM EDTA pH 8.0 pH 8.0
10x PCR buffer	670 mM TrisHCl, pH 8.8 67 mM $MgCl_2$ 1.7 mg/ml BSA 166 mM $(NH_4)_2SO_4$
Decalcification buffer	0.4 M EDTA pH 7.2 adjusted with sodium hydroxide
DNase I stock solution	Lyophilized Dnase I (1500 Kunitz units) dissolved in 550 µl Rnase-free H_2O aliquoted and stored at -20°C
Dnase treatment	µl Dnase solution 35 µl buffer RDD (provided in the Rnase-free Dnase Set)
DNA gel loading buffer	0.25 % bromophenol blue 0.25 % xylencyanol 15 % glycerol in 10 ml dH_2O
Giemsa solution	14.3% Giemsa in modified Sörensen buffer
HBSS+	Hanks' Balanced Salt Solution supplemented with 2% fetal calf serum and a final concentration of 10 mM HEPES
May-Grünwald solution	50% May-Grünwald in modified Sörensen buffer
modified Sörensen buffer	8 mM Na_2HPO_4 3.6 mM KH_2PO_4 pH 6.8

Table 5.3: Buffers

5.1.4 Antibodies for flow cytometry

Antigen	Label	Clone	Company
B220	PE-Cy5, PE-Cy7, APCeFluor®780	RA3-6B2	eBioscience
B220	biotin	RA3-6B2	BioLegend
CD4	FITC, PE-Cy7, Pacific Blue	GK1.5	eBioscience
CD4	biotin	GK1.5	BioLegend
CD8a	PE-Cy5, PE-Cy7	53-6.7	eBioscience
CD8a	biotin	53-6.7	BioLegend
CD11b	AlexaFluor®700, PE-Cy7	M1/70	eBioscience
CD11b	biotin	M1/70	BioLegend
CD16/32 (FcγR)	Pacific Blue	93	eBioscience
CD25	PE	PC61.5	eBioscience
CD34	AlexaFluor®700, FITC	RAM34	eBioscience
CD41	eFluor®450, FITC, PE-Cy7	MWReg30	eBioscience
CD44	Pacific Blue	IM7	BioLegend
CD45	AlexaFluor®700	30-F11	eBioscience
CD45.1	FITC, PE, PE-Cy7	A20.1	eBioscience
CD45.2	Pacific Blue	104	BioLegend
CD45.2	AlexaFluor®700	104	BD Pharmingen
CD48	Pacific Blue	HM48-1	BioLegend
CD48	PE, PE-Cy7	HM48-1	eBioscience
CD71	PE	OKT9	eBioscience
CD117 (c-Kit)	APC-eFluor®780	2B8	eBioscience
CD127 (IL7Rα)	PE	A7R34	eBioscience
CD135	PE	A2F10	eBioscience
CD150	PE-Cy5	TC15-12F12.2	BioLegend
Ki67	FITC	B56	BD Pharmingen
Gr-1 (Ly6-G)	APC, PE-Cy7	RB6-8C5	eBioscience
Gr-1 (Ly6-G)	biotin	RB6-8C5	BioLegend
Sca-1	APC	D7	eBioscience
Streptavidin	PE-TexasRed	-	BD Pharmingen
Ter119	APC-eFluor®780, PE-Cy7	TER-119	eBioscience
Ter119	biotin	TER-119	BioLegend

Table 5.4: Antibodies for flow cytometry
Abbreviations: APC, allophycocyanin; FITC, fluorescein isothiocyanate; PE, phycoerythrin; PE-Cy5, phycoerythrin-Cyanine 5; PE-Cy7, phycoerythrin-Cyanine 7; PE-TxRed, phycoerythrin-Texas Red.

5.1.5 Kits

Name	Company
SuperScript® VILO™ cDNA Synthesis Kit	Thermo Fisher Scientific (Waltham, USA)
Arcturus® PicoPure® RNA Isolation Kit	Thermo Fisher Scientific (Waltham, USA)
DNeasy Blood & Tissue Kit	Qiagen (Hilden, Germany)

Table 5.5: Kits

5.1.6 Consumables

Item	Company
384-well PCR plates	Thermo Fisher Scientific (Waltham, USA)
BD Micro-Fine (1 ml, 29 Gx8 mm)	Becton Dickinson (Franklin Lakes, USA)
Cell strainer (40 µm nylon)	Becton Dickinson (Franklin Lakes, USA)
Cover Slips (24x60 mm)	Thermo Fisher Scientific (Waltham, USA)
Disposable scalpel (20)	Feather Safety Razor (Osaka, Japan)
Eppendorf tubes (1.5 and 2 ml safe-lock)	Eppendorf (Hamburg, Germany)
FACS-tubes (5 ml)	Becton Dickinson (Franklin Lakes, USA)
Falcon tubes (sterile, 15 ml)	Sarstedt (Nümbrecht, Germany)
Falcon tubes (sterile, 50 ml)	Greiner (Frickenhausen, Germany)
Folded Filters	Munktell (Falun, Sweden)
Microscope slides	Thermo Fisher Scientific (Waltham, USA)
Microvette 200K3E	Sarstedt (Nümbrecht, Germany)
Mortar and pestle	Sigma-Aldrich (St. Louis, USA)
Multiwell culture plate (6-well, 12-well)	Corning Inc. (Corning, USA)
paper towels tissue	WEPA Hygieneprodukte (Arnsberg, Germany)
Pasteur pipettes	WU Mainz (Bamberg, Germany)
Petri dishes (sterile, 35 mm)	Becton Dickinson (Franklin Lakes, USA)
Petri dishes (sterile, 100 mm)	TPP Techno Plastic Products AG (Trasadingen Switzerland)
PCR-Reaction tubes (0.2 ml SingleCap 8-er SoftStripes)	Biozym Scientific (Hessisch Oldendorf, Germany)
Rnase-free microtubes	Axygen (Union City, USA)
Serological Pipettes (5 ml, 10 ml, 25 ml, 50 ml)	Becton Dickinson (Franklin Lakes, USA)
Sterile filtered and not filtered tips (10 µl, 20 µl, 200 µl, 1000 µl)	Starlab (Milton Keynes, UK)
Syringe without needle (5 ml)	Terumo (Leuven, Germany)

Table 5.6: Consumables

5.1.7 Equipment

Equipment	Company
Analytical Balance ALC-1100.2	Acculab (Göttingen, Germany)
Bench centrifuge Eppendorf 5810r centrifuge	Eppendorf (Hamburg, Germany)
Cell culture hood Safe2020	Thermo Fisher Scientific (Waltham, USA)
DynaMag™ magnets	Thermo Fisher Scientific (Waltham, USA)
Electronic pipette Eppendorf Research Pro (5-100 µl)	Eppendorf (Hamburg, Germany)
Electrophoresis power supply (PowerPac Basic Power Supply)	Bio-Rad Laboratories (Hercules, USA)
Electrophoresis unit (Sub-Cell GT)	Bio-Rad Laboratories (Hercules, USA)
FACS Arial, FACS Aria II, FACS Aria III	Becton Dickinson (Franklin Lakes, USA)
Heating block (MHR23)	Ditabis (Pforzheim, Germany)
Hemavet HV 950 Hematology System	ERBA Diagnostics (Miami, USA)
Cs-137 γ-irradiator (1990)	Buchler GmbH (Braunschweig, Germany)
LSR II	Becton Dickinson (Franklin Lakes, USA)
LSR Fortessa	Becton Dickinson (Franklin Lakes, USA)
Microwave oven	Sharp (Osaka, Japan)
Millipore H_2O-production unit	Milli-Q plus Millipore (Eschborn, Germany)
Neubauer counting chamber	Braun (Melsungen, Germany)
pH211 Microprocessor pH-Meter	Hanna Instruments (Woonsocket, USA)
Pipettes (p-2, p-20, p-200, p-1000)	Gilson (Bad Camberg, Germany)
Pipetboy acu	Integra Biosciences (Fernwald, Germany)
Precision weighing balance ALC-110.4	Acculab (Göttingen, Germany)
Refrigerator 4°C	Liebherr (Biberach an der Riß, Germany)
Refrigerator -20°C	Liebherr (Biberach an der Riß, Germany)
Refrigerator -80°C	SANYO Electric Co. (Wood Dale, USA)
Staining dish for microscope slides	Roth (Karlsruhe, Germany)
Stuart roller mixer SRT2	Sigma-Aldrich (St. Louis, USA)
Thermocycler (T3000)	Biometra (Göttingen, Germany)
UV-Transluminator and video system	Intas (Göttingen, Germany)
ViiA™ 7 Real-Time PCR System with 384-well block	Thermo Fisher Scientific (Waltham, USA)
Vi-CELL Series Cell Viability Analyzer	Beckman Coulter, Brea, USA
Vortex-Genie 2	Scientific Industries (Bohemia, USA)
Zeiss Axioplan microscope equipped with a AxioCam Icc 3 colour camera	Zeiss (Jena, Germany)
Zeiss Primo Vert inverted microscope equipped with an AxioCam Erc 5s	Zeiss (Jena, Germany)

Table 5.7: Equipment

5.1.8 Computer, printer and software

Computer, printer or software	Company
Adobe Illustrator CS6	Adobe (San Jose, USA)
Adobe Photoshop CS5	Adobe (San Jose, USA)
AxioVs40 V4.8.2.0	Carl Zeiss MicroImaging (Jena, Germany)
BD FACSDiva software	Becton Dickinson (Franklin Lakes, USA)
CloneManager 9	Scientific & Educational Software (Cary, USA)
DataAssist software 3.01	Thermo Fisher Scientific (Waltham, USA)
EndNote X3	Thompson Reuters (New York, USA)
FACSDiva Software	Becton Dickinson (Franklin Lakes, USA)
Fiji (SCHINDELIN *et al.* 2012)	Open Source image processing package
FlowJo 9.6.4 Software	TreeStar (Ashland, USA)
GraphPad Software Prism	GraphPad (La Jolla, USA)
Intas GDS	Intas (Göttingen, Germany)
MacBookPro notebook	Apple (Cupertino, USA)
Microsoft Office 2008 for Mac	Microsoft Corporation (Redmond, USA)
Microsoft Windows 7	Microsoft Corporation (Redmond, USA)
Parallels Desktop 6 for Mac	Parallels Holdings (Renton, USA)
ViiA7 software v 1.1	Thermo Fisher Scientific (Waltham, USA)
Printer HP Colour Laserjet CP2025	Hewlett-Packard (Palo Alto, USA)
Printer HP Laserjet P2035	Hewlett-Packard (Palo Alto, USA)
Printer Lexmark C544dn	Lexmark (Lexington, USA)
Printer Lexmark E460dn	Lexmark (Lexington, USA)
Printer Mitsubishi P93D	Mitsubishi Electric (Tokio, Japan)
Zen 2011 lite	Carl Zeiss Microscopy (Jena, Germany)

Table 5.8: Computer, printer and software

5.1.9 Internet resources

Tool	Internet address
Epigenome Browser	http://www.epigenomebrowser.org/
NCBI databases and tools	http://ncbi.nlm.nih.gov
TAD Data visualization	http://yuelab.org/hi-c/database.php
TRACER database	http://www.ebi.ac.uk/panda-srv/tracer/index.php
UCSC Genome Browser	http://genome.ucsc.edu
VISTA Browser	http://genome.lbl.gov/vista

Table 5.9: Internet resources

5.2 Methods

5.2.1 Animals

Mice were maintained in the animal facility of the German Cancer Research Center (DKFZ, Heidelberg) or at the European Molecular Biology Laboratory (EMBL, Heidelberg) under specific pathogen-free conditions (SPF) and housed in individually ventilated cages (IVC). If not indicated differently, the mice were on a C57Bl/6 background. Adult mice used for experiments were between 6 and 12 weeks old at the beginning of the respective experiment if not specified differently. The age of embryos or newborn mice is specified.

Mouse strains

C57Bl/6 J. C57Bl/6 J mice are referred to as ($CD45.2^+$) wild type (Wt) mice. These mice were either purchased from Harlan Laboratories or were bred at the DKFZ or EMBL.

B6.SJL-Ptprca-Pep3b-/BoyJ. B6.SJL-Ptprca-Pep3b-/BoyJ mice are referred to as $CD45.1^+$ wt mice. These mice were purchased from Charles River Laboratories, Italy or were bred at the DKFZ.

$Myc^{tm2.1Atp}$/Myc^{tm1Atp}. $Myc^{tm2.1Atp}$/Myc^{tm1Atp} mice are referred to as $c\text{-}myc^{flox/KO}$ mice. The knockout allele (*c-myc*^{KO}) has been generated by replacing the entire *c-myc* open reading frame (ORF) with a *Pgk-Hprt* cassette (TRUMPP *et al.* 2001). These mice were on a mixed background and bred at DKFZ.

Tg(Mx1-cre)1Cgn $Myc^{tm2.1Atp}$/$Myc^{tm2.1Atp}$. Tg(Mx1-cre)1Cgn $Myc^{tm2.1Atp}$/$Myc^{tm2.1Atp}$ mice are referred to as MxCre $c\text{-}myc^{flox/flox}$ mice. The *c-myc* allele is flanked by *loxP* recognition sites (TRUMPP *et al.* 2001), therefore expression of Cre recombinase causes the flanked gene to be removed. The Cre recombinase is under the control of the myxovirus resistance (*Mx1*) promoter, which can be induced by administration of the synthetic double-stranded RNA polymer polyinosinic-polycytidylic acid (polyI:C) (KÜHN *et al.* 1995). This leads to efficient deletion of *c-myc* in several tissues, e.g. the hematopoietic system, the liver and the BM stroma.

To induce deletion of loxP-flanked alleles, mice were injected intraperitoneally (i.p.) with 100 µg polyI:C in 200 µl PBS 5 times every other day. Control mice were injected with an equal volume of PBS. These mice were bred at DKFZ.

Transgenic mouse lines with transposon insertions and deletions/duplications

Mice carrying a transgenic insertion generated by the *Sleeping Beauty* transposon-based system were established in the laboratory of Dr. François Spitz (RUF *et al.* 2011). In Table 5.10 the respective position of the transposons as well as their direction and the parental transposon is indicated. These data are also available in the TRACER Database. In Table 5.11 the transgenic mouse lines are listed that were generated using targeted meiotic recombination as explained in chapter 3.1. Short names are used throughout the thesis. Most of these animals were maintained at EMBL and genotyping was performed by Dr. Veli V. Uslu. Only the lines del(14-17) and del(15-17) were also bred at DKFZ on a mixed background (derived from breedings below).

Line name	Short name	Chr	Position (mm9)	LoxP	Transposon parent
196231	c17	15	60133316	minus	179039
205880	c8a	15	61051281	minus	196231 or 194578
194578	3a	15	62168343	plus	179039
184347	8a	15	62668548	plus	179039
193058	14b	15	63185343	plus	179039
193637	14c	15	63196469	plus	179039
192339	15a	15	63291835	plus	179039
193315	16a	15	63461422	minus	179039
179039	17a	15	63550550	plus	176598
192857	17b	15	63550550	minus	179039

Table 5.10: Transgenic mouse lines with transposon insertions
Table specifies position of insertions, direction of loxP (strand) and parental transposon.

Line name	Centromeric breakpoint	Telomeric breakpoint	Region spanned (mm9)	Length (bp)
del(8-17)	184347	179039	chr15:62668548-63550550	882002
del(14-15)	193058	192339	chr15:63185343-63291835	106492
del(14-17)	193637	179039	chr15:63196469-63550550	354081
del(15-17)	192339	179039	chr15:63291835-63550550	258715
dup(15-17)	192339	179039	chr15:63291835-63550550	258715
dup(c17-17)	196231	192857	chr15:60133316-63550550	3417234

Table 5.11: Transgenic mouse lines carrying deletions or duplications
Table specifies breakpoints, spanned regions and length of deleted/duplicated region.

del(14-17)/c-myc^{flox} or del(14-17)/c-myc^{KO}. Del(14-17) mice were crossed with Myc$^{tm2.1Atp}$/Myc^{tm1Atp} mice to generate compound heterozygous mice. These were on a mixed background and were bred at DKFZ.

del(15-17)/c-myc^{flox} or del(15-17)/c-myc^{KO}. Del(15-17) mice were crossed with Myc$^{tm2.1Atp}$/Myc^{tm1Atp} mice to generate compound heterozygous mice. These were on a mixed background and were bred at DKFZ.

5.2.2 Genotyping

5.2.2.1 Genomic DNA extraction

Mice maintained at the German Cancer Research Center were marked using numbered ear tags or ear punches. Approximately 3 mm of the tail was cut and subsequently incubated with 100 µl Direct PCR Tail Lysis Reagent containing 0.2 mg/ml proteinase K at 55°C for 3 to 16 hours until the tissue was completely enzymatically digested. Inactivation of proteinase K was achieved by incubation at 85°C for 45 min. Samples were stored at 4°C and 1 µl used for genotyping by polymerase chain reaction.

Genomic DNA from lineage depleted cells (5.2.3.4) of MxCre c-myc$^{flox/flox}$ mice was extracted using the DNeasy Blood & Tissue Kit according to the manufacturers instructions.

5.2.2.2 Polymerase chain reaction

The polymerase chain reaction (PCR) was used to amplify specfic DNA fragments (MULLIS 1990). Usage of two oligonucleotide pairs (primers) allows amplification of a particular DNA sequence. Primers used for genotyping are listed Table 5.12.

All PCR amplifications were performed in an end volume of 30 µl according to the standard protocol shown in Table 5.13. Specific PCRs required addition of either 10% DMSO (c-myc^{KO}) or 0.13% Triton (c-myc^{flox} and c-myc$^{del\ ORF}$).

PCRs were performed according to the standard program shown in Table 5.14 on a T3000 thermocycler. Genotyping for the MxCre transgene was performed with 62°C annealing temperature. Finally, the PCR product was loaded onto an agarose gel.

Genotype	Primer name	Sequence (5'-3')	Amplicon
del(14-17) / del(15-17)	KOF 2432	GGT TCT CTC TCA TGG AGT GTA TCA GG	KO: 285 bp
	KOR 426	AAG TAG ATG TCC TAA CTG ACT TTGC	
del(14-17) / del(15-17)	WTF 2646	GAT GGG ACT TCC CAC ATA ACA GC	WT: 850 bp
	WTR 2647	AAT GCC AAA GAC AAG GAC TCC AG	
del(14-17)	KOF 193637	CCT CCT GGG ATT TCC ATG ACT C	KO: 294 bp
	KOR 429	TCC TAA CTG ACC TAA GAC AGG	
del(15-17)	KOF 2646	GAT GGG ACT TCC CAC ATA ACA GC	KO: 548 bp
	KOR 429	TCC TAA CTG ACC TAA GAC AGG	
c-myc^{flox}	5'floxB	ACA ACG TCT TGG AAC GTC AGA GG	WT: 350 bp
	3'floxB	GCA TTT TAA TTC CAG CGC ATC AG	Flox: 500 bp
c-myc^{KO}	cmyc KOA2F	GTA ATT CCA GCG AGA GAC AGA GG	KO: 850 bp
	cmyc KOA2R	AAC CTG GTT CAT CAT CGC TAA TC	
MxCre	MxU121	GGC AGG GCT CCT CAG TGA TTC	tg: 550 bp
	Cre21L	CTG GCG ATC CCT GAA CAT GTC	
c-myc$^{del\ ORF}$	cmyc del1	AAA TAG TGA TCG TAG TAA AAT TTA GCC TG	del: 200 bp
	cmyc del2	ACC GTT CTC CTT AGC TCT CAC G	

Table 5.12: Genotyping primers

reagent	volume
1/10 10x PCR buffer	3,0 µl
dNTP mix (10 mM)	2.1 µl
forward primer (10 µM)	0.6 µl
reverse primer (10 µM)	0.6 µl
DreamTaq DNA Polymerase (5 U/µl)	0.2 µl
DNA	1,0 µl
dH_2O	fill up to 30 µl

Table 5.13: PCR reaction conditions

Step	Temperature	Time	Number of cycles
Denaturation	95°C	2 min	1
Denaturation	94°C	45 s	
Annealing	60°C	45 s	35
Elongation	72°C	45 s	
Final elongation	72°C	5 min	1

Table 5.14: PCR thermal cycling program

5.2.2.3 Electrophoresis of DNA

In order to separate the DNA fragments amplified by PCR according to their molecular weight, PCR products were subjected to gel electrophoresis. The gel composed of 1-2% agarose diluted in 1x TBE buffer was boiled using a microwave oven. Ethidium bromide solution at a concentration of 30 µg/100 ml gel was added before the solution was filled into a gel tray that contained a comb at one side. After polymerization the gel was transferred into a chamber filled with 1x TBE and the comb was removed. The PCR-products were mixed with a loading buffer containing bromophenol blue and then loaded onto the gel along with a DNA ladder. The gel was run at a voltage of 120 V until fragments were separated. DNA fragments were visualized with an UV transilluminator and documented with a camera system.

5.2.3 Cell preparation

5.2.3.1 Isolation of cells from bone marrow

After sacrificing the mice by cervical dislocation, hematopoietic organs were removed and kept in PBS on ice. Bones from hind legs (femur, tibia), hips (ilium) and/or vertebrae (columna vertebralis) were isolated and muscle and connective tissue was removed using a scalpel and tissue. Bones were crushed with mortar and pestle in RPMI-1640 medium supplemented with 2% fetal calf serum (FCS). Cell suspensions were filtered through a 40 µm cell strainer. Viable cell numbers were determined with a Vi-CELL cell counter or manually using a Neubauer chamber.

5.2.3.2 Isolation of cells from liver and thymus

Liver and thymus were passed through a 40 µm cell strainer into RPMI-1640 medium supplemented with 2% FCS. Viable cell numbers were determined with a Vi-CELL cell counter.

5.2.3.3 Peripheral blood isolation

For isolation of peripheral blood (PB), 4-5 drops of blood were collected from the vena facialis into an EDTA containing tube. A blood cell count was performed using the automated Hemavet counter. For flow cytometric analysis erythrocytes were lysed twice with 1 ml of ACK lysing buffer at room temperature for 5 min. All centrifugation steps were conducted at 1,600 rpm for 5 min at 4°C with an Eppendorf 5810r

centrifuge. All wash steps were performed with ice-cold PBS supplemented with 2% FCS.

5.2.3.4 Lineage depletion

BM cells depleted for lineage positive cells were prepared by staining with a cocktail of rat anti-mouse monoclonal antibodies (mAbs) against the following lineage markers: CD4 (GK1.5), CD8a (53.6.7), B220 (RA3-6B2), Gr1 (RB6.8C5), Ter119 (Ter119) and CD11b (M1/70). These antibodies were purified and conjugated in our laboratory according to standard protocols. Labeled cells were then removed by incubation with sheep anti-rat IgG coated Dynabeads® (4.5 μm diameter superparamagnetic polystyrene beads) at a 2:1 bead-to-target cell ratio and subsequent magnetic separation. All centrifugation steps were conducted at 1,600 rpm for 5 min at 4°C with an Eppendorf 5810r centrifuge. All wash steps were performed with ice-cold PBS supplemented with 2% FCS.

5.2.3.5 Cell surface staining

All antibody cell surface stainings were performed in a solution of 50% RPMI-1640 supplemented with 2% FCS and 50% cultured supernatant from the 24G2 hybridoma cell line, which produces a rat monoclonal antibody directed against the CD16/32 or FcγR antigen. Cell surface stainings that aimed to identify committed progenitor cells by CD16/32 (FcγR) expression were performed in RPMI-1640 supplemented with 2% FCS only. All antibodies used in the experiments were titrated before usage.

For hematopoietic stem and progenitor cell identification, total or lineage depleted cells were stained using lineage antibodies (CD4, CD8, CD11b, Gr-1, B220 and TER119) and antibodies against c-Kit, Sca-1, CD150, CD48, CD135, CD34 and in part also CD41. All experiments with the del(8-17) mouse line did not include the CD135 marker, therefore MPP3 and MPP4 are combined as MPP3/4.

For staining of progenitor cells, cells were stained using lineage antibodies (CD4, CD8, CD11b, Gr-1, B220 and TER119) and antibodies against c-Kit, Sca-1, CD16/32, CD34, CD127 and CD135.

For staining of mature hematopoietic cells antibodies against CD4, CD8, CD11b, CD41, CD71, B220, Gr-1 and TER119 were used.

Mean fluorescence intensities for lacZ stainings and CD41 expression in HSCs were determined as geometric mean of the respective fluorescence signal.

Abbreviation	Population name	Cell surface phenotype
Lin	lineage (adult mice)	$CD11b^+$ $Gr\text{-}1^+$ $B220^+$ $CD4^+$ $CD8a^+$ $Ter119^+$
Lin	lineage (fetuses)	$Gr\text{-}1^+$ $B220^+$ $CD4^+$ $CD8a^+$ $Ter119^+$
LSK	hematopoietic stem and progenitor cells	Lin^- $Sca\text{-}1^+$ $c\text{-}Kit^+$
HSC	hematopoietic stem cell	LSK $CD150^+$ $CD48^-$ $CD34^-$ ($CD135^-$)
MPP1	multipotent progenitor 1	LSK $CD150^+$ $CD48^-$ $CD34^+$ ($CD135^-$)
MPP2	multipotent progenitor 2	LSK $CD150^+$ $CD48^+$ $CD34^+$ ($CD135^-$)
MPP3	multipotent progenitor 3	LSK $CD150^-$ $CD48^+$ $CD34^+$ $CD135^-$
MPP4	multipotent progenitor 4	LSK $CD150^-$ $CD48^+$ $CD34^+$ $CD135^+$
MPP3/4	multipotent progenitors 3 and 4	LSK $CD150^-$ $CD48^+$ $CD34^+$
LS^-K	myeloid committed progenitors	Lin^- $Sca\text{-}1^-$ $c\text{-}Kit^+$
CMP	common myeloid progenitor	Lin^- $Sca\text{-}1^-$ $c\text{-}Kit^+$ $IL7R\alpha^-$ $CD34^+$ $Fc\gamma R^{low}$
GMP	granulocyte macrophage progenitor	Lin^- $Sca\text{-}1^-$ $c\text{-}Kit^+$ $IL7R\alpha^-$ $CD34^+$ $Fc\gamma R^{high}$
MEP	megakaryocyte erythrocyte progenitor	Lin^- $Sca\text{-}1^-$ $c\text{-}Kit^+$ $IL7R\alpha^-$ $CD34^-$ $Fc\gamma R^{low}$
CLP	common lymphoid progenitor	Lin^- $Sca\text{-}1^{int}$ $c\text{-}Kit^{int}$ $IL7R\alpha^+$
gran / My	granulocytes	$CD11b^+$ $Gr\text{-}1^+$
mac	macrophages	$CD11b^+$ $Gr\text{-}1^-$
B	B lymphocytes	$B220^+$
T	T lymphocytes	$CD4^+$ cells and $CD8a^+$ cells
$CD4^+$ T	$CD4^+$ T lymphocytes	$CD4^+$
$CD8^+$ T	$CD8^+$ T lymphocytes	$CD8a^+$
DP	double positive thymocytes	$CD4^+$ $CD8a^+$
SP CD4	single positive CD4 thymocytes	$CD4^+$
SP CD8	single positive CD8 thymocytes	$CD8a^+$
DN	double negative thymocytes	$CD4^-$ $CD8a^-$
DN1	DN1 thymocytes	$CD4^-$ $CD8a^-$ $CD44^+$ $CD25^-$
DN2	DN2 thymocytes	$CD4^-$ $CD8a^-$ $CD44^+$ $CD25^+$
DN3	DN3 thymocytes	$CD4^-$ $CD8a^-$ $CD44^-$ $CD25^+$
DN4	DN4 thymocytes	$CD4^-$ $CD8a^-$ $CD44^-$ $CD25^-$
ProE	proerythroblasts	$CD71^+$ $Ter119^-$
EB	erythroblasts	$CD71^+$ $Ter119^+$
EP	erythrocyte progenitors	$CD71^+$
RBC	red blood cells	$Ter119^+$
Mgk	megakaryocytes	$CD41^+$

Table 5.15: Hematopoietic populations and corresponding cell surface markers

Detection of chimerism in BM and peripheral blood cells was achieved by using CD45.1 and CD45.2 antibodies.

For staining of developing T cells thymocytes were stained with antibodies against CD4, CD8, CD44, CD25, c-Kit, Ter119.

To calculate the number of a cell type, the absolute frequency of the population determined by flow cytometry was multiplied by the number of cells in the tissue determined by the Vi-CELL cell counter.

All monoclonal antibody conjugates were purchased from companies indicated in Table 5.4. The cell surface phenotypes used to identify and purify each population are listed in Table 5.15.

5.2.3.6 Cell cycle staining

For cell cycle analysis, cell surface stained cells were fixed and permeabilized with Cytofix/Cytoperm according to manufacturers instructions. Cells were then stained with anti-Ki67 antibody for at least one hour on ice followed by addition of Hoechst33342 for 5 min. After washing cells were immediately acquired at the flow cytometer.

5.2.3.7 LacZ staining

Cell surface stained BM cells were pelleted, resuspended in 200 µl (differentiated cell and progenitor cell staining) or 500 µl (HSC staining) of HBSS+ buffer and warmed for 10 min to 37°C. Hypotonic loading was accomplished by diluting the cells in a 2:1 ratio with warmed 2 mM fluorescein di-(β-D-galactopyranoside) (FDG) containing 1% DMSO and 1% ethanol and incubation at 37°C for exactly 1 min. Loading was stopped by adding 2 ml of ice-cold HBSS+ solution and intracellular hydrolysis of FDG to fluorescein catalyzed by β-galactosidase was allowed to proceed on ice for 1 h. Cells were immediately acquired at the flow cytometer.

5.2.4 Flow cytometry

5.2.4.1 Flow cytometry for cell analysis

Cells were analyzed by flow cytometry on either a LSRII or LSR Fortessa cell analyzer equipped with a 350 nm, 405 nm, 488 nm, 561 nm, and 640 nm laser. Prior to analysis of multicolor samples, compensation was manually adjusted according to signals from OneComp eBeads stained with single antibodies.

5.2.4.2 Fluorescence-activated cell sorting (FACS)

Fluorescence-activated cell sorting (FACS) was performed on a FACSAria I, a FACSAria II or a FACSAria III cell sorter at the DKFZ Flow Cytometry Service Unit.

5.2.4.3 Analysis of flow cytometric data

Analysis of flow cytometric data was performed using the FlowJo software version 9.6.4. Analysis was performed on live cells gated according to forward and side scatter characteristics.

5.2.5 Competitive transplantation

BM cells were isolated as described in 5.2.3.1. Cells were mixed in a 80:20 ratio with BM cells of $CD45.1^+/CD45.2^+$ mice and an aliquot of this cell suspension was cell surface stained for differentiated cells and hematopoietic stem and progenitor cells to determine the input ratio by flow cytometry. A volume of 100 µl containing $3x10^6$ cells was intravenously injected into the tail vein of lethally irradiated (2x4.5 Gy using a Cs 137 γ-irradiator on the day before) $CD45.1^+$ mice. Mice were kept on antibiotic (trimethoprim/sulfamethoxazole) containing water for 3 weeks post transplantation.
Peripheral blood chimerism was assessed by flow cytometry at 4, 8 and 12 weeks after transplantation. Mice were sacrificed after 16 weeks for peripheral blood and BM analysis by flow cytometry.

5.2.6 Colony forming unit assay

10,000 freshly prepared BM cells were mixed with 1 ml of semi-solid MethoCult M3434 medium and plated on a 35 mm culture plate. Colonies were counted after ten days using an Zeiss Primo Vert inverted microscope (4x and 10x objective) and images were captured using an AxioCam Erc 5s.

5.2.7 mRNA expression analysis

5.2.7.1 RNA isolation

500-50,000 cells were sorted in Extraction Buffer and RNA isolation was performed as described in the manual of the PicoPure RNA Isolation Kit including Rnase-free Dnase digestion to avoid unwanted contamination of genomic.

5.2.7.2 Reverse transcription

RNA samples were transcribed using the SuperScript VILO cDNA synthesis kit according to the manufacturer's instructions. cDNA was diluted in Rnase-free water.

5.2.7.3 Quantitative real-time polymerase chain reaction

Quantitative real-time PCR (qRT-PCR) reactions were performed on a ViiA 7 Real-Time PCR System using the Power SYBR Green Master Mix (at DKFZ). PCR reactions were performed in 384-well plates in a reaction volume of 10 µl with primer concentrations of 0.5 µM. The initial denaturation step of 95°C for 10 min was followed by 40 cycles of 15 seconds denaturation step at 95°C and 45 s annealing and extension step at 60°C. To confirm the specificity of the reaction a melting curve analysis was performed after the amplification cycles (denaturation at 95°C followed by continuous melting steps (0.5°C/s) starting from 65°C to 95°C). The fluorescent signal was monitored at the end of the extension step for each cycle as well as during the temperature ramp. Results were analyzed using the supplied ViiA 7 Software. The cycle number at which the fluorescence exceeds the background signal (cycle threshold; Ct) for each sample was determined with the baseline threshold algorithm that subtracts a baseline component and sets a fluorescent threshold in the exponential region for gene quantification.

Genotype	Direction	Sequence (5'-3')	Product size
c-myc	forward	CCC TAG TGC TGC ATG AGG AGA CAC	93 bp
	reverse	CCA CAG ACA CCA CAT CAA TTT CTT CC	
N-myc	forward	CTC CGG AGA GGA TAC CTT GA	89 bp
	reverse	TCT CTA CGG TGA CCA CAT CG	
Ddef1	forward	AAG AAC GGG ATC CTG ACC ATC TCC	74 bp
	reverse	TGG CAG GTG AGG AGG TTT AAC TTA GC	
Fam84b	forward	CCA GGG AAA GGA TTC AAT TAA GG	61 bp
	reverse	CAC AAC AGC AGG CCA AAA ACA	
Fam49b	forward	TGG CCA CGA AAT ACG AGA G	81 bp
	reverse	CGC CTT CTC TTG CAA CTT CT	
OAZ1	forward	TTT CAG CTA GCA TCC TGT ACT CC	77 bp
	reverse	GAC CCT GGT CTT GTC GTT AGA	

Table 5.16: qRT-PCR primer
Lyophilized oligonucleotides were resuspended with dH_2O and stored at 4°C overnight. Primers were diluted to a final concentration of 10 pM/µl and stored at -20 °C.

Primers used in this study are listed in Table 5.16. Efficiency of all primers was validated for the relevant Ct range. Expression levels were normalized to the levels of OAZ1 expression, which were previously identified by Dr. Armin Ehninger as being stably expressed in BM cells. Relative gene expression was calculated by the $2^{(-\Delta\Delta Ct)}$-method (LIVAK and SCHMITTGEN 2001).

5.2.8 Histology

5.2.8.1 Peripheral blood smears

2 µl of peripheral blood was placed close to the end of a glass slide. A second spreader slide was hold at an angle of approximately 30° and slowly moved backwards towards the blood drop. After the blood was spread along the edge of the spreader slide, the blood smear was produced moving the spreader slide forward. Air-dried smears were fixed with 100% of methanol for 5 min and then kept at room temperature until further processing.

5.2.8.2 May-Grünwald-Giemsa staining

Peripheral blood smears were stained for 7 min in May-Grünwald solution mixed 1:1 with modified Sörensen buffer. Slides were 10 s air-dried and then immersed for 20 min into freshly prepared Giemsa solution. Stainings were allowed to differentiate in three wash steps in modified Sörensen buffer solution (one time for 10 s and two times for 4 min), then air-dried and mounted with in Entellan after immersing in Xylol for 15 min. Slides were analyzed on an Zeiss Axioplan widefield microscope (20, 40 and 63x objective) and images were captured using an AxioCam Icc3.

5.2.8.3 Image analysis of peripheral blood smears

Image analysis was done using FIJI, employing the automated macro shown below. Correct encircling of red blood cells was always verified and corrected by visual inspection of the processed image.

```
run(‘‘Set Measurements...’’, ‘‘area perimeter fit shape feret’s
skewness kurtosis redirect=None decimal=3’’);
run(‘‘Set Scale...’’, ‘‘distance=0 known=0 pixel=1 unit=pixel
global’’);
run(‘‘Clear Results’’);
roiManager(‘‘Reset’’);
run(‘‘Duplicate...’’, ‘‘title=dupl.czi duplicate’’);
```

```
run(‘‘Split Channels’’);
close();
run(‘‘Invert’’);
run(‘‘Grays’’);
run(‘‘Subtract Background...’’, ‘‘rolling=50 sliding’’);
run(‘‘Median...’’, ‘‘radius=2’’);
run(‘‘Unsharp Mask...’’, ‘‘radius=4 mask=0.90’’);
//run(‘‘Threshold...’’);
setAutoThreshold(‘‘Default dark’’);
setThreshold(9, 255);
run(‘‘Convert to Mask’’);
run(‘‘Fill Holes’’);
run(‘‘Watershed’’);
setAutoThreshold(‘‘Default dark’’);
run(‘‘Analyze Particles...’’, ‘‘size=200-1000 circularity=0.85-1.00
show=Nothing display exclude summarize add’’);
close();
close();
roiManager(‘‘Show None’’);
roiManager(‘‘Show All’’);
```

5.2.9 Chromatin Immunoprecipitation (ChIP)

Cell suspensions of BM cells were crosslinked directly after isolation by adding PFA to a final concentration of 1%. After 10 min shaking at room temperature, PFA was quenched by adding 10% volume of a 1 M glycine solution. After centrifugation for 5 min and 500 g at room temperature, cell surface staining was performed as described in chapter 5.2.3.5.

Chromatin immunoprecipitation (ChIP) experiments were carried out according to protocols from the group of François Spitz at EMBL.

5.2.10 Statistics

For statistical analysis and graphical representation of data the GraphPad Prism software version 6.0b was used. If not specified differently graphs show the mean value and error bars indicate standard error of the mean (SEM). Significance of differences between samples was determined using unpaired two-tailed t-tests. Significance was plotted with *** ($p < 0.001$; extremely significant), ** ($0.001 > p < 0.01$; very significant), * ($0.01 > p < 0.05$; significant), ns ($p > 0.05$; not significant).

6 APPENDIX

6.1 Supplementary Figures

6.1.1 Chromatin modifications in hematopoietic cell types

Global chromatin modifications were published in August 2014 for several murine hematopoietic cell types (LARA-ASTIASO *et al.* 2014). Cells were isolated by FACS from wild type mice using cell surface staining as indicated in Table 6.1. ChIP profiles for H3K4me1, H3K27ac and H3K4me3 chromatin modifications in the DHEC region are shown in Figure 6.1 and 6.2 together with the position of the enhancer modules and ChIP profiles of several transcription factors (WILSON *et al.* 2010).

cell type	tissue/organ	cell surface staining
LT-HSC	BM	Lin^- c-Kit^+ Sca-1^+ $Flk2^-$ $CD34^-$
ST-HSC	BM	Lin^- c-Kit^+ Sca-1^+ $Flk2^-$ $CD34^+$
MPP	BM	Lin^- c-Kit^+ Sca-1^+ $Flk2^+$ $CD34^+$
CMP	BM	Lin^- c-Kit^- Sca-1^+ FcgRII^{low} $CD34^+$
GMP	BM	Lin^- c-Kit^- Sca-1^+ FcgRII^{high} $CD34^+$
MEP	BM	Lin^- c-Kit^- Sca-1^+ FcgRII^{low} $CD34^-$
CLP	BM	Lin^- c-Kit^+ Sca-1^+ $Flk2^+$ $IL7R^+$
granulocytes (gran)	BM	$CD3^-$ $B220^-$ $Nk1.1^-$ $CD11b^+$ Gr-1^+ High SSC
macrophages (mac)	BM	$CD3^-$ $B220^-$ $F4/80^+$ $CD115^-$ Low SSC
B cells (B)	spleen	$CD3^-$ $B220^+$ $CD19^+$
$CD4^+$ T cells (CD4 T)	spleen	$CD3^+$ $B220^-$ $CD4^+$ $CD8^-$
$CD8^+$ T cells (CD8 T)	spleen	$CD3^+$ $B220^-$ $CD4^-$ $CD8^+$
EryA	spleen	$Ter119^+$ $CD71^+$ high FSC
EryB	spleen	$Ter119^+$ $CD71^+$ low FSC

Table 6.1: Cell surface marker for hematopoietic cell isolation used by LARA-ASTIASO *et al.* 2014.

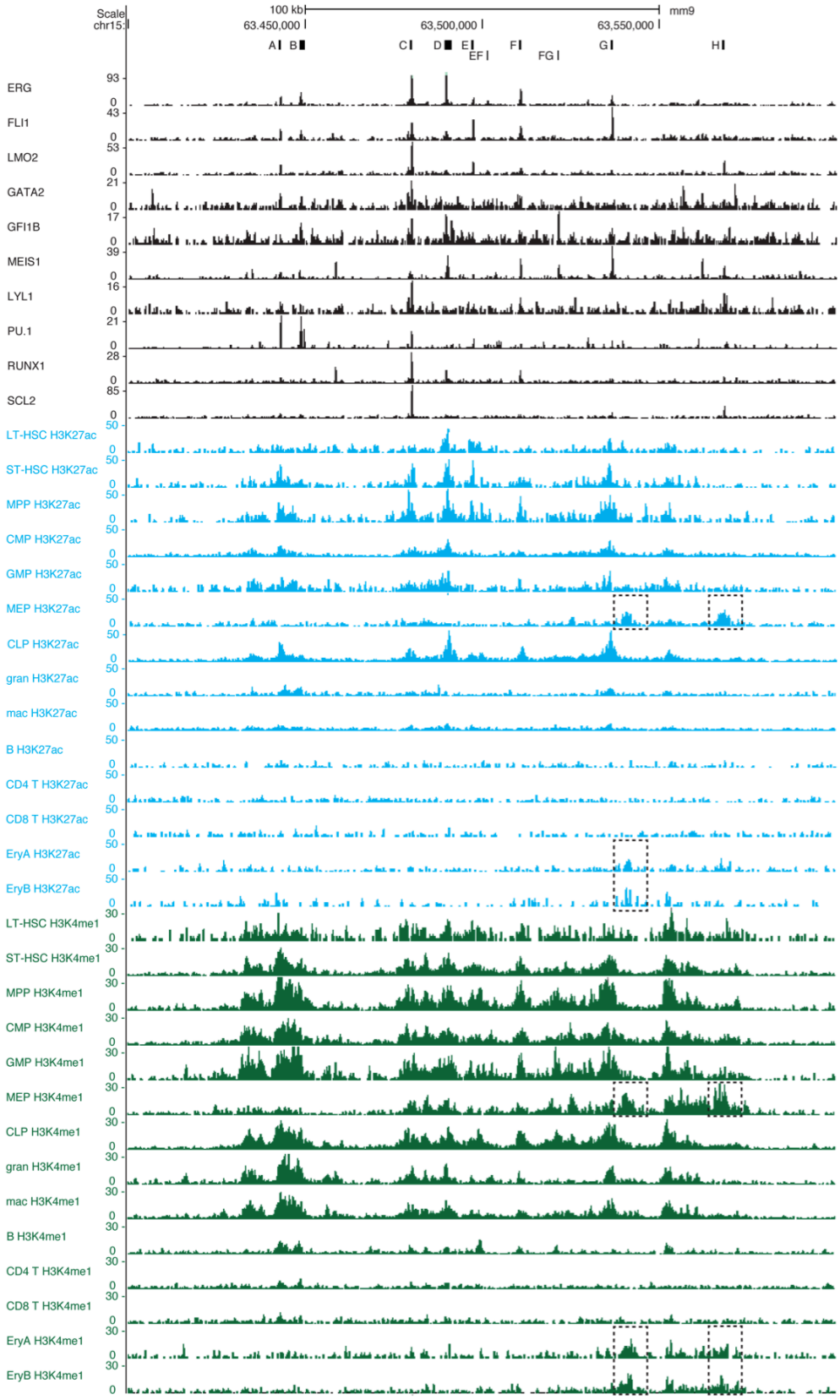

Figure 6.1: Enhancer-associated chromatin modifications in the DHEC region
Positions of enhancer modules are indicated at the top. Below the ChIP data for transcription factors in the HP-7 hematopoietic cell line are shown in black (WILSON *et al.* 2010). Enhancer-associated chromatin marks are shown in blue (H3K4me1) and green (H3K427ac) for different murine hematopoietic cell types (Table 6.1) (LARA-ASTIASO *et al.* 2014). Dashed boxes highlight erythroid lineage related prominent marks at module H.

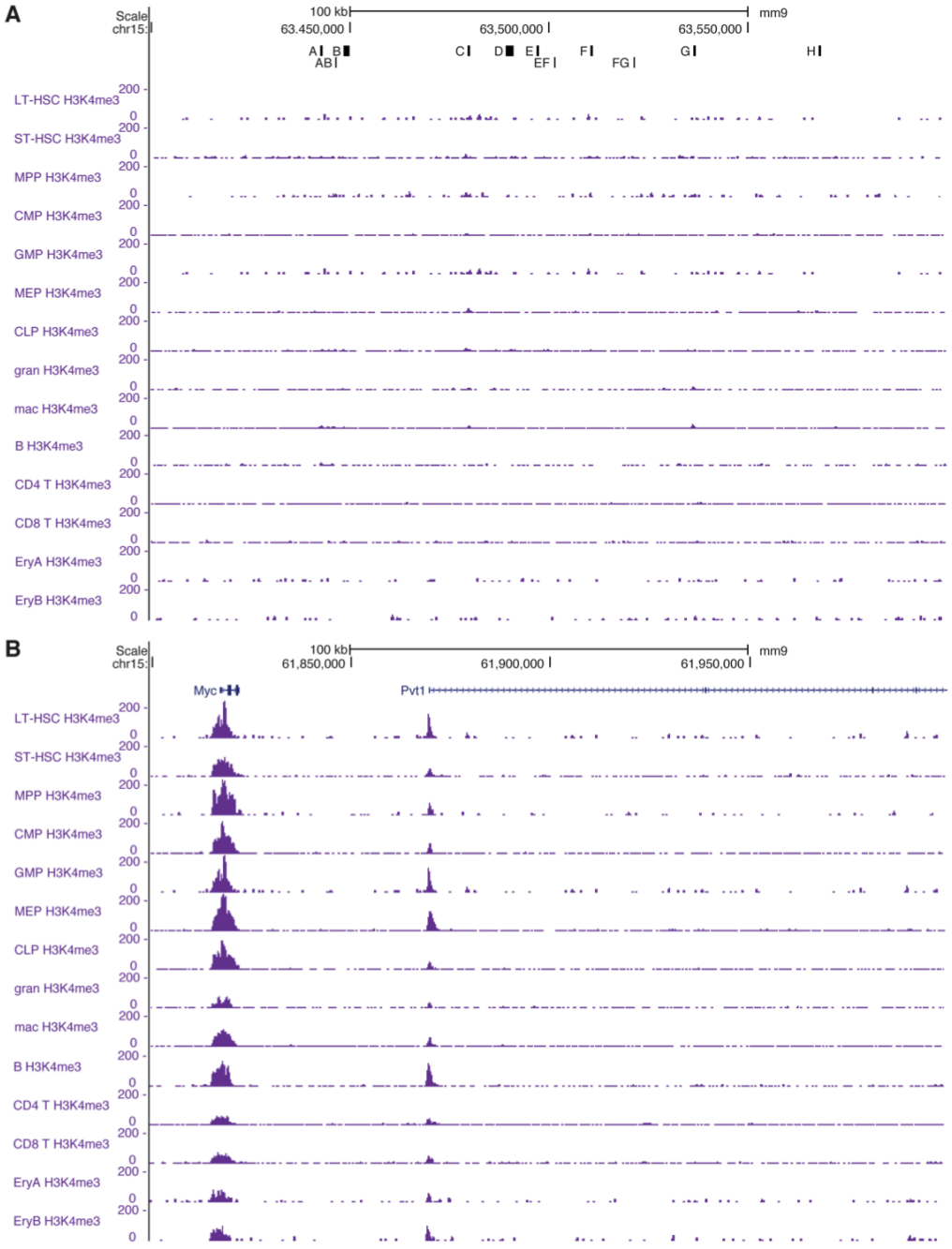

Figure 6.2: Active promoter-associated chromatin marks in the DHEC region
A Positions of enhancer modules are indicated at the top. H3K4me3 in different murine hematopoietic populations in the DHEC region reveals non-coding gene desert. **B** Same modification as in **A** for the *c-myc* locus showing high signal for active promoter mark H3K4me3 for *c-myc* and *Pvt1* using the same signal range (LARA-ASTIASO *et al.* 2014).

6.1.2 DNA methylation and RNA transcript in the DHEC region

RNA-seq results from HSCs, defined as side population LSK CD150^{+} cells, showed a low expressed, not yet annotated transcript in the DHEC region (CHALLEN *et al.* 2014; SUN *et al.* 2014) and decreased expression of *c-myc* and *N-myc* in Dnmt3a knockout and Dnmt3ab double knockout mice (CHALLEN *et al.* 2014).

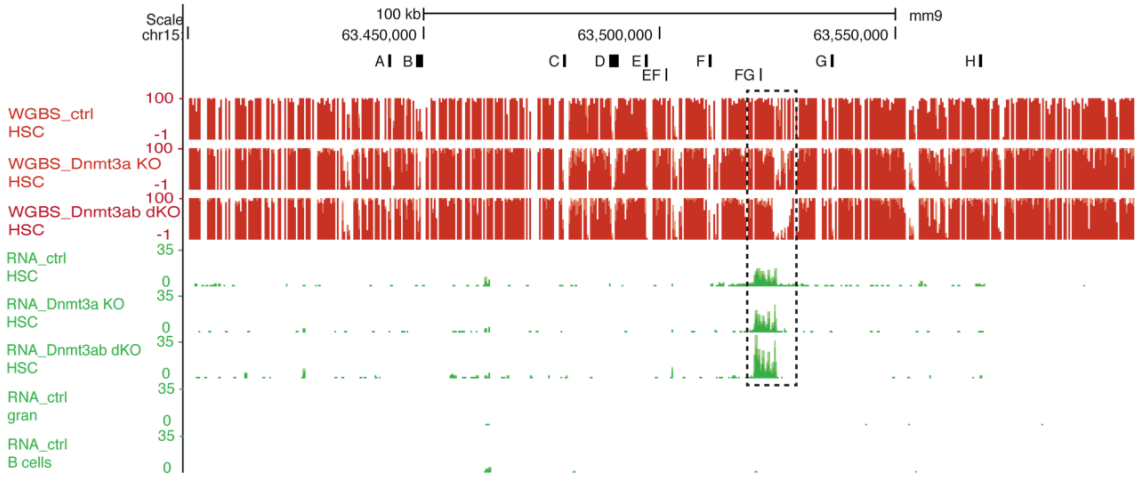

Figure 6.3: Presence of a transcript within the DHEC region in HSCs
On the top the positions of enhancer modules are indicated. Results from whole-genome bisulfite sequencing (WGBS) and RNA-seq results (RNA) of age-matched control (ctrl) versus tertiary-transplanted Dnmt3a knockout (KO) and Dnmt3ab double knockout (dKO) HSCs are depicted in the first 6 lanes. RNA-seq results for granulocytes (gran) and B cells reveal no transcript in the DHEC region. The dashed box highlights a differentially methylated region that coincides with a low level of transcription (CHALLEN *et al.* 2012; CHALLEN *et al.* 2014).

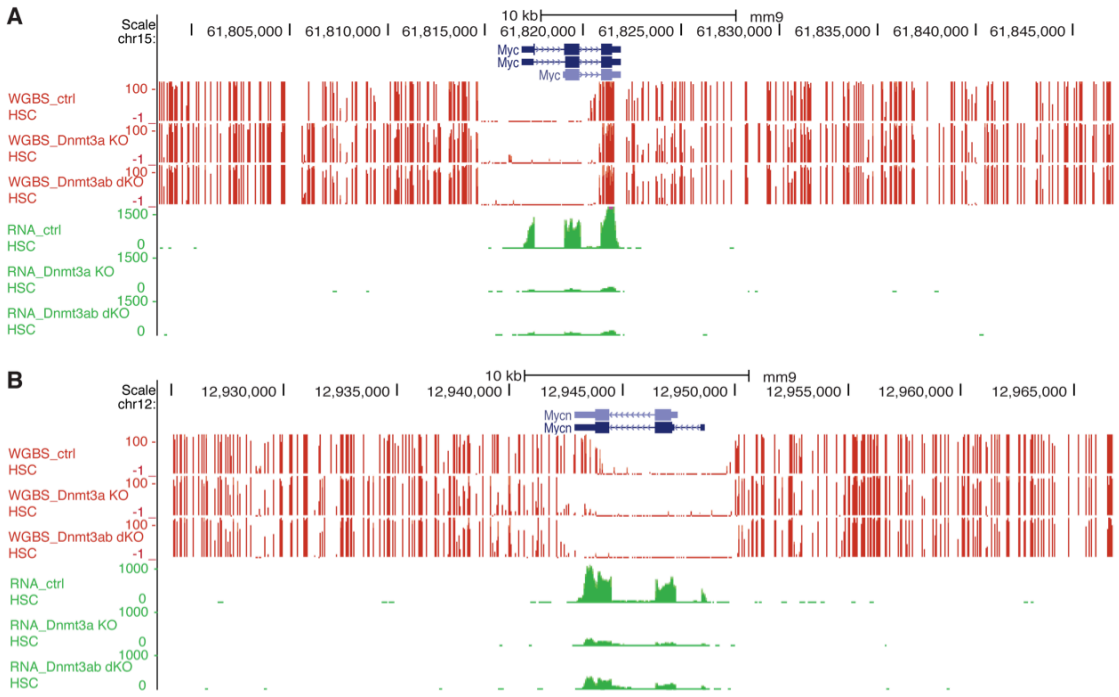

Figure 6.4: *c-myc* and *N-myc* transcripts are decreased upon Dnmt3a and Dnmt3ab knockout
Data as in Figure 6.3 for the *c-myc* (**A**) and the *N-myc* (**B**) locus (CHALLEN *et al.* 2012; CHALLEN *et al.* 2014). Range for RNA-seq signals is adjusted (compare to Figure 6.3).

6.2 Abbreviations

%	percent
°C	degree Celsius
<	inferior
>	superior
2i	2 inhibitor
3C	chromosome conformation capture
3D	three-dimensional
4C	circularized 3C
5C	3C carbon copy
ac	acetylation
ACK	ammonium-chloride-potassium
ADP	adenosine diphosphate
AF9	ALL1 fused gene from chromosome 9
AGM	aorta-gonad-mesonephros
AML	acute myeloid leukemia
APC	allophycocyanin
ATP	adenosine triphosphate
B	B cells
BAC	bacterial artifical chromosome
BAT	brown adipose tissue
BL-CFC	blast colony-forming cell
bp	base pair(s)
bHLH-Zip	basic-helix-loop-helix leucine zipper
BL-CSC	blast colony-forming cell
BM	bone marrow
BMDM	bone marrow derived macrophages
BrdU	5-Bromo-2-deoxyuridine
BRE	TFIIB-recognition site
BSA	bovine serum albumin
CAFC	cobblestone area-forming cell
CB	cord blood
CD	cluster of differentiation
CDK	cycline-dependent kinase
CEU	Utah residents of northern and western European ancestry
CFU	colony forming unit
CFU-S	spleen colony forming unit
CHB	Han Chinese individuals from Beijing, China
CHD	chromo-ATPase-helicase-DNA-binding protein
ChIA-PET	chromosome interaction analysis by paired-end tag sequencing
ChIP	chromatin immunoprecipitation
chr	chromosome
c-Kit	v-kit Hardy-Zuckerman 4 feline sarcoma viral oncogene homolog
CLP	common lymphoid progenitor
CMP	common myeloid progenitor
c-Myc	cellular myelocytomatosis homologue
CP	committed progenitor
CpG	cytosine phosphodiester bond guanine
Cs	cesium
Ct	cycle threshold
CTCF	CCCTC-binding factor
CTD	carboxy-terminal domain
CRC	chromatin remodeling complex
CRU	competitive repopulating unit
Cy5	cyanine 5
Cy7	cyanine 7
DC	dendritic cell
DCE	downstream core element
Ddef1	development and differen–tiation enhancing factor 1
del	deletion
dH_2O	distilled water
DHEC	distal hematopoietic enhancer cluster
DHS	Dnase hypersensitivity site

DKFZ	German Cancer Research Center
dKO	double knock-out
dl	deciliter
DMSO	dimethylsulfoxid
dMyc	Drosophila Myc
DN	double negative
DNA	deoxyribonucleic acid
Dnase	deoxyribonuclease
DNMT	DNA methyl transferase
dNTP	deoxyribonucleotide triphosphate
DP	double positive
dpc	days postcoitus
DPE	downstream promoter element
dup	duplication
dUTP	deoxyuridine triphosphate
E	embryonic day
E-box	enhancer box
EB	proerythroblast population
EDTA	ethylenediamine tetra-acetic acid
EMBL	European Molecular Biology Laboratory
ENCODE	Encyclopedia of DNA elements
EP/E-P	erythrocyte progenitors
EPCR	Endothelial protein C receptor
eRNA	enhancer RNA
ESAM	endothelial cell adhesion molecule
EtOH	ethanol
EryA	erythroblast population A
EryB	erythroblast population B
EryC	erythroblast population C
ESC/ES cells	embryonic stem cells
EYFP	enhanced yellow fluorescent protein
FACS	fluorescence activated cell sorting
Fbw7	F-box and WD-40 domain protein 7
FCS	fetal calf serum
FDG	fluorescein di-(β-D-galactopyranoside)
FIJI	Fiji is just imageJ
FISH	fluorescent in situ hybridization
FITC	fluorescein isothiocyanate
fl	femtoliter
Flk2	fetal liver kinase-2
FLT3	FMS-related tyrosine kinase 3
g	gram or G-force
G0	resting phase
G1	Gap1 phase
GCN5	general control of amino-acid synthesis 5
GERP	genomic evolutionary rate profiling
GFP	green fluorescent protein
GMP	granulocyte/macrophage progenitor
GO	gene ontology
gran	granulocytes
GROMIT	genome regulatory organization mapping with itegrated transposons
GSK-3β	Glycogen synthase kinase-3 β
GTF	general transcription factor
GWAS	genome-wide association studies
Gy	Gray
h	hour
H2A	histone 2A
H2A.Z	H2A family, member Z
H2B	histone 2B
H3	histone 3
H4	histone 4
HapMap	haplotype map
HAT	histone acetyltransferase
Hb	hemoglobin
HBB	hemoglobin subunit beta
HBSS	Hanks' Balanced Salt Solution
HCl	hydrochloric acid

HCT	hematocrit
HDAC	histone deacetylase
HEPES	4-(2-hydroxyethyl)-1-piperazineethanesulfonic acid
hg18	human Mar. 2006 (NCBI36/ hg18) browser sequences
hg19	human Feb. 2009 (GRCh37/ hg19) browser sequences
Hi-C	a genome-wide 3C analysis method
hox genes	homeotic genes
HS	hypersensitivity site
HSC	hematopoietic stem cell
Hsp	heat shock protein
HSZ	hämatopoetische Stammzelle
IDH1	isocitrate dehydrogenase 1
IFN	Interferon
IgG	immunoglobulin G
INO80	inositol requiring mutant 80
ISWI	Imitation Switch
IVC	individually ventilated cages
JPT	Japanese individuals from Tokyo, Japan
Inr	initiator element
K	lysine or 1000
kb	kilobase(s)
KH_2PO_4	potassium dihydrogen phosphate
KO	knock-out
LacZ	β-galactosidase
LCR	locus control region
LD	linkage disequilibrium
LIF	leukemia inhibitory factor
Lin	lineage
LMPP	lymphoid-primed multipotent progenitor
L-Myc	Lung cancer amplified myelocytomatosis homologue
lncRNA	long non-coding RNA
LSK	Lin^- $Sca\text{-}1^+$ $c\text{-}kit^+$
LS^-K	Lin^- $Sca\text{-}1^-$ $c\text{-}kit^+$
LTC-IC	long-term culture-initiating cell
M	molar or million
mac	macrophages
Mad	mitotic arrest deficient
Max	Myc-associated factor X
Mb	megabase(s)
MBD	methyl-binding domain
MC29	myelocytoma virus 29
MCD34	mobilized $CD34^+$ HSCs
m(e)1	monomethylation
m(e)2	dimethylation
m(e)3	trimethylation
MEF	mouse embryonic fibroblast
Mek	mitogen-activated protein kinase kinase
MEP	megakaryocyte/erythroid-progenitor
MeOH	methanol
MkEP	megakaryocyte/erythrocyte progenitor
MFI	mean fluorescence intensity
µg	microgram
mg	milligram
$MgCl_2$	magnesium chloride
Mgk	megakaryocytes
Mgk-P	megakaryocyte progenitor
min	minute(s)
Miz1	Myc-interacting Zinc finger protein 1
MkEP	megakaryocyte/erythrocyte progenitor
µl	microliter
ml	milliliter
MLL	mixed lineage leukemia
µm	micrometer
µM	micromolar
mm	millimeter
mM	millimolar
mm9	mouse July 2007 (NCBI37/ mm9) browser sequences
Mnt	MAX network transcriptional repressor
MPP	multipotent progenitor

MPV	mean platelet volume
mRNA	messenger RNA
MTE	motif ten element
My	myeloid cells
Myc	myelocytomatosis viral oncogene homolog
NaCl	sodium chloride
NaOH	sodium hydroxide
Na_2HPO_4	sodium dihydrogen phosphate
$(NH_4)_2SO_4$	ammonium sulfate
NK	natural killer
N-Myc	Neuroblastoma amplified myelocytomatosis homologue
nm	nanometer
NPM	nucleophosmin
Olfact	olfactory bulb
PB	peripheral blood
PBS	phosphate buffered saline
PcG	polycomb group
PCR	polymerase chain reaction
PFA	paraformaldehyde
pH	power of hydrogen
PIC	pre-initiation complex
pM	picomolar
polyA	poly adenosine tail
poly(I:C)	Polyinosinic-polycytidylic acid
PRC	polycomb repressive complex
PRE	polycomb response element
P1	promoter 1
P2	promoter 2
P3	promoter 3
PE	phycoerythrin
PLT	platelet count
pM	picomolar
Pol2	RNA polymerase II
Pvt1	plasmacytoma variant translocation 1
qRT-PCR	quantitative real-time polymerase chain reaction
R	arginine
RBC	red blood cells
RET	rearranged during transfection
RNA	ribonucleic acid
RNAPII	RNA polymerase II
Rnase	ribonuclease
RNA-seq	RNA sequencing
Rnf32	Ring finger protein 32
RPMI	Roswell Park Memorial Institute
rRNA	ribosomal RNA
RU	repopulating unit
s	seconds
Sca-1	stem cell antigen-1
SD	standard deviation
SEM	standard error of the mean
Seq	sequencing
S/G2/M	synthesis/gap2/mitotic phase
Shh	sonic hedgehog
shRNA	small hairpin RNA
Sin3	Swi-independent 3
SLAM	signaling lymphocytic activation molecule
Smint	small intestine
SNP	single-nucleotide polymorphism
snRNA	small nuclear ribonucleic acid
SP	single positive
SPF	specific pathogen-free conditions
SV40	Simian virus 40
SWI/SNF	SWItch/Sucrose NonFermentable
SWR1	Swi2/Snf2 related 1
T	T cells
TAD	topological associating domain
T-ALL	T-cell acute lymphoblastic leukemia
TBE	TRIS-borat-EDTA buffer
TBP	TATA-binding protein
TF	transcription factor
TSS	transcriptional start site

TRACER	transposase and recombi–nase-associated chromosomal engineering resource
TRIS	tris(hydroxymethyl)amino-methane
tRNA	transfer RNA
TRRAP	Transformation/transcription domain-associated protein
TUNEL	terminal deoxynucleotide transferase dUTP nick end labeling
TxRed	Texas Red
UCSC	University of California, Santa Cruz
UV	ultraviolet
V	volt
WBC	white blood cell count
WGBS	whole-genome bisulfite sequencing
Wt	wild type

6.3 List of figures

6.4 List of tables

6.5 Publications

VON PALESKE, L., USLU, V.U., PETRETICH, M. SPITZ, F., TRUMPP, A. A novel enhancer region 1.7 Mb downstream of the *c-myc* gene drives its expression in hematopoietic stem and progenitor cells. Abstract chosen for oral presentation at the 56th ASH Annual Meeting in San Francisco, Dec. 2014.

KLIMMECK, D., CABEZAS-WALLSCHEID, N., REYES, A., **VON PALESKE, L.**, RENDERS, HANSSON, J., KRIJGSVELD, J., HUBER, W., TRUMPP, 2014. Transcriptome-wide Profiling and Posttranscriptional Analysis of Hematopoietic Stem/Progenitor Cell Differentiation toward Myeloid Commitment. Stem Cell Reports *3:* 1-18.

CABEZAS-WALLSCHEID, N., KLIMMECK, D., HANSSON, J., LIPKA, D. B., REYES, A., WANG, Q., WEICHENHAN, D., LIER, A., **VON PALESKE, L.**, RENDERS, S., WÜNSCHE, P., ZEISBERGER, P., BROCKS, D., GU, L., HERRMANN, C., HAAS, S., ESSERS, M. A., BRORS, B., EILS, R., HUBER, W., MILSOM, M. D., PLASS, C., KRIJGSVELD, J., TRUMPP, A., 2014. Identification of Regulatory Networks in HSCs and Their Immediate Progeny via Integrated Proteome, Transcriptome, and DNA Methylome Analysis. Cell Stem Cell *15*(4):507-22.

DOHRN L., SALLES D., SIEHLER S.Y., KAUFMANN J., WIESMÜLLER L., 2012. BRCA1-mediated repression of mutagenic end-joining of DNA double-strand breaks requires complex formation with BACH1. Biochem J. *441*(3):919-26.

7 CONTRIBUTIONS

The completion of this thesis would not have been possible without the help of many people ranging from technical support to the contributions of ideas.

All experiments were performed in collaboration with Dr. Veli V. Uslu and Massimo Petretich from the lab of Dr. François Spitz at EMBL therefore I clarify their respective contributions to the project. Dr. Veli V. Uslu generated the transposon-mediated transgenic mouse strains and performed the genotyping of the mice housed at EMBL (mouse strains used for lacZ stainings, del(8-17), dup(15-17), dup(c17-17) and del(15-17) mice used for transplantation). He dissected mice from EMBL and assisted in bone marrow cell isolation. He provided sequences for primers for genotyping of the transgenic mouse strains as well as the primers for qRT-PCR. qRT-PCR analysis of del(8-17) and dup(c17-17) were performed by him. Massimo Petretich performed ChIP experiments with FACS-sorted cells provided by me. The results were evaluated and visualized by a joint effort of Dr. Veli V. Uslu, Dr. François Spitz, Prof. Dr. Andreas Trumpp and me.

At DKFZ great technical support, including bleeding, cell preparation and injections of mice, was provided by Petra Zeisberger, Katja Müdder, Adriana Przybylla and Daniel Baumgärtner.

Genotyping of mice housed at DKFZ was done in part by Melanie Neubauer and Adriana Przybylla. The animal care takers under supervision of Anja Rathgeb contributed to the maintenance of the mouse facility as well as the irradiation of mice.

The FACS sorts were performed together with Steffen Schmitt, Klaus Hexel, Jens Hartwig, Ann Atzberger and Tobias Rubner of the DKFZ FACS Core Facility.

Dr. Damir Krunic helped in writing the Fiji macro for analysis of microscope images.

Dr. Simon Raffel provided me with the qRT-PCR data for *c-MYC* expression in human AML samples.

8 Acknowledgements

9 BIBLIOGRAPHY

ABRAMSON, S., MILLER, R. G. and PHILLIPS, R. A., 1977. The identification in adult bone marrow of pluripotent and restricted stem cells of the myeloid and lymphoid systems. J Exp Med *145:* 1567-1579.

ADAMS, J. M., HARRIS, A. W., PINKERT, C. A., CORCORAN, L. M., ALEXANDER, W. S., CORY, S., PALMITER, R. D. and BRINSTER, R. L., 1985. The c-myc oncogene driven by immunoglobulin enhancers induces lymphoid malignancy in transgenic mice. Nature *318:* 533-538.

ADELMAN, K., and LIS, J. T., 2012. Promoter-proximal pausing of RNA polymerase II: emerging roles in metazoans. Nat Rev Genet *13:* 720-731.

ADHIKARY, S., and EILERS, M., 2005. Transcriptional regulation and transformation by Myc proteins. Nat Rev Mol Cell Biol *6:* 635-645.

ADOLFSSON, J., BORGE, O. J., BRYDER, D., THEILGAARD-MONCH, K., ASTRAND-GRUNDSTROM, I., SITNICKA, E., SASAKI, Y. and JACOBSEN, S. E., 2001. Upregulation of Flt3 expression within the bone marrow Lin(-)Sca1(+)c-kit(+) stem cell compartment is accompanied by loss of self-renewal capacity. Immunity *15:* 659-669.

ADOLFSSON, J., MANSSON, R., BUZA-VIDAS, N., HULTQUIST, A., LIUBA, K. *et al.*, 2005. Identification of Flt3+ lympho-myeloid stem cells lacking erythro-megakaryocytic potential a revised road map for adult blood lineage commitment. Cell *121:* 295-306.

AHMADIYEH, N., POMERANTZ, M. M., GRISANZIO, C., HERMAN, P., JIA, L. *et al.*, 2010. 8q24 prostate, breast, and colon cancer risk loci show tissue-specific long-range interaction with MYC. Proc Natl Acad Sci U S A *107:* 9742-9746.

AKASHI, K., TRAVER, D., MIYAMOTO, T. and WEISSMAN, I. L., 2000. A clonogenic common myeloid progenitor that gives rise to all myeloid lineages. Nature *404:* 193-197.

ALBERTS, B., JOHNSON, A., LEWSI, J., RAFF, M., ROBERTS, K. and WALTER, P., 2008 *Molecular Biology of the Cell*. Garland Science, New York.

AMATI, B., BROOKS, M. W., LEVY, N., LITTLEWOOD, T. D., EVAN, G. I. and LAND, H., 1993. Oncogenic activity of the c-Myc protein requires dimerization with Max. Cell *72:* 233-245.

AMERICO, J., WHITELEY, M., BROWN, J. L., FUJIOKA, M., JAYNES, J. B. and KASSIS, J. A., 2002. A complex array of DNA-binding proteins required for pairing-sensitive silencing by a polycomb group response element from the Drosophila engrailed gene. Genetics *160:* 1561-1571.

ANDERSSON, R., GEBHARD, C., MIGUEL-ESCALADA, I., HOOF, I., BORNHOLDT, J. *et al.*, 2014. An atlas of active enhancers across human cell types and tissues. Nature *507:* 455-461.

ARA, T., TOKOYODA, K., SUGIYAMA, T., EGAWA, T., KAWABATA, K. and NAGASAWA, T., 2003. Long-term hematopoietic stem cells require stromal cell-derived factor-1 for colonizing bone marrow during ontogeny. Immunity *19:* 257-267.

ARNOSTI, D. N., and KULKARNI, M. M., 2005. Transcriptional enhancers: Intelligent enhanceosomes or flexible billboards? J Cell Biochem *94:* 890-898.

ATCHLEY, W. R., and FITCH, W. M., 1995. Myc and Max: molecular evolution of a family of proto-oncogene products and their dimerization partner. Proc Natl Acad Sci U S A *92:* 10217-10221.

AYER, D. E., KRETZNER, L. and EISENMAN, R. N., 1993. Mad: a heterodimeric partner for Max that antagonizes Myc transcriptional activity. Cell *72:* 211-222.

AYER, D. E., LAWRENCE, Q. A. and EISENMAN, R. N., 1995. Mad-Max transcriptional repression is mediated by ternary complex formation with mammalian homologs of yeast repressor Sin3. Cell *80:* 767-776.

BAENA, E., GANDARILLAS, A., VALLESPINOS, M., ZANET, J., BACHS, O., REDONDO, C., FABREGAT, I., MARTINEZ, A. C. and DE ALBORAN, I. M., 2005. c-Myc regulates cell size and ploidy but is not essential for postnatal proliferation in liver. Proc Natl Acad Sci U S A *102:* 7286-7291.

BAENA, E., ORTIZ, M., MARTINEZ, A. C. and DE ALBORAN, I. M., 2007. c-Myc is essential for hematopoietic stem cell differentiation and regulates Lin(-)Sca-1(+)c-Kit(-) cell generation through p21. Exp Hematol *35:* 1333-1343.

BAINES, P., and VISSER, J. W., 1983. Analysis and separation of murine bone marrow stem cells by H33342 fluorescence-activated cell sorting. Exp Hematol *11:* 701-708.

BALAZS, A. B., FABIAN, A. J., ESMON, C. T. and MULLIGAN, R. C., 2006. Endothelial protein C receptor (CD201) explicitly identifies hematopoietic stem cells in murine bone marrow. Blood *107:* 2317-2321.

BALDRIDGE, M. T., KING, K. Y., BOLES, N. C., WEKSBERG, D. C. and GOODELL, M. A., 2010. Quiescent haematopoietic stem cells are activated by IFN-gamma in response to chronic infection. Nature *465:* 793-797.

BANERJI, J., RUSCONI, S. and SCHAFFNER, W., 1981. Expression of a beta-globin gene is enhanced by remote SV40 DNA sequences. Cell *27:* 299-308.

BANNISTER, A. J., and KOUZARIDES, T., 2011. Regulation of chromatin by histone modifications. Cell Res *21:* 381-395.

BARON, M. H., 2013. Concise Review: early embryonic erythropoiesis: not so primitive after all. Stem Cells *31:* 849-856.

BARSKI, A., CUDDAPAH, S., CUI, K., ROH, T. Y., SCHONES, D. E., WANG, Z., WEI, G., CHEPELEV, I. and ZHAO, K., 2007. High-resolution profiling of histone methylations in the human genome. Cell *129:* 823-837.

BAUS, J., LIU, L., HEGGESTAD, A. D., SANZ, S. and FLETCHER, B. S., 2005. Hyperactive transposase mutants of the Sleeping Beauty transposon. Mol Ther *12:* 1148-1156.

BECKER, A. J., MC, C. E. and TILL, J. E., 1963. Cytological demonstration of the clonal nature of spleen colonies derived from transplanted mouse marrow cells. Nature *197:* 452-454.

BEER, S., ZETTERBERG, A., IHRIE, R. A., MCTAGGART, R. A., YANG, Q. *et al.*, 2004. Developmental context determines latency of MYC-induced tumorigenesis. PLoS Biol *2:* e332.

BEISEL, C., and PARO, R., 2011. Silencing chromatin: comparing modes and mechanisms. Nat Rev Genet *12:* 123-135.

BENZ, C., COPLEY, M. R., KENT, D. G., WOHRER, S., CORTES, A. *et al.*, 2012. Hematopoietic stem cell subtypes expand differentially during development and display distinct lymphopoietic programs. Cell Stem Cell *10:* 273-283.

BERGSAGEL, P. L., and KUEHL, W. M., 2001. Chromosome translocations in multiple myeloma. Oncogene *20:* 5611-5622.

BERNSTEIN, B. E., MIKKELSEN, T. S., XIE, X., KAMAL, M., HUEBERT, D. J. *et al.*, 2006. A bivalent chromatin structure marks key developmental genes in embryonic stem cells. Cell *125:* 315-326.

BERNSTEIN, B. E., STAMATOYANNOPOULOS, J. A., COSTELLO, J. F., REN, B., MILOSAVLJEVIC, A. *et al.*, 2010. The NIH Roadmap Epigenomics Mapping Consortium. Nat Biotechnol *28:* 1045-1048.

BERTA, M. A., BAKER, C. M., COTTLE, D. L. and WATT, F. M., 2010. Dose and context dependent effects of Myc on epidermal stem cell proliferation and differentiation. EMBO Mol Med *2:* 16-25.

BERTONCELLO, I., HODGSON, G. S. and BRADLEY, T. R., 1985. Multiparameter analysis of transplantable hemopoietic stem cells: I. The separation and enrichment of stem cells homing to marrow and spleen on the basis of rhodamine-123 fluorescence. Exp Hematol *13:* 999-1006.

BETTESS, M. D., DUBOIS, N., MURPHY, M. J., DUBEY, C., ROGER, C., ROBINE, S. and TRUMPP, A., 2005. c-Myc is required for the formation of intestinal crypts but dispensable for homeostasis of the adult intestinal epithelium. Mol Cell Biol *25:* 7868-7878.

BIEDA, M., XU, X., SINGER, M. A., GREEN, R. and FARNHAM, P. J., 2006. Unbiased location analysis of E2F1-binding sites suggests a widespread role for E2F1 in the human genome. Genome Res *16:* 595-605.

BIRNEY, E., STAMATOYANNOPOULOS, J. A., DUTTA, A., GUIGO, R., GINGERAS, T. R. *et al.*, 2007. Identification and analysis of functional elements in 1% of the human genome by the ENCODE pilot project. Nature *447:* 799-816.

BLACKWELL, T. K., HUANG, J., MA, A., KRETZNER, L., ALT, F. W., EISENMAN, R. N. and WEINTRAUB, H., 1993. Binding of myc proteins to canonical and noncanonical DNA sequences. Mol Cell Biol *13:* 5216-5224.

BLACKWELL, T. K., KRETZNER, L., BLACKWOOD, E. M., EISENMAN, R. N. and WEINTRAUB, H., 1990. Sequence-specific DNA binding by the c-Myc protein. Science *250:* 1149-1151.

BLACKWOOD, E. M., and EISENMAN, R. N., 1991. Max: a helix-loop-helix zipper protein that forms a sequence-specific DNA-binding complex with Myc. Science *251:* 1211-1217.

BLACKWOOD, E. M., LUSCHER, B. and EISENMAN, R. N., 1992. Myc and Max associate in vivo. Genes Dev *6:* 71-80.

BLANCO-BOSE, W. E., MURPHY, M. J., EHNINGER, A., OFFNER, S., DUBEY, C., HUANG, W., MOORE, D. D. and TRUMPP, A., 2008. C-Myc and its target FoxM1 are critical downstream effectors of constitutive androstane receptor (CAR) mediated direct liver hyperplasia. Hepatology *48:* 1302-1311.

BLOW, M. J., MCCULLEY, D. J., LI, Z., ZHANG, T., AKIYAMA, J. A. *et al.*, 2010. ChIP-Seq identification of weakly conserved heart enhancers. Nat Genet *42:* 806-810.

BONAL, C., THOREL, F., AIT-LOUNIS, A., REITH, W., TRUMPP, A. and HERRERA, P. L., 2009. Pancreatic inactivation of c-Myc decreases acinar mass and transdifferentiates acinar cells into adipocytes in mice. Gastroenterology *136:* 309-319 e309.

BOUCHARD, C., DITTRICH, O., KIERMAIER, A., DOHMANN, K., MENKEL, A., EILERS, M. and LUSCHER, B., 2001. Regulation of cyclin D2 gene expression by the

Myc/Max/Mad network: Myc-dependent TRRAP recruitment and histone acetylation at the cyclin D2 promoter. Genes Dev *15:* 2042-2047.

BOWIE, M. B., KENT, D. G., DYKSTRA, B., MCKNIGHT, K. D., MCCAFFREY, L., HOODLESS, P. A. and EAVES, C. J., 2007. Identification of a new intrinsically timed developmental checkpoint that reprograms key hematopoietic stem cell properties. Proc Natl Acad Sci U S A *104:* 5878-5882.

BOWIE, M. B., MCKNIGHT, K. D., KENT, D. G., MCCAFFREY, L., HOODLESS, P. A. and EAVES, C. J., 2006. Hematopoietic stem cells proliferate until after birth and show a reversible phase-specific engraftment defect. J Clin Invest *116:* 2808-2816.

BOYER, L. A., PLATH, K., ZEITLINGER, J., BRAMBRINK, T., MEDEIROS, L. A. *et al.*, 2006. Polycomb complexes repress developmental regulators in murine embryonic stem cells. Nature *441:* 349-353.

BOYLE, A. P., DAVIS, S., SHULHA, H. P., MELTZER, P., MARGULIES, E. H., WENG, Z., FUREY, T. S. and CRAWFORD, G. E., 2008. High-resolution mapping and characterization of open chromatin across the genome. Cell *132:* 311-322.

BRENNER, C., DEPLUS, R., DIDELOT, C., LORIOT, A., VIRE, E. *et al.*, 2005. Myc represses transcription through recruitment of DNA methyltransferase corepressor. EMBO J *24:* 336-346.

BRYDER, D., ROSSI, D. J. and WEISSMAN, I. L., 2006. Hematopoietic stem cells: the paradigmatic tissue-specific stem cell. Am J Pathol *169:* 338-346.

BULGER, M., and GROUDINE, M., 2011. Functional and mechanistic diversity of distal transcription enhancers. Cell *144:* 327-339.

BUSHEY, A. M., DORMAN, E. R. and CORCES, V. G., 2008. Chromatin insulators: regulatory mechanisms and epigenetic inheritance. Mol Cell *32:* 1-9.

CABEZAS-WALLSCHEID, N., KLIMMECK, D., HANSSON, J., LIPKA, D. B., REYES, A. *et al.*, 2014. Identification of Regulatory Networks in HSCs and Their Immediate Progeny via Integrated Proteome, Transcriptome, and DNA Methylome Analysis. Cell Stem Cell.

CAI, H. N., and SHEN, P., 2001. Effects of cis arrangement of chromatin insulators on enhancer-blocking activity. Science *291:* 493-495.

CAMPOS, E. I., and REINBERG, D., 2009. Histones: annotating chromatin. Annu Rev Genet *43:* 559-599.

CAO, R., WANG, L., WANG, H., XIA, L., ERDJUMENT-BROMAGE, H., TEMPST, P., JONES, R. S. and ZHANG, Y., 2002. Role of histone H3 lysine 27 methylation in Polycomb-group silencing. Science *298:* 1039-1043.

CARRAMUSA, L., CONTINO, F., FERRO, A., MINAFRA, L., PERCONTI, G., GIALLONGO, A. and FEO, S., 2007. The PVT-1 oncogene is a Myc protein target that is overexpressed in transformed cells. J Cell Physiol *213:* 511-518.

CARTWRIGHT, P., MCLEAN, C., SHEPPARD, A., RIVETT, D., JONES, K. and DALTON, S., 2005. LIF/STAT3 controls ES cell self-renewal and pluripotency by a Myc-dependent mechanism. Development *132:* 885-896.

CASHMAN, J., HENKELMAN, D., HUMPHRIES, K., EAVES, C. and EAVES, A., 1983. Individual BFU-E in polycythemia vera produce both erythropoietin dependent and independent progeny. Blood *61:* 876-884.

CAWLEY, S., BEKIRANOV, S., NG, H. H., KAPRANOV, P., SEKINGER, E. A. *et al.*, 2004. Unbiased mapping of transcription factor binding sites along human chromosomes 21 and 22 points to widespread regulation of noncoding RNAs. Cell *116:* 499-509.

CHALLEN, G. A., SUN, D., JEONG, M., LUO, M., JELINEK, J. *et al.*, 2012. Dnmt3a is essential for hematopoietic stem cell differentiation. Nat Genet *44:* 23-31.

CHALLEN, G. A., SUN, D., MAYLE, A., JEONG, M., LUO, M. *et al.*, 2014. Dnmt3a and dnmt3b have overlapping and distinct functions in hematopoietic stem cells. Cell Stem Cell *15:* 350-364.

CHANG, T. C., YU, D., LEE, Y. S., WENTZEL, E. A., ARKING, D. E., WEST, K. M., DANG, C. V., THOMAS-TIKHONENKO, A. and MENDELL, J. T., 2008. Widespread microRNA repression by Myc contributes to tumorigenesis. Nat Genet *40:* 43-50.

CHANG, T. C., ZEITELS, L. R., HWANG, H. W., CHIVUKULA, R. R., WENTZEL, E. A. *et al.*, 2009. Lin-28B transactivation is necessary for Myc-mediated let-7 repression and proliferation. Proc Natl Acad Sci U S A *106:* 3384-3389.

CHARRON, J., MALYNN, B. A., FISHER, P., STEWART, V., JEANNOTTE, L., GOFF, S. P., ROBERTSON, E. J. and ALT, F. W., 1992. Embryonic lethality in mice homozygous for a targeted disruption of the N-myc gene. Genes Dev *6:* 2248-2257.

CHEN, C. Z., LI, M., DE GRAAF, D., MONTI, S., GOTTGENS, B. *et al.*, 2002. Identification of endoglin as a functional marker that defines long-term repopulating hematopoietic stem cells. Proc Natl Acad Sci U S A *99:* 15468-15473.

CHEN, T., and LI, E., 2006. Establishment and maintenance of DNA methylation patterns in mammals. Curr Top Microbiol Immunol *301:* 179-201.

CHESI, M., ROBBIANI, D. F., SEBAG, M., CHNG, W. J., AFFER, M. *et al.*, 2008. AID-dependent activation of a MYC transgene induces multiple myeloma in a conditional mouse model of post-germinal center malignancies. Cancer Cell *13:* 167-180.

CHOI, K., KENNEDY, M., KAZAROV, A., PAPADIMITRIOU, J. C. and KELLER, G., 1998. A common precursor for hematopoietic and endothelial cells. Development *125:* 725-732.

CHRISTENSEN, J. L., and WEISSMAN, I. L., 2001. Flk-2 is a marker in hematopoietic stem cell differentiation: a simple method to isolate long-term stem cells. Proc Natl Acad Sci U S A *98:* 14541-14546.

CHRISTENSEN, J. L., WRIGHT, D. E., WAGERS, A. J. and WEISSMAN, I. L., 2004. Circulation and chemotaxis of fetal hematopoietic stem cells. PLoS Biol *2:* E75.

CLAASSEN, G. F., and HANN, S. R., 2000. A role for transcriptional repression of p21CIP1 by c-Myc in overcoming transforming growth factor beta -induced cell-cycle arrest. Proc Natl Acad Sci U S A *97:* 9498-9503.

CLAMP, M., FRY, B., KAMAL, M., XIE, X., CUFF, J., LIN, M. F., KELLIS, M., LINDBLAD-TOH, K. and LANDER, E. S., 2007. Distinguishing protein-coding and noncoding genes in the human genome. Proc Natl Acad Sci U S A *104:* 19428-19433.

COLE, M. D., and COWLING, V. H., 2008. Transcription-independent functions of MYC: regulation of translation and DNA replication. Nat Rev Mol Cell Biol *9:* 810-815.

COOPER, G. M., STONE, E. A., ASIMENOS, G., GREEN, E. D., BATZOGLOU, S. and SIDOW, A., 2005. Distribution and intensity of constraint in mammalian genomic sequence. Genome Res *15:* 901-913.

COUILLARD, M., and TRUDEL, M., 2009. C-myc as a modulator of renal stem/progenitor cell population. Dev Dyn *238:* 405-414.

COURT, E. L., SMITH, M. A., AVENT, N. D., HANCOCK, J. T., MORGAN, L. M., GRAY, A. G. and SMITH, J. G., 2004. DNA microarray screening of differential gene expression in bone marrow samples from AML, non-AML patients and AML cell lines. Leuk Res *28:* 743-753.

COWLING, V. H., and COLE, M. D., 2007. The Myc transactivation domain promotes global phosphorylation of the RNA polymerase II carboxy-terminal domain independently of direct DNA binding. Mol Cell Biol *27:* 2059-2073.

CRAWFORD, G. E., DAVIS, S., SCACHERI, P. C., RENAUD, G., HALAWI, M. J. *et al.*, 2006a. DNase-chip: a high-resolution method to identify DNase I hypersensitive sites using tiled microarrays. Nat Methods *3:* 503-509.

CRAWFORD, G. E., HOLT, I. E., WHITTLE, J., WEBB, B. D., TAI, D. *et al.*, 2006b. Genome-wide mapping of DNase hypersensitive sites using massively parallel signature sequencing (MPSS). Genome Res *16:* 123-131.

CREYGHTON, M. P., CHENG, A. W., WELSTEAD, G. G., KOOISTRA, T., CAREY, B. W. *et al.*, 2010. Histone H3K27ac separates active from poised enhancers and predicts developmental state. Proc Natl Acad Sci U S A *107:* 21931-21936.

CUMANO, A., DIETERLEN-LIEVRE, F. and GODIN, I., 1996. Lymphoid potential, probed before circulation in mouse, is restricted to caudal intraembryonic splanchnopleura. Cell *86:* 907-916.

CUMANO, A., FERRAZ, J. C., KLAINE, M., DI SANTO, J. P. and GODIN, I., 2001. Intraembryonic, but not yolk sac hematopoietic precursors, isolated before circulation, provide long-term multilineage reconstitution. Immunity *15:* 477-485.

CZERMIN, B., MELFI, R., MCCABE, D., SEITZ, V., IMHOF, A. and PIRROTTA, V., 2002. Drosophila enhancer of Zeste/ESC complexes have a histone H3 methyltransferase activity that marks chromosomal Polycomb sites. Cell *111:* 185-196.

DALLA-FAVERA, R., BREGNI, M., ERIKSON, J., PATTERSON, D., GALLO, R. C. and CROCE, C. M., 1982. Human c-myc onc gene is located on the region of chromosome 8 that is translocated in Burkitt lymphoma cells. Proc Natl Acad Sci U S A *79:* 7824-7827.

DANG, C. V., 2012. MYC on the path to cancer. Cell *149:* 22-35.

DANG, C. V., O'DONNELL, K. A., ZELLER, K. I., NGUYEN, T., OSTHUS, R. C. and LI, F., 2006. The c-Myc target gene network. Semin Cancer Biol *16:* 253-264.

DARZYNKIEWICZ, Z., ROBINSON, J. P. and MARIO ROEDERER, M., 2009 *Essential Cytometry Methods*. Academic Press.

DATHE, K., KJAER, K. W., BREHM, A., MEINECKE, P., NURNBERG, P. *et al.*, 2009. Duplications involving a conserved regulatory element downstream of BMP2 are associated with brachydactyly type A2. Am J Hum Genet *84:* 483-492.

DAVIS, A. C., WIMS, M., SPOTTS, G. D., HANN, S. R. and BRADLEY, A., 1993. A null c-myc mutation causes lethality before 10.5 days of gestation in homozygotes and reduced fertility in heterozygous female mice. Genes Dev *7:* 671-682.

DE BRUIJN, M. F., SPECK, N. A., PEETERS, M. C. and DZIERZAK, E., 2000. Definitive hematopoietic stem cells first develop within the major arterial regions of the mouse embryo. EMBO J *19:* 2465-2474.

DE WIT, E., and DE LAAT, W., 2012. A decade of 3C technologies: insights into nuclear organization. Genes Dev *26:* 11-24.

DEATON, A. M., and BIRD, A., 2011. CpG islands and the regulation of transcription. Genes Dev *25:* 1010-1022.

DEVIDO, S. K., KWON, D., BROWN, J. L. and KASSIS, J. A., 2008. The role of Polycomb-group response elements in regulation of engrailed transcription in Drosophila. Development *135:* 669-676.

DIXON, J. R., SELVARAJ, S., YUE, F., KIM, A., LI, Y., SHEN, Y., HU, M., LIU, J. S. and REN, B., 2012. Topological domains in mammalian genomes identified by analysis of chromatin interactions. Nature *485:* 376-380.

DJEBALI, S., DAVIS, C. A., MERKEL, A., DOBIN, A., LASSMANN, T. *et al.*, 2012. Landscape of transcription in human cells. Nature *489:* 101-108.

DOMINGUEZ-SOLA, D., YING, C. Y., GRANDORI, C., RUGGIERO, L., CHEN, B. *et al.*, 2007. Non-transcriptional control of DNA replication by c-Myc. Nature *448:* 445-451.

DOSE, M., KHAN, I., GUO, Z., KOVALOVSKY, D., KRUEGER, A., VON BOEHMER, H., KHAZAIE, K. and GOUNARI, F., 2006. c-Myc mediates pre-TCR-induced proliferation but not developmental progression. Blood *108:* 2669-2677.

DOUAGI, I., VIEIRA, P. and CUMANO, A., 2002. Lymphocyte commitment during embryonic development, in the mouse. Semin Immunol *14:* 361-369.

DOUGLAS, N. C., JACOBS, H., BOTHWELL, A. L. and HAYDAY, A. C., 2001. Defining the specific physiological requirements for c-Myc in T cell development. Nat Immunol *2:* 307-315.

DUBOIS, N. C., ADOLPHE, C., EHNINGER, A., WANG, R. A., ROBERTSON, E. J. and TRUMPP, A., 2008. Placental rescue reveals a sole requirement for c-Myc in embryonic erythroblast survival and hematopoietic stem cell function. Development *135:* 2455-2465.

DYKSTRA, B., KENT, D., BOWIE, M., MCCAFFREY, L., HAMILTON, M., LYONS, K., LEE, S. J., BRINKMAN, R. and EAVES, C., 2007. Long-term propagation of distinct hematopoietic differentiation programs in vivo. Cell Stem Cell *1:* 218-229.

DZIERZAK, E., and SPECK, N. A., 2008. Of lineage and legacy: the development of mammalian hematopoietic stem cells. Nat Immunol *9:* 129-136.

EDELMANN, J., HOLZMANN, K., MILLER, F., WINKLER, D., BUHLER, A. *et al.*, 2012. High-resolution genomic profiling of chronic lymphocytic leukemia reveals new recurrent genomic alterations. Blood *120:* 4783-4794.

EHNINGER, A., BOCH, T., UCKELMANN, H., ESSERS, M. A., MUDDER, K., SLECKMAN, B. P. and TRUMPP, A., 2014. Posttranscriptional regulation of c-Myc expression in adult murine HSCs during homeostasis and interferon-alpha-induced stress response. Blood *123:* 3909-3913.

ELLWOOD-YEN, K., GRAEBER, T. G., WONGVIPAT, J., IRUELA-ARISPE, M. L., ZHANG, J., MATUSIK, R., THOMAS, G. V. and SAWYERS, C. L., 2003. Myc-driven murine prostate cancer shares molecular features with human prostate tumors. Cancer Cell *4:* 223-238.

EMA, H., MORITA, Y., YAMAZAKI, S., MATSUBARA, A., SEITA, J., TADOKORO, Y., KONDO, H., TAKANO, H. and NAKAUCHI, H., 2006. Adult mouse hematopoietic stem cells: purification and single-cell assays. Nat Protoc *1:* 2979-2987.

EMA, H., and NAKAUCHI, H., 2000. Expansion of hematopoietic stem cells in the developing liver of a mouse embryo. Blood *95:* 2284-2288.

ERNST, J., KHERADPOUR, P., MIKKELSEN, T. S., SHORESH, N., WARD, L. D. *et al.*, 2011. Mapping and analysis of chromatin state dynamics in nine human cell types. Nature *473:* 43-49.

ESSERS, M. A., OFFNER, S., BLANCO-BOSE, W. E., WAIBLER, Z., KALINKE, U., DUCHOSAL, M. A. and TRUMPP, A., 2009. IFNalpha activates dormant haematopoietic stem cells in vivo. Nature *458:* 904-908.

FELSHER, D. W., and BISHOP, J. M., 1999. Reversible tumorigenesis by MYC in hematopoietic lineages. Mol Cell *4:* 199-207.

FERNANDEZ, P. C., FRANK, S. R., WANG, L., SCHROEDER, M., LIU, S., GREENE, J., COCITO, A. and AMATI, B., 2003. Genomic targets of the human c-Myc protein. Genes Dev *17:* 1115-1129.

FISCHLE, W., WANG, Y., JACOBS, S. A., KIM, Y., ALLIS, C. D. and KHORASANIZADEH, S., 2003. Molecular basis for the discrimination of repressive methyl-lysine marks in histone H3 by Polycomb and HP1 chromodomains. Genes Dev *17:* 1870-1881.

FISHER, S., GRICE, E. A., VINTON, R. M., BESSLING, S. L. and MCCALLION, A. S., 2006. Conservation of RET regulatory function from human to zebrafish without sequence similarity. Science *312:* 276-279.

FLANAGAN, J. F., MI, L. Z., CHRUSZCZ, M., CYMBOROWSKI, M., CLINES, K. L., KIM, Y., MINOR, W., RASTINEJAD, F. and KHORASANIZADEH, S., 2005. Double chromodomains cooperate to recognize the methylated histone H3 tail. Nature *438:* 1181-1185.

FORD, C. E., HAMERTON, J. L., BARNES, D. W. and LOUTIT, J. F., 1956. Cytological identification of radiation-chimaeras. Nature *177:* 452-454.

FORRESTER, W. C., EPNER, E., DRISCOLL, M. C., ENVER, T., BRICE, M., PAPAYANNOPOULOU, T. and GROUDINE, M., 1990. A deletion of the human beta-globin locus activation region causes a major alteration in chromatin structure and replication across the entire beta-globin locus. Genes Dev *4:* 1637-1649.

FORSBERG, E. C., SERWOLD, T., KOGAN, S., WEISSMAN, I. L. and PASSEGUE, E., 2006. New evidence supporting megakaryocyte-erythrocyte potential of flk2/flt3+ multipotent hematopoietic progenitors. Cell *126:* 415-426.

FRANK, S. R., PARISI, T., TAUBERT, S., FERNANDEZ, P., FUCHS, M., CHAN, H. M., LIVINGSTON, D. M. and AMATI, B., 2003. MYC recruits the TIP60 histone acetyltransferase complex to chromatin. EMBO Rep *4:* 575-580.

FRANK, S. R., SCHROEDER, M., FERNANDEZ, P., TAUBERT, S. and AMATI, B., 2001. Binding of c-Myc to chromatin mediates mitogen-induced acetylation of histone H4 and gene activation. Genes Dev *15:* 2069-2082.

FULCHER, D. A., and BASTEN, A., 1997. B cell life span: a review. Immunol Cell Biol *75:* 446-455.

GARTEL, A. L., YE, X., GOUFMAN, E., SHIANOV, P., HAY, N., NAJMABADI, F. and TYNER, A. L., 2001. Myc represses the p21(WAF1/CIP1) promoter and interacts with Sp1/Sp3. Proc Natl Acad Sci U S A *98:* 4510-4515.

GAWAZ, M., LANGER, H. and MAY, A. E., 2005. Platelets in inflammation and atherogenesis. J Clin Invest *115:* 3378-3384.

GEKAS, C., DIETERLEN-LIEVRE, F., ORKIN, S. H. and MIKKOLA, H. K., 2005. The placenta is a niche for hematopoietic stem cells. Dev Cell *8:* 365-375.

GERSHENZON, N. I., and IOSHIKHES, I. P., 2005. Synergy of human Pol II core promoter elements revealed by statistical sequence analysis. Bioinformatics *21:* 1295-1300.

GEYER, P. K., 1997. The role of insulator elements in defining domains of gene expression. Curr Opin Genet Dev *7:* 242-248.

GEYER, P. K., and CORCES, V. G., 1992. DNA position-specific repression of transcription by a Drosophila zinc finger protein. Genes Dev *6:* 1865-1873.

GOHL, D., AOKI, T., BLANTON, J., SHANOWER, G., KAPPES, G. and SCHEDL, P., 2011. Mechanism of chromosomal boundary action: roadblock, sink, or loop? Genetics *187:* 731-748.

GOLL, M. G., and BESTOR, T. H., 2005. Eukaryotic cytosine methyltransferases. Annu Rev Biochem *74:* 481-514.

GOMEZ-ROMAN, N., GRANDORI, C., EISENMAN, R. N. and WHITE, R. J., 2003. Direct activation of RNA polymerase III transcription by c-Myc. Nature *421:* 290-294.

GOODELL, M. A., BROSE, K., PARADIS, G., CONNER, A. S. and MULLIGAN, R. C., 1996. Isolation and functional properties of murine hematopoietic stem cells that are replicating in vivo. J Exp Med *183:* 1797-1806.

GREAVES, M., and MALEY, C. C., 2012. Clonal evolution in cancer. Nature *481:* 306-313.

GROSVELD, F., VAN ASSENDELFT, G. B., GREAVES, D. R. and KOLLIAS, G., 1987. Position-independent, high-level expression of the human beta-globin gene in transgenic mice. Cell *51:* 975-985.

GRUNSTEIN, M., 1997. Histone acetylation in chromatin structure and transcription. Nature *389:* 349-352.

GUO, W., and WU, H., 2008. Detection of LacZ expression by FACS-Gal analysis.

GUO, Y., NIU, C., BRESLIN, P., TANG, M., ZHANG, S. *et al.*, 2009. c-Myc-mediated control of cell fate in megakaryocyte-erythrocyte progenitors. Blood *114:* 2097-2106.

GUY, C. T., WEBSTER, M. A., SCHALLER, M., PARSONS, T. J., CARDIFF, R. D. and MULLER, W. J., 1992. Expression of the neu protooncogene in the mammary epithelium of transgenic mice induces metastatic disease. Proc Natl Acad Sci U S A *89:* 10578-10582.

HAAS, S., HANSSON, J., KLIMMECK, D., LÖFFLER, D., VELTEN, L. *et al.*, 2014. Inflammation-driven fast-track differentiation of HSCs into the megakaryocytic lineage. Experimental Hematology *42:* S14.

HAH, N., DANKO, C. G., CORE, L., WATERFALL, J. J., SIEPEL, A., LIS, J. T. and KRAUS, W. L., 2011. A rapid, extensive, and transient transcriptional response to estrogen signaling in breast cancer cells. Cell *145:* 622-634.

HAH, N., MURAKAMI, S., NAGARI, A., DANKO, C. G. and KRAUS, W. L., 2013. Enhancer transcripts mark active estrogen receptor binding sites. Genome Res *23:* 1210-1223.

HAHN, S., 2004. Structure and mechanism of the RNA polymerase II transcription machinery. Nat Struct Mol Biol *11:* 394-403.

HALLIKAS, O., PALIN, K., SINJUSHINA, N., RAUTIAINEN, R., PARTANEN, J., UKKONEN, E. and TAIPALE, J., 2006. Genome-wide prediction of mammalian enhancers based on analysis of transcription-factor binding affinity. Cell *124:* 47-59.

HANDOKO, L., XU, H., LI, G., NGAN, C. Y., CHEW, E. *et al.*, 2011. CTCF-mediated functional chromatin interactome in pluripotent cells. Nat Genet *43:* 630-638.

HANNAH, R., JOSHI, A., WILSON, N. K., KINSTON, S. and GOTTGENS, B., 2011. A compendium of genome-wide hematopoietic transcription factor maps supports the identification of gene regulatory control mechanisms. Exp Hematol *39:* 531-541.

HARDISON, R., SLIGHTOM, J. L., GUMUCIO, D. L., GOODMAN, M., STOJANOVIC, N. and MILLER, W., 1997. Locus control regions of mammalian beta-globin gene clusters: combining phylogenetic analyses and experimental results to gain functional insights. Gene *205:* 73-94.

HARE, E. E., PETERSON, B. K., IYER, V. N., MEIER, R. and EISEN, M. B., 2008. Sepsid even-skipped enhancers are functionally conserved in Drosophila despite lack of sequence conservation. PLoS Genet *4:* e1000106.

HARRISON, D. E., JORDAN, C. T., ZHONG, R. K. and ASTLE, C. M., 1993. Primitive hemopoietic stem cells: direct assay of most productive populations by competitive repopulation with simple binomial, correlation and covariance calculations. Exp Hematol *21:* 206-219.

HASSAN, A. H., PROCHASSON, P., NEELY, K. E., GALASINSKI, S. C., CHANDY, M., CARROZZA, M. J. and WORKMAN, J. L., 2002. Function and selectivity of bromodomains in anchoring chromatin-modifying complexes to promoter nucleosomes. Cell *111:* 369-379.

HASSIG, C. A., FLEISCHER, T. C., BILLIN, A. N., SCHREIBER, S. L. and AYER, D. E., 1997. Histone deacetylase activity is required for full transcriptional repression by mSin3A. Cell *89:* 341-347.

HATA, K., OKANO, M., LEI, H. and LI, E., 2002. Dnmt3L cooperates with the Dnmt3 family of de novo DNA methyltransferases to establish maternal imprints in mice. Development *129:* 1983-1993.

HATTON, B. A., KNOEPFLER, P. S., KENNEY, A. M., ROWITCH, D. H., DE ALBORAN, I. M., OLSON, J. M. and EISENMAN, R. N., 2006. N-myc is an essential downstream effector of Shh signaling during both normal and neoplastic cerebellar growth. Cancer Res *66:* 8655-8661.

HATTON, K. S., MAHON, K., CHIN, L., CHIU, F. C., LEE, H. W., PENG, D., MORGENBESSER, S. D., HORNER, J. and DEPINHO, R. A., 1996. Expression and activity of L-Myc in normal mouse development. Mol Cell Biol *16:* 1794-1804.

HEINTZMAN, N. D., HON, G. C., HAWKINS, R. D., KHERADPOUR, P., STARK, A. *et al.*, 2009. Histone modifications at human enhancers reflect global cell-type-specific gene expression. Nature *459:* 108-112.

HEINTZMAN, N. D., STUART, R. K., HON, G., FU, Y., CHING, C. W. *et al.*, 2007. Distinct and predictive chromatin signatures of transcriptional promoters and enhancers in the human genome. Nat Genet *39:* 311-318.

HERAULT, Y., RASSOULZADEGAN, M., CUZIN, F. and DUBOULE, D., 1998. Engineering chromosomes in mice through targeted meiotic recombination (TAMERE). Nat Genet *20:* 381-384.

HERMEKING, H., RAGO, C., SCHUHMACHER, M., LI, Q., BARRETT, J. F. *et al.*, 2000. Identification of CDK4 as a target of c-MYC. Proc Natl Acad Sci U S A *97:* 2229-2234.

HERRANZ, D., AMBESI-IMPIOMBATO, A., PALOMERO, T., SCHNELL, S. A., BELVER, L. *et al.*, 2014. A NOTCH1-driven MYC enhancer promotes T cell development, transformation and acute lymphoblastic leukemia. Nat Med.

HNISZ, D., ABRAHAM, B. J., LEE, T. I., LAU, A., SAINT-ANDRE, V., SIGOVA, A. A., HOKE, H. A. and YOUNG, R. A., 2013. Super-enhancers in the control of cell identity and disease. Cell *155:* 934-947.

HOBEIKA, E., THIEMANN, S., STORCH, B., JUMAA, H., NIELSEN, P. J., PELANDA, R. and RETH, M., 2006. Testing gene function early in the B cell lineage in mb1-cre mice. Proc Natl Acad Sci U S A *103:* 13789-13794.

HODGES, E., MOLARO, A., DOS SANTOS, C. O., THEKKAT, P., SONG, Q. *et al.*, 2011. Directional DNA methylation changes and complex intermediate states accompany lineage specificity in the adult hematopoietic compartment. Mol Cell *44:* 17-28.

HORIE, K., YUSA, K., YAE, K., ODAJIMA, J., FISCHER, S. E. *et al.*, 2003. Characterization of Sleeping Beauty transposition and its application to genetic screening in mice. Mol Cell Biol *23:* 9189-9207.

HUANG, C. Y., BREDEMEYER, A. L., WALKER, L. M., BASSING, C. H. and SLECKMAN, B. P., 2008. Dynamic regulation of c-Myc proto-oncogene expression during lymphocyte development revealed by a GFP-c-Myc knock-in mouse. Eur J Immunol *38:* 342-349.

HUANG, S., LI, X., YUSUFZAI, T. M., QIU, Y. and FELSENFELD, G., 2007. USF1 recruits histone modification complexes and is critical for maintenance of a chromatin barrier. Mol Cell Biol *27:* 7991-8002.

HUBER, T. L., KOUSKOFF, V., FEHLING, H. J., PALIS, J. and KELLER, G., 2004. Haemangioblast commitment is initiated in the primitive streak of the mouse embryo. Nature *432:* 625-630.

HURLIN, P. J., QUEVA, C. and EISENMAN, R. N., 1997. Mnt, a novel Max-interacting protein is coexpressed with Myc in proliferating cells and mediates repression at Myc binding sites. Genes Dev *11:* 44-58.

HURLIN, P. J., QUEVA, C., KOSKINEN, P. J., STEINGRIMSSON, E., AYER, D. E., COPELAND, N. G., JENKINS, N. A. and EISENMAN, R. N., 1996. Mad3 and Mad4: novel Max-interacting transcriptional repressors that suppress c-myc dependent transformation and are expressed during neural and epidermal differentiation. EMBO J *15:* 2030.

IKUTA, K., and WEISSMAN, I. L., 1992. Evidence that hematopoietic stem cells express mouse c-kit but do not depend on steel factor for their generation. Proc Natl Acad Sci U S A *89:* 1502-1506.

IOSHIKHES, I. P., and ZHANG, M. Q., 2000. Large-scale human promoter mapping using CpG islands. Nat Genet *26:* 61-63.

JABBARI, K., and BERNARDI, G., 2004. Cytosine methylation and CpG, TpG (CpA) and TpA frequencies. Gene *333:* 143-149.

JOHNSON, G. R., and MOORE, M. A., 1975. Role of stem cell migration in initiation of mouse foetal liver haemopoiesis. Nature *258:* 726-728.

JOHNSTON, L. A., PROBER, D. A., EDGAR, B. A., EISENMAN, R. N. and GALLANT, P., 1999. Drosophila myc regulates cellular growth during development. Cell *98:* 779-790.

JONES, P. A., 2012. Functions of DNA methylation: islands, start sites, gene bodies and beyond. Nat Rev Genet *13:* 484-492.

JUVEN-GERSHON, T., and KADONAGA, J. T., 2010. Regulation of gene expression via the core promoter and the basal transcriptional machinery. Dev Biol *339:* 225-229.

KAIKKONEN, M. U., SPANN, N. J., HEINZ, S., ROMANOSKI, C. E., ALLISON, K. A. *et al.*, 2013. Remodeling of the enhancer landscape during macrophage activation is coupled to enhancer transcription. Mol Cell *51:* 310-325.

KASSIS, J. A., 1994. Unusual properties of regulatory DNA from the Drosophila engrailed gene: three "pairing-sensitive" sites within a 1.6-kb region. Genetics *136:* 1025-1038.

KASSIS, J. A., VANSICKLE, E. P. and SENSABAUGH, S. M., 1991. A fragment of engrailed regulatory DNA can mediate transvection of the white gene in Drosophila. Genetics *128:* 751-761.

KASTEN, M., SZERLONG, H., ERDJUMENT-BROMAGE, H., TEMPST, P., WERNER, M. and CAIRNS, B. R., 2004. Tandem bromodomains in the chromatin remodeler RSC recognize acetylated histone H3 Lys14. EMBO J *23:* 1348-1359.

KENG, V. W., YAE, K., HAYAKAWA, T., MIZUNO, S., UNO, Y. *et al.*, 2005. Region-specific saturation germline mutagenesis in mice using the Sleeping Beauty transposon system. Nat Methods *2:* 763-769.

KIEL, M. J., YILMAZ, O. H., IWASHITA, T., TERHORST, C. and MORRISON, S. J., 2005. SLAM family receptors distinguish hematopoietic stem and progenitor cells and reveal endothelial niches for stem cells. Cell *121:* 1109-1121.

KIM, T. K., HEMBERG, M., GRAY, J. M., COSTA, A. M., BEAR, D. M. *et al.*, 2010. Widespread transcription at neuronal activity-regulated enhancers. Nature *465:* 182-187.

KING, B., TRIMARCHI, T., REAVIE, L., XU, L., MULLENDERS, J. *et al.*, 2013. The ubiquitin ligase FBXW7 modulates leukemia-initiating cell activity by regulating MYC stability. Cell *153:* 1552-1566.

KNOEPFLER, P. S., CHENG, P. F. and EISENMAN, R. N., 2002. N-myc is essential during neurogenesis for the rapid expansion of progenitor cell populations and the inhibition of neuronal differentiation. Genes Dev *16:* 2699-2712.

KOCH, F., FENOUIL, R., GUT, M., CAUCHY, P., ALBERT, T. K. *et al.*, 2011. Transcription initiation platforms and GTF recruitment at tissue-specific enhancers and promoters. Nat Struct Mol Biol *18:* 956-963.

KOHL, N. E., KANDA, N., SCHRECK, R. R., BRUNS, G., LATT, S. A., GILBERT, F. and ALT, F. W., 1983. Transposition and amplification of oncogene-related sequences in human neuroblastomas. Cell *35:* 359-367.

KOMURO, K., ITAKURA, K., BOYSE, A. and JOHN, M., 1975. Ly-5; A New T-Lymphocyte Antigen System. Immunogenetics*:* 452-456.

KONDO, M., WEISSMAN, I. L. and AKASHI, K., 1997. Identification of clonogenic common lymphoid progenitors in mouse bone marrow. Cell *91:* 661-672.

KOPECKY, B., SANTI, P., JOHNSON, S., SCHMITZ, H. and FRITZSCH, B., 2011. Conditional deletion of N-Myc disrupts neurosensory and non-sensory development of the ear. Dev Dyn *240:* 1373-1390.

KOPECKY, B. J., DECOOK, R. and FRITZSCH, B., 2012. N-Myc and L-Myc are essential for hair cell formation but not maintenance. Brain Res *1484:* 1-14.

KOULNIS, M., POP, R., PORPIGLIA, E., SHEARSTONE, J. R., HIDALGO, D. and SOCOLOVSKY, M., 2011. Identification and analysis of mouse erythroid progenitors using the CD71/TER119 flow-cytometric assay. J Vis Exp.

KOUZARIDES, T., 2007. Chromatin modifications and their function. Cell *128:* 693-705.

KROON, E., KROSL, J., THORSTEINSDOTTIR, U., BABAN, S., BUCHBERG, A. M. and SAUVAGEAU, G., 1998. Hoxa9 transforms primary bone marrow cells through specific collaboration with Meis1a but not Pbx1b. EMBO J *17:* 3714-3725.

KUHN, M. W., RADTKE, I., BULLINGER, L., GOORHA, S., CHENG, J. *et al.*, 2012. High-resolution genomic profiling of adult and pediatric core-binding factor acute myeloid leukemia reveals new recurrent genomic alterations. Blood *119:* e67-75.

KÜHN, R., SCHWENK, F., AGUET, M. and RAJEWSKY, K., 1995. Inducible gene targeting in mice. Science *269:* 1427-1429.

KULKARNI, M. M., and ARNOSTI, D. N., 2003. Information display by transcriptional enhancers. Development *130:* 6569-6575.

KUMARAVELU, P., HOOK, L., MORRISON, A. M., URE, J., ZHAO, S., ZUYEV, S., ANSELL, J. and MEDVINSKY, A., 2002. Quantitative developmental anatomy of definitive haematopoietic stem cells/long-term repopulating units (HSC/RUs): role of the aorta-gonad-mesonephros (AGM) region and the yolk sac in colonisation of the mouse embryonic liver. Development *129:* 4891-4899.

KUZMICHEV, A., NISHIOKA, K., ERDJUMENT-BROMAGE, H., TEMPST, P. and REINBERG, D., 2002. Histone methyltransferase activity associated with a human multiprotein complex containing the Enhancer of Zeste protein. Genes Dev *16:* 2893-2905.

LACKNER, D. H., and BAHLER, J., 2008. Translational control of gene expression from transcripts to transcriptomes. Int Rev Cell Mol Biol *271:* 199-251.

LAHERTY, C. D., YANG, W. M., SUN, J. M., DAVIE, J. R., SETO, E. and EISENMAN, R. N., 1997. Histone deacetylases associated with the mSin3 corepressor mediate mad transcriptional repression. Cell *89:* 349-356.

LAM, M. T., CHO, H., LESCH, H. P., GOSSELIN, D., HEINZ, S. *et al.*, 2013. Rev-Erbs repress macrophage gene expression by inhibiting enhancer-directed transcription. Nature *498:* 511-515.

LANDER, E. S., LINTON, L. M., BIRREN, B., NUSBAUM, C., ZODY, M. C. *et al.*, 2001. Initial sequencing and analysis of the human genome. Nature *409:* 860-921.

LARA-ASTIASO, D., WEINER, A., LORENZO-VIVAS, E., ZARETSKY, I., JAITIN, D. A. *et al.*, 2014. Immunogenetics. Chromatin state dynamics during blood formation. Science *345:* 943-949.

LAURENTI, E., VARNUM-FINNEY, B., WILSON, A., FERRERO, I., BLANCO-BOSE, W. E. *et al.*, 2008. Hematopoietic stem cell function and survival depend on c-Myc and N-Myc activity. Cell Stem Cell *3:* 611-624.

LAURENTI, E., WILSON, A. and TRUMPP, A., 2009. Myc's other life: stem cells and beyond. Curr Opin Cell Biol *21:* 844-854.

LAVENU, A., POURNIN, S., BABINET, C. and MORELLO, D., 1994. The cis-acting elements known to regulate c-myc expression ex vivo are not sufficient for correct transcription in vivo. Oncogene *9:* 527-536.

LEDER, A., PATTENGALE, P. K., KUO, A., STEWART, T. A. and LEDER, P., 1986. Consequences of widespread deregulation of the c-myc gene in transgenic mice: multiple neoplasms and normal development. Cell *45:* 485-495.

LEE, L. K., UENO, M., VAN HANDEL, B. and MIKKOLA, H. K., 2010. Placenta as a newly identified source of hematopoietic stem cells. Curr Opin Hematol *17:* 313-318.

LEE, T. I., JENNER, R. G., BOYER, L. A., GUENTHER, M. G., LEVINE, S. S. *et al.*, 2006. Control of developmental regulators by Polycomb in human embryonic stem cells. Cell *125:* 301-313.

LEHNERTZ, B., UEDA, Y., DERIJCK, A. A., BRAUNSCHWEIG, U., PEREZ-BURGOS, L. *et al.*, 2003. Suv39h-mediated histone H3 lysine 9 methylation directs DNA methylation to major satellite repeats at pericentric heterochromatin. Curr Biol *13:* 1192-1200.

LEMISCHKA, I. R., RAULET, D. H. and MULLIGAN, R. C., 1986. Developmental potential and dynamic behavior of hematopoietic stem cells. Cell *45:* 917-927.

LETTICE, L. A., HEANEY, S. J., PURDIE, L. A., LI, L., DE BEER, P. *et al.*, 2003. A long-range Shh enhancer regulates expression in the developing limb and fin and is associated with preaxial polydactyly. Hum Mol Genet *12:* 1725-1735.

LEVENS, D., 2010. You Don't Muck with MYC. Genes Cancer *1:* 547-554.

LEWIS, E. B., 1978. A gene complex controlling segmentation in Drosophila. Nature *276:* 565-570.

LEY, T. J., DING, L., WALTER, M. J., MCLELLAN, M. D., LAMPRECHT, T. *et al.*, 2010. DNMT3A mutations in acute myeloid leukemia. N Engl J Med *363:* 2424-2433.

LI, G., RUAN, X., AUERBACH, R. K., SANDHU, K. S., ZHENG, M. *et al.*, 2012. Extensive promoter-centered chromatin interactions provide a topological basis for transcription regulation. Cell *148:* 84-98.

LI, H., ILIN, S., WANG, W., DUNCAN, E. M., WYSOCKA, J., ALLIS, C. D. and PATEL, D. J., 2006. Molecular basis for site-specific read-out of histone H3K4me3 by the BPTF PHD finger of NURF. Nature *442:* 91-95.

LI, Q., PETERSON, K. R., FANG, X. and STAMATOYANNOPOULOS, G., 2002. Locus control regions. Blood *100:* 3077-3086.

LI, W., NOTANI, D., MA, Q., TANASA, B., NUNEZ, E. *et al.*, 2013. Functional roles of enhancer RNAs for oestrogen-dependent transcriptional activation. Nature *498:* 516-520.

LI, Z., VAN CALCAR, S., QU, C., CAVENEE, W. K., ZHANG, M. Q. and REN, B., 2003. A global transcriptional regulatory role for c-Myc in Burkitt's lymphoma cells. Proc Natl Acad Sci U S A *100:* 8164-8169.

LIEBERMAN, L., BERCOVITZ, R. S., SHOLAPUR, N. S., HEDDLE, N. M., STANWORTH, S. J. and ARNOLD, D. M., 2014. Platelet transfusions for critically ill patients with thrombocytopenia. Blood *123:* 1146-1151; quiz 1280.

LIEBERMAN-AIDEN, E., VAN BERKUM, N. L., WILLIAMS, L., IMAKAEV, M., RAGOCZY, T. *et al.*, 2009. Comprehensive mapping of long-range interactions reveals folding principles of the human genome. Science *326:* 289-293.

LIN, C. Y., LOVEN, J., RAHL, P. B., PARANAL, R. M., BURGE, C. B., BRADNER, J. E., LEE, T. I. and YOUNG, R. A., 2012. Transcriptional amplification in tumor cells with elevated c-Myc. Cell *151:* 56-67.

LIU, J., and LEVENS, D., 2006. Making myc. Curr Top Microbiol Immunol *302:* 1-32.

LIVAK, K. J., and SCHMITTGEN, T. D., 2001. Analysis of relative gene expression data using real-time quantitative PCR and the 2(-Delta Delta C(T)) Method. Methods *25:* 402-408.

LOHAN, S., SPIELMANN, M., DOELKEN, S. C., FLOTTMANN, R., MUHAMMAD, F. *et al.*, 2014. Microduplications encompassing the Sonic hedgehog limb enhancer ZRS are associated with Haas-type polysyndactyly and Laurin-Sandrow syndrome. Clin Genet.

LOVEN, J., HOKE, H. A., LIN, C. Y., LAU, A., ORLANDO, D. A., VAKOC, C. R., BRADNER, J. E., LEE, T. I. and YOUNG, R. A., 2013. Selective inhibition of tumor oncogenes by disruption of super-enhancers. Cell *153:* 320-334.

LUGER, K., MADER, A. W., RICHMOND, R. K., SARGENT, D. F. and RICHMOND, T. J., 1997. Crystal structure of the nucleosome core particle at 2.8 A resolution. Nature *389:* 251-260.

LUO, G., IVICS, Z., IZSVAK, Z. and BRADLEY, A., 1998. Chromosomal transposition of a Tc1/mariner-like element in mouse embryonic stem cells. Proc Natl Acad Sci U S A *95:* 10769-10773.

LUO, H., LI, Q., O'NEAL, J., KREISEL, F., LE BEAU, M. M. and TOMASSON, M. H., 2005. c-Myc rapidly induces acute myeloid leukemia in mice without evidence of lymphoma-associated antiapoptotic mutations. Blood *106:* 2452-2461.

MALYNN, B. A., DE ALBORAN, I. M., O'HAGAN, R. C., BRONSON, R., DAVIDSON, L., DEPINHO, R. A. and ALT, F. W., 2000. N-myc can functionally replace c-myc in murine development, cellular growth, and differentiation. Genes Dev *14:* 1390-1399.

MANZ, M. G., TRAVER, D., MIYAMOTO, T., WEISSMAN, I. L. and AKASHI, K., 2001. Dendritic cell potentials of early lymphoid and myeloid progenitors. Blood *97:* 3333-3341.

MARTINS, R. A., ZINDY, F., DONOVAN, S., ZHANG, J., POUNDS, S. *et al.*, 2008. N-myc coordinates retinal growth with eye size during mouse development. Genes Dev *22:* 179-193.

MASTON, G. A., EVANS, S. K. and GREEN, M. R., 2006. Transcriptional regulatory elements in the human genome. Annu Rev Genomics Hum Genet *7:* 29-59.

MATSUOKA, S., EBIHARA, Y., XU, M., ISHII, T., SUGIYAMA, D. *et al.*, 2001. CD34 expression on long-term repopulating hematopoietic stem cells changes during developmental stages. Blood *97:* 419-425.

MATSUZAKI, Y., KINJO, K., MULLIGAN, R. C. and OKANO, H., 2004. Unexpectedly efficient homing capacity of purified murine hematopoietic stem cells. Immunity *20:* 87-93.

MAURANO, M. T., HUMBERT, R., RYNES, E., THURMAN, R. E., HAUGEN, E. *et al.*, 2012. Systematic localization of common disease-associated variation in regulatory DNA. Science *337:* 1190-1195.

MAUTNER, J., BEHRENDS, U., HORTNAGEL, K., BRIELMEIER, M., HAMMERSCHMIDT, W., STROBL, L., BORNKAMM, G. W. and POLACK, A., 1996. c-myc expression is activated by the immunoglobulin kappa-enhancers from a distance of at least 30 kb but not by elements located within 50 kb of the unaltered c-myc locus in vivo. Oncogene *12:* 1299-1307.

MAYOR, C., BRUDNO, M., SCHWARTZ, J. R., POLIAKOV, A., RUBIN, E. M., FRAZER, K. A., PACHTER, L. S. and DUBCHAK, I., 2000. VISTA : visualizing global DNA sequence alignments of arbitrary length. Bioinformatics *16:* 1046-1047.

MCGAUGHEY, D. M., VINTON, R. M., HUYNH, J., AL-SAIF, A., BEER, M. A. and MCCALLION, A. S., 2008. Metrics of sequence constraint overlook regulatory sequences in an exhaustive analysis at phox2b. Genome Res *18:* 252-260.

MCGRATH, K. E., FRAME, J. M., FROMM, G. J., KONISKI, A. D., KINGSLEY, P. D., LITTLE, J., BULGER, M. and PALIS, J., 2011. A transient definitive erythroid lineage with unique regulation of the beta-globin locus in the mammalian embryo. Blood *117:* 4600-4608.

MCKNIGHT, S. L., and KINGSBURY, R., 1982. Transcriptional control signals of a eukaryotic protein-coding gene. Science *217:* 316-324.

MCMAHON, S. B., WOOD, M. A. and COLE, M. D., 2000. The essential cofactor TRRAP recruits the histone acetyltransferase hGCN5 to c-Myc. Mol Cell Biol *20:* 556-562.

MEDVINSKY, A., and DZIERZAK, E., 1996. Definitive hematopoiesis is autonomously initiated by the AGM region. Cell *86:* 897-906.

MELGAR, M. F., COLLINS, F. S. and SETHUPATHY, P., 2011. Discovery of active enhancers through bidirectional expression of short transcripts. Genome Biol *12:* R113.

MELO, C. A., DROST, J., WIJCHERS, P. J., VAN DE WERKEN, H., DE WIT, E. *et al.*, 2013. eRNAs are required for p53-dependent enhancer activity and gene transcription. Mol Cell *49:* 524-535.

MERIKA, M., WILLIAMS, A. J., CHEN, G., COLLINS, T. and THANOS, D., 1998. Recruitment of CBP/p300 by the IFN beta enhanceosome is required for synergistic activation of transcription. Mol Cell *1:* 277-287.

MEYER, N., and PENN, L. Z., 2008. Reflecting on 25 years with MYC. Nat Rev Cancer *8:* 976-990.

MIKKOLA, H. K., and ORKIN, S. H., 2006. The journey of developing hematopoietic stem cells. Development *133:* 3733-3744.

MILLER, B. A., ANTOGNETTI, G. and SPRINGER, T. A., 1985. Identification of cell surface antigens present on murine hematopoietic stem cells. J Immunol *134:* 3286-3290.

MILLER, C. L., and EAVES, C. J., 1997. Expansion in vitro of adult murine hematopoietic stem cells with transplantable lympho-myeloid reconstituting ability. Proc Natl Acad Sci U S A *94:* 13648-13653.

MIN, J., ZHANG, Y. and XU, R. M., 2003. Structural basis for specific binding of Polycomb chromodomain to histone H3 methylated at Lys 27. Genes Dev *17:* 1823-1828.

MORRISON, S. J., HEMMATI, H. D., WANDYCZ, A. M. and WEISSMAN, I. L., 1995. The purification and characterization of fetal liver hematopoietic stem cells. Proc Natl Acad Sci U S A *92:* 10302-10306.

MOUSAVI, K., ZARE, H., DELL'ORSO, S., GRONTVED, L., GUTIERREZ-CRUZ, G., DERFOUL, A., HAGER, G. L. and SARTORELLI, V., 2013. eRNAs promote transcription by establishing chromatin accessibility at defined genomic loci. Mol Cell *51:* 606-617.

MÜLLER, A. M., MEDVINSKY, A., STROUBOULIS, J., GROSVELD, F. and DZIERZAK, E., 1994. Development of hematopoietic stem cell activity in the mouse embryo. Immunity *1:* 291-301.

MÜLLER, J., HART, C. M., FRANCIS, N. J., VARGAS, M. L., SENGUPTA, A. *et al.*, 2002. Histone methyltransferase activity of a Drosophila Polycomb group repressor complex. Cell *111:* 197-208.

MÜLLER-SIEBURG, C. E., CHO, R. H., KARLSSON, L., HUANG, J. F. and SIEBURG, H. B., 2004. Myeloid-biased hematopoietic stem cells have extensive self-renewal capacity but generate diminished lymphoid progeny with impaired IL-7 responsiveness. Blood *103:* 4111-4118.

MÜLLER-SIEBURG, C. E., CHO, R. H., THOMAN, M., ADKINS, B. and SIEBURG, H. B., 2002. Deterministic regulation of hematopoietic stem cell self-renewal and differentiation. Blood *100:* 1302-1309.

MÜLLER-SIEBURG, C. E., TOWNSEND, K., WEISSMAN, I. L. and RENNICK, D., 1988. Proliferation and differentiation of highly enriched mouse hematopoietic stem cells and progenitor cells in response to defined growth factors. J Exp Med *167:* 1825-1840.

MÜLLER-SIEBURG, C. E., WHITLOCK, C. A. and WEISSMAN, I. L., 1986. Isolation of two early B lymphocyte progenitors from mouse marrow: a committed pre-pre-B cell and a clonogenic Thy-1-lo hematopoietic stem cell. Cell *44:* 653-662.

MULLIS, K. B., 1990. Target amplification for DNA analysis by the polymerase chain reaction. Ann Biol Clin (Paris) *48:* 579-582.

MUNCAN, V., SANSOM, O. J., TERTOOLEN, L., PHESSE, T. J., BEGTHEL, H. *et al.*, 2006. Rapid loss of intestinal crypts upon conditional deletion of the Wnt/Tcf-4 target gene c-Myc. Mol Cell Biol *26:* 8418-8426.

MURAVYOVA, E., GOLOVNIN, A., GRACHEVA, E., PARSHIKOV, A., BELENKAYA, T., PIRROTTA, V. and GEORGIEV, P., 2001. Loss of insulator activity by paired Su(Hw) chromatin insulators. Science *291:* 495-498.

MURRAY, P. D. F., 1932. The development in vitro of the blood of the early chicken embryo. Proc R Soc Lond B Biol Sci *11:* 497-521.

NAGAO, M., CAMPBELL, K., BURNS, K., KUAN, C. Y., TRUMPP, A. and NAKAFUKU, M., 2008. Coordinated control of self-renewal and differentiation of neural stem cells by Myc and the p19ARF-p53 pathway. J Cell Biol *183:* 1243-1257.

NALLS, M. A., COUPER, D. J., TANAKA, T., VAN ROOIJ, F. J., CHEN, M. H. *et al.*, 2011. Multiple loci are associated with white blood cell phenotypes. PLoS Genet *7:* e1002113.

NATOLI, G., and ANDRAU, J. C., 2012. Noncoding transcription at enhancers: general principles and functional models. Annu Rev Genet *46:* 1-19.

NAU, M. M., BROOKS, B. J., BATTEY, J., SAUSVILLE, E., GAZDAR, A. F. *et al.*, 1985. L-myc, a new myc-related gene amplified and expressed in human small cell lung cancer. Nature *318:* 69-73.

NEELY, K. E., HASSAN, A. H., WALLBERG, A. E., STEGER, D. J., CAIRNS, B. R., WRIGHT, A. P. and WORKMAN, J. L., 1999. Activation domain-mediated targeting of the SWI/SNF complex to promoters stimulates transcription from nucleosome arrays. Mol Cell *4:* 649-655.

NEGRE, N., HENNETIN, J., SUN, L. V., LAVROV, S., BELLIS, M., WHITE, K. P. and CAVALLI, G., 2006. Chromosomal distribution of PcG proteins during Drosophila development. PLoS Biol *4:* e170.

NIE, Z., HU, G., WEI, G., CUI, K., YAMANE, A. *et al.*, 2012. c-Myc is a universal amplifier of expressed genes in lymphocytes and embryonic stem cells. Cell *151:* 68-79.

NISHIOKA, K., CHUIKOV, S., SARMA, K., ERDJUMENT-BROMAGE, H., ALLIS, C. D., TEMPST, P. and REINBERG, D., 2002. Set9, a novel histone H3 methyltransferase that facilitates transcription by precluding histone tail modifications required for heterochromatin formation. Genes Dev *16:* 479-489.

NOCKA, K., TAN, J. C., CHIU, E., CHU, T. Y., RAY, P., TRAKTMAN, P. and BESMER, P., 1990. Molecular bases of dominant negative and loss of function mutations at the murine c-kit/white spotting locus: W37, Wv, W41 and W. EMBO J *9:* 1805-1813.

NORA, E. P., LAJOIE, B. R., SCHULZ, E. G., GIORGETTI, L., OKAMOTO, I. *et al.*, 2012. Spatial partitioning of the regulatory landscape of the X-inactivation centre. Nature *485:* 381-385.

NOWELL, P. C., COLE, L. J., HABERMEYER, J. G. and ROAN, P. L., 1956. Growth and continued function of rat marrow cells in x-radiated mice. Cancer Res *16:* 258-261.

O'DONNELL, K. A., WENTZEL, E. A., ZELLER, K. I., DANG, C. V. and MENDELL, J. T., 2005. c-Myc-regulated microRNAs modulate E2F1 expression. Nature *435:* 839-843.

OGAWA, M., MATSUZAKI, Y., NISHIKAWA, S., HAYASHI, S., KUNISADA, T., SUDO, T., KINA, T. and NAKAUCHI, H., 1991. Expression and function of c-kit in hemopoietic progenitor cells. J Exp Med *174:* 63-71.

OGBOURNE, S., and ANTALIS, T. M., 1998. Transcriptional control and the role of silencers in transcriptional regulation in eukaryotes. Biochem J *331 (Pt 1):* 1-14.

OKADA, Y., HIROTA, T., KAMATANI, Y., TAKAHASHI, A., OHMIYA, H. *et al.*, 2011. Identification of nine novel loci associated with white blood cell subtypes in a Japanese population. PLoS Genet *7:* e1002067.

OKANO, M., BELL, D. W., HABER, D. A. and LI, E., 1999. DNA methyltransferases Dnmt3a and Dnmt3b are essential for de novo methylation and mammalian development. Cell *99:* 247-257.

OKUBO, T., KNOEPFLER, P. S., EISENMAN, R. N. and HOGAN, B. L., 2005. Nmyc plays an essential role during lung development as a dosage-sensitive regulator of progenitor cell proliferation and differentiation. Development *132:* 1363-1374.

ONG, C. T., and CORCES, V. G., 2011. Enhancer function: new insights into the regulation of tissue-specific gene expression. Nat Rev Genet *12:* 283-293.

OOI, A. G., KARSUNKY, H., MAJETI, R., BUTZ, S., VESTWEBER, D., ISHIDA, T., QUERTERMOUS, T., WEISSMAN, I. L. and FORSBERG, E. C., 2009. The adhesion molecule esam1 is a novel hematopoietic stem cell marker. Stem Cells *27:* 653-661.

ORIAN, A., VAN STEENSEL, B., DELROW, J., BUSSEMAKER, H. J., LI, L. *et al.*, 2003. Genomic binding by the Drosophila Myc, Max, Mad/Mnt transcription factor network. Genes Dev *17:* 1101-1114.

OSAWA, M., HANADA, K., HAMADA, H. and NAKAUCHI, H., 1996. Long-term lymphohematopoietic reconstitution by a single CD34-low/negative hematopoietic stem cell. Science *273:* 242-245.

OSKARSSON, T., ESSERS, M. A., DUBOIS, N., OFFNER, S., DUBEY, C. *et al.*, 2006. Skin epidermis lacking the c-Myc gene is resistant to Ras-driven tumorigenesis but can reacquire sensitivity upon additional loss of the p21Cip1 gene. Genes Dev *20:* 2024-2029.

OTA, S., ZHOU, Z. Q., KEENE, D. R., KNOEPFLER, P. and HURLIN, P. J., 2007. Activities of N-Myc in the developing limb link control of skeletal size with digit separation. Development *134:* 1583-1592.

PANNE, D., 2008. The enhanceosome. Curr Opin Struct Biol *18:* 236-242.

PATEL, J. H., LOBODA, A. P., SHOWE, M. K., SHOWE, L. C. and MCMAHON, S. B., 2004. Analysis of genomic targets reveals complex functions of MYC. Nat Rev Cancer *4:* 562-568.

PATEL, S. R., RICHARDSON, J. L., SCHULZE, H., KAHLE, E., GALJART, N., DRABEK, K., SHIVDASANI, R. A., HARTWIG, J. H. and ITALIANO, J. E., JR., 2005. Differential roles of microtubule assembly and sliding in proplatelet formation by megakaryocytes. Blood *106:* 4076-4085.

PENGELLY, A. R., COPUR, O., JACKLE, H., HERZIG, A. and MULLER, J., 2013. A histone mutant reproduces the phenotype caused by loss of histone-modifying factor Polycomb. Science *339:* 698-699.

PENN, L. J., BROOKS, M. W., LAUFER, E. M. and LAND, H., 1990a. Negative autoregulation of c-myc transcription. EMBO J *9:* 1113-1121.

PENN, L. J., LAUFER, E. M. and LAND, H., 1990b. C-MYC: evidence for multiple regulatory functions. Semin Cancer Biol *1:* 69-80.

PENNACCHIO, L. A., AHITUV, N., MOSES, A. M., PRABHAKAR, S., NOBREGA, M. A. *et al.*, 2006. In vivo enhancer analysis of human conserved non-coding sequences. Nature *444:* 499-502.

PESCHON, J. J., BEHRINGER, R. R., PALMITER, R. D. and BRINSTER, R. L., 1989. Expression of mouse protamine 1 genes in transgenic mice. Ann N Y Acad Sci *564:* 186-197.

PETRIE, H. T., 2003. Cell migration and the control of post-natal T-cell lymphopoiesis in the thymus. Nat Rev Immunol *3:* 859-866.

PEUKERT, K., STALLER, P., SCHNEIDER, A., CARMICHAEL, G., HANEL, F. and EILERS, M., 1997. An alternative pathway for gene regulation by Myc. EMBO J *16:* 5672-5686.

PHILLIPS-CREMINS, J. E., SAURIA, M. E., SANYAL, A., GERASIMOVA, T. I., LAJOIE, B. R. *et al.*, 2013. Architectural protein subclasses shape 3D organization of genomes during lineage commitment. Cell *153:* 1281-1295.

PLANK, J. L., and DEAN, A., 2014. Enhancer function: mechanistic and genome-wide insights come together. Mol Cell *55:* 5-14.

PLOEMACHER, R. E., VAN DER SLUIJS, J. P., VOERMAN, J. S. and BRONS, N. H., 1989. An in vitro limiting-dilution assay of long-term repopulating hematopoietic stem cells in the mouse. Blood *74:* 2755-2763.

POMERANTZ, M. M., AHMADIYEH, N., JIA, L., HERMAN, P., VERZI, M. P. *et al.*, 2009. The 8q24 cancer risk variant rs6983267 shows long-range interaction with MYC in colorectal cancer. Nat Genet *41:* 882-884.

PRONK, C. J., ROSSI, D. J., MANSSON, R., ATTEMA, J. L., NORDDAHL, G. L., CHAN, C. K., SIGVARDSSON, M., WEISSMAN, I. L. and BRYDER, D., 2007. Elucidation of the phenotypic, functional, and molecular topography of a myeloerythroid progenitor cell hierarchy. Cell Stem Cell *1:* 428-442.

PSHENICHNAYA, I., SCHOUWEY, K., ARMARO, M., LARUE, L., KNOEPFLER, P. S., EISENMAN, R. N., TRUMPP, A., DELMAS, V. and BEERMANN, F., 2012. Constitutive gray hair in mice induced by melanocyte-specific deletion of c-Myc. Pigment Cell Melanoma Res *25:* 312-325.

PTASHNE, M., 1986. Gene regulation by proteins acting nearby and at a distance. Nature *322:* 697-701.

PURTON, L. E., and SCADDEN, D. T., 2007. Limiting factors in murine hematopoietic stem cell assays. Cell Stem Cell *1:* 263-270.

RADA-IGLESIAS, A., BAJPAI, R., SWIGUT, T., BRUGMANN, S. A., FLYNN, R. A. and WYSOCKA, J., 2011. A unique chromatin signature uncovers early developmental enhancers in humans. Nature *470:* 279-283.

RADTKE, I., MULLIGHAN, C. G., ISHII, M., SU, X., CHENG, J. *et al.*, 2009. Genomic analysis reveals few genetic alterations in pediatric acute myeloid leukemia. Proc Natl Acad Sci U S A *106:* 12944-12949.

RAHL, P. B., LIN, C. Y., SEILA, A. C., FLYNN, R. A., MCCUINE, S., BURGE, C. B., SHARP, P. A. and YOUNG, R. A., 2010. c-Myc regulates transcriptional pause release. Cell *141:* 432-445.

RALPH, S. J., and BERRIDGE, M. V., 1984. Expression of antigens of the 'T200' family of glycoproteins on hemopoietic stem cells: evidence that thymocyte cell lineage antigens are represented on 'T200'. J Immunol *132:* 2510-2514.

RAMALHO-SANTOS, M., and WILLENBRING, H., 2007. On the origin of the term "stem cell". Cell Stem Cell *1:* 35-38.

REAVIE, L., BUCKLEY, S. M., LOIZOU, E., TAKEISHI, S., ARANDA-ORGILLES, B. *et al.*, 2013. Regulation of c-Myc ubiquitination controls chronic myelogenous leukemia initiation and progression. Cancer Cell *23:* 362-375.

REAVIE, L., DELLA GATTA, G., CRUSIO, K., ARANDA-ORGILLES, B., BUCKLEY, S. M. *et al.*, 2010. Regulation of hematopoietic stem cell differentiation by a single ubiquitin ligase-substrate complex. Nat Immunol *11:* 207-215.

REINBERG, D., ORPHANIDES, G., EBRIGHT, R., AKOULITCHEV, S., CARCAMO, J. *et al.*, 1998. The RNA polymerase II general transcription factors: past, present, and future. Cold Spring Harb Symp Quant Biol *63:* 83-103.

RHODES, K. E., GEKAS, C., WANG, Y., LUX, C. T., FRANCIS, C. S. *et al.*, 2008. The emergence of hematopoietic stem cells is initiated in the placental vasculature in the absence of circulation. Cell Stem Cell *2:* 252-263.

RIETHOVEN, J. J., 2010. Regulatory regions in DNA: promoters, enhancers, silencers, and insulators. Methods Mol Biol *674:* 33-42.

ROSS, M. E., MAHFOUZ, R., ONCIU, M., LIU, H. C., ZHOU, X. *et al.*, 2004. Gene expression profiling of pediatric acute myelogenous leukemia. Blood *104:* 3679-3687.

RUF, S., SYMMONS, O., USLU, V. V., DOLLE, D., HOT, C., ETTWILLER, L. and SPITZ, F., 2011. Large-scale analysis of the regulatory architecture of the mouse genome with a transposon-associated sensor. Nat Genet *43:* 379-386.

SABIN, F. R., 1920. Studies on the origin of blood vessels and of red corpuscles as seen in the living blastoderm of chicks during the second day of incubation. Contrib. Embryol. *9:* 213-262.

SABÒ, A., KRESS, T. R., PELIZZOLA, M., DE PRETIS, S., GORSKI, M. M. *et al.*, 2014. Selective transcriptional regulation by Myc in cellular growth control and lymphomagenesis. Nature *511:* 488-492.

SABO, P. J., HAWRYLYCZ, M., WALLACE, J. C., HUMBERT, R., YU, M. *et al.*, 2004a. Discovery of functional noncoding elements by digital analysis of chromatin structure. Proc Natl Acad Sci U S A *101:* 16837-16842.

SABO, P. J., HUMBERT, R., HAWRYLYCZ, M., WALLACE, J. C., DORSCHNER, M. O., MCARTHUR, M. and STAMATOYANNOPOULOS, J. A., 2004b. Genome-wide identification of DNaseI hypersensitive sites using active chromatin sequence libraries. Proc Natl Acad Sci U S A *101:* 4537-4542.

SAHA, A., WITTMEYER, J. and CAIRNS, B. R., 2006. Chromatin remodelling: the industrial revolution of DNA around histones. Nat Rev Mol Cell Biol *7:* 437-447.

SALVATORI, B., IOSUE, I., DJODJI DAMAS, N., MANGIAVACCHI, A., CHIARETTI, S. *et al.*, 2011. Critical Role of c-Myc in Acute Myeloid Leukemia Involving Direct Regulation of miR-26a and Histone Methyltransferase EZH2. Genes Cancer *2:* 585-592.

SANDELIN, A., CARNINCI, P., LENHARD, B., PONJAVIC, J., HAYASHIZAKI, Y. and HUME, D. A., 2007. Mammalian RNA polymerase II core promoters: insights from genome-wide studies. Nat Rev Genet *8:* 424-436.

SANJUAN-PLA, A., MACAULAY, I. C., JENSEN, C. T., WOLL, P. S., LUIS, T. C. *et al.*, 2013. Platelet-biased stem cells reside at the apex of the haematopoietic stem-cell hierarchy. Nature *502:* 232-236.

SATO, T., ONAI, N., YOSHIHARA, H., ARAI, F., SUDA, T. and OHTEKI, T., 2009. Interferon regulatory factor-2 protects quiescent hematopoietic stem cells from type I interferon-dependent exhaustion. Nat Med *15:* 696-700.

SAUER, B., and HENDERSON, N., 1988. Site-specific DNA recombination in mammalian cells by the Cre recombinase of bacteriophage P1. Proc Natl Acad Sci U S A *85:* 5166-5170.

SAWAI, S., SHIMONO, A., WAKAMATSU, Y., PALMES, C., HANAOKA, K. and KONDOH, H., 1993. Defects of embryonic organogenesis resulting from targeted disruption of the N-myc gene in the mouse. Development *117:* 1445-1455.

SAXONOV, S., BERG, P. and BRUTLAG, D. L., 2006. A genome-wide analysis of CpG dinucleotides in the human genome distinguishes two distinct classes of promoters. Proc Natl Acad Sci U S A *103:* 1412-1417.

SCHEID, M. P., and TRIGLIA, D., 1979. Further description of the Ly-5 system. Immunogenetics*:* 423-433.

SCHMITT, T. M., and ZUNIGA-PFLUCKER, J. C., 2002. Induction of T cell development from hematopoietic progenitor cells by delta-like-1 in vitro. Immunity *17:* 749-756.

SCHNEIDER, R., BANNISTER, A. J., WEISE, C. and KOUZARIDES, T., 2004. Direct binding of INHAT to H3 tails disrupted by modifications. J Biol Chem *279:* 23859-23862.

SCHOENFELDER, S., CLAY, I. and FRASER, P., 2010. The transcriptional interactome: gene expression in 3D. Curr Opin Genet Dev *20:* 127-133.

SCHREIBER-AGUS, N., CHIN, L., CHEN, K., TORRES, R., RAO, G., GUIDA, P., SKOULTCHI, A. I. and DEPINHO, R. A., 1995. An amino-terminal domain of Mxi1 mediates anti-Myc oncogenic activity and interacts with a homolog of the yeast transcriptional repressor SIN3. Cell *80:* 777-786.

SCHWAB, M., ALITALO, K., KLEMPNAUER, K. H., VARMUS, H. E., BISHOP, J. M., GILBERT, F., BRODEUR, G., GOLDSTEIN, M. and TRENT, J., 1983. Amplified DNA with limited homology to myc cellular oncogene is shared by human neuroblastoma cell lines and a neuroblastoma tumour. Nature *305:* 245-248.

SCHWARTZ, Y. B., KAHN, T. G., NIX, D. A., LI, X. Y., BOURGON, R., BIGGIN, M. and PIRROTTA, V., 2006. Genome-wide analysis of Polycomb targets in Drosophila melanogaster. Nat Genet *38:* 700-705.

SEMPLE, J. W., ITALIANO, J. E., JR. and FREEDMAN, J., 2011. Platelets and the immune continuum. Nat Rev Immunol *11:* 264-274.

SEOANE, J., LE, H. V. and MASSAGUE, J., 2002. Myc suppression of the p21(Cip1) Cdk inhibitor influences the outcome of the p53 response to DNA damage. Nature *419:* 729-734.

SEOANE, J., POUPONNOT, C., STALLER, P., SCHADER, M., EILERS, M. and MASSAGUE, J., 2001. TGFbeta influences Myc, Miz-1 and Smad to control the CDK inhibitor p15INK4b. Nat Cell Biol *3:* 400-408.

SHEINESS, D., FANSHIER, L. and BISHOP, J. M., 1978. Identification of nucleotide sequences which may encode the oncogenic capacity of avian retrovirus MC29. J Virol *28:* 600-610.

SHEN, Y., YUE, F., MCCLEARY, D. F., YE, Z., EDSALL, L. *et al.*, 2012. A map of the cis-regulatory sequences in the mouse genome. Nature *488:* 116-120.

SHI, J., WHYTE, W. A., ZEPEDA-MENDOZA, C. J., MILAZZO, J. P., SHEN, C. *et al.*, 2013. Role of SWI/SNF in acute leukemia maintenance and enhancer-mediated Myc regulation. Genes Dev *27:* 2648-2662.

SHLUSH, L. I., ZANDI, S., MITCHELL, A., CHEN, W. C., BRANDWEIN, J. M. *et al.*, 2014. Identification of pre-leukaemic haematopoietic stem cells in acute leukaemia. Nature *506:* 328-333.

SIMINOVITCH, L., MCCULLOCH, E. A. and TILL, J. E., 1963. The Distribution of Colony-Forming Cells among Spleen Colonies. J Cell Physiol *62:* 327-336.

SING, A., PANNELL, D., KARAISKAKIS, A., STURGEON, K., DJABALI, M., ELLIS, J., LIPSHITZ, H. D. and CORDES, S. P., 2009. A vertebrate Polycomb response element governs segmentation of the posterior hindbrain. Cell *138:* 885-897.

SMALE, S. T., and KADONAGA, J. T., 2003. The RNA polymerase II core promoter. Annu Rev Biochem *72:* 449-479.

SMITH, K. N., SINGH, A. M. and DALTON, S., 2010. Myc represses primitive endoderm differentiation in pluripotent stem cells. Cell Stem Cell *7:* 343-354.

SOTELO, J., ESPOSITO, D., DUHAGON, M. A., BANFIELD, K., MEHALKO, J. *et al.*, 2010. Long-range enhancers on 8q24 regulate c-Myc. Proc Natl Acad Sci U S A *107:* 3001-3005.

SPANGRUDE, G. J., HEIMFELD, S. and WEISSMAN, I. L., 1988. Purification and characterization of mouse hematopoietic stem cells. Science *241:* 58-62.

SPITZ, F., and FURLONG, E. E., 2012. Transcription factors: from enhancer binding to developmental control. Nat Rev Genet *13:* 613-626.

STADLER, M. B., MURR, R., BURGER, L., IVANEK, R., LIENERT, F. *et al.*, 2011. DNA-binding factors shape the mouse methylome at distal regulatory regions. Nature *480:* 490-495.

STANTON, B. R., PERKINS, A. S., TESSAROLLO, L., SASSOON, D. A. and PARADA, L. F., 1992. Loss of N-myc function results in embryonic lethality and failure of the epithelial component of the embryo to develop. Genes Dev *6:* 2235-2247.

STEIGER, D., FURRER, M., SCHWINKENDORF, D. and GALLANT, P., 2008. Max-independent functions of Myc in Drosophila melanogaster. Nat Genet *40:* 1084-1091.

STERNBERG, N., and HAMILTON, D., 1981. Bacteriophage P1 site-specific recombination. I. Recombination between loxP sites. J Mol Biol *150:* 467-486.

STIREWALT, D. L., MESHINCHI, S., KOPECKY, K. J., FAN, W., POGOSOVA-AGADJANYAN, E. L. *et al.*, 2008. Identification of genes with abnormal expression changes in acute myeloid leukemia. Genes Chromosomes Cancer *47:* 8-20.

STOCK, J. K., GIADROSSI, S., CASANOVA, M., BROOKES, E., VIDAL, M., KOSEKI, H., BROCKDORFF, N., FISHER, A. G. and POMBO, A., 2007. Ring1-mediated ubiquitination of H2A restrains poised RNA polymerase II at bivalent genes in mouse ES cells. Nat Cell Biol *9:* 1428-1435.

STOELZLE, T., SCHWARB, P., TRUMPP, A. and HYNES, N. E., 2009. c-Myc affects mRNA translation, cell proliferation and progenitor cell function in the mammary gland. BMC Biol *7:* 63.

SUN, D., LUO, M., JEONG, M., RODRIGUEZ, B., XIA, Z. *et al.*, 2014. Epigenomic profiling of young and aged HSCs reveals concerted changes during aging that reinforce self-renewal. Cell Stem Cell *14:* 673-688.

SUR, I. K., HALLIKAS, O., VAHARAUTIO, A., YAN, J., TURUNEN, M. *et al.*, 2012. Mice lacking a Myc enhancer that includes human SNP rs6983267 are resistant to intestinal tumors. Science *338:* 1360-1363.

SUTHERLAND, H. J., EAVES, C. J., EAVES, A. C., DRAGOWSKA, W. and LANSDORP, P. M., 1989. Characterization and partial purification of human marrow cells capable of initiating long-term hematopoiesis in vitro. Blood *74:* 1563-1570.

SYKES, M., CHESTER, C. H., SUNDT, T. M., ROMICK, M. L., HOYLES, K. A. and SACHS, D. H., 1989. Effects of T cell depletion in radiation bone marrow chimeras. III. Characterization of allogeneic bone marrow cell populations that increase allogeneic chimerism independently of graft-vs-host disease in mixed marrow recipients. J Immunol *143:* 3503-3511.

SYMMONS, O., and SPITZ, F., 2013. From remote enhancers to gene regulation: charting the genome's regulatory landscapes. Philos Trans R Soc Lond B Biol Sci *368:* 20120358.

SYMMONS, O., USLU, V. V., TSUJIMURA, T., RUF, S., NASSARI, S., SCHWARZER, W., ETTWILLER, L. and SPITZ, F., 2014. Functional and topological characteristics of mammalian regulatory domains. Genome Res *24:* 390-400.

SZILVASSY, S. J., HUMPHRIES, R. K., LANSDORP, P. M., EAVES, A. C. and EAVES, C. J., 1990. Quantitative assay for totipotent reconstituting hematopoietic stem cells by a competitive repopulation strategy. Proc Natl Acad Sci U S A *87:* 8736-8740.

TASWELL, C., 1981. Limiting dilution assays for the determination of immunocompetent cell frequencies. I. Data analysis. J Immunol *126:* 1614-1619.

TAUB, R., KIRSCH, I., MORTON, C., LENOIR, G., SWAN, D., TRONICK, S., AARONSON, S. and LEDER, P., 1982. Translocation of the c-myc gene into the immunoglobulin heavy chain locus in human Burkitt lymphoma and murine plasmacytoma cells. Proc Natl Acad Sci U S A *79:* 7837-7841.

TEWARI, R., GILLEMANS, N., HARPER, A., WIJGERDE, M., ZAFARANA, G., DRABEK, D., GROSVELD, F. and PHILIPSEN, S., 1996. The human beta-globin locus control

region confers an early embryonic erythroid-specific expression pattern to a basic promoter driving the bacterial lacZ gene. Development *122:* 3991-3999.

THON, J. N., and ITALIANO, J. E., 2010. Platelet formation. Semin Hematol *47:* 220-226.

THURMAN, R. E., RYNES, E., HUMBERT, R., VIERSTRA, J., MAURANO, M. T. *et al.*, 2012. The accessible chromatin landscape of the human genome. Nature *489:* 75-82.

TILL, J. E., and MCCULLOCH, E. A., 1961. A direct measurement of the radiation sensitivity of normal mouse bone marrow cells. Radiat Res *14:* 213-222.

TOLHUIS, B., DE WIT, E., MUIJRERS, I., TEUNISSEN, H., TALHOUT, W., VAN STEENSEL, B. and VAN LOHUIZEN, M., 2006. Genome-wide profiling of PRC1 and PRC2 Polycomb chromatin binding in Drosophila melanogaster. Nat Genet *38:* 694-699.

TOLHUIS, B., PALSTRA, R. J., SPLINTER, E., GROSVELD, F. and DE LAAT, W., 2002. Looping and interaction between hypersensitive sites in the active beta-globin locus. Mol Cell *10:* 1453-1465.

TRUMPP, A., REFAELI, Y., OSKARSSON, T., GASSER, S., MURPHY, M., MARTIN, G. R. and BISHOP, J. M., 2001. c-Myc regulates mammalian body size by controlling cell number but not cell size. Nature *414:* 768-773.

TSENG, Y. Y., MORIARITY, B. S., GONG, W., AKIYAMA, R., TIWARI, A. *et al.*, 2014. PVT1 dependence in cancer with MYC copy-number increase. Nature *512:* 82-86.

TZONEVA, G., and FERRANDO, A. A., 2012. Recent advances on NOTCH signaling in T-ALL. Curr Top Microbiol Immunol *360:* 163-182.

USLU, V. V., PETRETICH, M., RUF, S., LANGENFELD, K., FONSECA, N. A., MARIONI, J. C. and SPITZ, F., 2014. Long-range enhancers regulating Myc expression are required for normal facial morphogenesis. Nat Genet *46:* 753-758.

VALK, P. J., VERHAAK, R. G., BEIJEN, M. A., ERPELINCK, C. A., BARJESTEH VAN WAALWIJK VAN DOORN-KHOSROVANI, S. *et al.*, 2004. Prognostically useful gene-expression profiles in acute myeloid leukemia. N Engl J Med *350:* 1617-1628.

VALLESPINOS, M., FERNANDEZ, D., RODRIGUEZ, L., ALVARO-BLANCO, J., BAENA, E. *et al.*, 2011. B Lymphocyte commitment program is driven by the proto-oncogene c-Myc. J Immunol *186:* 6726-6736.

VAN KEUREN, M. L., GAVRILINA, G. B., FILIPIAK, W. E., ZEIDLER, M. G. and SAUNDERS, T. L., 2009. Generating transgenic mice from bacterial artificial chromosomes: transgenesis efficiency, integration and expression outcomes. Transgenic Res *18:* 769-785.

VAN OS, R., KAMMINGA, L. M. and DE HAAN, G., 2004. Stem cell assays: something old, something new, something borrowed. Stem Cells *22:* 1181-1190.

VAN RIGGELEN, J., YETIL, A. and FELSHER, D. W., 2010. MYC as a regulator of ribosome biogenesis and protein synthesis. Nat Rev Cancer *10:* 301-309.

VARLAKHANOVA, N. V., COTTERMAN, R. F., DEVRIES, W. N., MORGAN, J., DONAHUE, L. R., MURRAY, S., KNOWLES, B. B. and KNOEPFLER, P. S., 2010. myc maintains embryonic stem cell pluripotency and self-renewal. Differentiation *80:* 9-19.

VENNSTROM, B., SHEINESS, D., ZABIELSKI, J. and BISHOP, J. M., 1982. Isolation and characterization of c-myc, a cellular homolog of the oncogene (v-myc) of avian myelocytomatosis virus strain 29. J Virol *42:* 773-779.

VENTER, J. C., ADAMS, M. D., MYERS, E. W., LI, P. W., MURAL, R. J. *et al.*, 2001. The sequence of the human genome. Science *291:* 1304-1351.

VIRE, E., BRENNER, C., DEPLUS, R., BLANCHON, L., FRAGA, M. *et al.*, 2006. The Polycomb group protein EZH2 directly controls DNA methylation. Nature *439:* 871-874.

VISEL, A., RUBIN, E. M. and PENNACCHIO, L. A., 2009. Genomic views of distant-acting enhancers. Nature *461:* 199-205.

WALSH, C. T., GARNEAU-TSODIKOVA, S. and GATTO, G. J., JR., 2005. Protein posttranslational modifications: the chemistry of proteome diversifications. Angew Chem Int Ed Engl *44:* 7342-7372.

WALZ, S., LORENZIN, F., MORTON, J., WIESE, K. E., VON EYSS, B. *et al.*, 2014. Activation and repression by oncogenic MYC shape tumour-specific gene expression profiles. Nature *511:* 483-487.

WANG, D., GARCIA-BASSETS, I., BENNER, C., LI, W., SU, X. *et al.*, 2011. Reprogramming transcription by distinct classes of enhancers functionally defined by eRNA. Nature *474:* 390-394.

WANG, H., WANG, L., ERDJUMENT-BROMAGE, H., VIDAL, M., TEMPST, P., JONES, R. S. and ZHANG, Y., 2004. Role of histone H2A ubiquitination in Polycomb silencing. Nature *431:* 873-878.

WASKOW, C., MADAN, V., BARTELS, S., COSTA, C., BLASIG, R. and RODEWALD, H. R., 2009. Hematopoietic stem cell transplantation without irradiation. Nat Methods *6:* 267-269.

WATERSTON, R. H., LINDBLAD-TOH, K., BIRNEY, E., ROGERS, J., ABRIL, J. F. *et al.*, 2002. Initial sequencing and comparative analysis of the mouse genome. Nature *420:* 520-562.

WATT, F. M., FRYE, M. and BENITAH, S. A., 2008. MYC in mammalian epidermis: how can an oncogene stimulate differentiation? Nat Rev Cancer *8:* 234-242.

WENG, A. P., FERRANDO, A. A., LEE, W., MORRIS, J. P. T., SILVERMAN, L. B., SANCHEZ-IRIZARRY, C., BLACKLOW, S. C., LOOK, A. T. and ASTER, J. C., 2004. Activating

mutations of NOTCH1 in human T cell acute lymphoblastic leukemia. Science *306:* 269-271.

WHITE, R. J., 2011. Transcription by RNA polymerase III: more complex than we thought. Nat Rev Genet *12:* 459-463.

WHITLOCK, C. A., and WITTE, O. N., 1982. Long-term culture of B lymphocytes and their precursors from murine bone marrow. Proc Natl Acad Sci U S A *79:* 3608-3612.

WIERSTRA, I., and ALVES, J., 2008. The c-myc promoter: still MysterY and challenge. Adv Cancer Res *99:* 113-333.

WILSON, A., LAURENTI, E., OSER, G., VAN DER WATH, R. C., BLANCO-BOSE, W. *et al.*, 2008. Hematopoietic stem cells reversibly switch from dormancy to self-renewal during homeostasis and repair. Cell *135:* 1118-1129.

WILSON, A., MURPHY, M. J., OSKARSSON, T., KALOULIS, K., BETTESS, M. D. *et al.*, 2004. c-Myc controls the balance between hematopoietic stem cell self-renewal and differentiation. Genes Dev *18:* 2747-2763.

WILSON, N. K., FOSTER, S. D., WANG, X., KNEZEVIC, K., SCHUTTE, J. *et al.*, 2010. Combinatorial transcriptional control in blood stem/progenitor cells: genome-wide analysis of ten major transcriptional regulators. Cell Stem Cell *7:* 532-544.

WINSTON, F., and ALLIS, C. D., 1999. The bromodomain: a chromatin-targeting module? Nat Struct Biol *6:* 601-604.

WOEHRER, S., MILLER, C. L. and EAVES, C. J., 2013. Long-term culture-initiating cell assay for mouse cells. Methods Mol Biol *946:* 257-266.

WOLF, N. S., KONE, A., PRIESTLEY, G. V. and BARTELMEZ, S. H., 1993. In vivo and in vitro characterization of long-term repopulating primitive hematopoietic cells isolated by sequential Hoechst 33342-rhodamine 123 FACS selection. Exp Hematol *21:* 614-622.

WOO, C. J., KHARCHENKO, P. V., DAHERON, L., PARK, P. J. and KINGSTON, R. E., 2010. A region of the human HOXD cluster that confers polycomb-group responsiveness. Cell *140:* 99-110.

WOYCHIK, N. A., and HAMPSEY, M., 2002. The RNA polymerase II machinery: structure illuminates function. Cell *108:* 453-463.

WU, A. M., TILL, J. E., SIMINOVITCH, L. and MCCULLOCH, E. A., 1967. A cytological study of the capacity for differentiation of normal hemopoietic colony-forming cells. J Cell Physiol *69:* 177-184.

WU, S., CETINKAYA, C., MUNOZ-ALONSO, M. J., VON DER LEHR, N., BAHRAM, F., BEUGER, V., EILERS, M., LEON, J. and LARSSON, L. G., 2003. Myc represses

differentiation-induced p21CIP1 expression via Miz-1-dependent interaction with the p21 core promoter. Oncogene *22:* 351-360.

WU, S., YING, G., WU, Q. and CAPECCHI, M. R., 2007. Toward simpler and faster genome-wide mutagenesis in mice. Nat Genet *39:* 922-930.

XI, H., SHULHA, H. P., LIN, J. M., VALES, T. R., FU, Y. *et al.*, 2007. Identification and characterization of cell type-specific and ubiquitous chromatin regulatory structures in the human genome. PLoS Genet *3:* e136.

YAMAMOTO, R., MORITA, Y., OOEHARA, J., HAMANAKA, S., ONODERA, M., RUDOLPH, K. L., EMA, H. and NAKAUCHI, H., 2013. Clonal analysis unveils self-renewing lineage-restricted progenitors generated directly from hematopoietic stem cells. Cell *154:* 1112-1126.

YANG, H., WANG, H. and JAENISCH, R., 2014. Generating genetically modified mice using CRISPR/Cas-mediated genome engineering. Nat Protoc *9:* 1956-1968.

YANT, S. R., and KAY, M. A., 2003. Nonhomologous-end-joining factors regulate DNA repair fidelity during Sleeping Beauty element transposition in mammalian cells. Mol Cell Biol *23:* 8505-8518.

YATES, L. R., and CAMPBELL, P. J., 2012. Evolution of the cancer genome. Nat Rev Genet *13:* 795-806.

YEE, S. P., and RIGBY, P. W., 1993. The regulation of myogenin gene expression during the embryonic development of the mouse. Genes Dev *7:* 1277-1289.

YING, Q. L., WRAY, J., NICHOLS, J., BATLLE-MORERA, L., DOBLE, B., WOODGETT, J., COHEN, P. and SMITH, A., 2008. The ground state of embryonic stem cell self-renewal. Nature *453:* 519-523.

YOKOTA, T., ORITANI, K., BUTZ, S., KOKAME, K., KINCADE, P. W., MIYATA, T., VESTWEBER, D. and KANAKURA, Y., 2009. The endothelial antigen ESAM marks primitive hematopoietic progenitors throughout life in mice. Blood *113:* 2914-2923.

YOON, Y. S., JEONG, S., RONG, Q., PARK, K. Y., CHUNG, J. H. and PFEIFER, K., 2007. Analysis of the H19ICR insulator. Mol Cell Biol *27:* 3499-3510.

YUAN, R., ASTLE, C. M., CHEN, J. and HARRISON, D. E., 2005. Genetic regulation of hematopoietic stem cell exhaustion during development and growth. Exp Hematol *33:* 243-250.

YUDKOVSKY, N., LOGIE, C., HAHN, S. and PETERSON, C. L., 1999. Recruitment of the SWI/SNF chromatin remodeling complex by transcriptional activators. Genes Dev *13:* 2369-2374.

ZANET, J., PIBRE, S., JACQUET, C., RAMIREZ, A., DE ALBORAN, I. M. and GANDARILLAS, A., 2005. Endogenous Myc controls mammalian epidermal cell size,

hyperproliferation, endoreplication and stem cell amplification. J Cell Sci *118:* 1693-1704.

ZELLER, K. I., ZHAO, X., LEE, C. W., CHIU, K. P., YAO, F. *et al.*, 2006. Global mapping of c-Myc binding sites and target gene networks in human B cells. Proc Natl Acad Sci U S A *103:* 17834-17839.

ZERVOS, A. S., GYURIS, J. and BRENT, R., 1993. Mxi1, a protein that specifically interacts with Max to bind Myc-Max recognition sites. Cell *72:* 223-232.

ZHANG, Y., WONG, C. H., BIRNBAUM, R. Y., LI, G., FAVARO, R. *et al.*, 2013. Chromatin connectivity maps reveal dynamic promoter-enhancer long-range associations. Nature *504:* 306-310.

ZHAO, H., and DEAN, A., 2004. An insulator blocks spreading of histone acetylation and interferes with RNA polymerase II transfer between an enhancer and gene. Nucleic Acids Res *32:* 4903-4919.

ZHOU, V. W., GOREN, A. and BERNSTEIN, B. E., 2011. Charting histone modifications and the functional organization of mammalian genomes. Nat Rev Genet *12:* 7-18.

ZHU, X., LING, J., ZHANG, L., PI, W., WU, M. and TUAN, D., 2007. A facilitated tracking and transcription mechanism of long-range enhancer function. Nucleic Acids Res *35:* 5532-5544.

ZILBERMAN, D., COLEMAN-DERR, D., BALLINGER, T. and HENIKOFF, S., 2008. Histone H2A.Z and DNA methylation are mutually antagonistic chromatin marks. Nature *456:* 125-129.

ZILLER, M. J., GU, H., MULLER, F., DONAGHEY, J., TSAI, L. T. *et al.*, 2013. Charting a dynamic DNA methylation landscape of the human genome. Nature *500:* 477-481.

ZIMMERMAN, K., and ALT, F. W., 1990. Expression and function of myc family genes. Crit Rev Oncog *2:* 75-95.